Pharmacological Characterisation of Novel Oxytocin and Vasopressin Receptor Ligands

Damien Gulliver

A thesis submitted in fulfilment of the requirements for the degree of Doctor of Philosophy

Faculty of Medicine
School of Medical Sciences
The University of Sydney
December 10th 2020

Statement of Originality

I certify that to the best of my knowledge, this thesis contains no material previously published by any other person except where due acknowledgement has been made. This thesis has not been submitted for any degree or other purposes.

I certify that the intellectual content of this thesis is the product of my own work and that all the assistance received in preparing this thesis and sources have been acknowledged.

Damien Gulliver
30.09.20

Acknowledgements

First and foremost, I would like to thank my supervisor, Prof. Michael Kassiou, for giving me the opportunity to work within the Drug Discovery Group on this project. A well-funded, smoothly running laboratory and interesting areas of research makes the experience of a PhD immeasurably more enjoyable. I appreciate the autonomy I was given to explore new ideas and establish new assays, and the direction I was given when it was sought after. Most of all, I appreciate your humour and your sensitivity, which shone through at the moments when I needed it most.

To my colleague and mentor Dr. Eryn Werry - thank you for teaching me what it means to be a scientist. You have been there from the very beginning, since I was a fledgling honours student, and I can only say that without your steadfast support and gentle guidance, I would never have made it this far. Your unshakeable composure, easy-going nature and incredible abilities as a researcher leave me in awe, and I will always have boundless respect for you.

To the chemists of the Drug Discovery Group – Dr. Will Jorgensen, Dr. Tristan Reekie and Timothy Katte. Thank you for your tireless efforts in synthesising the molecules investigated in this thesis. It was a pleasure to collaborate with you, and I appreciate the knowledge and technical expertise which you brought to various aspects of the oxytocin project.

To my fellow students in the Drug Discovery Group – thank you for sharing this experience with me and I wish you all the best in future endeavours. Erick, I always felt that there was a tacit understanding between us, and I appreciated that solidarity. Kiyan, I admire your passion for science, I appreciate the assistance you provided me with the bias work, and I enjoyed our conversations around the intricacies of pharmacology. Michael, Alison and Sam – your presence created a positive and uplifting work environment which I valued immensely.

I would also like to thank Donna Lai, Sheng Hua and the Molecular Biology Facility, who provided many of the instruments I used in this research, and the training on how to operate them. Thank you also to thank Dr. Ben Crossett and David Maltby from the Sydney Mass Spectrometry Core Facility, who tried valiantly for many months to assist me in establishing a mass-spectrometry assay, and to Dr. Markus Muttenthaler from the University of Queensland, who synthesised and generously gifted some of the molecules investigated in this thesis.

To my friends and family, thank you for supporting me when I was low and sharing in my excitement when things were going well. A PhD can be a hard and sometimes dark road, but a strong network of people that love you provides much needed security, comfort and resilience.

Athena, we met what feels like an age ago, and who knew then that we would go, as one, through the entire journey? We weathered the storms and celebrated the triumphs which arose through ten long years of study, and were shaped by them together. Many times, there was no one who truly understood how I felt but you. Thank you for your endlessly giving and caring nature, without which I would not be where I am, or who I am.

Authorship Attribution Statement

Chapter 1 of this thesis contains material published in:

Gulliver D, Werry E, Reekie T, Katte T, Jorgensen W, Kassiou M.* Targeting the Oxytocin System: New Pharmacotherapeutic Approaches. Trends Pharmacol Sci. 2019;40(1):22-37.

This has been adapted from the published manuscript, and is throughout Section 1.1 - 1.5. I conducted the literature review, wrote the manuscript and designed the figures for this publication.

Chapter 3 of this thesis contains material published in:

Jorgensen W[a], **Gulliver D**[b], Katte T, Werry E, Reekie T, Connor M, Kassiou M.* Conformationally rigid derivatives of WAY-267,464: Synthesis and pharmacology at the human oxytocin and vasopressin 1A receptors. Eur J Med Chem. 2018;143:1644-1656.

This is Section 3.2.1; Figure 3.3 and Table 3.1, which corresponds to data in Table 1 of the published manuscript. I was involved in the experimental design, data collection, data management and statistical analysis for this publication.

Chapter 5 of this thesis contains unpublished experimental data collected by Dr. Eryn Werry and included with her permission. This is in Section 5.3.3; Figure 5.4.

In addition to the statements above, in cases where I am not the corresponding author of a published item, permission to include the published material has been granted by the corresponding author.

Damien Gulliver
30.09.20

As supervisor for the candidature upon which this thesis is based, I can confirm that the authorship attribution statements above are correct.

Michael Kassiou
30.09.20

Abstract

Deficits in social behavioural domains such as interpersonal communication and emotion recognition are a symptom of many neuropsychiatric conditions, including autism spectrum disorder, schizophrenia and social anxiety disorder. Often, these symptoms are intractable, profoundly affecting patient quality of life. Current therapeutic interventions do not target core social deficits and display considerable adverse effect profiles, thus, novel approaches are urgently needed to address the medical needs of this patient population.

The hypothalamic peptides oxytocin (OT) and vasopressin (AVP) have emerged as key regulators of social behaviour in vertebrates, with converging evidence indicating that OT signalling exerts broadly prosocial effects in animal studies and human cohorts. Consequently, the oxytocin receptor (OTR) has been identified as a potential therapeutic target for improving social behavioural deficits. The use of OT in this context is complicated by rapid metabolism and poor CNS penetration of the peptide, low receptor selectivity between the OTR and vasopressin receptors ($V_{1A}R$, $V_{1B}R$, V_2R), and desensitisation of the OTR with chronic administration.

This thesis sought to identify OTR agonists which mitigate limitations inherent to the native peptide. Drug candidates were screened from a library of (A) pyrazolobenzodiazepine small molecules and (B) peptide ligands derived from endogenous metabolites of OT. Although the small-molecule discovery program did not identify novel OTR agonists, two selective $V_{1A}R$ ligands (**4a**, **5f**) were characterised, which may have alternate therapeutic applications. In contrast, the peptide discovery program identified biologically active fragments of OT (**9a**, **9b**). Structural modification of these metabolites produced selective OTR agonists (**11c**, **12c**) with enhanced receptor affinity and signalling efficacy. Relative to OT, these modified peptides displayed a bias toward activation of G-protein signalling, and away from β-arrestin recruitment – factors which may prolong therapeutic efficacy *in vivo*. The lower molecular weight and reduced polarity of **11c** and **12c** relative to OT may also facilitate greater CNS penetration, positioning them as superior candidates for further development as oxytocinergic therapeutics.

List of Abbreviations

5-HT$_{1A}$ 5-HT type 1A receptor
5-HT$_{1B}$ 5-HT type 1B receptor
ACTH Adrenocorticotropic hormone
ADME Absorption, distribution, metabolism, excretion
ANOVA Analysis of variance
ASD Autism spectrum disorder
AVP Arginine-vasopressin
AVPR Vasopressin receptor
BRET Bioluminescence resonance energy transfer
BSA Bovine serum albumin
cAMP Cyclic adenosine monophosphate
CB1 Cannabinoid type 1 receptor
CD38 Cyclic ADP ribose hydrolase
CNS Central nervous system
CRH Corticotrophin-releasing hormone
CSF Cerebrospinal fluid
D$_2$R Dopamine type 2 receptor
DMEM Dulbecco's modified eagle medium
DMSO Dimethyl sulfoxide
DRN Dorsal raphe nuclei
ECL Extracellular loop
EPSA Exposed polar surface area
FBS Foetal bovine serum
fMRI Functional magnetic resonance imaging
FRET Fluorescence resonance energy transfer
GPCR G-protein coupled receptor
GRK G-protein coupled receptor kinase
HBSS Hank's buffered salts solution
HEK293 Human epithelial kidney cells
HPA Hypothalamic-pituitary-adrenal axis
HTRF Homogenous time-resolved fluorescence
IBMX 3-isobutyl-1-methyxanthine
ICV Intracerebroventricular
IMHB Intramolecular hydrogen bond
IP Intraperitoneal
IP$_1$ Inositol monophosphate
IRAP Insulin-regulated aminopeptidase
LB Luria-bertani broth
LC-MS Liquid chromatography-mass spectrometry
LVA Linear vasopressin
MAPK Mitogen-activated protein kinase
MCS Multiple cloning site
MIF-1 Melanocyte inhibiting factor
NAcc Nucleus accumbens
Nluc Nanoluciferase
OT Oxytocin
OTR Oxytocin receptor
OVTA Ornithine vasotocin
PDE Phosphodiesterase
PET Positron emission tomography
PKA Protein kinase A
P-LAP Placental leucine aminopeptidase
PLGA Poly(lactic-co-glycolic acid)
PTSD Post-traumatic stress disorder
PVN Paraventricular nuclei
RAGE Receptor for advanced glycation end products

RCT Randomised controlled trial
SAD Social anxiety disorder
SNP Single nucleotide polymorphism
SON Supraoptic nuclei
TM Transmembrane domain
TRPV2 Transient receptor potential cation channel subfamily V member 2
$V_{1A}R$ Vasopressin type 1A receptor
$V_{1B}R$ Vasopressin type 1B receptor
V_2R Vasopressin type 2 receptor
VTA Ventral tegmental area

Contents

1 Introduction **1**

1.1 Neuropeptide Regulation of Social Behaviour 2

1.1.1 Mammalian Social Behaviour 2

1.1.2 Oxytocin and Vasopressin: Social Neuropeptides 3

1.1.3 The Effects of Oxytocin and Vasopressin in Animal Behavioural Studies 5

1.1.4 The Effects of Oxytocin and Vasopressin in Healthy Human Cohorts 6

1.1.5 Dysregulation of Oxytocin Signalling in Neuropsychiatric Conditions 7

1.2 Neurobiology of the Oxytocin System 9

1.2.1 The Oxytocin Signalling Network in the Central Nervous System 9

1.2.2 Oxytocin in the Basal Forebrain: Reward, Attention and Dopaminergic Signalling 12

1.2.3 Oxytocin in the Amygdala: Anxiolysis and 5-HT Signalling . . 14

1.2.4 Oxytocin in the Hypothalamus: Stress Inhibition and Opioid Signalling 16

1.3 Receptor Pharmacology 18

1.3.1 Oxytocin Receptor Structure 18

1.3.2 Intracellular Signalling Pathways Coupled to the Oxytocin Receptor 20

1.4 The State of Therapeutic Development for the Oxytocin Receptor . . 23

1.4.1 Intranasal Oxytocin 23

1.4.2 Small-Molecule Oxytocin Receptor Agonists: The Benzodiazepine Pharmacophore 25

1.4.3 Peptide Oxytocin Receptor Agonists 26

1.5 Oxytocin Receptor Ligands: New Avenues for Therapeutic Development 29

1.5.1 Small-molecule Oxytocin Receptor Ligands: Improving Selectivity Through Structural Rigidity 29

1.5.2 Peptide Oxytocin Receptor Ligands: Exploration of Bioactive Metabolites 30

1.5.3 Peptide Oxytocin Receptor Ligands: Counteracting Receptor Downregulation with Biased Agonists 31

1.5.4 Summary and Aims 32

2 Materials and Methods **34**

2.1 Chemicals 35
2.2 Cell Culture 35
2.2.1 Cell Line Maintenance 35
2.2.2 Transfections 35
2.3 Cloning 36
2.3.1 Plasmids 36
2.3.2 Isolation of DNA for Cloning Procedures 37
2.3.3 DNA Ligation and Bacterial Transformation 37
2.4 Ligand Affinity and Kinetics Binding Assays 38
2.4.1 Membrane Homogenate Preparation 38
2.4.2 Competition Radioligand Binding: Affinity 38
2.4.3 Competition Radioligand Binding: Kinetics 39
2.4.4 Radioactivity Detection 39
2.5 Ligand Biological Activity: Cellular Signalling Assays: 40
2.5.1 $G\alpha_q$ Signalling: IP_1 Accumulation Assay 40
2.5.2 $G\alpha_s$ Signalling: cyclic AMP Production Assay 42
2.5.3 Real-Time Calcium Flux Assay 44
2.5.4 β-arrestin Recruitment Assay 44
2.5.5 Endosomal Trafficking Assay 47
2.6 Statistical Analyses 48
2.6.1 Ligand Affinity and Binding Kinetics Data 48
2.6.2 Ligand Functional Activity Data 48
2.6.3 Ligand Signalling Bias Analysis 48

3 Small Molecule Ligands: Derivatives of WAY-267,464 **50**

3.1 Introduction and Rationale 51
3.2 Ligand Affinity at the Oxytocin and Vasopressin 1A Receptors 56
3.2.1 Phenylpiperazine WAY-267,464 Derivatives 56
3.2.2 Truncated WAY-267,464 Derivatives 57
3.3 Ligand Functional Activity: $G\alpha_q$ Signalling 57
3.4 Discussion 62
3.4.1 Summary of Findings 62
3.4.2 Structure-Affinity Relationships: Phenylpiperazine Derivatives 63
3.4.3 Structure-Affinity Relationships: Truncated Derivatives 65
3.4.4 Phenylpiperazine and Truncated Derivatives: Functional Activity 66
3.4.5 Conclusions and Future Directions 68

4 Bioactive Metabolites of Oxytocin **69**
4.1 Introduction and Rationale 70
4.2 Pharmacological Evaluation of Oxytocin Metabolites 72
4.2.1 Ligand Affinity at the Oxytocin and Vasopressin 1A Receptors 72
4.2.2 Ligand Functional Activity: $G\alpha_q$ Signalling 72
4.3 Discussion 77
4.3.1 Summary of Findings 77
4.3.2 Cyclic and Linear Metabolites: Receptor Affinity 77
4.3.3 Cyclic Metabolites: Functional Activity 79
4.3.4 Metabolite Bioactivity in the Physiological Context 80
4.3.5 Conclusions and Future Directions 82

5 Structural Modification of Bioactive Oxytocin Metabolites **84**
5.1 Introduction and Rationale 85
5.2 Pharmacological Evaluation of Modified Oxytocin Metabolites 89
5.2.1 Ligand Affinity at the Oxytocin Receptor 89
5.2.2 Ligand Functional Activity: $G\alpha_q$ Signalling 89
5.2.3 Ligand Functional Activity: Intracellular Calcium Flux 90
5.3 Lead Development of C-Amidated Cyclic Peptides 96
5.3.1 Ligand Effects on β-arrestin Recruitment to the Oxytocin Receptor 99
5.3.2 Quantitative Analysis of Ligand Signalling Bias 100
5.3.3 Ligand Effects on Endosomal Trafficking of β-arrestin 100
5.3.4 Ligand Effects on $G\alpha_s$ Signalling 103
5.3.5 Kinetics of Ligand Binding at the Oxytocin Receptor 105
5.4 Discussion 107
5.4.1 Summary of Findings 107
5.4.2 Assessing the Impact of Structural Modifications on Metabolite Biological Activity 108
5.4.3 C-Amidated Cyclic Peptides: Signalling Bias 111
5.4.4 C-Amidated Cyclic Peptides: Receptor Binding Kinetics . . . 115
5.4.5 Conclusions and Future Directions 118

6 Summary and Conclusions **121**
6.0.1 Small Molecule Ligands 121
6.0.2 Peptide Ligands 123
6.0.3 Concluding Remarks 128

Appendices

A Instrument Settings

B Assay Optimisation Data

List of Figures

1.1 Amino acid sequence and structure of oxytocin and arginine-vasopressin. 4
1.2 Overview of the oxytocin signalling network in the central nervous system. 10
1.3 Overview of oxytocinergic interactions with dopamine neurotransmission in the mesolimbic reward pathway 13
1.4 Overview of oxytocinergic interactions with 5-HT neurotransmission in the limbic system. 15
1.5 Overview of oxytocinergic interactions with the μ-opioid system and the hypothalamic-pituitary-adrenal axis. 17
1.6 An overview of major signalling pathways and functional outcomes associated with the oxytocin receptor in neurons. 21
1.7 Molecular structures of small-molecule oxytocin receptor agonists WAY-267,464, TC OT 39, and LIT-001, derived from a functionalised benzodiazepine scaffold. 26
1.8 Structural modifications That influence stability, potency, and selectivity in oxytocin analogues. 27
1.9 Peptide analogues of oxytocin and structural determinants of ligand signalling bias. 28

2.1 Vectors used to generate fusion constructs for β-arrestin recruitment assays. 36
2.2 Ligand-induced $G\alpha_q$ signalling through the OTR leads to release of intracellular Ca^{2+} stores and production of IP_1. 41
2.3 Ligand-induced recruitment of labelled β-arrestin2 to the OTR leads to bioluminescence resonance energy transfer from nanoluciferase to the HaloTag^{618} fluorophore. 45

3.1 Conserved structural features between first-generation non-peptide OTR agonists and our efforts to systematically characterise their pharmacological importance. 54
3.2 Structural modifications in a library of WAY-267,464 derivatives. . . . 55
3.3 Binding affinity of WAY-267,464 1,3-dimethoxybenzene derivatives at the human vasopressin 1A receptor 59
3.4 Binding affinity of truncated benzazepine WAY-267,464 derivatives at the human vasopressin 1A receptor 60

4.1 Binding affinity of cyclic, N-terminal fragments of oxytocin at the human oxytocin receptor and vasopressin 1A receptor 74
4.2 Functional activity of cyclic, N-terminal fragments of oxytocin at the human oxytocin and vasopressin 1A receptor 75

5.1 Binding affinity curves for modified, cyclic derivatives of oxytocin at the human oxytocin receptor. 92
5.2 Functional activity of modified, cyclic derivatives of oxytocin at the $G\alpha_q$ signalling pathway 93
5.3 Functional effects of modified, cyclic derivatives of oxytocin on intracellular Ca^{2+} flux at the human oxytocin receptor (OTR) 94
5.4 Functional effects of oxytocin, carbetocin and C-amidated, cyclic derivatives of oxytocin (**11c**, **12c**) on β-arrestin recruitment and intracellular trafficking of the human oxytocin receptor 102
5.5 Functional effects of oxytocin, atosiban and C-amidated derivatives of oxytocin **11c** and **12c** at the $G\alpha_s$ signalling pathway. 104
5.6 Binding kinetics of radiolabelled oxytocin ([^{3}H]-OT) at the human oxytocin receptor. 106
5.7 Intramolecular hydrogen bonds (IMHBs) which stabilise the secondary structure of oxytocin. 109
5.8 Structural modifications of **12c** to improve metabolic stability, passive permeability and oxytocin receptor affinity. 120

B.1 Homogenous time-resolved fluorescence (HTRF) cAMP production assay optimisation (part 1) . . . . . .
B.2 Homogenous time-resolved fluorescence (HTRF) cAMP production assay optimisation (part 2) . . . . . .
B.3 Bioluminescence resonance energy transfer (BRET) β-arrestin recruitment assay - optimisation of luminescence donor and acceptor fluorophore concentration. . . . . .

List of Tables

2.1 Restriction enzymes used in cloning procedures. 38
2.2 Transfection conditions for bioluminescence resonance energy transfer (BRET) assays. 46

3.1 Affinity and functional data of a WAY-267,464 derivative library at the human oxytocin and vasopressin 1A receptor. 61
3.1 Affinity and functional data of a WAY-267,464 derivative library at the human oxytocin and vasopressin 1A receptor. 62

4.1 Sequence information for compound library **9** - peptide fragments derived from the known metabolism of oxytocin. 71
4.2 Affinity and functional data of an oxytocin metabolite library at the human oxytocin and vasopressin 1A receptors. 76

5.1 Putative stability-enhancing structural modifications incorporated into full-length oxytocin and cyclic, N-terminal fragments of the peptide sequence. 87
5.2 Affinity and functional activity of modified, cyclic derivatives of oxytocin (**10** - **12**) at the human oxytocin receptor. 95
5.3 Physiochemical properties of oxytocin and C-amidated derivatives calculated *in silico* 96
5.4 Effects of modified, cyclic derivatives of oxytocin on ligand-induced β-arrestin recruitment to the human oxytocin receptor. 99
5.5 Binding kinetics of [^{3}H]-oxytocin, carbetocin and C-amidated, cyclic derivatives of oxytocin at the human oxytocin receptor. 106

A.1 Instrument settings for microplate readers and radioactivity detectors.

Chapter 1

Introduction

1.1 Neuropeptide Regulation of Social Behaviour

1.1.1 Mammalian Social Behaviour

Social behaviour is an evolutionary strategy that promotes the survival of a species [1]. Successful interaction between individual members within a group is the cornerstone of cooperativity, reproduction, and avoidance of conflict and predation [2]. As no living organism exists in isolation, but rather within a vast and contiguous network of other lifeforms, all organisms must engage in social behaviour to a greater or lesser extent.

Cooperative prosocial behaviours such as resource sharing and parental care provide a collective benefit to a species and are the dominant form of social behaviour in stable groups [3]. In contrast, negative social behaviours such as aggression may promote individual or in-group survival, but can be detrimental to the species as a whole [4]. Prosocial behaviours are thus advantageous from an evolutionary perspective and are highly conserved through natural selection across all taxa of life, from prokaryotes to placental mammals [5]. Species that express strong prosocial behaviours, including primates, rodents, cetaceans, and insects of the Hymenoptera order (ants, bees and wasps) often exist in highly organised, mutually beneficial group structures that provide greater resilience to environmental stressors and advantages in resource acquisition [6].

Humans rank amongst the most social animals, and the breadth and complexity of our social structures are a testament to our essentially cooperative nature. Sociality is a core element of the human experience, and the emotional drivers of prosocial behaviour - altruism, empathy, and love - often form the basis of our most rewarding interactions. Socioemotional skills are a key predictor of success in adulthood, while impaired social behaviour is a hallmark feature of some of the most debilitating psychiatric disorders, including autism spectrum disorder (ASD), major depression, post-traumatic stress disorder (PTSD), schizophrenia and social anxiety disorder (SAD) [7, 8]. The presence of a strong social support network is now known to be a key factor in the maintenance of long-term human physical and psychological health, whilst the lack of a support network is associated with increases in overall morbidity and mortality [9]. Taken together, these findings highlight the vital importance of positive social behaviour in our lives, and the impact that dysregulated social behaviour can have on both wellbeing and longevity. Moreover, the

possibility of enhancing prosocial behaviour through pharmacotherapy represents an attractive potential strategy to improve health outcomes for vulnerable populations such as those living with chronic psychiatric disorders or without strong social support networks [9].

1.1.2 Oxytocin and Vasopressin: Social Neuropeptides

Sociobehavioural characteristics emerge from biology, and to realise the goal of developing therapeutics that can enhance prosocial behaviour, the neurobiological pathways that underpin this behaviour must first be understood from a mechanistic perspective. However, deciphering the nuance and complexity inherent in human interactions has so far proven a daunting task for the research community. Although much is still unknown about the human social psyche, recent advances in animal behavioural research alongside pioneering studies in humans have now vastly expanded our understanding of how these behaviours are regulated. From these studies, hypothalamic neuropeptides have emerged as key regulators of social behaviour in mammals, reptiles and birds [10]. Although manifestations of social behaviour in these animals differ markedly, the molecules that drive it are highly conserved, indicating a common origin and an evolution in function over time [10].

Among the most widely studied of these neuropeptides are the hypothalamic hormones oxytocin (OT) and arginine-vasopressin (AVP), and a compelling body of evidence now suggests that alongside their physiological endocrine functions, which include facilitation of reproduction (OT) and maintenance of fluid homeostasis (AVP), these neuropeptides also play pivotal roles in the regulation of social behaviour by acting within the central nervous system (CNS) [11]. OT signalling in the CNS has been implicated in pair-bonding, sexual behaviour and maternal care in animal behavioural studies [12–14], and trust, emotional perceptivity, and empathy in human cohorts [15–17]. In contrast, AVP signalling in the CNS is associated with increased avoidance behaviour, arousal and anxiogenic effects in animals [18, 19], and ruthlessness, decreased emotional perceptivity and aggression in humans [20–23]. Overall, OT signalling appears to exert anxiolytic and rewarding effects which reinforce affiliative behaviour, whereas AVP signalling drives behaviour that arises from increased arousal, anxiety and vigilance [24]. In many species the influence of these neuropeptides is sexually dimorphic, with OT signalling generally playing a more dominant role in female social behaviour, and AVP playing a greater role in male social behaviour [25]. Nonetheless, converging lines of evidence indicate that activation of the OT signalling network facilitates prosocial behaviour in both sexes

by acting on the neural substrates of reward, attention and fear [26, 27].

OT is a polypeptide comprised of nine amino acids, differing from AVP by only two substitutions at position 3 and 8 of the amino acid sequence (see Figure 1.1). Both neuropeptides contain a cyclic motif formed by a disulfide bridge between residues 1-6, a linear tripeptide tail, and an amidated C-terminal. Orthologues of these neuropeptides are present in all vertebrates, including placental mammals (OT/AVP), bony fish (isotocin/vasotocin), amphibians, reptiles and birds (mesotocin/vasotocin), as well as some insects (inotocin) [28, 29].

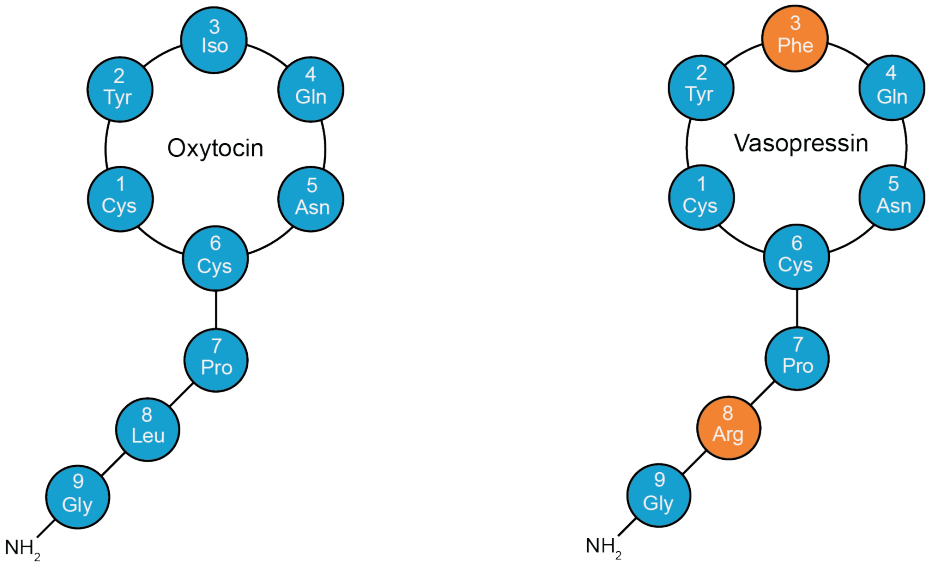

Figure 1.1: Amino acid sequence and structure of oxytocin and arginine-vasopressin.

The OT/AVP family is thought to have evolved via a gain-of-function gene duplication from the ancestral vasotocin peptide of jawed vertebrates at least 600 million years ago [30]. The highly conserved nature of these neuropeptides across species implies a fundamentally important role in the maintenance of life. Broadly speaking, the contrasting effects of OT and AVP on physiology and behaviour can be understood through a homeostasis model, whereby OT regulates processes that facilitate survival of the species, whilst AVP regulates behaviours that promote the survival of the individual.

1.1.3 The Effects of Oxytocin and Vasopressin in Animal Behavioural Studies

Our current understanding of OT and AVP neurobiology has emerged from an extensive body of animal research investigating the influence of hypothalamic peptides on behaviour since the 1970s. The earliest studies in this field focused on characterising the behavioural effects of intracranially administered OT or AVP in rodents, identifying a role for these peptides in regulating reproduction, locomotion, satiety, maternal behaviour, aggression and avoidance [31, 32]. The development of autoradiography tracers [^{125}I]-ornithine vasotocin (^{125}I-OVTA) and [^{125}I]-linear vasopressin (^{125}I-LVA) during the 1980s facilitated the identification of the endogenous rodent OT/AVP receptor family and their distribution within the brain, mapping them to functional networks involved in social behaviour centred on the limbic system [33–35]. The OT/AVP receptor family, comprised of the oxytocin receptor (OTR) and three closely related AVP receptor subtypes ($V_{1A}R$, $V_{1B}R$, V_2R), was found to be shared between rodents and humans. Due to structural similarities between the OT/AVP receptor family and their endogenous ligands, OT and AVP bind to all receptors of the family with varying degrees of affinity, an effect which is more pronounced in the human OT/AVP receptors [36].

At this time, pioneering research into the neurobiological processes that underlie pair-bonding and monogamy in the prairie vole (*Microtus ochrogaster*) elucidated a regulatory role for OT and AVP in the expression of these social behaviours. The process of pair-bonding was found to depend on interactions between OT, AVP and dopaminergic signalling networks in the limbic system, providing robust evidence of a neurobiological mechanism through which neuropeptides exert their behavioural effects [37]. This keystone finding led to the establishment of the prairie vole as a model organism for studying how the expression of OT, AVP and their cognate receptors influences social behavioural phenotypes, and mapping changes in peptide release and receptor expression related to age, sex and reproductive phases [38, 39].

With the delineation of the receptor family for OT and AVP and the advent of advanced genetic engineering techniques during the 1990s, manipulation of gene sequences in living organisms became feasible. Subsequently, a plethora of studies targeting the OT system in rodents demonstrated pervasive social deficits in *OXTR*$^{-/-}$ and *OXT*$^{-/-}$ knockout animals, including impaired maternal nurturing, increased aversive behaviour, increased aggression and autistic-like phenotypes [40]. In comparison, *AVPR1A*$^{-/-}$ and *AVPR1B*$^{-/-}$ knockout lines were found to exhibit reduced aggression, although the phenotypic changes were modest in comparison to

OXTR$^{-/-}$ knockout models, positioning the OTR as a more viable target for therapeutic interventions to improve social behavioural symptoms [41, 42].

As a consequence of the prosocial behavioural outcomes associated with OTR signalling in murine models, recent efforts have focused on elucidating OT-mediated behaviours in non-human primates. OT signalling influences attraction and monogamy in marmosets [43], food sharing in chimpanzees [44], as well as social stress and status in rhesus macaques [45, 46]. Although the peptide sequence of OT is highly conserved in primates, variations have been observed in New World monkey species of the Cebidae family, which display a high incidence of social monogamy and communal infant rearing [47]. These OT analogues induce parental care behaviour when administered to male rats, suggesting they may have evolved to facilitate greater induction of the OT signalling pathways that control social behaviour in males [48]. Taken together, these findings in primates highlight the synonymous role of OT and analogous peptides in mammalian social behaviour across species and represent a critical milestone in translating the findings of animal behavioural research to the pathophysiology of human neuropsychiatric disorders.

1.1.4 The Effects of Oxytocin and Vasopressin in Healthy Human Cohorts

In humans, research on the behavioural effects of OT has been hindered by a lack of selective, CNS-penetrant ligands for the OTR that can be used to examine OT signalling in the human brain. OT itself is metabolically unstable and does not cross the blood-brain barrier in physiologically relevant concentrations, precluding the use of peripheral drug delivery routes in clinical studies of OT administration in humans [49]. Intranasal administration of aerosolised OT has been widely adopted as a strategy in investigative trials to overcome this constraint. Although the efficacy of this approach has been questioned [49], preliminary evidence indicates that exogenous OT reinforces prosocial behaviour in humans, just as is in other species.

In healthy subjects, a single-dose of intranasal OT (40 IU) increased the willingness to accept social risks (the possibility of betrayal) in a trust-based financial game [15]. Visual information is a key component of human social interactions, and in a visual stimulus task with healthy subjects, 40 IU intranasal OT increases the emotional empathic response to images which depict negative scenarios, but only for those images with a social context [16]. A meta-analysis of studies utilising facial emotion recognition tasks also demonstrated that OT enhances emotional perceptivity or

the ability to accurately infer emotional states from images of human faces [17]. These behavioural findings are further supported by functional magnetic resonance imaging (fMRI) studies in healthy subjects, which have found that intranasally-administered OT increases functional connectivity between brain regions associated with assigning salience to visual stimuli, as well as decreased reactivity in regions associated with anxiety, providing a correlation between neurobiological processes and prosocial behavioural outcomes [50, 51].

Although there has been less of a focus on examining the role of AVP in human social behavioural research, the reported effects of AVP support earlier findings in animal models, namely that AVP signalling is associated with vigilance, aggression and decreased emotional perception, particularly in males. The concentration of endogenous AVP in the cerebrospinal fluid (CSF) is positively correlated with the aggressive life histories in individuals with personality-disorder [23]. Single dose, intranasally-administered AVP stimulates agonistic facial motor patterns and decreases friendliness ratings to same-sex facial expressions in men [20, 52], and has been shown to decrease the accuracy in inferring emotions from eyes of others in a visual recognition task [22].

1.1.5 Dysregulation of Oxytocin Signalling in Neuropsychiatric Conditions

Based on preliminary findings in animal behavioural models and healthy human cohorts, dysregulation of the OT system has been suggested as a putative pathophysiology contributing to social behavioural deficits in neuropsychiatric disorders. On a fundamental level, dysregulation of the OT system means alterations in OT release or OTR expression patterns in the CNS, which are subject to strict spatiotemporal control but highly variable between individuals [53, 54]. The expression of social behaviour represents a convergence of predisposing genetic factors and environmental influences through social conditioning. Together, these factors influence the patterns of OT synthesis and OTR expression in the CNS. Single nucleotide polymorphisms (SNPs) in the *OXTR* gene have been associated with social impairments in the general population, and ASD symptom severity in different ethnic populations [55–59]. The majority of *OXTR* SNPs correlated with behavioural deficits in human populations are intronic, and thus influence *OXTR* gene splicing, transcription factor binding and mRNA degradation, factors which alter the expression patterns of the OTR, rather than the signalling or ligand binding properties of the translated receptor. This suggests that heritable *OXTR* SNP mutations may contribute to

individual differences in human social functioning, including the severe social impairments which characterise ASD. OT synthesis and OTR expression variability are also subject to epigenetic mechanisms, such as DNA methylation, which act as a secondary layer of genetic regulation, influencing gene expression levels without changing underlying DNA sequences [60]. Epigenetic states of genes are sensitive to a variety of external factors, particularly during development, and are thus viewed as a key biological mechanism linking environmental influences with behaviour [60].

There is evidence to suggest that epigenetic regulation of the OT system is disrupted in neuropsychiatric disorders. On a transcriptional level, *OXTR* promoter hypermethylation is inversely correlated with *OXTR* mRNA levels in human and murine myometrium cells, as well as murine hypothalamic, olfactory bulb, centromedial amygdala and cortical tissues [61, 62]. High levels of *OXT* methylation in human salivary samples (presumed to indicate lower levels of OT peptide production) have been linked to insecure attachment styles and reduced ability to recognize emotional facial expressions [63]. Changes in *OXTR* methylation patterns from human plasma and salivary samples have also been associated with a range of social-cognitive deficits, including callous-unemotional traits in youth [64], anxiety and severity of social symptoms in ASD [65], postnatal depression in women [66], anhedonia in schizophrenia [67] and interestingly, prenatal and early life stress – risk factors for the development of mental illness and addiction in adulthood [68]. It should be stressed that it is not yet clear whether *OXTR* methylation patterns from peripheral tissue samples are an accurate predictor of methylation patterns in the CNS. Nonetheless, fMRI studies have recently correlated altered *OXTR* methylation patterns in blood samples to changes in functional coupling between limbic-cortical networks, as well as the reactivity of regions associated with visual stimulus processing during social-cognitive tasks – providing preliminary evidence that peripheral *OXTR* methylation patterns correlate with altered social cognition in brain regions that express the OTR [63, 69].

Over forty years of pioneering behavioural research has confirmed the regulatory role of OT and AVP in rodent and primate social behaviour, and there is accumulating evidence for a synonymous role in humans. Overall, OT signalling appears to facilitate social interaction, highlighting the therapeutic potential of targeting the OTR for drug development. There is also evidence that the epigenetic regulation of the OT system may be disrupted in neuropsychiatric disorders, providing a putative link between dysfunctional OT signalling and pathophysiology. Extending this body of research, the neurobiological aspects of OT signalling are now being elucidated with ever greater detail, consolidating our understanding of how social behaviour is regulated and providing further support for the development of OTR-targeting

therapeutics to treat social impairments in neuropsychiatric disorders.

1.2 Neurobiology of the Oxytocin System

1.2.1 The Oxytocin Signalling Network in the Central Nervous System

OT and AVP are synthesised in the supraoptic nucleus (SON) and paraventricular nucleus (PVN) of the hypothalamus by spatially discrete magnocellular neuron populations. Synthesis of both neuropeptides occurs through enzymatic cleavage of an inactive precursor neurophysin protein, followed by packaging into dense-core vesicles that are transported to axon terminals for depolarisation-coupled release [53]. Hypothalamic neurons innervate the posterior lobe of the pituitary gland as well as numerous structures in the CNS that express the OTR and V1aR (see Figure 1.2) [70–73]. Pituitary OT and AVP are released into peripheral circulation to exert their endocrine effects [74], whereas centrally released neuropeptides modulate signalling networks in the limbic system that are associated with fear, reward and attention [53]. The distribution of OT signalling networks in the CNS reflect the primary mode of social communication used by that particular species [75]. Accordingly, OT-containing neurons and OTR expression in rodents is concentrated heavily in regions associated with auditory and olfactory processing, whereas in primates the receptor density and innervation from the hypothalamus is highest in brain regions involved in visual processing and attention [75].

In rodents, social interactions are driven by chemical communication through scent-marking and sniffing. Social recognition of offspring, kin, potential mates and unknown individuals is based on olfactory processing of major urinary proteins [84]. With this context in mind, receptor autoradiography studies have revealed that in the rodent CNS, OTR expression is localised to the olfactory bulb and accessory olfactory nucleus, as well as downstream limbic regions that receive projections from this primary sensory area, including the amygdala, which is associated with fear-processing and emotion regulation, and the bed nucleus of the stria terminalis, an integrative centre for limbic information [75, 85].

Outside of the olfactory pathway, OTR expression has been detected in other limbic structures including the hypothalamus, where OT is synthesised, as well as the ventral tegmental area (VTA) and nucleus accumbens (NAcc). OTR-expressing

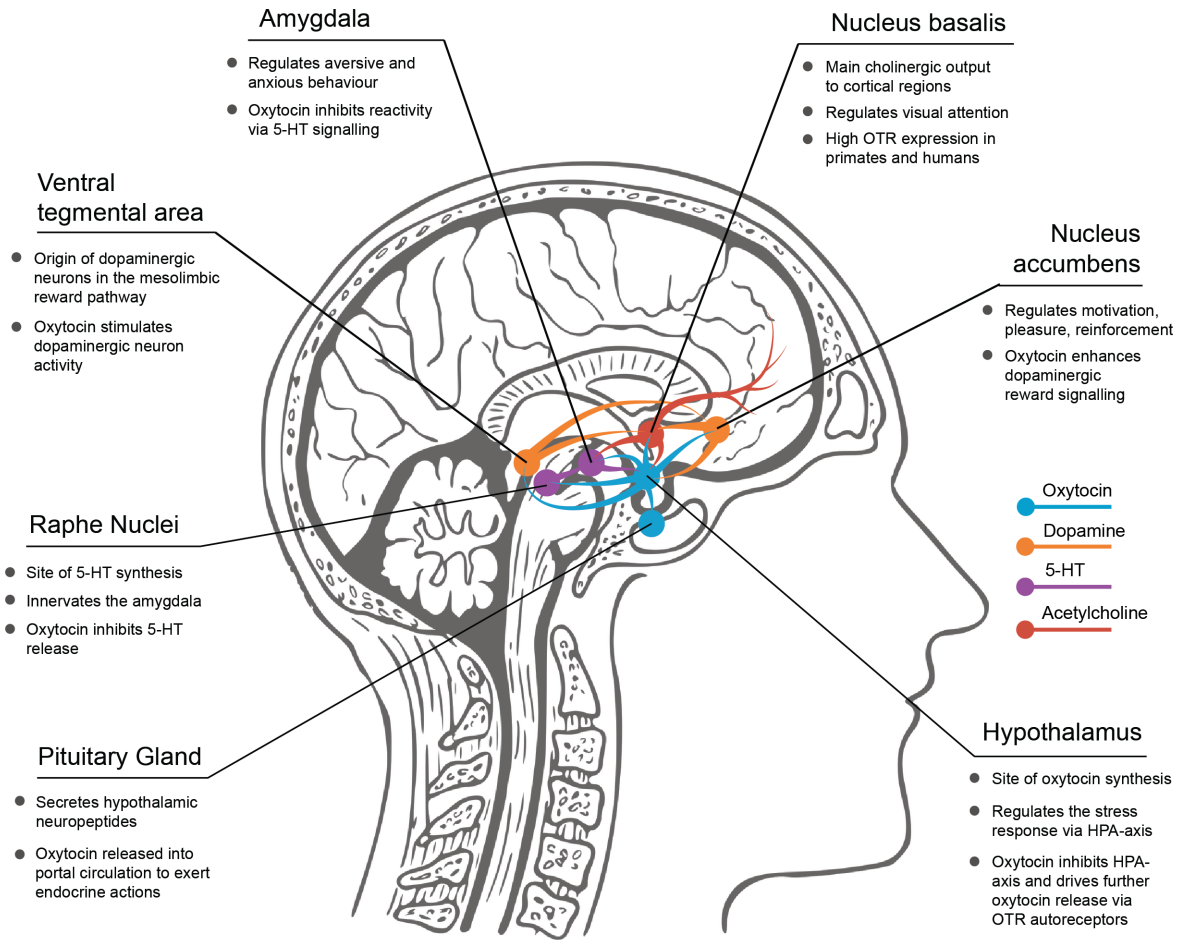

Figure 1.2: Overview of the oxytocin signalling network in the central nervous system. Abbreviations: *OTR*; oxytocin receptor, *HPA-axis*; hypothalamic-pituitary-adrenal axis. Based on [53, 70–83].

dopaminergic neurons projecting from the VTA to the NAcc comprise the mesolimbic reward pathway, which regulates motivation, reinforcement and reward-related motor function learning [72, 76]. In rodents, high levels of *OXTR* mRNA have been detected in limbic structures such as the hypothalamus, amygdala and VTA alongside the olfactory pathway, suggesting a correlation between receptor mRNA and the spatial distribution of the OTR identified through autoradiography studies [86]. Furthermore, increasing or decreasing *OXTR* mRNA concentrations in the NAcc modulates partner preference formation in the monogamous prairie vole, indicating a correspondence between *OXTR* mRNA distribution patterns and social behaviour [87, 88].

In humans and non-human primates, mapping the OT signalling network has been

historically complicated by the non-selectivity of available autoradiography ligands and immunohistochemical antibodies, arising from a high sequence similarity between the primate OTR and $V_{1A}R$ [89]. This hurdle has been recently overcome through the development of high-affinity radiotracers for the OTR and improved autoradiography protocols, facilitating the identification of OTR populations in the primate brain [77]. With these techniques, high OTR expression has been detected in a conserved network of limbic structures including the hypothalamus and amygdala, as well as regions that regulate attention and processing of visual stimuli in primates, such as the nucleus basalis in the basal forebrain, and the superior colliculus in the midbrain [77–79].

Gene expression maps of *OXTR* mRNA in the human brain have recently been constructed using the Allen Human Brain Atlas [80, 90]. Under this approach, *OXTR* mRNA expression patterns mirror the distribution of OTR-binding sites identified in non-human primate autoradiography studies, with high expression in the limbic system and basal forebrain [80]. Within these brain regions, interactions between OTR signalling and other neurotransmission systems provide a complex network through which OT is able to influence discrete neurobiological processes. There is robust evidence for a physiological relationship between OT and dopaminergic [81], cholinergic [80], 5-HT [82] and opioid [83] neurotransmission systems. Disruptions in these neurotransmission networks have been identified in ASD, schizophrenia, SAD and major depression [91–97], indicating that OTR-targeting therapeutics may be able to normalise pathophysiological states in multiple signalling networks.

Multiple lines of evidence support the existence of a highly conserved OT signalling network in the mammalian brain, with OTR expression heavily concentrated in sensory processing pathways and limbic structures that regulate attention, reward and fear. These findings provide a neurobiological context for the behavioural effects elicited by OT in animal studies and highlight the domains of behaviour where OTR targeting therapeutics may be effective in ameliorating symptoms. In addition, information on the distribution of the OTR has elucidated the regions where OT signalling interacts with other neurotransmission systems that regulate social behaviour, deepening our understanding of how pathophysiological states may arise.

1.2.2 Oxytocin in the Basal Forebrain: Reward, Attention and Dopaminergic Signalling

Alterations in dopaminergic reward signalling are thought to contribute to the social deficits and stereotyped behaviours in ASD, social-cognitive deficits and anhedonia in schizophrenia, as well as the development and reinforcement of addiction, a frequent comorbidity of neuropsychiatric disorders [81, 91–93]. Converging evidence indicates that the OT and dopaminergic systems interact synergistically within the mesolimbic reward pathway to motivate social interaction (see Figure 1.3). Hypothalamic OT neurons innervate the VTA and NAcc, key components of the reward system, where OT influences dopamine release from OTR-expressing neurons directly [98].

The OTR and dopamine 2 receptor (D_2R) are co-expressed within the NAcc, and concerted activation of NAcc OT and dopaminergic signalling is required to elicit maternal behaviour and pair-bonding in animal models [31, 99]. Recent findings suggest that the OTR and D_2R may form heteromers that enhance dopaminergic neurotransmission in the NAcc, indicating an additional mechanism for facilitative interactions between these systems [100]. NAcc dopaminergic fibres project to the SON of the hypothalamus and stimulate OT release directly through activation of the D_2R expressed on OT-containing neurons, providing evidence for a bi-directional positive feedback relationship between OT and dopaminergic systems [14, 101, 102]. Decreased mesolimbic OTR and D_2R expression has been identified in ASD and schizophrenic cohorts [103, 104], highlighting the possibility that social-reward signalling is disrupted in these conditions.

The NAcc may also act as a central hub for OT interactions with other neurotransmission systems. In animal models, reinforcement of social learning requires coordinated OT and 5-HT signalling in the NAcc core [70]. OT release in the NAcc also drives endocannabinoid signalling via cannabinoid receptor type 1 (CB_1) receptors, which is linked to anxiolysis and inhibition of the stress response [105]. Dopaminergic neurons of the NAcc innervate the nucleus basalis, a basal forebrain structure involved in visual attention and the main cholinergic output to cortical regions associated with cognition [106]. The OTR is highly expressed in the nucleus basalis of humans and non-human primates [77–79], and may influence social cognition and the salience of visual stimuli by modulating cholinergic neurotransmission in the nucleus basalis [83]. Altered cholinergic signalling is associated with cognitive deficits in schizophrenia, and relieves social deficits and cognitive rigidity in mouse models of ASD [94, 95, 107], Furthermore, OTR expression in the nucleus basalis

is low in post-mortem brain tissue from ASD subjects [103], indicating a neurobiological link between the OT system, cholinergic neurotransmission and behavioural deficits related to cognition and visual attention.

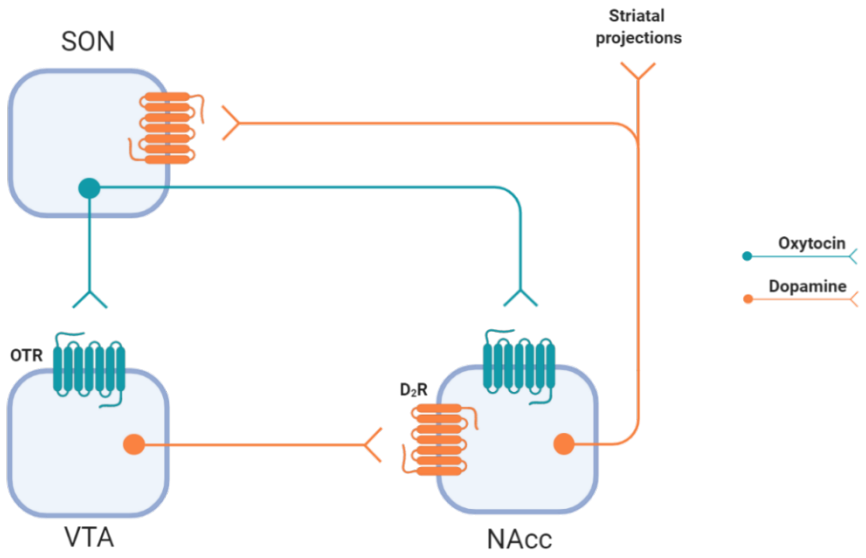

Figure 1.3: Overview of oxytocinergic interactions with dopamine neurotransmission in the mesolimbic reward pathway. Abbreviations: D_2R, dopamine 2 receptor; *NAcc*, nucleus accumbens; *OTR*, oxytocin receptor; *SON*, supraoptic nuclei of the hypothalamus; *VTA*, ventral tegmental area. Based on [31, 98, 99, 101, 102, 108].

Taken together, these findings indicate that OT influences motivation and reward signalling through facilitative interactions with dopamine, 5-HT and endocannabinoids in the mesolimbic pathway. There is also evidence that OT regulates visual attention in primates through an interaction with cholinergic neurotransmission in the basal forebrain. Reduced OTR expression has been observed in these regions in ASD and schizophrenic cohorts, highlighting a possible deficit in OT-mediated reward signalling and cholinergic neurotransmission that may contribute to the behavioural symptoms of schizophrenia and ASD such as reduced motivation, social-cognitive deficits, impaired eye gaze and facial emotion recognition. The development of OTR-targeting therapeutics thus represents an untapped pathway to treat the intractable core symptoms of ASD and schizophrenia, by enhancing social reward and attention to visual social cues.

1.2.3 Oxytocin in the Amygdala: Anxiolysis and 5-HT Signalling

Considerable neurobiological overlap also exists between the OT and 5-HT signalling networks, suggesting an interface between these two systems in the regulation of social behaviour. 5-HT neurotransmission regulates the expression of harm-avoidance behaviours, and has been consistently linked to the pathophysiology of mood and anxiety disorders [96]. Comparatively, OT produces anxiolysis and inhibits reactivity in the amygdala - the integrative centre for fear conditioning and a major hub of 5-HT neurotransmission in the limbic system [109]. There is robust evidence for a bidirectional relationship between OT and 5-HT signalling systems (see Figure 1.4). 5-HT neurons originating in the dorsal raphe nucleus (DRN) - the main site of 5-HT synthesis in the brain – project to the SON of the hypothalamus and regulate the release of OT from magnocellular neurons, which express a number of 5-HT receptor subtypes [110, 111]. Similarly, OT neurons originating in the hypothalamus innervate the DRN and influence 5-HT release patterns from neurons expressing the OTR [27, 82]. Hypothalamic and DRN neuronal projections also localise in the amygdala, suggesting that bi-directional influences between OT and 5-HT signalling systems may contribute to the expression of fear-associated behaviours [71, 112].

Activation of inhibitory 5-HT signalling is a putative mechanism through which OT may exert its anxiolytic effects. Based on the high density of 5-HT_{1A} and 5-HT_{1B} receptors in the limbic system, these subtypes are considered to be two of the major inhibitory 5-HT receptors involved in regulating emotion and aversive behaviour in the human brain [113, 114]. Within the DRN, serotonergic neurons express somatodendritic 5-HT_{1A} autoreceptors that suppress 5-HT synthesis, 5-HT turnover and 5-HT release in projection areas [27, 115, 116]. By contrast, 5-HT_{1A} and 5-HT_{1B} heteroreceptors are expressed post-synaptically in the hypothalamus, where they modulate neuropeptide release in response to 5-HT [111, 117, 118] and in the amygdala, where they exert a hyperpolarising effect on GABAergic interneurons following activation [116]. Thus, OT release in the DRN may lead to greater activation of 5-HT_{1A} and 5-HT_{1B} autoreceptor populations, enhancing the inhibitory tone of 5-HT signalling in the amygdala and hypothalamus.

Diminished 5-HT_{1A} and 5-HT_{1B} autoreceptor expression in the DRN has been reported in post-mortem studies of SAD and major depression, and is a predictor of amygdala reactivity [116, 119–121]. In fMRI studies, amygdala reactivity increases in response to fearful or negative stimuli in mood and anxiety disorders [122], suggesting a functional link between reduced 5-HT inhibitory tone in the DRN and

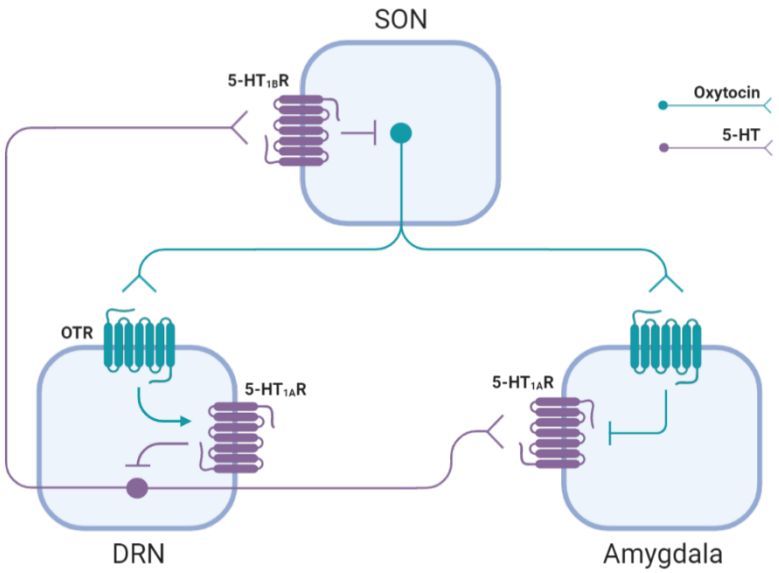

Figure 1.4: Overview of oxytocinergic interactions with 5-HT neurotransmission in the limbic system. Abbreviations: *DRN*, dorsal raphe nucleus; *OTR*, oxytocin receptor; *SON*, supraoptic nuclei of the hypothalamus; *5-HT$_{1A}$R*, serotonin type 1A receptor; *5-HT$_{1B}$R*, serotonin type 1B receptor. Based on [27, 82, 110, 111, 115–118].

atypical emotion processing. OT has been reported to increase the non-displaceable binding potential of a 5-HT$_{1A}$ receptor antagonist, [^{18}F]MPPF in the DRN, indicating 5-HT$_{1A}$ autoreceptor expression increases following OT exposure in humans [27]. This supports the hypothesis that OT mediates anxiolytic effects through inhibitory 5-HT signalling, but also highlights the possibility that deficient OT production could reduce 5-HT autoreceptor inhibition in the DRN, leading to anxiogenesis in mood and anxiety disorders. Decreased 5-HT$_{1A}$ and 5-HT$_{1B}$ autoreceptor inhibition in the DRN could also drive 5-HT release into the hypothalamus, subsequently inhibiting OT release via 5-HT$_{1A}$ and 5-HT$_{1B}$ heteroreceptors. In support of this concept, plasma OT levels in major depression, SAD and ASD are reduced when compared with healthy controls, suggesting the presence of inhibitory influences on OT production [123, 124]. Electroconvulsive-shock therapy, a mainstay treatment for major depression, downregulates 5-HT$_{1A}$ and 5-HT$_{1B}$ receptor expression in the hypothalamus and concurrently increases plasma OT levels [117]. In addition, administration of a selective 5-HT$_{1B}$ agonist induces autistic-like social and attention deficits in mice, which are rescued by OT administration [125].

In summary, OT release in the amygdala and DRN exerts an anxiolytic effect that may be mediated through inhibitory 5-HT signalling. The tone of 5-HT inhibition is disrupted in mood and anxiety disorders, which may negatively influence OT production. Supporting this hypothesis, circulating plasma OT concentrations are low in a range of neuropsychiatric disorders associated with 5-HT signalling, indicating

a deficit in OT production or secretion. From a therapeutic perspective, the finding that exogenous OT exposure increases expression of 5-HT_{1A} and 5-HT_{1B} autoreceptors in the DRN positions OTR ligands as a novel drug development pipeline for anxiety disorders, one which ameliorates anxious behaviour by restoring the inhibitory tone of 5-HT signalling networks in the limbic system.

1.2.4 Oxytocin in the Hypothalamus: Stress Inhibition and Opioid Signalling

Alongside focal release in extra-hypothalamic projection areas, OT is also released somatodendritically within the hypothalamus itself. Somatodendritic OT stimulates OTR autoreceptors in the SON, which increases the excitation of OT-containing neurons via Ca^{2+} signalling, priming the system for further OT release in a positive feedback loop [126, 127]. Somatodendritic OT in the SON also diffuses locally within the hypothalamus, acting on neuropeptide-secreting neurons in the adjacent PVN, which form part of the hypothalamic-pituitary-adrenal (HPA) axis involved in the stress response (see Figure 1.5) [128].

Stress typically activates corticotrophin-releasing hormone (CRH) neurons in the PVN, inducing the secretion of CRH, which in turn releases adrenocorticotropic hormone (ACTH) into the bloodstream from corticotropic cells in the anterior pituitary [129]. Circulating ACTH stimulates the synthesis and secretion of cortisol from the adrenal glands, which mediates physiological effects associated with sympathetic nervous system activation. During chronic stress, CRH-synthesising cells in the PVN co-synthesise and co-secrete AVP with CRH into the portal circulation, where it interacts with AVP receptors in the anterior pituitary to facilitate CRH-induced ACTH secretion and potentiate the stress response [130].

Dysregulation of the HPA-axis is a pathophysiological symptom that decreases stress-resilience in many neuropsychiatric conditions. Exposure to mild stressors early in life has been shown to enhance HPA-axis regulation and promote lifelong stress tolerance [136]. In contrast, prolonged or extreme trauma can induce HPA-axis hyperactivity that persists into adulthood, and is a developmental risk factor for psychological disorders during later life [137, 138]. Children with ASD display elevated plasma and serum cortisol concentrations following exposure to stress when compared with healthy controls, indicating stress-induced HPA-axis hyperactivity [139]. In adulthood, chronic elevation of circulating cortisol and HPA-axis activation is associated with persistent depressive symptoms [140], while patients with

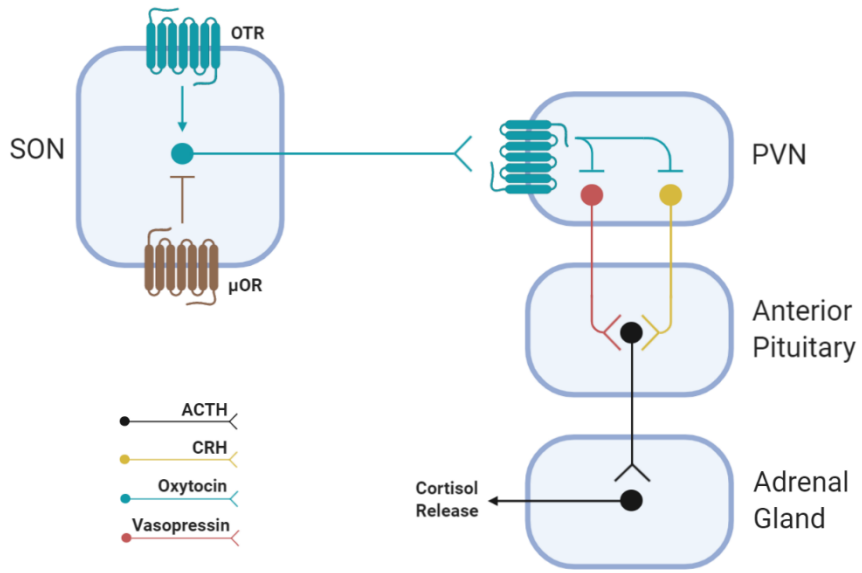

Figure 1.5: Overview of oxytocinergic interactions with the μ-opioid system and the hypothalamic-pituitary-adrenal axis. Oxytocin receptor signalling activates interneurons in the paraventricular nucleas that inhibit the release of pituitary and adrenal stress hormones, a regulatory mechanism inhibited by μ-opioid receptor activation in the hypothalamus. Abbreviations: *ACTH*, adrenocorticotropic hormone; *CRH*, corticotrophin releasing hormone; *OTR*, oxytocin receptor; *PVN*, paraventricular nucleus of the hypothalamus; *SON*, supraoptic nucleus of the hypothalamus; μR, μ-opioid receptor. Based on [126–135]

SAD show greater HPA hyperactivity and cortisol release in response to visually presented social threat cues (angry faces) than healthy controls, associated with a concomitant increase in avoidance behaviour [141].

OT inhibits the basal and stress-induced activity of the HPA-axis [131–133]. This is achieved through inhibitory regulation of AVP- and CRH-releasing neurons in the PVN by magnocellular OT neurons in the SON (see Figure 1.5) [134, 135]. As such, deficits in endogenous OT production or release can reduce the inhibitory tone that OT exerts on the HPA-axis, producing abnormal stress responses. Pathophysiological inhibition of OT production could arise from a range of sources - the hypothalamus receives multiple inputs from limbic brain regions, and intra-hypothalamic OT release is differentially regulated by dopamine, 5-HT, acetylcholine and opioid neurotransmission systems [83, 142].

μ-opioid receptors have been studied in relation to reward, emotion, and behavior in the social domain [143], are strongly expressed in reward-related regions of the primate brain [144] and exert a powerful regulatory influence on OT release [83]. Endogenous opioids directly inhibit OT release from axon terminals in the posterior pituitary, and reduce the functional activity and somatodendritic release of OT

from magnocellular OT neurons in the hypothalamus [145, 146]. Chronic administration of morphine, a μ-opioid receptor agonist, inhibits OT synthesis, reduces OT secretion and delays the onset of labour [145, 147]. Supporting this functional association, endogenous opioid inhibition triggers central OT release [148], while the high-affinity μ-opioid receptor antagonist naloxone drives OT release from the posterior pituitary and SON [146, 149]. Excessive opioid activity in the brain has been proposed as a hypothesis to explain the aetiology of ASD [97], and μ-opioid receptor antagonists have shown promise in ameliorating social symptoms of ASD in clinical trials [150]. In addition, a recent report found that mothers prescribed opioids during early pregnancy were 2.5-fold more likely to have a child born with ASD, or other developmental disabilities with autistic symptoms [151].

In summary, OT released in the hypothalamus binds to OTR autoreceptors, facilitating further OT release. Hypothalamic OT also diffuses locally to other structures in the hypothalamus, including the PVN, where it exerts an inhibitory, anti-stressor effect on the HPA-axis. Excessive HPA-axis activation has been identified in multiple neuropsychiatric disorders and may contribute to maladaptive stress responses that precipitate adverse health outcomes. The μ-opioid system inhibits somatodendritic OT release in the hypothalamus, and there is evidence that OT production may be reduced in some neuropsychiatric conditions as a consequence of excessive opioid signalling, producing HPA-axis hyperactivity. From a therapeutic perspective, exogenous OTR ligands in this context could supplement endogenous OT production, mitigating the effects of excessive μ-opioid receptor inhibition and restoring HPA-axis regulation.

1.3 Receptor Pharmacology

1.3.1 Oxytocin Receptor Structure

The OTR and $V_{1A}R$ are typical members of the class-A (rhodopsin-like) family of G-protein coupled receptors (GPCRs). The high homology between OT and AVP is reflected in their corresponding receptors, which co-evolved alongside the endogenous ligands through duplication of a single ancestral receptor gene during the Cambrian Era, producing receptors with new properties and functionality [152]. As a result of this early evolution, orthologous receptors for OT and AVP are widely conserved and have been identified in all vertebrates studied to date [152]. In humans, the OTR and $V_{1A}R$ share approximately 50% overall sequence homology, and share

80% homology in the extracellular loops and transmembrane domains of the receptor [153]. Common structural features in these regions are critical for ligand recognition and binding, which gives rise to a low ligand-selectivity profile between the OTR and AVP receptor subtypes [154]. The lowest homology between receptors is found in the intracellular loops, which may be the basis for differences in OTR and $V_{1A}R$ coupling to intracellular signalling pathways [154].

Evidence from computational modelling and site-directed mutagenesis studies indicate that OT and AVP bind to their cognate receptors through a multimodal interaction with transmembrane domains (TMs), extracellular loops (ECLs) and the flexible N-terminal domain. The crystal structure of a peptide ligand-bound OTR has recently been solved, confirming the existence of a deep binding cavity formed by α-helices of TM2 - 7, which accommodates peptide ligands, cholesterol and Mg^{2+}, with the latter two acting as positive allosteric modulators of OTR signalling [155]. In the rat $V_{1A}R$, substitution of highly conserved glutamine and lysine residues localised within this binding pocket decreased affinity for OT, AVP and the evolutionarily related peptide vasotocin. Because these residues are highly conserved between receptors, the TM2 - 7 binding pocket is shared by all subtypes of the OT/AVP receptor family, and may contribute to the low ligand selectivity profile of the OTR [156, 157]. Small-molecule ligands are also thought to bind to the OTR via this transmembrane cavity, although direct experimental evidence of this interaction is lacking [154]. In contrast, epitopes in ECL1 have been found to be crucial determinants of peptide ligand selectivity in the human OTR, $V_{1A}R$ and V_2R. When tyrosine^{115} in ECL1 of the $V_{1A}R$ is substituted with an asparagine or phenylalanine residue (the corresponding residues in the OTR and V_2R), the ligand selectivity profile switches accordingly. This modification produces a 19-fold increase in OT affinity at the mutant $V_{1A}R$ relative to the native receptor [158].

Overcoming the low ligand-selectivity of the OTR is an ongoing challenge for both social behavioural research and oxytocinergic drug design. Non-selective binding of autoradiography ligands has hindered the accurate mapping of OTR distribution in functional networks of the brain implicated in social behaviour. Crosstalk between OT and AVP signalling pathways also complicates the interpretation of behavioural studies and limits our understanding of the respective roles OT and AVP play in social behaviour. The AVP receptor subtypes are widely distributed in the body and regulate stress hormone release from the anterior pituitary ($V_{1B}R$), fluid homeostasis in the kidney (V_2R) and vasoconstriction in cardiac tissues ($V_{1A}R$) [159]. Non-selective activation of these receptors could produce wide-ranging and potentially severe side effects that may stall or entirely preclude the development of novel oxytocinergic therapeutics. Thus, engineering receptor selectivity is a critical factor

in the design of ligands that target the OTR.

1.3.2 Intracellular Signalling Pathways Coupled to the Oxytocin Receptor

As a class-A GPCR, the OTR couples with trimeric G-protein complexes, comprised of Gα and Gβγ subunits. Ligand binding initiates separation of the G-protein complex and activation of Gα and Gβγ associated intracellular signalling cascades. Investigations in myometrium and neuronal cell systems have shown that the OTR can exert different sub-cellular effects depending on the tissue-specific expression of G-protein subtypes. In these heterologous expression systems, the OTR can functionally associate with $G\alpha_q$, $G\alpha_s$ and $G\alpha_{i/o}$ proteins (see Figure 1.6), although activation of the $G\alpha_s$ pathway has been detected primarily in myometrial tissues [160, 161], and activation of $G\alpha_{i/o}$ associated pathways requires at least tenfold higher concentrations of OT than $G\alpha_{q/11}$ [162].

$G\alpha_q$ proteins are expressed ubiquitously in all tissues, although $G\alpha_q$ expression in the CNS is particularly abundant throughout the limbic system, overlapping with OTR distribution in regions associated with emotion regulation [163]. Genetic knockout of $G\alpha_q$ and downstream signalling proteins in the rodent limbic system produces anxious phenotypes and deficits in maternal behaviour, domains commonly associated with OT signalling [164, 165]. On a cellular level, OTR-$G\alpha_q$ signalling promotes the release of Ca^{2+} from intracellular stores and influx through Ca^{2+}-selective ion channels [166, 167]. In hypothalamic neurons, OTR-Ca^{2+} signalling recruits cyclic ADP hydrolase (CD38) and transient receptor potential vallinoid type-2 channels (TRPV2), which further amplify Ca^{2+} signalling cascades, promoting somatodendritic and axonal OT secretion [126, 127].

In addition to inducing OT release, Ca^{2+} signalling also promotes the release of other neurotransmitters from neurons expressing the OTR, providing a mechanism through which OT is able to modulate other neurotransmission networks in the limbic system and mesolimbic reward pathway (see Figure 1.6: 1) [168]. OTR-Ca^{2+} signalling in the hypothalamus also activates the mitogen-activated protein kinase (MAPK) pathway, which is necessary for social memory and OT-induced anxiolysis in vivo (see Figure 1.6: 2) [127, 169]. Taken together, these findings indicate that the OTR-$G\alpha_q$ signalling pathway has a fundamental role in facilitating OT release from hypothalamic neurons and mediating the social behavioural outcomes associated with OT.

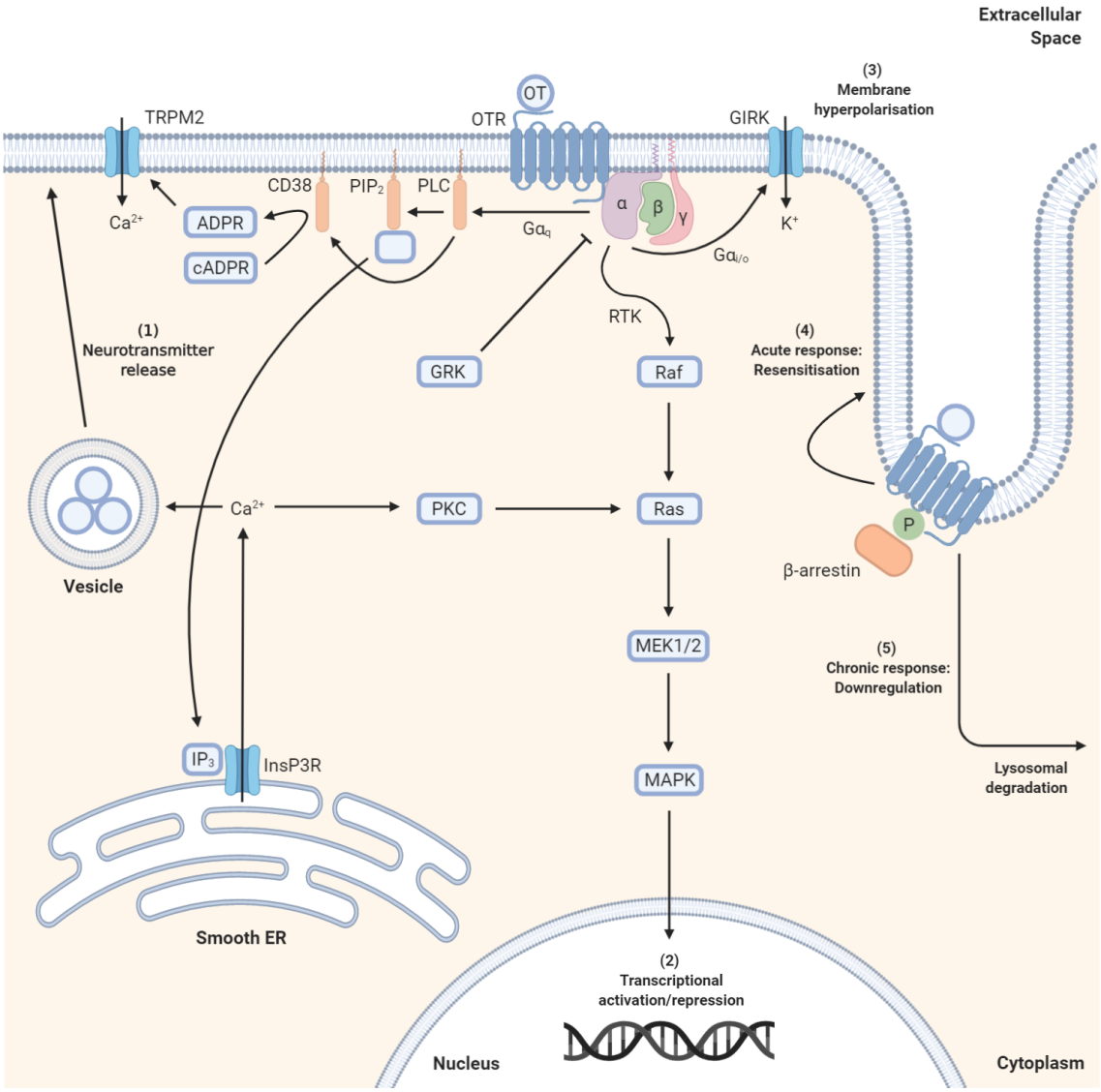

Figure 1.6: An overview of major signalling pathways and functional outcomes associated with the oxytocin receptor in neurons. **(1)** $G\alpha_q$-signalling mobilises Ca^{2+} stores, leading to neurotransmitter release. **(2)** $G\alpha_{i/o}$-signalling activates inwardly rectifying ion channels, producing membrane hyperpolarisation. **(3)** $G\alpha_q$-signalling activates kinase signalling cascades which alter gene transcription. **(4)** Acute exposure to oxytocin leads to rapid internalisation and recycling of the oxytocin receptor. **(5)** Chronic exposure to oxytocin leads to downregulation of the oxytocin receptor. Abbreviations: *ADPR*; ADP-ribose, *DAG*; diacylglycerol, *cADPR*; cyclic ADP-ribose, *CD38*; cyclic ADP ribose hydrolase, *ER*; endoplasmic reticulum, *GIRK*; G-protein-coupled inwardly rectifying potassium channel, *GRK*; G-protein coupled receptor kinase, *InsP3R*; inositol triphosphate receptor, IP_3; inositol triphosphate, *MAPK*; mitogen-activated protein kinase, *MEK1/2*; mitogen-activated protein kinase kinase 1/2, *OT*; oxytocin, *OTR*, oxytocin receptor; *P*; phosphate, PIP_2; phosphatidylinositol 4,5-bisphosphate, *PLC*; phospholipase C, *Ras*; Ras GTPase, *Raf*; Raf kinase, *RTK*; receptor tyrosine kinase, *TRPM2*; Transient receptor potential cation channel, subfamily M, member 2. Based on REF

The $G\alpha_{i/o}$ family is heterogeneously distributed throughout the CNS and periphery, and expression of each subtype varies over time, suggesting changing roles for $G\alpha_{i/o}$ signalling over the course of development [170]. OTR-$G\alpha_{i/o}$ signalling is also known to have a crucial role in neurodevelopment, although the signalling cascades involved are poorly characterised [163]. *In vitro*, OTR-$G\alpha_{i/o}$ signalling inhibits cell proliferation and drives expression of cytokines known to be associated with the onset of labour, indicating a potential role for OTR-$G\alpha_{i/o}$ signalling in neuronal migration and facilitating reproduction [171, 172].

In immortalised GN11 olfactory neurons, OT differentially regulates membrane excitability in a dose-dependent manner [162]. High concentrations of OT activate OTR-$G\alpha_{i/o}$ signalling, which stimulates inwardly rectifying potassium currents (see Figure 1.6: 3). By contrast, low concentrations of OT activate OTR-$G\alpha_{q}$ signalling, which inhibits inwardly-rectifying currents [173]. This dose dependent relationship extends to cultured hypothalamic neurons, where low concentrations of OT (<100 nM) reduce, and high concentrations (>500 nM) promote OT secretion and oxytocinergic neuron burst firing, by inhibiting OTR-expressing GABAergic interneurons that control OT release [174]. This preliminary evidence suggests that OTR-$G\alpha_{i/o}$ signalling constitutes an important regulatory pathway, and that the high-threshold for activation of $G\alpha_{i/o}$ signalling may act as an excitatory switch in oxytocinergic positive feedback loops which is only activated during periods of greater OT release, such as early development or during the female reproductive cycle [175, 176].

Following agonist stimulation, the COOH-terminus of the OTR is phosphorylated by GPCR kinase (GRK), which recruits β-arrestin scaffold proteins to the receptor [177].

β-arrestin complexing inhibits further G-protein signalling – a process known as desensitisation. Receptor-bound β-arrestin acts as a scaffold for clathrin, a protein which initiates endocytosis and receptor internalisation [178, 179]. Depending on the cellular context, internalised receptors are targeted to different intracellular compartments, where they may be recycled to the plasma membrane (resensitisation) or transported to lysosomes for degradation (downregulation) (see Figure 1.6: 4,5) The fate of the OTR appears to be linked to the duration of agonist stimulation. Following acute OT exposure in cultured human myocytes, OTR-arrestin complexes are transported to vesicles expressing Rab4/5 GTPases, markers of the 'short cycle', which rapidly recycle the OTR to the plasma membrane [180]. In contrast, prolonged OT exposure in human myometrium desensitizes the OTR, reduces Ca^{2+}-signalling response and leads to a reduction in *OXTR* mRNA, indicating

receptor downregulation [181, 182].

In vivo, acute and chronic OT exposure elicit divergent effects on rodent social behaviour, with acute administration increasing social exploration of novel opposite-sex stimuli and chronic administration decreasing this behaviour, alongside a concomitant decrease in OTR expression throughout the brain [183]. This finding is of particular relevance to oxytocinergic drug development, as it suggests that the efficacy of OTR-targeted therapeutics that recruit β-arrestin may be compromised in the majority of neuropsychiatric disorders that require long-term drug treatment regimes. A potential strategy to mitigate β-arrestin induced OTR downregulation may lie in so-called 'biased ligands', which exhibit preferential signalling via G-protein pathways over β-arrestin pathways. The OT variants found in the highly social Cebidae family of New World Monkeys exhibit selectivity for $G\alpha_q$ over β-arrestin signalling [48]. $G\alpha_q$ signalling bias in these peptides may have evolved as a strategy to maintain non-desensitising OTR signalling in the brain, thus increasing the tone of OTR neuromodulation and the expression of prosocial behaviour.

1.4 The State of Therapeutic Development for the Oxytocin Receptor

1.4.1 Intranasal Oxytocin

The robust preclinical evidence supporting a role for OT in social behaviour has led to immense interest in exploring the therapeutic applications of OT in humans. As such, the last two decades have seen a growing body of randomised controlled trials (RCTs) investigating OT as a primary or adjunct therapy in neuropsychiatric disorders. The rapid metabolism and extremely poor oral absorption and distribution of OT has necessitated the use of intranasal administration of aerosolised OT, although the efficacy of this approach has not been firmly established. The outcome of OT intervention RCTs have yielded inconclusive results in a number of different conditions, with generally weak effect sizes and issues with replicability. A recent meta-analysis of OT RCT studies in schizophrenia (n=238) found no improvement in negative symptoms following acute intranasal OT administration [184]. Similarly, a meta-analysis of intranasal OT RCTs in anxiety disorders found no improvements in self-reported mood or anxiety scores following acute intranasal OT administration (n=228) [185]. The therapeutic outcome of OT in ASD has been more promising, with a meta-analysis (n=101) finding that a regimen of intranasal OT as primary or

adjunct therapy can lead to moderate improvements in ASD core symptoms including repetitive behaviour, eye gaze and emotion recognition. However, symptomatic improvements were not maintained beyond 6 weeks of treatment, indicating a potential issue with the long-term clinical efficacy of intranasal OT [186]. Taken together, the viability of using intranasal OT as a therapeutic intervention in neuropsychiatric disorders is far from certain.

Intranasally delivered drugs are hypothesized to passively diffuse along perineuronal channels associated with the olfactory and trigeminal nerve pathways innervating the nasal cavity, thus providing a direct link to the CNS that bypasses the blood-brain barrier and first-pass metabolism [187]. Studies in rodents and non-human primates have demonstrated that intranasal administered OT can lead to a modest increase in peptide concentrations in the CSF [188], although this increase often corresponds to minute fractions of the total administered dose (as little as 0.002%) [49]. The limited efficacy of intranasal OT administration necessitates the use of supra-physiological doses in human studies, a practice that leads to sustained elevations of OT in systemic circulation [189]. Although the physiological consequences of this process are not well characterised, it can be reasonably argued that high levels of OT in circulation may induce prolonged activation of OTRs in peripheral tissues, increasing the risk of adverse events associated with disrupted endocrine signalling, while also confounding the interpretation of behavioural outcomes in clinical trials that seek to study a target population of OTRs in the CNS.

In addition, many of the trials investigating intranasal OT over the past decade have been considerably underpowered, with small patient cohorts and effect sizes, large variations in dosing regimens (10–7000 IU) and heterogeneous behavioural readouts further complicating the interpretation of study data [190]. The use of preclinical findings in the design of human studies has been rendered difficult by the limited construct validity of animal social behaviour models, which often use monogenic knockout strains to investigate neuropsychiatric disorders with complex genetics, and show diverse manifestations of social behaviour that may not always be representative of the human condition [191]. A further obstacle lies in the partial agonist activity of OT at the vasopressin receptor subtypes $V_{1A}R$, $V_{1B}R$ and V_2R. Although the binding affinity of OT at these receptors is 10-100 fold lower than at the OTR [89], large doses of exogenous OT could drive AVP signalling, which may mask the prosocial effects of OT mediated through the OTR.

Increasingly, the therapeutic shortfalls associated with intranasal OT, as well as a lack of patentability have driven interest in developing alternative ligands for the OTR. Two schools of thought have emerged in this field, which utilise different

strategies to develop novel drug candidates. Small-molecule based approaches attempt to develop novel OTR ligands by utilising an OTR-active benzodiazepine pharmacophore previously identified from high-throughput screening of $V_{1A}R$ and $V_{1B}R$ antagonist libraries by the pharmaceutical industry [192]. In comparison, peptide-based approaches attempt to produce OT analogues with improved metabolic stability and pharmacodynamic characteristics by optimising functional moieties in the OT scaffold itself. Both approaches have yielded promising lead candidates for OTR drug development, but the majority of these candidates remain in the early preclinical stages of the development pipeline, with questions of dosage, safety and efficacy in human cohorts still to be answered.

1.4.2 Small-Molecule Oxytocin Receptor Agonists: The Benzodiazepine Pharmacophore

Relative to peptides, small-molecule GPCR ligands often display more favourable drug-like properties, such as improved metabolic stability and CNS distribution, and are more easily synthesized, providing inherent advantages over peptide-based drugs. However, developing small-molecule agonists for neuropeptide receptors such as the OTR presents a unique set of challenges. Neuropeptide ligands are large and structurally complex, interacting with their receptors across multiple spatially separated domains [154]. Small-molecule agonists cannot replicate this property; thus, it is difficult to rival the exquisite potency displayed by endogenous peptides. Perhaps reflecting this limitation, most small-molecule ligands for the OTR reported in the literature are antagonists [193].

Examination of small-molecule agonists reported for the OTR, $V_{1A}R$, $V_{1B}R$ and V_2R over the past decade reveals the existence of a pyrazolobenzodiazepine motif shared by many compounds with high affinity at one or more of these receptors. WAY-267,474 (see Figure 1.7), developed by Wyeth, displays low-nanomolar affinity at the human OTR and produces prosocial effects (100 mg/kg, intraperitoneal (IP) administration) and anxiolysis (3 µg, intracerebroventricular (ICV) administration) in rodent behavioural paradigms [194, 195]. TC-OT 39 (see Figure 1.7), developed by Ferring pharmaceuticals, shows full agonist activity at the human OTR and 200-fold selectivity over the V_2R in cell-based binding and functional assays, although behavioural efficacy has not been reported [192]. More recently, Frantz et al. reported the development of LIT-001 (see Figure 1.7), which displays greater OTR potency than WAY-267,464 and improves social interaction in a mouse model of ASD [196]. These molecules display a mixed agonist/antagonist profile in the OT/AVPR

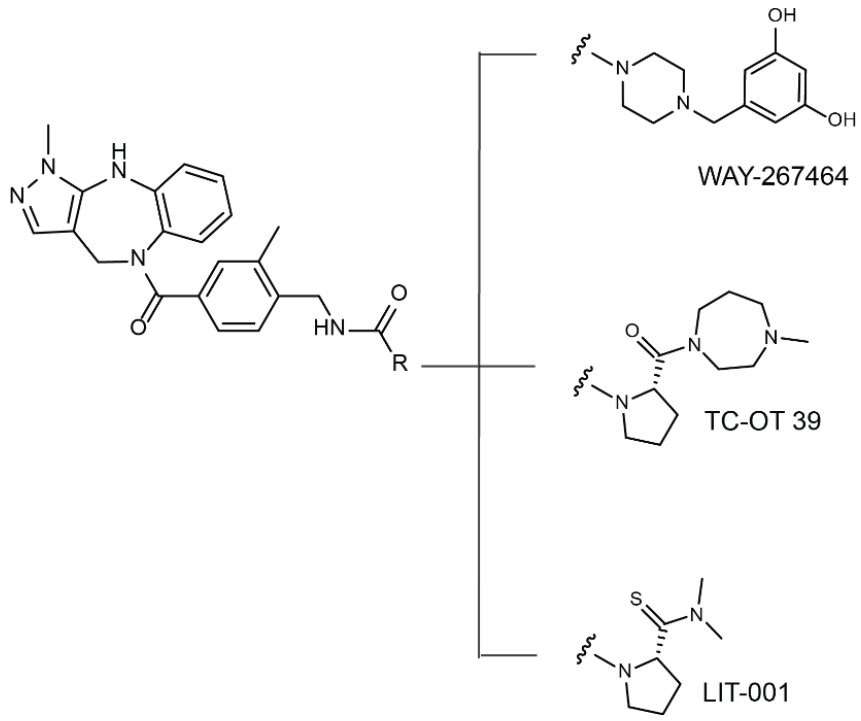

Figure 1.7: Molecular structures of small-molecule oxytocin receptor agonists WAY-267,464, TC OT 39, and LIT-001, derived from a functionalised benzodiazepine scaffold.

family, with low selectivity between the OTR and $V_{1A}R$ and functional antagonism of the $V_{1A}R$ *in vitro*, limiting their utility as therapeutics or investigational tools [197, 198].

Overall, small-molecule OTR agonists based on the benzodiazepine pharmacophore display improved metabolic stability relative to OT, and exert behavioural effects when administered peripherally, indicating CNS penetration. However, the receptor selectivity of these ligands is not substantially improved, with all reported OTR agonists displaying varying degrees of affinity and functional effects at the $V_{1A}R$, $V_{1B}R$ or V_2R. As such, further exploration of the structural determinants of receptor affinity and functional effects in these molecules will be required to optimise their pharmacological characteristics and advance therapeutic development.

1.4.3 Peptide Oxytocin Receptor Agonists

Structural motifs in the OT scaffold that influence stability, potency, and receptor selectivity have been identified, allowing the design of peptide OT analogues with improved pharmacological properties. Replacing the metabolically unstable disulfide bond of OT with alternatives, such as *meta*-xylene and diselenide bridges (see

Figure 1.8: 1) produces analogues with extended biological half-lives and selectivity over AVP receptor subtypes, albeit with a small reduction in potency at the human OTR [199, 200]. Wisniewski et al. [201] recently reported a series of OT analogues containing an alkyl-halide substitution at position 7 (see Figure 1.8: 2) that exhibit subnanomolar potency at the human OTR and 1000-fold selectivity with the $V_{1A}R$, $V_{1B}R$, and V_2R. In another approach, Kablaoui et al. [202] sought to increase the CNS uptake of peptide OTR agonists by designing hybrid molecules that incorporate non-polar elements from small-molecule agonists (see Figure 1.8:3) Although these compounds display full agonist activity at the OTR and do not activate the $V_{1A}R$, permeability is not substantially improved, suggesting that pairing with other polarity-lowering strategies is necessary to produce CNS-penetrating ligands with this approach.

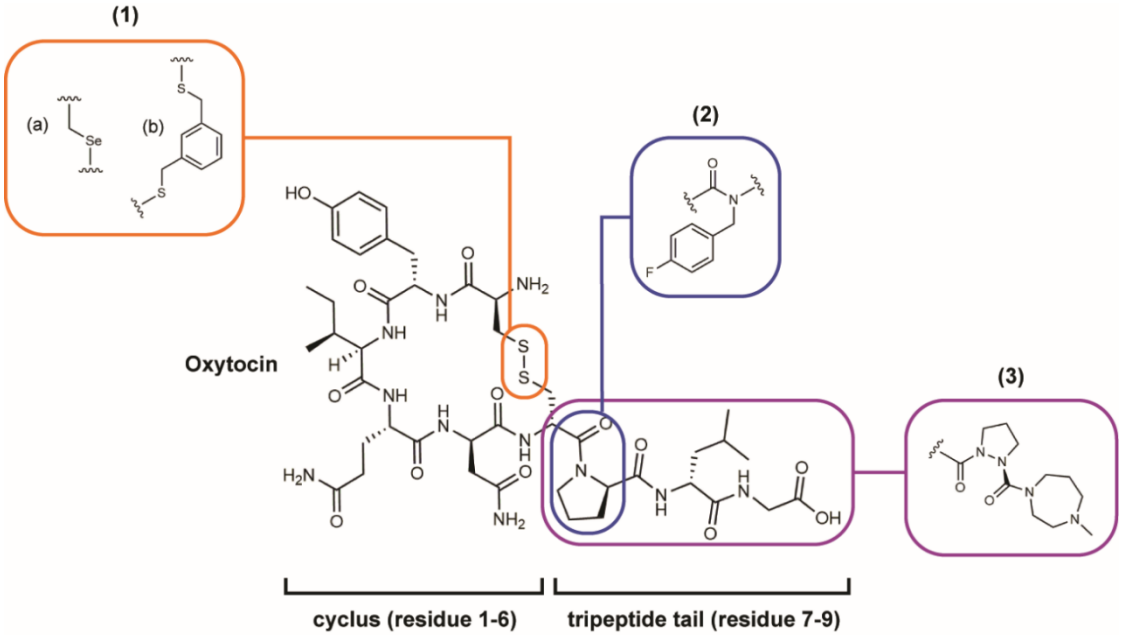

Figure 1.8: Structural modifications That influence stability, potency, and selectivity in oxytocin analogues. **(1)** Replacement of the disulfide bond with either (a) diselenide or (b) meta-xylene bridge increases metabolic stability. **(2)** N-alkyl halide substitution at position 7 increases potency at the oxytocin receptor and selectivity over vasopressin receptors. **(3)** Replacement of the tripeptide tail with a functional motif from a small-molecule oxytocin receptor agonist produces molecules with reduced polarity that retain oxytocin receptor potency but do not activate the vasopressin 1A receptor.

Other subtle modifications influence the ability of ligands to activate specific G-protein subtype pathways associated with the OTR (see Figure 1.9). The synthetic OT analogues, DNalOVT and atosiban, share bulky substituents at position 2 and in cell-based functional assays preferentially activate $G\alpha_{i1}$ and $G\alpha_{i3}$-isoform mediated OTR signalling, respectively - indicating a role for this residue in $G\alpha_{i/o}$ functional selectivity [162]. By contrast, the disulfide-stabilised OT analogue carbetocin (see

Figure 1.9) selectively engages the $G\alpha_q$-signalling and does not activate $G\alpha_{i/o}$ signalling [203].

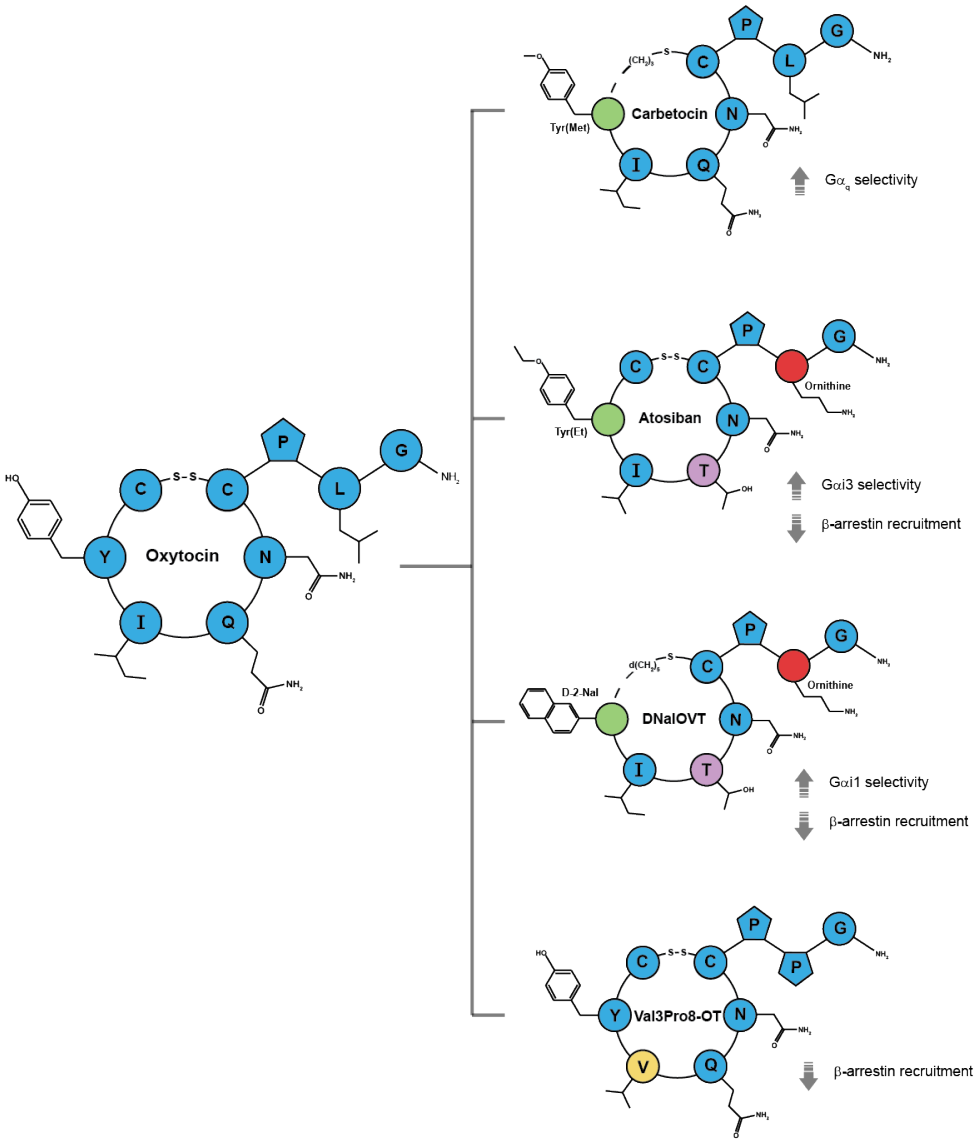

Figure 1.9: Peptide analogues of oxytocin and structural determinants of ligand signalling bias. Oxytocin binding at the oxytocin receptor promotes recruitment of $G\alpha_q$, $G\alpha_{i/o}$ ($G\alpha_{1-3}$, $G\alpha o_{A,B}$)-signaling proteins and β-arrestin. Structural modification at key points in the OT scaffold produces ligands that preferentially recruit individual $G\alpha_q$ or $G\alpha_{i/o}$ subtypes and display a reduced propensity for β-arrestin recruitment. *D-2-Nal*: D-2-Napthyl alanine.

Functionally selective ligands for the OTR can be used to explore the cellular and behavioural effects of OTR-mediated $G\alpha_{i/o}$ and $G\alpha_q$ signalling and may have a range of therapeutic applications. Atosiban was recently used to identify a new population of oxytocinergic neurons involved in pain signalling, constituting further evidence for OTR-$G\alpha_{i/o}$ inhibitory coupling in the CNS [204]. In addition, OTR-stimulated $G\alpha_{i/o}$ signalling has been shown to exert an anti-proliferative effect on cell growth in myometrium tissue [172]. These findings point towards the possibility of devel-

oping $G\alpha_{i/o}$-selective OT analogues as a novel pipeline for analgesic or anticancer therapeutics [205].

$G\alpha_q$ signalling through the phospholipase-C pathway is involved in the regulation of anxiety in the central amygdala, and likely has a pivotal role in the anxiolytic effects of OT [164, 206]. In line with this possibility, carbetocin exerts OT-like anxiolytic and antidepressant effects in rodents, but differs from the behavioural profile of OT in other key areas [207–209]. However, it is not conclusively known whether these divergent effects are the result of $G\alpha_q$ functional selectivity *in vivo*, potential antagonism of the $V_{1A}R$, or altered OTR internalisation dynamics induced by carbetocin, highlighting the need for further characterisation.

The most salient findings that emerge from peptide-based drug discovery approaches are that the OT scaffold is highly sensitive to modification, and substitution of functional motifs in the cyclic and linear components of the molecule can dramatically influence metabolic stability, receptor selectivity and potency. Additionally, some modified OT analogues preferentially activate $G\alpha_q$ or $G\alpha_{i/o}$-isoform coupled signalling, highlighting the possibility of developing biased ligands that produce targeted therapeutic outcomes that are associated with activation of a specific, OTR-coupled intracellular signalling pathway. Although attempts have been made to reduce the size and polarity of peptide OT analogues, these efforts have been largely unsuccessful, and as such, limited oral bioavailability and CNS penetration remain major barriers to the future therapeutic development of these molecules.

1.5 Oxytocin Receptor Ligands: New Avenues for Therapeutic Development

1.5.1 Small-molecule Oxytocin Receptor Ligands: Improving Selectivity Through Structural Rigidity

Small-molecule ligands based on the pyrazolobenzodiazepine pharmacophore have shown the greatest potential for therapeutic development as OTR agonists. At present, there are no other structural scaffolds with demonstrable binding affinity and efficacy at the OT/AVP receptor family. Nonetheless, poor functional selectivity between receptors is a recurrent theme in all pyrazolobenzodiazepine derivatives, which limits their use as investigative tools or candidates for therapeutic development. Overcoming this limitation requires a systematic exploration of the fac-

tors that contribute to the affinity and functional effects of pyrazolobenzodiazepine derivatives at the OTR and $V_{1A}R$. While many structural modifications to this class of molecules have already been characterised, the contribution of molecular flexibility towards OTR and $V_{1A}R$ affinity and efficacy remain largely unexplored.

WAY-267,464, TC-OT 39 and LIT-001 are highly flexible molecules, containing 11 freely rotatable bonds each. A high number of rotatable bonds (>10) negatively impacts oral bioavailability and binding specificity, and is thus a prime target for structural optimisation of these ligands. We have previously reported on the synthesis and pharmacology of WAY-267,464 analogues that retain the pyrazolobenzene and resorcinol moieties of WAY-267,464 tethered by a flexible alkyl-linker [198]. All flexible analogues evaluated in this study lost OT receptor affinity and activity, resulting in the generation of highly selective $V_{1A}R$ ligands. As such, we hypothesise that engineering molecules in the opposite direction towards greater rigidity is a potential strategy to enhance selective activation of the OTR.

1.5.2 Peptide Oxytocin Receptor Ligands: Exploration of Bioactive Metabolites

Although many peptide ligands based on the OT scaffold have been engineered for enhanced OTR affinity and subtype selectivity, there are some inherent disadvantages to this approach. The large size and polarity of OT presents a key obstacle - these factors substantially reduce CNS permeability, in turn reducing the efficacy of orally administered peptide formulations. Limited metabolic stability is another concern, as the biological half-life of OT ranges between 2 – 8 minutes in peripheral circulation to 30 minutes in the CNS [210, 211]. The rapid metabolism of OT *in vivo* is catalysed by peptidases, which sequentially cleave residues from the N- and C-termini of the molecule.

Interestingly, there is evidence to suggest that the products of OT metabolism are bioactive in the CNS [212–214]. The anxiolytic effects associated with central OT administration in mice are dependent on the presence of insulin-regulated aminopeptidase (IRAP), suggesting these behaviours may be attributable to a product of IRAP-mediated OT metabolism, rather than OT itself [215]. Linear products of OT metabolism - $OT_{4\text{-}9}$ and $OT_{4\text{-}8}$ - exhibit strong effects on social memory and social recognition, and increase sociability in models of ASD [213, 214, 216]. $OT_{7\text{-}9}$, otherwise known as melanocyte-inhibiting factor (MIF-1) is another product of OT metabolism with a broad range of effects in the CNS, blocking the effects of μ-opioid

receptor activation and acting as a positive allosteric modulator of dopamine receptors [217, 218]. These properties may in turn potentiate OT release and contribute to the anti-addictive and reward-enhancing effects associated with OT administration [93].

Based on these findings, products of OT metabolism represent a novel, promising and largely unexplored avenue for OTR ligand development. The opportunity is twofold – the smaller size and reduced polarity of OT metabolites may improve CNS penetration, while the distinct structural characteristics of OT metabolites may improve OTR affinity and functional efficacy relative to the parent molecule. However, a number of fundamental questions remain surrounding the pharmacological properties of OT metabolites. Remarkably, the behaviourally-active $OT_{4\text{-}9}$ and $OT_{4\text{-}8}$ fragments have not yet been assessed for binding affinity and signalling efficacy at the OTR *in vitro*, raising the possibility that these molecules may exert their effects via another target in the brain. Moreover, there is limited information on the bioactivity of other linear and cyclic fragments arising from degradation of OT in cellular or behavioural contexts, highlighting the need for a comprehensive characterisation of OT metabolite pharmacology.

1.5.3 Peptide Oxytocin Receptor Ligands: Counteracting Receptor Downregulation with Biased Agonists

The observation that the OTR downregulates following chronic agonist exposure is a major concern for both small-molecule and peptide-based approaches to oxytocinergic drug development. Overcoming this hurdle is a critical step towards developing OTR ligands that maintain therapeutic efficacy over the long-term treatment regimens commonly required in neuropsychiatric disorders. The reports of ligand signalling bias in the clinically used OTR ligands carbetocin and atosiban indicates that ligand morphology can impact signalling pathway selectivity in the OT system. Moreover, the discovery of $G\alpha_q$-biased OT variants in the highly social Cebidae family of New World Monkeys suggests that optimising OTR ligands for $G\alpha_q$ pathway activation over β-arrestin recruitment could be a potential strategy to mitigate OTR downregulation in a therapeutic context.

1.5.4 Summary and Aims

Social dysfunction in multiple domains is a characteristic feature of many neuropsychiatric disorders, most notably ASD, schizophrenia, depression, SAD and PTSD. While our understanding of human social behaviour is incomplete, the neuropeptides OT and AVP appear to play a key role in regulating social behaviour. Research summarised in the preceding sections suggests that targeting the OTR may be an effective strategy to improve social behavioural deficits in neuropsychiatric conditions, however, OT itself is unlikely to ever be used in a therapeutic capacity due to its poor drug-like properties.

Previous approaches in the design of OTR agonists have focused on small molecule ligands derived from a benzodiazepine pharmacophore (Figure 1.7, or peptide analogues derived from the structure of OT (Figure 1.8, 1.9). Remaining barriers in the therapeutic development of these ligands include a lack of OTR selectivity in small molecules, and limited stability and CNS penetration in peptide analogues of OT. Densensitisation and downregulation of the OTR associated with chronic agonist exposure represents another obstacle faced by both small molecule and peptide ligands for the OTR.

The overarching aim of thesis is to identify novel OTR agonists to serve as lead candidates for the treatment of social behavioural deficits and anxiety in neuropsychiatric disorders. To achieve this aim, the preclinical *in vitro* pharmacology of putative OTR ligands derived from small-molecule and peptide scaffolds will be evaluated in a suite of cellular assays. The following objectives are associated specifically with each chapter of the thesis and support achievement of the overarching aim:

1. To evaluate the receptor binding affinity, receptor selectivity and functional effects of novel WAY-267,464 derivatives in cells expressing the human OTR or $V_{1A}R$ (Chapter 3).

2. To investigate the biological activity of peptide fragments derived from the endogenous metabolism of OT, and characterise the receptor binding affinity and functional effects of active fragments in cells expressing the human OTR or $V_{1A}R$ (Chapter 4).

3. To explore the impact of structural modifications on the pharmacology of bioactive OT metabolites in cells expressing the human OTR or $V_{1A}R$, and from this analysis, identify novel peptide agonists with improved OTR affinity and potency or reduced propensity to induce OTR internalisation (Chapter

5).

Chapter 2

Materials and Methods

2.1 Chemicals

Small molecule derivatives of WAY-267,464 (Chapter 3) were synthesised by Dr. Will Jorgensen of the Kassiou Drug Discovery Chemistry Group. Peptide metabolites of OT (Chapter 4) were synthesised by Mimotopes Pty Ltd. (Victoria, Australia). Modified metabolites (Chapter 5) were a generous gift from Dr. Markus Muttenthaler. 100 mM stock solutions of WAY-267,464 derivatives were prepared by solubilising compounds in dimethyl sulfoxide (DMSO), whilst 10 mM stock solutions of peptidergic compounds were prepared by resuspension in molecular biology grade H_2O. All stock solutions were stored at -80°C until use.

2.2 Cell Culture

2.2.1 Cell Line Maintenance

Wild-type human epithelial kidney cells (HEK293) used for transient transfections were maintained in Dulbecco's Modified Eagle Medium (DMEM) (Sigma Aldrich; Missouri, USA) supplemented with heat-inactivated foetal bovine serum (FBS) 10% (v/v) (Sigma Aldrich). Stably transfected cell lines expressing the human OTR or $V_{1A}R$ (HEK293-OTR, HEK293-$V_{1A}R$) were maintained in DMEM supplemented with FBS 10% (v/v) , blasticidin-S hydrochloride (15 µg/mL; Sigma Aldrich), penicillin-streptomycin (100 U; Sigma Aldrich) and hygromycin B (100 µg/mL; Sigma Aldrich). The hygromycin B concentration that maintained selection pressure on stably transfected cell lines was optimised by incubating wild-type HEK293 cells with a range of hygromycin B concentrations (2-2000 µg/mL) for 7 days, then assessing cell viability with a CellTiter-Blue assay as per the manufacturers protocol (Promega; Wisconsin, USA). Receptor expression was induced in stable cell lines by the addition of tetracycline hydrochloride (2 µg/mL; Sigma Aldrich) to the culture media for 48 h prior to experiments. All cell lines were maintained at 37°C, 5% CO_2 and passaged routinely before reaching confluency.

2.2.2 Transfections

DNA transfections were carried out using Fugene^{HD} reagent (Promega) as per the manufacturers protocol. Briefly, wild-type HEK293 cells were plated into poly-*L*-

lysine coated, 6-well cell culture dishes (Corning; New York, USA) at a density of 8×10^5 cells/well and incubated at 37°C, 5% CO_2 for 4-6 h to allow cells to reattach to dish. Transfection mixtures containing DNA (2 µg/well) and Fugene^{HD} reagent (4 µL/µg DNA) in OptiMEM (Sigma Aldrich) were incubated for 10 min at ambient temperature and added dropwise to culture dishes, followed by a 24 h incubation at 37°C, 5% CO_2 to allow adequate gene expression for subsequent assays.

2.3 Cloning

2.3.1 Plasmids

To obtain fusion protein vectors used in β-arrestin assays (Methods 2.5.4), cDNAs encoding the human OTR and human β-arrestin2 (arr2) were synthesized by Life Technologies in the pMA-RQ cloning vector. cDNAs for the OTR and arr2 were then subcloned from pMA-RQ into pNLF1-C and pHTC mammalian expression vectors (Promega), respectively. These vectors encode the protein partners nanoluciferase (Nluc; pNLF1-C) and HaloTag (pHTC). OTR and arr2 encoding cDNAs were inserted into the multiple cloning site (MCS) upstream of protein coding regions in each vector to generate C-terminal fusion sequences (see Figure 2.1).

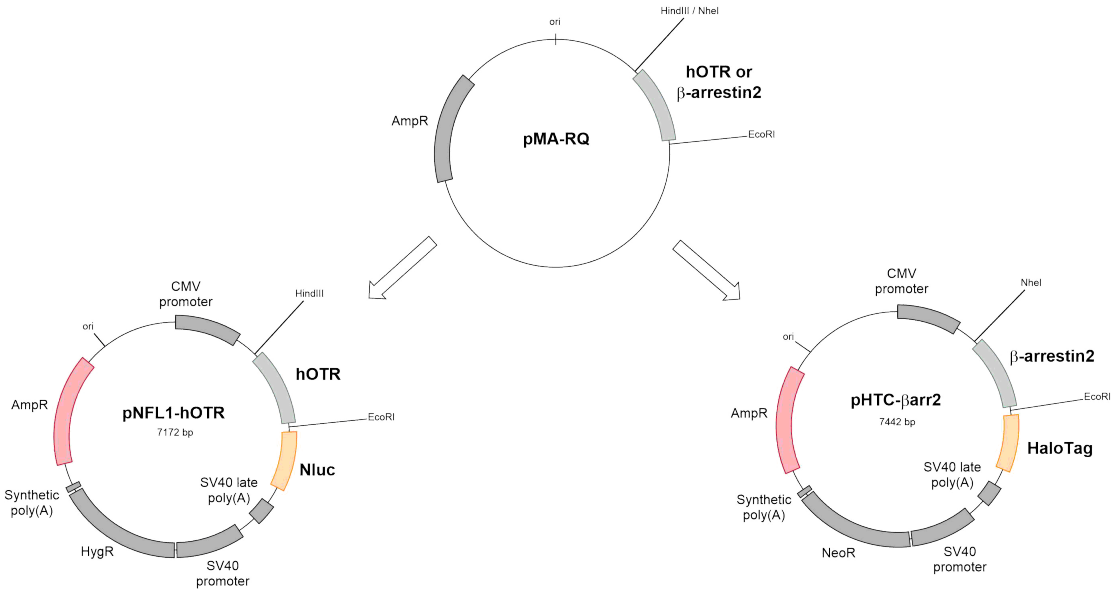

Figure 2.1: Vectors used to generate fusion constructs for β-arrestin recruitment assays. *hOTR*: human oxytocin receptor, *Nluc*: nanoluciferase.

2.3.2 Isolation of DNA for Cloning Procedures

Origin and destination vectors (1 µg/50 µL reaction) were double digested with restriction enzymes (10 U/50 µL reaction) (see Table 2.1) in CutSmart buffer (New England Biolabs; MA, USA) for 15 min at 37°C, and the reaction terminated by heat inactivation at 65°C for 20 min. Digests were cooled to room temperature and 6X gel loading dye (New England Biolabs) added to each sample. DNA bands were separated by running 20 µL aliquots of digest on a 1.2% agarose E-gel (Invitrogen) for 30 min alongside 1 Kb Plus DNA ladder (Invitrogen), then imaged using a Safe Imager^{TM} blue-light transilluminator (Invitrogen). Bands which corresponded in size to gene insert and destination vectors were excised and purified using a QIAquick gel extraction kit (Qiagen; Hilden, Germany) according to the manufacturers protocol. DNA extracts were resuspended in Tris-HCl 10 mM, EDTA 0.1 mM, pH 8.0, followed by purity assessment and DNA quantification using a Nanodrop UV/VIS spectrophotometer (Thermofisher Scientific, Massachusetts, USA). Extracts were stored at −20°C prior to further use.

2.3.3 DNA Ligation and Bacterial Transformation

Purified gene inserts and cut destination vectors were mixed at a 3:1 molar ratio and ligated by incubation with Instant Sticky-end Ligase Master Mix (2X) (New England Biolabs) for 10 min at 4°C. Ligations were transformed directly into XL1-blue supercompetent cells (Agilent Technologies; California, USA) as per the manufacturers protocol. Briefly, 50 µL aliquots of XL-1 blue cells were thawed on ice for 15 min, then treated with β-mercaptoethanol (0.5 µL/50 µL cells) for 10 min and incubated with ligation reaction (5 µL/50 µL cells) for 30 min. Cells were then transformed by heat-shock at 42°C for 30 seconds and recovered for 1 h at 37°C in Luria-Bertani (LB) media.

Recovered cultures were spread onto LB-agar plates containing ampicillin (100 µg/mL; Sigma-Aldrich) and incubated overnight at 37°C. The following day, ampicillin resistant colonies were inoculated into LB-ampicillin (100 µg/mL) starter cultures and grown for 8 h, diluted 1:1000 and grown for a further 16 h. DNA was purified from cultures using a midiPREP DNA extraction kit (Qiagen) according to the manufacturers protocol, then resuspended in Tris-HCl 10 mM, EDTA 0.1 mM, pH 8.0 and DNA concentration quantified using a Nanodrop spectrophotometer (Thermofisher Scientific) prior to storage at −20°C until further use. Plasmid integrity following transformation was verified via DNA sequencing (Macrogen; Seoul, Korea).

Table 2.1: Restriction enzymes used in cloning procedures.

cDNA	Origin	Destination	Restriction Enzymes
OTR	pMA-RQ	pNLF1-C	HindIII, EcoRI
β-arrestin2	pMA-RQ	pHTC	NheI, EcoRI

2.4 Ligand Affinity and Kinetics Binding Assays

2.4.1 Membrane Homogenate Preparation

HEK293-OTR and HEK293-V_{1A}R cells were detached from culture vessels with PBS containing EDTA 5 mM, pH 7.4 and centrifuged at 1200 g for 5 min. The supernatant was removed and cells resuspended in HEPES 50 mM, EDTA 5 mM, $MgCl_2$ 5 mM, pH 7.4 prior to homogenisation using an Ultra-Turrax homogeniser (IKA; North Carolina, USA). Resulting homogenates were centrifuged twice at 48 000 g, 4°C for 30 min and pellets resuspended in Tris-HCl 50 mM, $MgCl_2$ 5 mM, pH 7.4. Final protein concentration in membrane fractions was calculated using the BCA protein-assay method (Bio-Rad; California, USA) according to manufacturer's protocols, followed by storage at −80°C until further use.

2.4.2 Competition Radioligand Binding: Affinity

The binding affinity (K_i) of compounds was indexed by competitive displacement of [^{3}H]-oxytocin ([^{3}H]-OT) or [^{3}H]-vasopressin ([^{3}H]-AVP) at K_d concentrations previously determined in-house using saturation radioligand binding assays [219]. Membrane fractions (50 µg/well) from OTR or V_{1A}R expressing cells were incubated in a final volume of 200 µL containing [^{3}H]-OT (10 nM) or [^{3}H]-AVP (3 nM) (Perkin-Elmer; MA, USA) alongside competing compounds (0.1 nM - 100 µM) in Tris-HCl 50 mM, $MgCl_2$ 5 mM, pH 7.4. Reactions were incubated for 90 min at 4°C to reach equilibrium, and terminated by rapid filtration over glass fibre filters (GF/A 1.6 µM, Whatman; Maidstone, UK), and washing with ice-cold reaction buffer. Non-specific binding was determined in the presence of 1 µM unlabelled OT or AVP (Sigma-Aldrich), respectively.

2.4.3 Competition Radioligand Binding: Kinetics

To determine the association (k_{on}) and dissociation (k_{off}) rate constants for [^{3}H]-OT, HEK293-OTR membranes (50 µg/well) were incubated with a $10\times K_d$ concentration of [^{3}H]-OT (100 nM) in Tris-HCl 50 mM, $MgCl_2$ 5 mM, pH 7.4 at 4°C. For association experiments, [^{3}H]-OT was added to OTR membranes sequentially over a 2 h timecourse. For dissociation experiments, [^{3}H]-OT was incubated with OTR membranes for 90 min at 4°C to allow reactions to reach equilibrium, then ligand-receptor complexes were dissociated with the addition of unlabelled OT (1 µM) over a 6 h timecourse.

k_{on} and k_{off} parameters for unlabelled, competing compounds were determined using the theoretical model of Motulsky and Mahan [220] and a novel assay methodology developed by Costa et al. [221] Unlike methods in which one compound is pre-equilibrated with the receptor, this approach involves the simultaneous addition of both [^{3}H]-OT and competing ligands to OTR membranes, so that at $t = 0$ all receptors are unoccupied. [^{3}H]-OT (10 nM) and competing ligand ($3\times K_i$ concentration, determined previously (Section 2.4.2) in Tris-HCl 50 mM, $MgCl_2$ 5 mM, pH 7.4 were added to OTR membranes (50 µg/well) over a 2 h timecourse at 4°C. All reactions were terminated by rapid filtration over glass fibre filters (Whatman), and washing with ice-cold reaction buffer. Non-specific binding at each time point was determined in the presence of 1 µM unlabelled OT (Sigma-Aldrich).

2.4.4 Radioactivity Detection

Filtered samples were dried for 24 h, then soaked in Microscint-0 scintillant (Perkin-Elmer) for 30 min. Radioactivity (counts per minute, CPM) was detected using a Microbeta^2 2450 microplate reader (Perkin-Elmer) (see Appendix A for instrument settings). Specific binding at each point was calculated from raw radioactivity data using Equation 2.1:

$$\frac{\text{CPM}_{\text{compound + [}^3\text{H]-OT}}}{\text{CPM}_{\text{[}^3\text{H]-OT}}} - \text{CPM}_{\text{non-specific binding}} = \text{Specific Binding} \tag{2.1}$$

2.5 Ligand Biological Activity: Cellular Signalling Assays:

2.5.1 $G\alpha_q$ Signalling: IP_1 Accumulation Assay

The $G\alpha_q$ pathway is the primary mediator of intracellular signal transduction coupled to the OTR and $V_{1A}R$[154]. To evaluate the functional effects of ligand binding at the OTR and $V_{1A}R$, activation of the $G\alpha_q$-coupled pathway was assessed using a homogenous-time resolved fluorescence (HTRF) IP_1 assay (Cisbio; Codolet, France). $G\alpha_q$ signaling leads to the production of inositol monophosphate (IP_1). Further metabolism of IP_1 can be inhibited by the addition of lithium chloride, and thus IP_1 accumulation can be used as an index of $G\alpha_q$ pathway activation (see Figure 2.2).

The HTRF system used in this assay is comprised of an IP_1 molecule labelled with an acceptor fluorophore (IP_1-d2) and an IP_1-specific antibody labelled with a lanthanide complex, terbium cryptate (Ab-cryptate). Laser excitation of the lanthanide complex produces a long-lived fluorescence emission at 620 nm, which reduces interference from rapidly decaying autofluorescence signals often observed in biological matrices. When IP_1-d2 and Ab-cryptate are in close proximity, fluorescence resonance energy transfer (FRET) occurs between the fluorophores and a characteristic fluorescence emission at 665 nm is produced by IP_1-d2. Endogenous IP_1 competes with IP_1-d2 for Ab-cryptate binding sites, and thus the fluorescence signal intensity at 665 nm is inversely proportional to the concentration of intracellular IP_1 present, and by extension the level of receptor activation induced by a ligand.

HEK293-OTR or HEK293-$V_{1A}R$ cells were seeded onto clear, poly-*L*-lysine coated 384 well plates (Corning) at a density of 8.75×10^3 cells/well and incubated for 48 h at 37°C, 5% CO_2 in the presence of tetracycline hydrochloride (2 µg/mL) to induce receptor expression. Agonist effects were evaluated by incubating cells with test compounds (1 nM – 10 µM) for 1 h at 37°C prior to the addition of Ab-Cryptate and IP_1-d2 in lysis buffer. The ligand concentration that induced a 50% maximal response (EC_{50}) was used to compare potency across compounds. The response induced by 10 µM of ligand (E_{max}), expressed as a percentage of maximal full agonist response (% OT or AVP) was used to evaluate the intrinsic efficacy of compounds.

For antagonist assessment, cells were pre-incubated with test compounds (1 nM - 10 µM) at 37°C for 30 min prior to the addition of an EC_{70}concentration of OT or

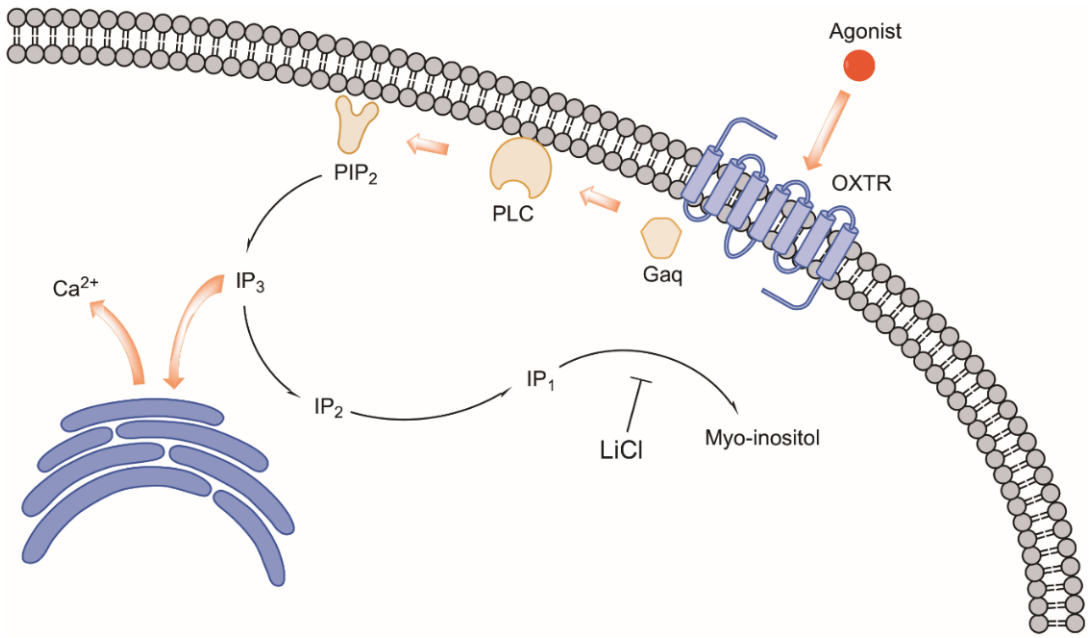

Figure 2.2: Ligand-induced $G\alpha_q$ signalling through the OTR leads to release of intracellular Ca^{2+} stores and production of IP_1. Metabolism of IP_1 can be inhibited by LiCl. *OTR*: human oxytocin receptor, *PLC* = phospholipase C, PIP_2 : Phosphatidylinositol 4,5-bisphosphate, IP_{1-3} : inositol mono/di/triphosphate, *LiCl*: Lithium chloride.

AVP mixed with either test compounds or DMSO (0.1% v/v) control. Cells were then incubated for a further 1 h at 37°C, and Ab-Cryptate and IP_1-d2 added. The ligand concentration that inhibited 50% of OT or AVP-induced response (IC_{50}) was used to evaluate antagonistic functional effects across compounds.

To explore the possibility of allosteric interactions between OT, AVP and test compounds, cells were incubated for 1 h at 37°C with an EC_{10} concentration of OT or AVP alone or in combination with test compounds (10 µM), prior to addition of Ab-Cryptate and IP_1-d2. In all assays, following addition of Ab-Cryptate and IP_1-d2, lysates were incubated for a further 1 h at ambient temperature, transferred to a low-volume, white-walled 384 well plate (Perkin-Elmer) and HTRF data acquired using a PHERAStar microplate reader (BMG Labtech; Ortenberg, Germany) (see Appendix A for instrument settings). Raw 665 nm fluorescence data was normalised to the nonvariable 620 nm emission of Ab-cryptate using Equation 2.2:

$$\frac{665 \text{ nm emission}}{620 \text{ nm emission}} \times 10000 = \text{HTRF Ratio} \tag{2.2}$$

2.5.2 $G\alpha_s$ Signalling: cyclic AMP Production Assay

Although $G\alpha_q$ proteins are the primary intracellular signal transduction partners associated with the OTR [154], interactions between the OTR and $G\alpha_s$ proteins which regulate the cyclic AMP/protein-kinase A (cAMP-PKA) signalling pathway have been detected in some cell types [160, 161, 222]. To evaluate the functional effects of ligand binding at the OTR, activation of the $G\alpha_s$-coupled intracellular signalling pathway was assessed using a cAMP production assay (Cisbio). This assay relies on the same HTRF technology to detect $G\alpha_q$ pathway activation described in Methods 2.5.1, but uses an acceptor dye-labelled cAMP biosensor (cAMP-d2) and a cAMP-specific, lanthanide-labelled antibody (Ab-cryptate) as the HTRF donor fluorophlore to detect $G\alpha_s$ pathway activation. To counteract the degradation of cAMP to AMP by the action of phosphodiesterase (PDE) enzymes, a PDE pan-inhibitor (3-isobutyl-1-methylxanthine, IBMX [223]) was supplemented in assay media to ensure proper cAMP accumulation and its subsequent measurement. Forskolin, a known activator of cAMP production [224], was used as a positive control to verify the functionality of the assay system. The OTR antagonist, atosiban, was used as a reference ligand to compare the $G\alpha_s$ pathway activity of test compounds. Data acquisition was performed using a PHERAStar microplate reader (BMG Labtech) fitted with a luminescence detection module (see Appendix A for instrument settings). Raw 665 nm fluorescence data was normalised to the nonvariable 620 nm emission of Ab-cryptate using Equation 2.2.

Prior to assessment of ligand-induced activation of cAMP signalling, the dynamic range of the HTRF cAMP assay was enhanced by optimising buffer composition, cell density, agonist stimulation and antibody incubation times. To determine optimal buffer composition and agonist stimulation times for the assay, HEK293-OTR cells were seeded at a density of 5×10^3 cells/well into white, poly-*L*-lysine coated 384 well plates, and incubated for 48 h at 37°C, 5% CO_2. After 48 h, culture media was aspirated and replaced with forskolin (1 µM) in assay buffer - either DMEM supplemented with IBMX (0.5 mM) or Hanks Buffered Salts Solution (HBSS) supplemented with HEPES 20 mM, IBMX 0.5 mM, pH 7.4, and incubated for 5 - 60 min at 20 °C. cAMP-d2 and Ab-cryptate in lysis buffer were added to cells and incubated for a further 1 h at 4°C prior to data acquisition. DMEM + IBMX 0.5 mM was selected for assay buffer composition, as it produced higher raw fluorescence values and greater assay sensitivity than HBSS buffer (optimisation data shown in Appendix B, Figure B.1). The maximal effect induced by forskolin was observed at 5 min, and did not increase with extended agonist incubation times.

Cell density optimisation was then performed by seeding HEK293-OTR cells at a range of densities (0.25 - 16 $\times$ 10^3 cells/well) into white, poly-*L*-lysine coated 384 well plates, followed by incubation for 48 h at 37°C, 5% CO_2. On the day of the experiment, culture media was aspirated and replaced with forskolin (1 - 10 µM) in DMEM + IBMX 0.5 mM and incubated for 5 min. cAMP-d2 and Ab-cryptate in lysis buffer were added to cells and incubated for a further 1 h at 4°C prior to HTRF data acquisition. The cell density which yielded the largest difference between basal and forskolin-induced cAMP response (2 $\times$ 10^3 cells/well) was utilised in subsequent experiments to maximise the dynamic range of the assay (optimisation data shown in Appendix B, Figure B.1).

Further attempts to increase assay sensitivity were made by extending antibody incubation times from 1 h to 24 h, and by reducing basal cAMP activity in HEK293-OTR cells through introduction of a serum-starvation step. Briefly, HEK293-OTR cells seeded at 2 $\times$ 10^3 cells/well were incubated for 48 h at 37°C, 5% CO_2. On the day of the experiment, the cell culture media was aspirated and replaced with DMEM supplemented with FBS 0.5% (v/v), and incubated for 3 h at 37°C, 5% CO_2 prior to the addition of test compounds in assay buffer. No statistically significant differences were seen between forskolin-induced cAMP responses in 1 h vs 24 h antibody incubation times (optimisation data shown in Appendix B, Figure B.2). Similarly, no differences were observed in constitutive cAMP production between 3 h serum-starve vs no-starve conditions (optimisation data shown in Appendix B, Figure B.2). Thus, the final experimental conditions consisted of a 1 h incubation with Ab-cryptate prior to data acquisition and maintenance of cells in complete culture media prior to test compound addition.

Following assay optimisation procedures, ligand functional activity at the $G\alpha_s$ pathway was indexed by measuring cAMP production following exposure to test compounds. HEK293-OTR cells were seeded at a density of 2×10^3 cells/well into white, poly-*L*-lysine coated 384 well plates, and incubated for 48 h at 37°C, 5% CO_2. On the day of the experiment, cell culture media was aspirated and replaced with test compounds (0.1 - 10 µM) in DMEM + IBMX 0.5 mM for a 5 min agonist incubation period. cAMP-d2 and Ab-cryptate in lysis buffer were then added to cells and incubated for a further 1 h at 4°C prior to HTRF data acquisition. The ligand concentration that induced a 50% maximal response (EC_{50}) was used to compare potency across compounds. The response induced by 10 µM of ligand (E_{max}) was used to evaluate the efficacy of compounds comparative to basal cAMP production.

2.5.3 Real-Time Calcium Flux Assay

Increases in cytosolic Ca^{2+} mobilized from intracellular stores and through ion channel influx is a key regulator of many cellular processes, and is a major downstream effector of OTR activation [225]. The level of Ca^{2+} mobilization induced by test compounds at the OTR was evaluated using the cell permeant Fluo-4 AM Ca^{2+} indicator dye (Invitrogen), which produces a peak fluorescence emission at 525 nm when bound to Ca^{2+}.

HEK293-OTR cells were seeded onto poly-*L*-lysine coated, black, clear-bottom 96 well plates (Corning) at a density of 3×10^4 cells/well in phenol-red free DMEM (Sigma Aldrich), containing 1% (v/v) FBS, HEPES 50 mM, penicillin-streptomycin (100 U) and tetracycline hydrochloride (2 µg/mL), then incubated for 48 h at 37°C, 5% CO_2. On the day of the experiment, culture media was replaced with Fluo-4 AM in assay buffer (HBSS supplemented with HEPES 20 mM, $MgCl_2$ 5 mM, probenecid 2.5 mM, pH 7.4) and incubated for 1 h at 37°C. Following a 90 second baseline reading, compounds (0.1 nM – 10 µM) were added to cells and fluorescence data simultaneously acquired for 5 min using a Flexstation 3 microplate reader fitted with an injector module (Molecular Devices; California, USA) (see Appendix A for instrument settings). The post-injection timepoint at which fluorescence peaked (t = 2 min) was used to generate normalised data (F/F_0) with Equation 2.3. EC_{50} and E_{max} values were used to evaluate the potency and efficacy for Ca^{2+} mobilisation across compounds.

$$\frac{525 \text{ nm emission }_{\text{peak}}}{525 \text{ nm emission }_{\text{baseline}}} = F/F_0 \tag{2.3}$$

2.5.4 β-arrestin Recruitment Assay

Ligand induced activation of the OTR recruits β-arrestin, a multifunctional protein which mediates receptor internalisation processes and simultaneously stimulates the MAPK transcriptional pathway [226]. A live-cell nanoBRET assay (Promega) was employed to explore the capacity of test compounds to induce recruitment of β-arrestin to the OTR. This assay uses bioluminescence energy transfer (BRET) phenomena to detect protein-protein interactions. In the assay system, the OTR is conjugated to nanoluciferase (Nluc), a luminescence donor protein, whilst β-arrestin is conjugated to an acceptor fluorophore, HaloTag^{618}. In the presence of the Nluc substrate, fumirazine, a glow-type luminescence signal is generated at 460 nm. Re-

cruitment of β-arrestin to the OTR brings the HaloTag^{618} acceptor moiety into close proximity with the luminescence donor Nluc, and a BRET interaction occurs, producing a fluorescence emission at 618 nm (see Figure 2.3). This signal can then be used to measure the extent of protein interaction between the OTR and β-arrestin.

Wild-type HEK293 cells were transiently transfected with plasmids encoding OTR-Nluc and arr2-HaloTag^{618} fusion proteins (see Methods 2.2.2 and 2.3.1 for details). To widen the dynamic range of the assay, the stoichiometry of BRET partners was first optimised with donor dilution and acceptor saturation assays. In dilution experiments, the optimal concentration of BRET donor was determined by sequentially diluting OTR-Nluc against a fixed concentration of arr2-HaloTag^{618}. In acceptor saturation assays, the optimal ratio of donor to acceptor was identified by titrating arr2-HaloTag^{618} against a fixed concentration of OTR-Nluc previously determined in the dilution assay. The optimised transfection conditions used in the final assay are shown in Table 2.2 (see Appendix B, Figure B.3 for optimisation data).

24 h following transfection, cells were detached with trypsin-EDTA 0.25 (% v/v), centrifuged at 1200 g for 5 min, and resuspended in optiMEM supplemented with FBS 4% (v/v). Density was adjusted to 2.2×10^5 cells/mL and arr2-HaloTag^{618} la-

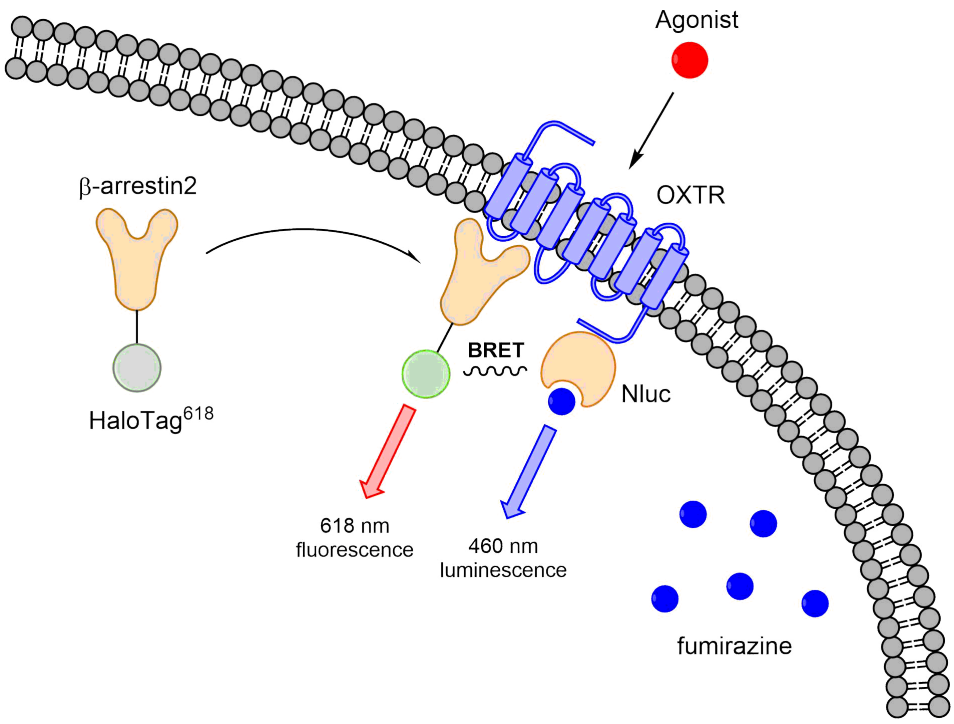

Figure 2.3: Ligand-induced recruitment of labelled β-arrestin2 to the OTR leads to bioluminescence resonance energy transfer from nanoluciferase to the HaloTag^{618} fluorophore. *OTR*: human oxytocin receptor, *Nluc*: nanoluciferase, *BRET*: bioluminescence resonance energy transfer.

Table 2.2: Transfection conditions for bioluminescence resonance energy transfer (BRET) assays.

Donor (µg)	Acceptor (µg)	Carrier (µg)	Total (µg)	D:A Ratio
Donor Dilution Assay				
1	1	0	2	1:1
0.2	1.8	0	2	1:10
0.02	2	0	2	1:100
0.002	2	0	2	1:1000
Acceptor Saturation Assay				
0.02	0.2	1.8	2	1:10
0.02	0.5	1.3	2	1:25
0.02	1	1	2	1:50
0.02	2	0	2	1:100
Optimised DNA Concentrations				
0.02	0.2	1.8	2	1:10

belled by incubating cells for 5 min with either 100 nM HaloTag^{618} ligand (Promega) or DMSO 0.1% (v/v) (control). Following incubation, cells were plated into poly-*L*-lysine coated, white walled, clear bottom 96-well plates (Corning) at a density of 2.2×10^4 cells/well and incubated for 24 h at 37°C, 5% CO_2.

On the day of experiment, test compounds (0.01 nM – 1 µM) in optiMEM supplemented with $MgCl_2$ (5 mM) were added directly to culture media and incubated for 5 min at ambient temperature. 5X fumirazine substrate (Promega) was then diluted into culture media and luminescence signals acquired immediately using a CLARIOStar microplate reader (BMG Labtech) fitted with a linear variable filter monochromator (see Appendix A for instrument settings). Raw luminescence data was converted into ratiometric milliBRET units (mBU) by normalising to the non-variable luminescence at 460 nm emission using Equation 2.4. EC_{50} and E_{max} values were used to evaluate test compound potency and intrinsic efficacy respectively for the β-arrestin recruitment pathway.

$$\frac{\text{618 nm emission}}{\text{460 nm emission}} \times 1000 = \text{BRET Ratio (mBU)} \tag{2.4}$$

2.5.5 Endosomal Trafficking Assay

Recruitment of β-arrestin to the OTR terminates G-protein dependent signalling and initiates internalisation and trafficking of the receptor to early endosomes [180]. To provide another experimental index of ligand-induced OTR internalisation alongside β-arrestin recruitment assays (Methods 2.5.4), we utilised a PathHunter eXpress assay (DiscoverX, CA, USA). This assay provides a quantitative measurement of internalised GPCR protein localised to early endosome using β-galactosidase (β-gal) enzyme fragment complementation. In this system, a 42 amino acid fragment of β-gal is localised to intracellular endosomes, while the larger β-gal fragment is fused to β-arrestin. Stimulation of the OTR results in β-arrestin binding to the receptor, followed by internalisation and trafficking of the receptor/β-arrestin complex to cellular endosomes. This action forces complementation of the β-gal fragments, resulting in the formation of a functional enzyme that is capable of hydrolysing substrate and generating a chemiluminescent signal.

Experimental procedures were conducted by Dr. Eryn Werry of the Kassiou Drug Discovery Lab. U2OS cells expressing the human OTR (supplied by kit manufacturer) were thawed, then seeded into white, poly-*L*-lysine coated 96-well plates (Corning) at a density of 1×10^4 cells/well in AssayComplete^{TM} plating buffer. Cultures were maintained for 48 h at 37°C, 5% CO_2. On the day of the experiment, test compounds (0.1 nM - 10 µM) were dispensed into each well and incubated for 3 h at 20 °C. Following agonist incubation, β-gal luminescent substrate (detection reagent) was prepared according to the manufacturers protocol, then incubated with cells for a further 1 h at 20 °C. Data acquisition was performed using a PHERAStar microplate reader (BMG Labtech) fitted with a luminescence module (see Appendix A for instrument settings). EC_{50} and E_{max} values were used to evaluate test compound potency and efficacy respectively for β-arrestin endosomal trafficking.

2.6 Statistical Analyses

Data represent the mean ± the standard deviation of at least three independent experiments, unless stated otherwise. All statistical analyses were performed using Graphpad Prism 7.0 Software (Graphpad Inc; California, USA).

2.6.1 Ligand Affinity and Binding Kinetics Data

K_i values for test compounds were determined by fitting equilibrium radioligand binding data to a one-site competition binding model (graphpad equation: One site – fit K_i) and analysing via nonlinear regression. Dissociation curves for [^{3}H]-OT were fitted to a one-phase exponential decay model (graphpad equation: Dissociation – one phase exponential decay) and k_{off} determined using nonlinear regression analysis. This parameter was then used to determine [^{3}H]-OT k_{on} using a non-global data fitting method (graphpad equation: Association – one concentration hot). k_{on} and k_{off} rate constants for test compounds were then calculated using previously determined [^{3}H]-OT k_{on} and k_{off} values as input parameters (graphpad equation: Kinetics of competition binding).

2.6.2 Ligand Functional Activity Data

Dose-response data from functional assays (Methods Section 2.5) were fitted to a sigmoidal, four-parameter logistic curve and analysed via nonlinear regression to yield E_{max} EC_{50} and IC_{50} values. For test compounds that did not exhibit agonist or antagonist effects, one-way analysis of variance (ANOVA) with Dunnett's multiple comparison test was used to confirm that the maximum ligand-response did not differ significantly from basal activity. Students t-test (unpaired) was used to determine statistically significant differences between means when comparing two groups.

2.6.3 Ligand Signalling Bias Analysis

A quantitative approach was used to determine if test compounds exhibited ligand signalling bias between the $G\alpha_q$ and β-arrestin coupled signalling pathways, two primary outcomes of OTR activation [154]. To provide a translatable and therapeutically useful measure of ligand bias, the method used to calculate bias factors must be independent of system variables such as membrane receptor density, as well

as altered coupling efficiency to intracellular transduction pathways in different cell types or tissues [227].

To this end, bias factors for each test compound were calculated by first fitting dose-response data from $G\alpha_q$ and β-arrestin signalling assays (Methods 2.5.1 and 2.5.4) to the Black and Leff operational model [228] to yield 'tranduction coefficients' $log\left(\frac{\tau}{K_A}\right)$, which are insensitive to changes in receptor density and encompass key elements required to describe GPCR agonism, namely, affinity (K_A) for the receptor and efficacy (τ) in activating a particular signaling pathway [228]. The operational model was reparametised according to the method of Christopoulos et. al, [229] to allow the direct fitting of dose-response data in Graphpad software using Equation 2.5.

$$E = \text{Basal} + \frac{E_{max} - \text{Basal}}{1 + \frac{\frac{[A]}{10^{logK_A}} + 1}{\frac{10^{logR}}{[A]}}^n} \tag{2.5}$$

Where E is the effect of the ligand, Basal is the response of the system in the absence of agonist, E_{max} is the maximum possible response of the system, $[A]$ is the concentration of agonist, $logK_A$ is the logarithm of the agonist binding dissociation constant, n is the slope of the transducer function and $logR$ is the logarithm of the transduction coefficient $\left(\frac{\tau}{K_A}\right)$. All agonist dose response curves at each pathway were globally fitted to the model with the parameters Basal, E_{max} and n shared between agonists. For full agonists, the $logK_A$ was constrained to a value of zero, whereas for partial agonists this was directly estimated by the curve fitting procedure. To overcome potential variances in $log\left(\frac{\tau}{K_A}\right)$ values obtained in different cellular contexts, $log\left(\frac{\tau}{K_A}\right)$ values for test compounds were normalised to the $log\left(\frac{\tau}{K_A}\right)$ value obtained for a reference agonist, OT, at each pathway using Equation 2.6. Final bias factors for each compound were then calculated by subtracting the difference in normalised $\Delta log\left(\frac{\tau}{K_A}\right)$ values between signalling pathways using Equation 2.7.

$$log\left(\frac{\tau}{K_A}\right)_{\text{compound}} - log\left(\frac{\tau}{K_A}\right)_{\text{oxytocin}} = \Delta log\left(\frac{\tau}{K_A}\right)_{\text{pathway}} \tag{2.6}$$

$$\Delta log\left(\frac{\tau}{K_A}\right)_{G\alpha_q} - \Delta log\left(\frac{\tau}{K_A}\right)_{\text{β-arrestin}} = \Delta\Delta log\left(\frac{\tau}{K_A}\right) \text{(Bias Factor)} \tag{2.7}$$

Chapter 3

Small Molecule Ligands: Derivatives of WAY-267,464

3.1 Introduction and Rationale

The simplicity of small-molecules confers a range of inherent advantages when used as a starting point for drug design. Compared with peptide-based scaffolds, the reduced complexity of small molecules limits the extent of modification possible, streamlining the process of lead optimisation. Small molecule scaffolds are also more amenable to oral delivery and are less susceptible to rapid metabolism than peptides, a property which increases their bioavailability and prolongs the duration of their therapeutic effects *in vivo* [230]. The reduced size and polarity of small molecules also generally indicates a higher propensity for CNS penetration, an important consideration when developing drugs for neuropsychiatric disorders with targets located in the CNS [231]. In addition, the greater ease of synthesis for small molecules relative to peptides often translates to more scalable and commercially viable synthetic procedures, an important factor in translating discoveries into new therapeutics which should be considered at the outset of any drug development program.

For these reasons, our group has been interested in understanding the intricacies surrounding the functional activity of WAY-267,464, one of the very few small-molecule, non-peptide OTR agonists reported in the literature. We have previously published the behavioural profile of WAY-267,464 and found significant pro-social effects (I.P., 100 mg/kg) [195] which were later in-part correlated to $V_{1A}R$ antagonism rather than its oxytocinergic effects [197]. In 2016, we reported the pharmacological binding and efficacy profile of WAY-267,464 along with its first published structure-activity relationship. WAY-267,464 was shown to be a non-selective OTR agonist/$V_{1A}R$ antagonist (OTR $K_i = 230$ nM; $V_{1A}R$ $K_i = 27$ nM; OTR $EC_{50} = 420$ nM; $V_{1A}R$ $IC_{50} = 613$ nM) [219].

Given the incomplete understanding of how OT and AVP signalling systems interact to modulate social behaviour, the non-selectivity of WAY-267,464 confounds the interpretation of studies that seek to delineate the behavioural effects regulated by activation of either receptor in isolation. Furthermore, the large size and polarity of WAY-267,464 is highly unfavourable for CNS penetration, highlighting the possibility that the behavioural effects observed in earlier studies may be mediated by binding to peripherally distributed OTR and $V_{1A}R$s, rather than the desired targets in the CNS. As such, additional structural optimisation is necessary to produce viable, OTR-selective drug candidates based on this scaffold.

WAY-267,464 can be broadly divided into three structural motifs: a heterocyclic

pyrazolo[1,4]-diazepine group, central benzylurea linker, and a pyrazine-resorcinol tail (see Figure 3.1). Whilst the initial disclosure of WAY-267,464 reported the synthesis of multiple analogues, derivatisation was focused on modifications to the heterocyclic pyrazolo[1,4]-diazepine motif or the pyrazine-resorcinol tail moiety. In 2010, Ring et al. performed a structure activity relationship analysis of TC-OT 39, a weak OTR partial agonist which shares structural motifs, including the benzylurea linker, with WAY-267,464 [194]. Whilst their work focused on the truncation of TC-OT 39 and elaboration through hybridisation with AVPR and OTR ligands, the benzylurea component was maintained. Similarly, a structure-activity relationship anaylsis of the OTR ligand LIT-001 by Frantz et al. [196] focused on derivatisation of the heterocyclic head group, but retained the benzylurea linker. As such, the majority of our work has focused on identifying the functional necessity of this central, structurally-conserved motif.

Previous work from our group involved replacing the rigid benzylurea with flexible alkyl tethers of varying lengths (see Figure 3.1). This modification abolished OTR activity and largely diminished OTR binding affinity. Marginal receptor affinity was gained at increasing chain lengths similar in distance to the lead molecule. Whilst deleterious to receptor pharmacology, these modifications were better tolerated at the $V_{1A}R$ and thus resulted in selective $V_{1A}R$ ligands. In addition, removal of hydrogen-bonding capabilities in the pyrazine-resorcinol tail through methyl-ethyl incorporation resulted in a reversal of WAY-267,464 functional activity (resulting in a weak OTR antagonist; IC_{50}= 4 µM), exemplifying the subtleties surrounding the ligand binding properties of the OTR [198].

Considering the lack of published structure-activity relationship studies surrounding the WAY-267,464 molecule and the previously observed subtleties surrounding the flexible alkyl-tethered analogues, the present chapter focused on evaluation of 32 conformationally restricted or truncated WAY-267,464 derivatives, designated as compound library **1** - **8**. Several considerations were necessary in the design of these molecules. Shortened chain lengths limited the number of freely rotatable bonds, minimising overall molecular flexibility. Phenylpiperazine derivatives (**1** – **4**, Figure 3.2) were designed to methodically explore sterically restrained analogues of WAY-267,464 in an attempt to re-establish the OTR activity which was lost upon the introduction of flexibility. For consistency, both methylated and resorcinol analogues were incorporated to correlate with the previous work in a sustained effort towards the identification of a viable OTR pharmacophore. Truncated derivatives, (**5** – **8**, Figure 3.2) were designed to evaluate whether the scaffold can be further truncated and retain affinity at the OTR or $V_{1A}R$, as well as explore the effects of ring-opening on OTR affinity and potency. Unfortunately, a full set of functional

group modifications for (**8**) could not be obtained due to synthesis issues.

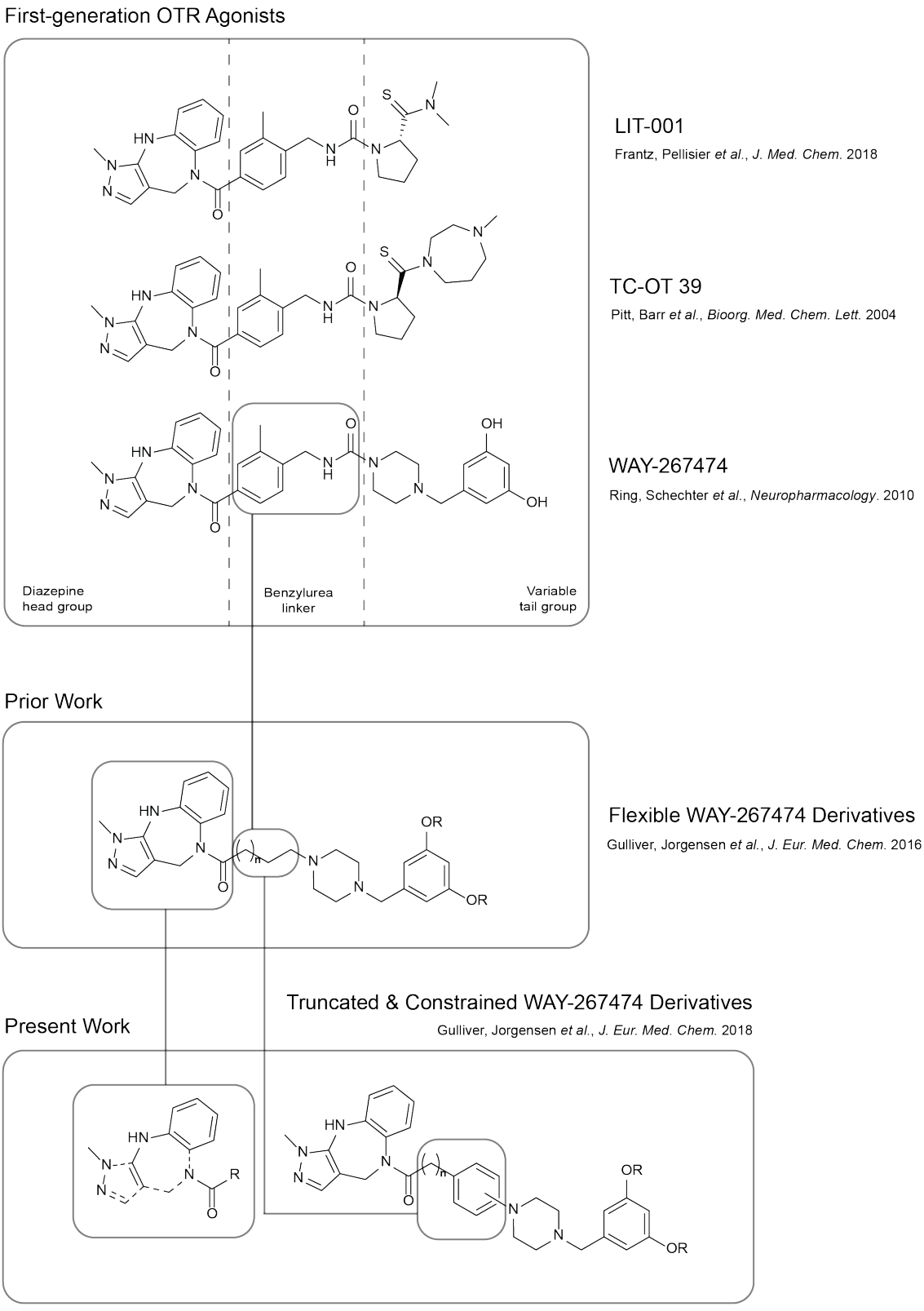

Figure 3.1: Conserved structural features between first-generation non-peptide OTR agonists and our efforts to systematically characterise their pharmacological importance.

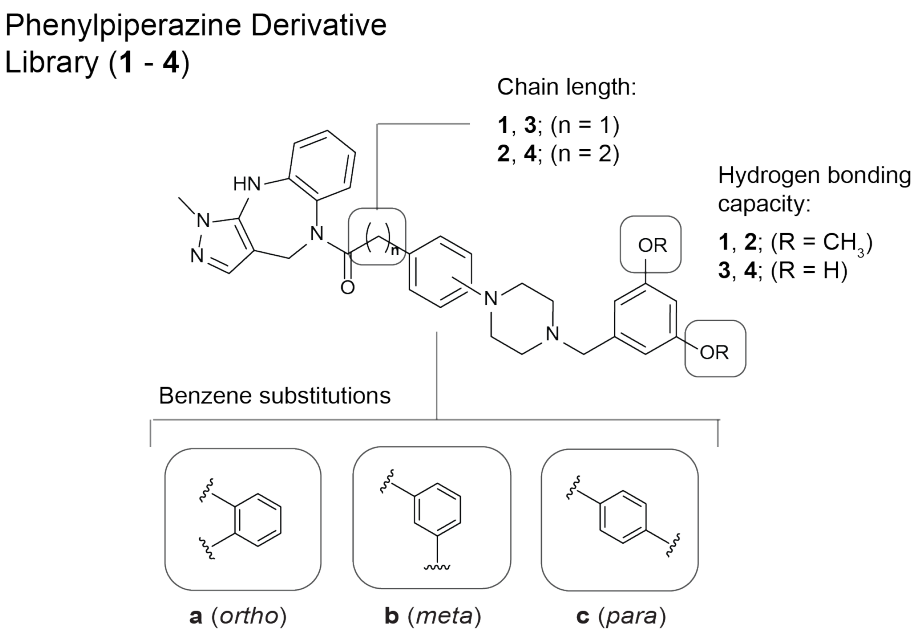

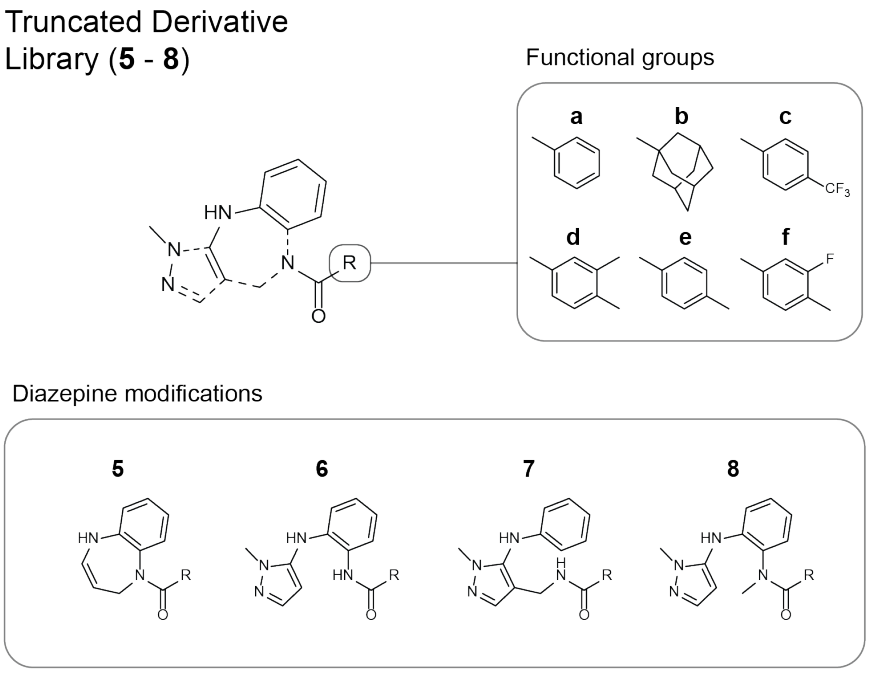

Figure 3.2: Structural modifications in a library of WAY-267,464 derivatives. Compound library **1** – **4** was synthesised to explore the pharmacophoric importance of chain length in the benzylurea linker (**1** and **3**; n = 1, **2** and **4**; n = 2), linker conformation (**1a** - **4a**; *ortho*-, **1b** - **4b**; *meta*-, **1c** - **4c**; *para*-) and hydrogen-bonding in the resorcinol tail (**1** and **2**; R = CH_3, **3** and **4**; R = H). Compound library **5** – **8** was synthesised to determine the effect of truncation and ring linearisation on affinity and potency at the human oxytocin and vasopressin 1A receptors. Compounds were functionalised via the adjacent amide group (**5a** – **8a**; toluene, **5b** – **8b**; adamantyl, **5c** – **8c**; 4-(trifluoromethyl)benzene, **5d** – **8d**; *o*-xylene, **5e** – **8e**; *p*-xylene, **5f** – **8f**; 4-fluoro-3-methylbenzene).

The aim of the present chapter was to characterise the binding affinity and functional efficacy of this library of WAY-267,464 derivatives at the human OTR and $V_{1A}R$. In Section 3.2, the OTR and $V_{1A}R$ affinity of WAY-267,464 derivatives were first evaluated using a competition radioligand binding assay (Methods 2.4.2) to determine K_i values under equilibrium conditions. In Section 3.3, a cell-based functional assay (Methods 2.5.1) was used to index the capacity of WAY-267,464 derivatives to activate, inhibit or allosterically modulate the $G\alpha_q$ signalling pathway at the OTR and $V_{1A}R$.

3.2 Ligand Affinity at the Oxytocin and Vasopressin 1A Receptors

3.2.1 Phenylpiperazine WAY-267,464 Derivatives

Reintroduction of molecular rigidity into the central linker moiety in derivative libraries **1** – **4** abolished OTR binding affinity compared with the parent molecule (summarised in Table 3.1) In contrast, all compounds evaluated in the library bound to the $V_{1A}R$, although with marked differences in affinity extending from the low nanomolar to high micromolar range (Figure 3.3). Restricting the number of freely rotatable bonds in the central linker led to a divergent effect on $V_{1A}R$ affinity. When spacer length (n) = 1 (compounds **1a** - **1c** and **3a** - **3c**), the pattern of arene substitution around the benzene ring determines $V_{1A}R$ affinity in the rank order of *para* > *meta* > *ortho*. Interestingly, when spacer length (n) = 2, (compounds **2a** - **2c** and **4a** - **4c**) and conformational flexibility is increased, this relationship reverses, such that the *ortho*-substituted derivatives display the highest binding affinity relative to *meta*- and *para*-substitutions (Figure 3.3).

Methylation of the 2,4-hydroxyl groups in the resorcinol moiety of the tail region in phenylpiperazine derivatives (**1** - **2**) produced a consistent 3-fold reduction in $V_{1A}R$ affinity when compared with non-methylated derivatives (**3** - **4**). Whilst all modifications in derivative libraries **1** - **4** led to a reduction in $V_{1A}R$ affinity relative to WAY-267,464, ($V_{1A}R$ K_i: 27 ± 3 nM), the extent of this effect varied - the non-methylated, *ortho*-substituted derivative **4a** retained the highest affinity in the series (K_i: 251 ± 33 nM), a value comparable with the parent molecule. Moreover, the lack of detectable affinity at the OTR up to a concentration of 10 µM indicates that compound **4a** displays at least 50-fold greater selectivity for the $V_{1A}R$ over the OTR, compared with the 8-fold $V_{1A}R$ selectivity displayed by WAY-267,464 [195].

3.2.2 Truncated WAY-267,464 Derivatives

Truncation of WAY-267,464 in compound library **5** – **8** led to a total loss of detectable OTR binding, similar to that observed in derivative library **1** – **4** (summarised in Table 3.1). With respect to the $V_{1A}R$, removal of the pyrazole moiety within the diazepine head group (**5a** – **5f**) was well-tolerated, with all compounds in the series displaying some degree of $V_{1A}R$ affinity (Figure 3.4: C,E). In contrast, breaking the central diazepine ring at positions 6, 7 (**6a** – **6f**) or 2 (**7a** – **7f**) introduced a high degree of conformational flexibility to the molecule, leading to a total loss of detectable $V_{1A}R$ binding. Interestingly, breakage of the diazepine at position 6 alone (**8a**, **8d**) did not entirely abolish $V_{1A}R$ affinity (Figure 3.4: D). A comparison between **8d** and its structural analogue **5d**, which contains an identical *o*-xylene functional group, reveals a 2-fold higher $V_{1A}R$ affinity for **8d**, indicating that removal of the pyrazole ring exerts a more detrimental effect on affinity than breakage of the diazepine ring at position 6.

Functionalisation of the amide motif in derivative library **5** with a toluene group (**5a**) produced the lowest affinity $V_{1A}R$ ligand of the series. Replacement with an adamantyl group (**5b**) increased $V_{1A}R$ affinity 3-fold, indicating that the active site of the $V_{1A}R$ may contain a binding pocket capable of accommodating large structural motifs at this position. Substituted benzenes (**5c** – **5f**), however, produced more favourable binding properties than either toluene or adamantyl groups. Of particular interest, inclusion of a methyl group at position 4 (4-methylbenzene, **5e**) produced 6-fold higher affinity than toluene (**5a**) and 2-fold higher affinity than its more electronegative counterpart 4-(trifluoromethyl)benzene, **5c**). Addition of a second methyl group at position 3 (3,4-(dimethyl)benzene, **5d**) led to a small reduction in affinity, whilst an organofluorine at this position generated a 2-fold increase in affinity relative to **5e**, producing the compound with the highest $V_{1A}R$ affinity in this library (3-(fluoro),4-methylbenzene, **5f**) (K_i: 230 ± 33 nM).

3.3 Ligand Functional Activity: $G\alpha_q$ Signalling

Consistent with a lack of observable OTR binding, no derivatives induced $G\alpha_q$ activation of the OTR up to 10 µM concentrations in a cell-based functional assay (summarised in Table 3.1). This lack of intrinsic agonist activity was mirrored at the $V_{1A}R$ despite the capacity for many derivatives evaluated to bind to the $V_{1A}R$ with moderate nanomolar affinity. Moreover, no derivatives were able to inhibit the native $G\alpha_q$ response induced by an EC_{70} concentration of OT or AVP at the OTR or

$V_{1A}R$, respectively, suggesting a lack of detectable competitive antagonism at either receptor. Finally, no derivatives were able influence the $G\alpha_q$ response induced by OT or AVP at either receptor (no significant differences between means relative to EC_{10} concentrations of OT or AVP (control), one-way ANOVA with Dunnett's test, F= 1.673, p=0.2735), indicating that they do not function as positive or negative allosteric modulators of OTR or $V_{1A}R$-mediated $G\alpha_q$ signalling.

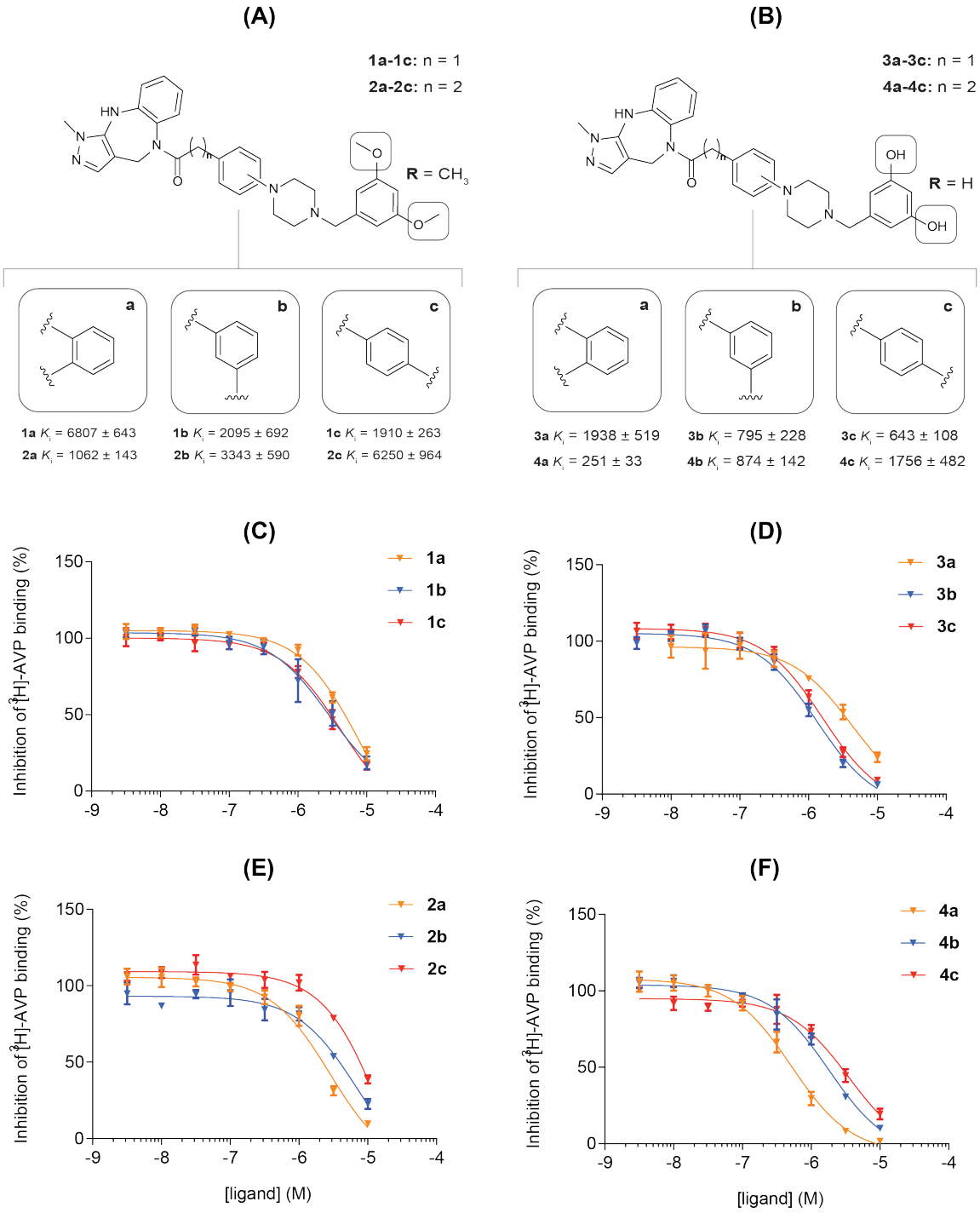

Figure 3.3: Binding affinity of WAY-267,464 1,3-dimethoxybenzene derivatives (**A**,**C**,**E**) and resorcinol derivatives (**B**,**D**,**F**) at the human vasopressin 1A receptor, measured by competitive displacement of radiolabelled arginine-vasopressin ([^{3}H]-AVP) in HEK293 membrane homogenate under equilibrium conditions. Data represent the mean ± the standard deviation of three independent experiments.

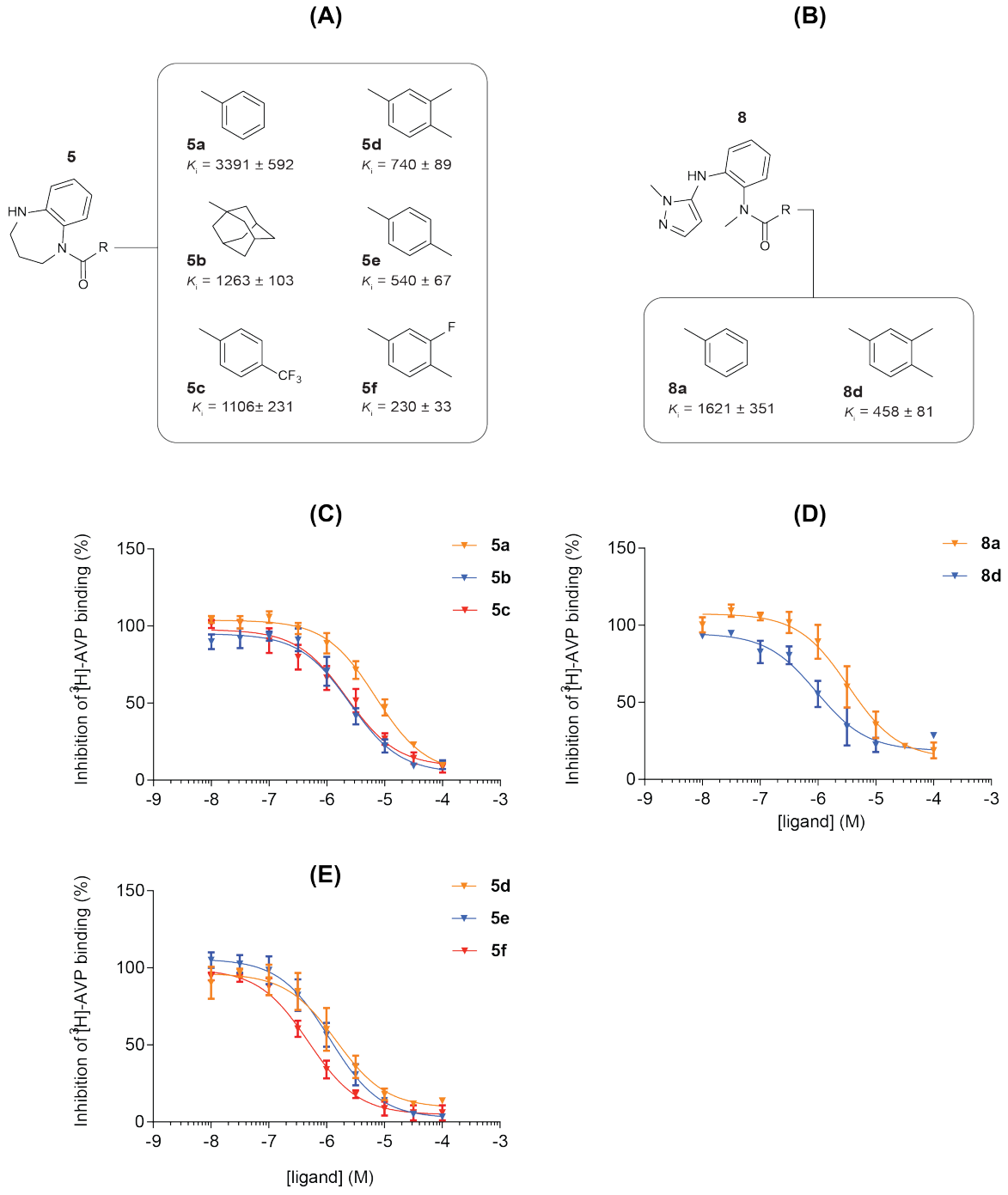

Figure 3.4: Binding affinity of truncated benzazepine WAY-267,464 derivatives (**A**,**C**,**E**) and 2-(pyrazol-5-amine)benzyl derivatives (**B**,**D**) at the human vasopressin 1A receptor, measured by competitive displacement of radiolabelled arginine-vasopressin ([^{3}H]-AVP) in HEK293 membrane homogenate under equilibrium conditions. Data represent the mean ± the standard deviation of three independent experiments.

Table 3.1: Affinity and functional data of a WAY-267,464 derivative library at the human oxytocin receptor (OTR) and vasopressin 1A receptor ($V_{1A}R$). Affinity was measured by competitive displacement of radiolabelled oxytocin or arginine-vasopressin ([^{3}H]-OT/AVP) in HEK293 membrane homogenate under equilibrium conditions. Functional effects were determined using a cell-based homogenous time-resolved fluorescence (HTRF) assay to index activation of the $G\alpha_q$ signalling pathway. Allosteric modulation properties were determined in $G\alpha_q$ functional assays by co-incubating WAY-267,464 derivatives (10 µM) with OT/AVP at EC_{10} concentrations. No significant differences were observed between the $G\alpha_q$ response induced by native ligand ($E_{10)}$ and native ligand + WAY-267,464 derivatives (one-way ANOVA, F= 1.673, p=0.2735). Data represent the mean ± the standard deviation of three independent experiments. *NAM*: negative allosteric modulator, *nd*: not determined, *OT*: oxytocin, *PAM*: positive allosteric modulator.

Compound	Affinity, K_i (nM)		$G\alpha_q$ EC_{50} (nM)		$G\alpha_q$ IC_{50} (nM)		PAM (10 µM)		NAM (10 µM)	
	OTR	$V_{1A}R$	OTR	$V_{1A}R$	OTR	$V_{1A}R$	OTR	$V_{1A}R$	OTR	$V_{1A}R$
6a	>10 000	>10 000	>10 000	>10 000	>10 000	>10 000	No	No	No	No
6b	>10 000	>10 000	>10 000	>10 000	>10 000	>10 000	No	No	No	No
6c	>10 000	>10 000	>10 000	>10 000	>10 000	>10 000	No	No	No	No
6d	>10 000	>10 000	>10 000	>10 000	>10 000	>10 000	No	No	No	No
6e	>10 000	>10 000	>10 000	>10 000	>10 000	>10 000	No	No	No	No
6f	>10 000	>10 000	>10 000	>10 000	>10 000	>10 000	No	No	No	No
7a	>10 000	>10 000	>10 000	>10 000	>10 000	>10 000	No	No	No	No
7b	>10 000	>10 000	>10 000	>10 000	>10 000	>10 000	No	No	No	No
7c	>10 000	>10 000	>10 000	>10 000	>10 000	>10 000	No	No	No	No
7d	>10 000	>10 000	>10 000	>10 000	>10 000	>10 000	No	No	No	No
1a	>10 000	6807 ± 643	>10 000	>10 000	>10 000	>10 000	No	No	No	No
1b	>10 000	2095 ± 692	>10 000	>10 000	>10 000	>10 000	No	No	No	No
1c	>10 000	1910 ± 263	>10 000	>10 000	>10 000	>10 000	No	No	No	No
2a	>10 000	1062 ± 143	>10 000	>10 000	>10 000	>10 000	No	No	No	No
2b	>10 000	3343 ± 59	>10 000	>10 000	>10 000	>10 000	No	No	No	No
2c	>10 000	6250 ± 964	>10 000	>10 000	>10 000	>10 000	No	No	No	No
3a	>10 000	1938 ± 519	>10 000	>10 000	>10 000	>10 000	No	No	No	No
3b	>10 000	795 ± 228	>10 000	>10 000	>10 000	>10 000	No	No	No	No
3c	>10 000	643 ± 108	>10 000	>10 000	>10 000	>10 000	No	No	No	No
4a	>10 000	251 ± 33	>10 000	>10 000	>10 000	>10 000	No	No	No	No
4b	>10 000	874 ± 142	>10 000	>10 000	>10 000	>10 000	No	No	No	No
4c	>10 000	1756 ± 482	>10 000	>10 000	>10 000	>10 000	No	No	No	No
5a	>10 000	3391 ± 592	>10 000	>10 000	>10 000	>10 000	No	No	No	No
5b	>10 000	1263 ± 103	>10 000	>10 000	>10 000	>10 000	No	No	No	No
5c	>10 000	1106 ± 231	>10 000	>10 000	>10 000	>10 000	No	No	No	No
5d	>10 000	740 ± 89	>10 000	>10 000	>10 000	>10 000	No	No	No	No
5e	>10 000	540 ± 67	>10 000	>10 000	>10 000	>10 000	No	No	No	No
5f	>10 000	230 ± 33	>10 000	>10 000	>10 000	>10 000	No	No	No	No

Continued on next page

Table 3.1: Affinity and functional data of a WAY-267,464 derivative library at the human oxytocin receptor (OTR) and vasopressin 1A receptor ($V_{1A}R$). Affinity was measured by competitive displacement of radiolabelled oxytocin or arginine-vasopressin ([^{3}H]-OT/AVP) in HEK293 membrane homogenate under equilibrium conditions. Functional effects were determined using a cell-based homogenous time-resolved fluorescence (HTRF) assay to index activation of the $G\alpha_q$ signalling pathway. Allosteric modulation properties were determined in $G\alpha_q$ functional assays by co-incubating WAY-267,464 derivatives (10 µM) with OT/AVP at EC_{10} concentrations. No significant differences were observed between the $G\alpha_q$ response induced by native ligand ($E_{10)}$ and native ligand + WAY-267,464 derivatives (one-way ANOVA, F= 1.673, p=0.2735). Data represent the mean ± the standard deviation of three independent experiments. *NAM*: negative allosteric modulator, *nd*: not determined, *OT*: oxytocin, *PAM*: positive allosteric modulator.

Compound	Affinity, K_i (nM)		$G\alpha_q$ EC_{50} (nM)		$G\alpha_q$ IC_{50} (nM)		PAM (10 µM)		NAM (10 µM)	
	OTR	$V_{1A}R$	OTR	$V_{1A}R$	OTR	$V_{1A}R$	OTR	$V_{1A}R$	OTR	$V_{1A}R$
7e	>10 000	>10 000	>10 000	>10 000	>10 000	>10 000	No	No	No	No
7f	>10 000	>10 000	>10 000	>10 000	>10 000	>10 000	No	No	No	No
8a	>10 000	1621 ± 351	>10 000	>10 000	>10 000	>10 000	No	No	No	No
8b	nd	nd	nd	nd	nd	nd	nd	nd	nd	nd
8c	nd	nd	nd	nd	nd	nd	nd	nd	nd	nd
8d	>10 000	458 ± 81	>10 000	>10 000	>10 000	>10 000	No	No	No	No
8e	nd	nd	nd	nd	nd	nd	nd	nd	nd	nd
8f	nd	nd	nd	nd	nd	nd	nd	nd	nd	nd
WAY-267,474	230 ± 31	27 ± 3	420 ± 59	>10 000	nd	613 ± 206	nd	nd	nd	nd
OT	4 ± 2	81 ± 25	4 ± 1	122 ± 36	nd	nd	nd	nd	nd	nd

3.4 Discussion

3.4.1 Summary of Findings

A library of non-peptide, WAY-267,464 derivatives were evaluated for affinity, selectivity and functional effects at the human OTR and $V_{1A}R$. Reintroduction of a structurally rigid in central linker motif in phenylpiperazine derivatives (**1** – **4**) abolished OTR affinity, however, $V_{1A}R$ affinity was retained by all compounds in the series. Compounds with hydrogen bonding capability in the tail motif (**3** – **4**) displayed increased $V_{1A}R$ affinity relative to methylated analogues (**1** – **2**), whilst increasing alkyl-chain length (n = 2) in the linker region and an *ortho*-substitution pattern around the central benzene ring were the most favourable modifications for $V_{1A}R$ affinity when compared against shorter linker lengths, *para*- and *meta*- substitutions. Combination of these structural elements in compound **4a** produced the strongest-binding $V_{1A}R$ characteristics of the series (K_i: 251 ± 33 nM) - a 10-fold reduction in $V_{1A}R$ affinity compared with the parent molecule, WAY-267,464 (K_i:

27 ± 3 nM)

Truncation of the WAY-267,464 molecule to the heterocyclic pyrazolo[1,4]-diazepine group (**5** – **8**), also abolished OTR affinity, whilst $V_{1A}R$ binding was retained to produce $V_{1A}R$ selective ligands. A comparison of the full set of functional group modifications in derivative library **5** suggests that 3-(fluoro),4-methylbenzene was the most favourable conjugate for $V_{1A}R$ affinity (**5f**, K_i: 230 ± 33 nM). With respect to heterocyclic group modifications, removal of the pyrazole motif was well-tolerated (derivative library **5**), whilst breakage of the diazepine ring in most cases was detrimental to affinity (derivative library **6** – **7**). An exception to this was seen in derivative library **8**, which retained $V_{1A}R$ affinity despite linearisation of the diazepine ring.

Although $V_{1A}R$ affinity was retained in 60% of derivatives evaluated, no ligands were able to induce $V_{1A}R$-$G\alpha_q$ activation directly, and neither inhibit or allosterically modulate AVP signalling through the $V_{1A}R$ in a cell-based assay. A lack of functional efficacy was mirrored at the OTR, although this outcome correlates with the lack of observable OTR affinity identified for these derivatives in competition radioligand binding assays.

3.4.2 Structure-Affinity Relationships: Phenylpiperazine Derivatives

Prior work from our group demonstrated that substituting the central benzylurea motif in WAY-267,464 with a flexible alkyl-chain linker abolishes OTR affinity, while affinity at the $V_{1A}R$ is retained [198]. Based on this finding, we hypothesised that OTR affinity could be reintroduced in WAY-267,464 derivatives by incorporation of a structurally rigid benzene ring in the linker region (compound library **1** – **4**). Unfortunately, this modification did not restore OTR affinity, indicating that the central urea group, which is highly conserved between first generation OTR ligands, participates in favourable binding interactions in the orthosteric site of the OTR. At the $V_{1A}R$, this modification reduced receptor affinity by 10-70 fold compared to WAY-267,464, indicating that the $V_{1A}R$ orthosteric site is more tolerant of sub-optimal binding partners.

The crystal structure of the OTR bound to the non-peptide antagonist, retosiban, has been recently published [155], providing new insights into the structural conformation and binding interactions that take place in the orthosteric site of the receptor. This study confirmed the existence of a deep and wide extracellular cavity

in the OTR that may have evolved to accommodate the large size of the endogenous neuropeptide ligand. The orthosteric site can be divided into two spatially separated regions: a polar interaction surface formed by a network of residues on TM1 to 6, ECL1,2 and the N-terminus of the receptor, and a hydrophobic hemisphere stretching from TM helices 5 to 7 [154, 155]. Within the OTR binding cavity, retosiban adopts an upright, elongated conformation, interacting with multiple residues located at the distal polar and hydrophobic surfaces. Based on the high sequence homology between the OTR and $V_{1A}R$, and the use of non-peptide antagonist to stabilise the receptor conformation, this reported crystal structure can be used to make inferences about the binding properties of the $V_{1A}R$ and the binding mode of WAY-267,464 derivatives explored in this study.

The enhancement of $V_{1A}R$ affinity with increasing alkyl-linker lengths (compound library **3** – **4**) indicates that WAY-267,464 derivatives may be interacting with spatially separated sites in the $V_{1A}R$, mirroring the extended conformation adopted by retosiban when bound to the OTR. Based on the presence of distal hydrophobic and polar regions in the OTR orthosteric site, it can be postulated that the conserved, planar pyrazolo[1,4]-diazepine group interacts with the TM 5-7 hydrophobic region of the binding pocket, while the resorcinol moiety participates in hydrogen-bonding interactions at the polar surface. In this paradigm, greater flexibility and length in the central linker region would facilitate binding interactions at multiple contact sites, which correlates well with the present findings at the $V_{1A}R$.

The reduced $V_{1A}R$ affinity of *o*-dimethyl analogues (**1** - **2**) compared with their non-methylated resorcinol counterparts (**3** - **4**) indicates that the tail group of WAY-267,464 derivatives participate in hydrogen bonding interactions, potentially with residues located at the polar interaction surface of the OTR or $V_{1A}R$ orthosteric site. This trend was also observed in our earlier work with flexible WAY-267,464 analogues [219], suggesting a conserved interaction that be optimised for in future OTR and $V_{1A}R$ drug development. Amino acid 103, located in ECL1 of the OTR and $V_{1A}R$ has been identified as a key regulator of ligand selectivity between receptors [153, 232] and may be a candidate for this interaction. In the $V_{1A}R$ a polar Tyr^{103} residue could participate in hydrogen bonding interactions with the resorcinal motif of phenylpiperazine derivatives, whereas a non-polar Phe^{103} residue in the OTR would not facilitate the formation of hydrogen bonding networks, thus leading to the $V_{1A}R$ selectivity observed for derivative library **1** - **4** in the present work. The involvement of Phe/Tyr^{103} in WAY-267,464 derivative affinity could be verified using newly developed computational models of ligand docking at the OTR and $V_{1A}R$ [233] in concert with the structural information provided by the newly resolved OTR crystal structure [155].

Interestingly, an inverse relationship was identified between linker length and benzene substitution position with respect to $V_{1A}R$ affinity in derivative library **1** – **4**. When the length of the alkyl-chain was restricted to one carbon atom, *para*-substituted derivatives displayed the highest affinity, followed by *meta*- and *ortho*-substituted derivatives. When the alkyl-chain length was increased to two carbon atoms, this relationship reversed, such that *ortho*-substituted derivatives displayed the highest affinity. It can be hypothesised that in shorter alkyl-linker lengths, *para*-subsitutions are preferenced as they provide the maximum extension of the molecule to reach distal interacting residues, and reduce intramolecular steric hindrance compared with *ortho*-substitutions. In longer alkyl-linker lengths with sufficient extension, the rigid linearity of *para*-substituted derivatives may be disadvantageous for ligand docking compared with the kinked structure formed by *ortho*-substitution. In support of this argument, the 2,5-diketopiperazine core of retosiban also adopts a kinked formation when bound to the OTR [155].

3.4.3 Structure-Affinity Relationships: Truncated Derivatives

Extending on our prior work exploring the importance of the central linker motif of WAY-267,464 molecule, we next evaluated a series of truncated derivatives (**5** – **8**) containing the pyrazolo[1,4]-diazepine functionalised through the adjacent amide group. Interestingly, removal of the central linker and resorcinol tail group abolished OTR binding, but did not substantially impact $V_{1A}R$ affinity. The strongest binding ligand in the truncated derivative library (**5f**, K_i: 230 ± 33 nM) displayed a higher $V_{1A}R$ affinity than **4a** (K_i: 251 ± 33 nM), the strongest binding ligand identified from the phenylpiperazine derivative library, despite being approximately half the size (**5f**: 284.13 g/mol, **4a**: 570.82 g/mol). This finding suggests that the benzylurea and resorcinol moieties are non-essential structural components for $V_{1A}R$ affinity, and thus, truncation provides a strategy to simultaneously halve the molecular weight and enhance the $V_{1A}R$ selectivity of derivatives based on the WAY-267,464 scaffold.

Modifications to the pyrazolo[1,4]-diazepine group revealed valuable information on the structural determinants of affinity in this region of the molecule. Removal of the pyrazole ring was well-tolerated, with derivative library **5** retaining $V_{1A}R$ affinity in the nanomolar range. In contrast, breakage of the diazepine ring in derivative library **6** and **7** abolished both OTR and $V_{1A}R$ affinity, confirming the importance of a bulky and sterically constrained heterocyclic structure in the molecule, which

likely participates in non-polar binding interactions with hydrophobic domains in the receptor orthosteric site. Interestingly, although the diazepine ring was linearised in compound library **8**, these molecules retained $V_{1A}R$ affinity. While this finding defies the affinity trend identified for other linearised, truncated derivatives, one possibility is that the diazepine ring-breaking modification in **8** is more amenable to spontaneous recyclisation than similar modifications introduced in **6** and **7**.

With respect to amide-conjugated functional groups **a** – **f** in truncated derivatives, substituted benzene motifs were preferenced over adamantyl groups for $V_{1A}R$ affinity. A planar, cyclic ring in this position is mirrored in the structurally conserved benzylurea motif of first generation OTR agonists WAY-267,464, TC OT-39 and LIT-001, suggesting that it may form part of the minimum viable pharmacophore of pyrazole[1,4]-diazepine OTR and $V_{1A}R$ agonists [192, 194, 196]. In support of this assessment, our previous work demonstrates that removal or rearrangement of the benzylurea linker in WAY-267,464 derivatives abolishes OTR affinity [198, 219].

3.4.4 Phenylpiperazine and Truncated Derivatives: Functional Activity

Although phenylpiperazine (**1** – **4**) and truncated (**5**, **8**) WAY-267,464 analogues retained $V_{1A}R$ affinity in competition radioligand binding studies, no derivatives were able to influence $V_{1A}R$-coupled $G\alpha_q$ signalling in a cell-based functional assay in either the agonist or antagonist format. While there is a possibility that these molecules are functionally silent – binding to the $V_{1A}R$ but not engaging intracellular signalling partners or interfering with AVP receptor interactions – it is highly improbable that a molecule binding interaction will exert no net effect on receptor conformation or the binding of competing ligands. A more viable explanation is that the potency and signalling efficacy of these derivatives for $V_{1A}R$-mediated $G\alpha_q$ activation or inhibition falls below the detectable limit of the signalling assay used.

We have observed in prior work that the EC_{50} value of non-peptide ligands evaluated in HTRF IP_1 assays used to index $G\alpha_q$ activation can exceed the K_i value determined through competition radioligand binding by as much as 20-fold [195]. Further, unpublished data from our laboratory indicates that in comparison to peptides, small molecule ligands based on the WAY-267,464 scaffold display low efficacy at the OTR and $V_{1A}R$ in cellular functional assays. This indicates that the conformational changes induced in the receptor by the binding of a non-peptide ligand have a lower likelihood of engaging intracellular signalling partners compared with the

endogenous ligands, OT or AVP. The HTRF IP_1 assays used to index $G\alpha_q$ pathway activation measure accumulation of a downstream intracellular signalling molecule, IP_1. As such, low efficacy relative to $V_{1A}R$ binding affinity in phenylpiperazine WAY-267,464 analogues may contribute to the lack of observable $G\alpha_q$ agonism for these compounds at the $V_{1A}R$.

While the lack of agonist effects in these molecules mirrors the pharmacological profile of WAY-267,464 at the $V_{1A}R$, and may be an intrinsic property related to efficacy, the lack of observable antagonism at the $V_{1A}R$ diverges from the functional effects of the parent molecule. This finding may have arisen through factors related to experimental design. The K_i of a ligand is an inherent property which describes compound binding affinity to a receptor in the absence of competition [234]. The influence of competing radioligand concentration ([^{3}H]-AVP) in binding experiments is factored into the calculation of K_i values using the equation of Cheng and Prusoff [234].

$$K_i = \frac{IC_{50}}{1 + \frac{[\text{radioligand}]}{K_d}} \tag{3.1}$$

In contrast to K_i, IC_{50} values determined through functional assays are not an inherent property of the ligand and may vary when experimental conditions are altered. The concentration of [^{3}H]-AVP used in competition radioligand binding experiments was 3 nM - the approximate K_d of AVP determined from saturation binding assays. In contrast, the concentration of competing AVP used in HTRF IP_1 assays was tenfold higher at 30 nM – the EC_{70} value of the ligand determined through HTRF IP_1 agonist assays. By definition, at a K_d concentration of a given ligand, the fractional occupancy of its associated receptor is 50% under equilibrium conditions. At 10x K_d ligand concentrations, receptor occupancy approaches 90%. Thus, the tenfold higher concentration of AVP used in the HTRF IP_1 assay substantially increases competition for $V_{1A}R$ binding sites, and may have masked weak antagonism of the receptor by phenylpiperazine WAY-267,464 analogues. Further studies could experimentally validate this hypothesis by performing HTRF IP_1 assays with a reduced concentration of competing AVP, thereby lowering the concentration threshold at which antagonism of the $V_{1A}R$ by phenylpiperazine derivatives could be observed in this assay.

Alternatively, phenylpiperazine and truncated WAY-267,464 derivatives may be activating other G-protein signalling pathways associated with the $V_{1A}R$ not evaluated in this assay, such as the $G\alpha_s$-cAMP-PKA pathway [235]. Potential activation of

$G\alpha_s$ signalling via the $V_{1A}R$ could be experimentally verified in future studies using cellular functional assays which index $G\alpha_s$ recruitment to the $V_{1A}R$, cAMP production or measure kinase phosphorylation following agonist stimulation. If $G\alpha_s$ activity is detected for the WAY-267,464 derivatives investigated in this study, they may be candidates for further therapeutic development with applications in treating psychostimulant addiction.

3.4.5 Conclusions and Future Directions

Based on the lack of observable functional effects for compound library **1** – **8**, additional structural optimisation will be desirable to produce $V_{1A}R$ ligands that can influence behaviour in a physiologically relevant concentration range. If $V_{1A}R$ antagonism emerges as a property of optimised WAY-267,464 derivatives, then these molecules could be repurposed as AVP-signalling inhibitors, with indications for hyponatremia, congestive heart failure and liver cirrhosis [236–238]. The observation that truncated WAY-267,464 derivatives (**5** – **8**) retain $V_{1A}R$ affinity is a valuable insight in this context, as it suggests that the structural complexity of lead molecules can be reduced to improve bioavailability while also enhancing $V_{1A}R$ selectivity.

The aim of the present chapter was to characterise the pharmacological properties of a WAY-267,464 derivative library at the OTR and $V_{1A}R$, with the objective of identifying novel lead molecules for OTR agonist development. While none of the derivatives characterised here bound to the OTR, our subsequent efforts to optimise the structure of the truncated derivative library **5** - **8** have since yielded novel, non-peptide agonists for the human OTR, which are currently under preclinical development in our laboratory [239].

Chapter 4

Bioactive Metabolites of Oxytocin

4.1 Introduction and Rationale

A growing body of evidence indicates that the products of endogenous OT metabolism are biologically active, and may play important roles in modulating social behaviour, memory and anxiety that are synergistic with, or distinct from the parent molecule [213, 216, 240, 241]. In the CNS, OT is metabolised by peptidases which sequentially cleave residues from the N- and C-termini of the peptide to produce truncated fragments. N-terminal metabolic products, $OT_{1\text{-}7}$ and $OT_{1\text{-}8}$, retain the cyclic core formed by the Cys^1-Cys^6 disulfide bridge of OT, whereas all C-terminal products are linearised via cleavage of the Cys^1-Tyr^2 peptide bond [212, 242].

Biologically active fragments derived from the metabolism of OT could serve as scaffolds in the design of novel OTR ligands. The advantages of this approach include the biological compatibility and straightforward metabolism of peptides into constituent amino acids, which help mitigate adverse effects that may arise from the uncharacterised metabolism of novel small molecules such as the formation of toxic metabolites [243]. In addition, peptide ligands often display superior receptor affinity and selectivity when compared with small molecule ligands, which typically translates to high potency drug candidates with reduced off-target effects [230]. The recent discovery of ligand signalling bias in naturally occurring and synthetic OT peptide analogues provides an additional layer of specificity, facilitating targeted activation of therapeutically desirable intracellular signalling pathways associated with the OTR [48, 162, 203].

The reduced metabolic stability and poor CNS penetration of peptide ligands compared with small molecules remains a caveat to their therapeutic use in neuropsychiatric disorders [230]. Previous efforts to improve the metabolic stability of OT through structural modification have been remarkably successful, producing the long-acting, clinically used OT analogues carbetocin and atosiban, as well as an extensive range of investigative OTR ligands used in animal behavioural research [244]. This suggests that the incorporation of stability-enhancing moeities is a viable strategy to offset the metabolic vulnerability of biologically active OT fragments. In addition, novel strategies to improve the delivery of peptide therapeutics across the blood-brain barrier are currently in development, including nanoparticle-mediated delivery, enhanced transcytosis, osmotic and ultrasound-mediated membrane disruption [245]. If these innovative approaches can overcome the drug distribution obstacle posed by the blood-brain barrier, then the diversity of peptide-based therapeutics targeting CNS-related disorders is likely to expand dramatically, justifying efforts to identify novel, peptide agonists for the OTR.

To identify OT fragments which could serve as lead molecules for further drug development, and gain insight into the potential contribution of OT metabolites toward the behavioural effects of OT, we first comprehensively characterised the pharmacological properties of a library of endogenous OT metabolites (see Table 4.1) by evaluating their affinity, potency and efficacy at the human OTR and $V_{1A}R$. Metabolites evaluated in this series included N-terminal fragments of OT (**9a**, **9b**) which retained the disulfide-bridged cyclic core of the parent molecule, but lack the amidated C-terminal of OT (Gly^9-NH_2), linear C-terminal fragments (**9c** – **9f**), linear fragments lacking both the N- and C- termini (**9g**, **9h**) and linear fragments containing pyroglutamate (**9i**, **9j**), a naturally occurring amino acid containing a lactam ring formed through spontaneous cyclisation of N-terminal glutamine residues *in vivo* [246].

Table 4.1: Sequence information for compound library **9** - peptide fragments derived from the known metabolism of oxytocin. *C (bolded)*: disulfide-bonded cysteine, *(C')*: cysteine dimer (cystine), *Cyt*: cystine, *Glu*: glutamine, *OT*: oxytocin, *pQ*: pyroglutamic acid.

Compound	Sequence	Fragment Size
OT	**C**YIQN**C**PLG-NH_2	$OT_{1\text{-}9}$
9a	**C**YIQN**C**PL	$OT_{1\text{-}8}$
9b	**C**YIQN**C**P	$OT_{1\text{-}7}$
9c	YIQN(C')PLG	$[Cyt^6]$-$OT_{2\text{-}9}$
9d	IQN(C')PLG	$[Cyt^6]$-$OT_{3\text{-}9}$
9e	QN(C')PLG	$[Cyt^6]$-$OT_{4\text{-}9}$
9f	N(C')PLG	$[Cyt^6]$-$OT_{5\text{-}9}$
9g	QN(C')PL	$[Cyt^6]$-$OT_{4\text{-}8}$
9h	N(C')PL	$[Cyt^6]$-$OT_{5\text{-}8}$
9i	*p*QN(C')PLG	$[pGlu^4Cyt^6]$-$OT_{4\text{-}9}$
9j	*p*QN(C')PL	$[pGlu^4Cyt^6]$-$OT_{4\text{-}9}$

4.2 Pharmacological Evaluation of Oxytocin Metabolites

4.2.1 Ligand Affinity at the Oxytocin and Vasopressin 1A Receptors

The OTR and $V_{1A}R$ affinity of compound library **9** was determined using a competition radioligand binding assay outlined previously (see Methods 2.4.2). OT displayed a K_i of 4 ± 2 nM at the OTR, and 66 ± 3 nM at the $V_{1A}R$, consistent with previously reported affinity values [154, 195]. Cyclic N-terminal fragments of OT (**9a**, **9b**) bound to both the OTR and $V_{1A}R$ with affinities in the nanomolar to low micromolar range. Removal of Gly^9-NH_2 of OT in **9a** led to a 260-fold reduction in binding affinity at the OTR, whilst at the $V_{1A}R$ this modification was better tolerated, producing a 31-fold decrease in affinity relative to OT (Figure 4.1: B). Further truncation of the OT molecule through removal of both Gly^9-NH_2 and Leu^8 in **9b** partially restored binding capacity, producing a 60-fold decrease in OTR affinity and 6-fold decrease in $V_{1A}R$ affinity relative to OT at each receptor. (Figure 4.1: C). No binding was detected for linear peptide fragments (**9c** – **9j**) at either the OTR or $V_{1A}R$ (Table 4.2).

4.2.2 Ligand Functional Activity: $G\alpha_q$ Signalling

To characterise the functional effects of fragment library **9** at the OTR and $V_{1A}R$ a cell-based HTRF IP_1 functional assay was used to index ligand-induced activation, inhibition or modulation of $G\alpha_q$ signalling, the major intracellular signaling pathway associated with the OTR and $V_{1A}R$ (see Methods 2.5.1) [154].

In $G\alpha_q$ activation studies, OT displayed a similar receptor selectivity to that observed in affinity studies, with a potency (EC_{50}) of 33 nM ± 3 nM at the OTR and 122 ± 36 nM at the $V_{1A}R$ (Table 4.2). At the $V_{1A}R$, OT was a partial agonist, with a maximal efficacy (E_{max}) 38 ± 8% of the $G\alpha_q$ response induced by the same concentration of AVP. The functional activity of cyclic OT metabolites also mirrored the trend observed with decreasing peptide length in affinity experiments; Removal of the C-terminal Gly^9-NH_2 of OT in **9a** led to an 18-fold reduction in potency and an E_{max} of 34 ± 5% of OT response at the OTR (Figure 4.2: B,D). Exclusion of residues Leu^8 and Gly^9-NH_2 in **9b** partially ameliorated this effect, producing a 12-fold reduction

in $G\alpha_q$ potency and an E_{max} 30 ± 11% of OT response at the OTR. At the $V_{1A}R$, the $G\alpha_q$ response induced by **9a** did not differ significantly from basal activity (*t*-test, unpaired, p=0.6783). **9b** displayed low maximal efficacy, with an E_{max} 5 ± 4% of AVP-induced response. As a consequence of low efficacy, a dose-response curve and EC_{50} value could not be extrapolated for **9b**.

Although linear metabolites **9c** – **9j** did not bind competitively to the OTR or $V_{1A}R$ orthosteric site in affinity assays, functional characterisation was still performed to rule out the possibility of receptor activation mediated by binding to an allosteric site. No linear metabolite (**9c** – **9j**) was able to induce statistically significant $G\alpha_q$ activation above basal activity at either the OTR or $V_{1A}R$ (one-way ANOVA with Dunnett's test: F=2.325, p=0.0719) (Table 4.2). Following agonist evaluation, all metabolites that did not show agonist activity in compound library **9** were also assessed for antagonist effects on $G\alpha_q$ activation at the OTR and $V_{1A}R$. No cyclic or linear metabolite was able to inhibit the $G\alpha_q$ response induced by the native ligands OT or AVP at the OTR or $V_{1A}R$, respectively (Table 4.2).

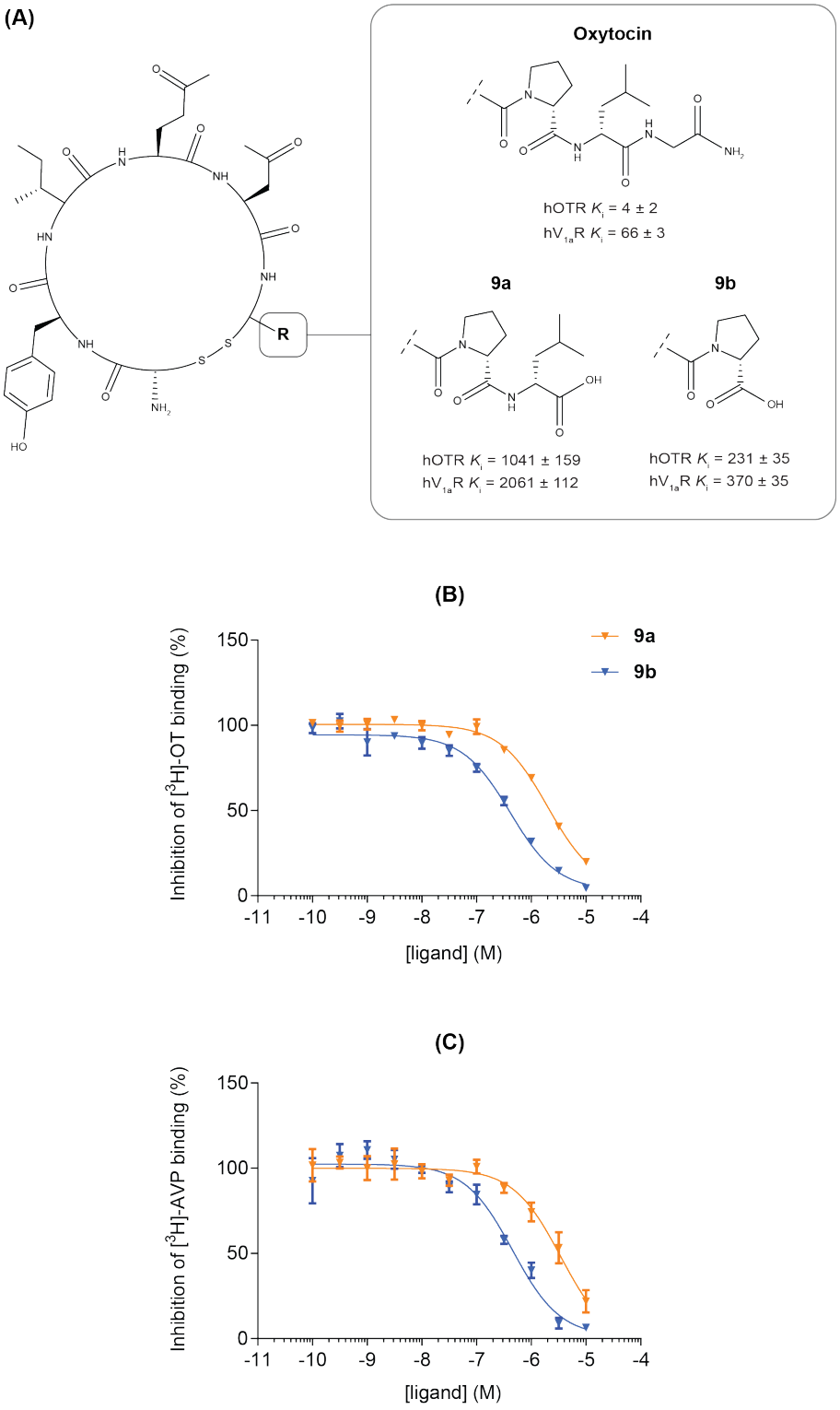

Figure 4.1: Binding affinity curves for cyclic, N-terminal fragments of oxytocin at the **(B)** human oxytocin receptor and **(C)** the human vasopressin 1A receptor, measured by competitive displacement of radiolabelled oxytocin or arginine-vasopressin ([^{3}H]-AVP) in HEK293 membrane homogenate under equilibrium conditions. Data represent the mean ± the standard deviation of three independent experiments.

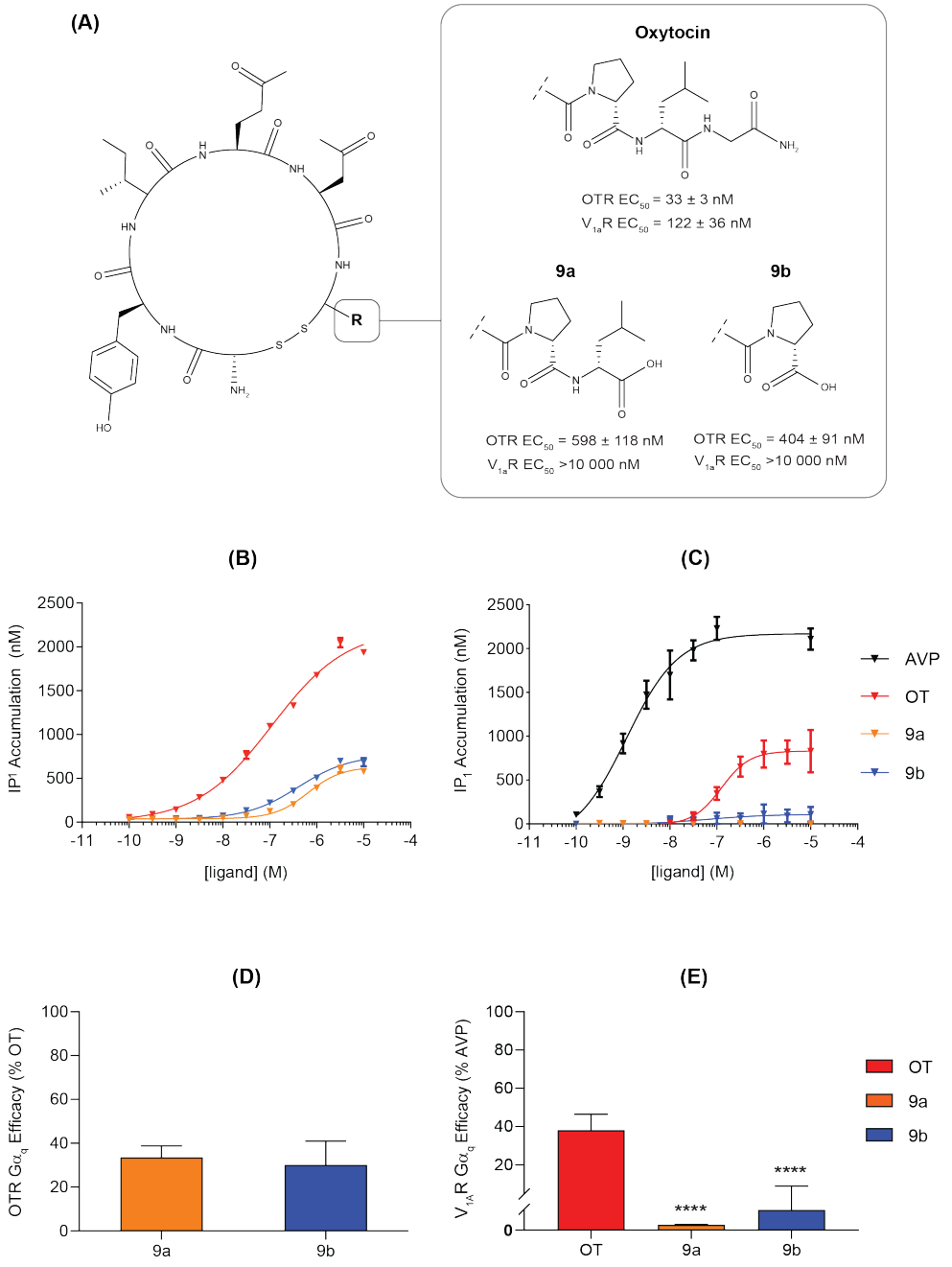

Figure 4.2: **(A)** Functional activity of cyclic, N-terminal fragments of oxytocin at the human oxytocin receptor (OTR) and vasopressin 1A receptor ($V_{1A}R$). Ligand potency and efficacy for the $G\alpha_q$ intracellular signalling pathway was evaluated using a cell-based, homogenous-time resolved fluorescence assay. **(B - C)** Potency of cyclic metabolites for $G\alpha_q$ activation at the OTR and$V_{1A}R$. **(D − E)** Efficacy of oxytocin and cyclic metabolites for $G\alpha_q$ activation at the OTR and $V_{1A}R$. Truncation of oxytocin led to a statistically significant reduction in ligand maximal efficacy at the $V_{1A}R$ (one-way ANOVA with Dunnett's test: F=448.7, $^{****}p$<0.0001) Data represent the mean ± the standard deviation of three independent experiments. *OT*: oxytocin, *AVP*: arginine-vasopressin.

Table 4.2: Affinity and functional data of an oxytocin metabolite library at the human oxytocin and vasopressin 1A receptors. Receptor affinity was measured by competitive displacement of radiolabelled oxytocin or arginine-vasopressin ([^{3}H]-OT/AVP) in HEK293 membrane homogenate under equilibrium binding conditions. Functional effects were determined using a cell-based homogenous time-resolved fluorescence (HTRF) assay to index activation or inhibition of the $G\alpha_q$ signalling pathway. Data represent the mean ± the standard deviation of three independent experiments. *na*: not applicable, *nd*: not determined, *OT*: oxytocin.

Compound	Affinity, K_i (nM)		$G\alpha_q$ EC_{50} (nM)		$G\alpha_q$ E_{max} (% OT/AVP)		$G\alpha_q$ IC_{50} (nM)	
	OTR	$V_{1A}R$	OTR	$V_{1A}R$	OTR	$V_{1A}R$	OTR	$V_{1A}R$
OT	33 ± 3	66 ± 3	4 ± 1	122 ± 36	na	38 ± 8	nd	nd
9a	1041 ± 159	2061 ± 112	598 ± 118	> 10 000	34 ± 5	2 ± 1	nd	> 10 000
9b	232 ± 35	371 ± 35	404 ± 91	> 10 000	30 ± 11	5 ± 4	nd	> 10 000
9c	> 10 000	> 10 000	> 10 000	> 10 000	nd	nd	> 10 000	> 10 000
9d	> 10 000	> 10 000	> 10 000	> 10 000	nd	nd	> 10 000	> 10 000
9e	> 10 000	> 10 000	> 10 000	> 10 000	nd	nd	> 10 000	> 10 000
9f	> 10 000	> 10 000	> 10 000	> 10 000	nd	nd	> 10 000	> 10 000
9g	> 10 000	> 10 000	> 10 000	> 10 000	nd	nd	> 10 000	> 10 000
9h	> 10 000	> 10 000	> 10 000	> 10 000	nd	nd	> 10 000	> 10 000
9i	> 10 000	> 10 000	> 10 000	> 10 000	nd	nd	> 10 000	> 10 000
9j	> 10 000	> 10 000	> 10 000	> 10 000	nd	nd	> 10 000	> 10 000

4.3 Discussion

4.3.1 Summary of Findings

A compound library (**9a** – **9j**) comprised of peptide fragments of the OT molecule were assessed for affinity, selectivity and functional activity at the human OTR and $V_{1A}R$. Removal of the Cys^1 residue in **9c** – **9i** produced linearised C-terminal fragments that did not bind to or activate either the OTR or $V_{1A}R$. In contrast, N-terminal OT fragments that retained the cyclic motif (**9a** – **9b**) bound to and activated both receptors with nanomolar affinity, suggesting the conserved, disulfide-bridged cyclic core of OT and AVP is a critical determinant of ligand affinity and signalling efficacy.

Binding interactions between cyclic OT metabolites and the OTR were highly sensitive to change, with truncation of the molecule producing 60-260 fold reductions in OTR affinity relative to the parent compound in **9a** and **9b**, respectively. This effect was less pronounced at the $V_{1A}R$ (6-31 fold decrease in **9a** and **9b** affinity relative to OT), where interactions between OT and the receptor are weaker than those with the OTR. The relative hydrophilicity of the C-terminal of the ligand influenced affinity and potency. Ligands containing a hydrophilic Gly-NH_2 or Pro residue (OT, **9b**) at the C-terminal of the molecule bound with substantially higher affinity than those with a strongly hydrophobic amino acid (Leu, **9a**) at both receptors.

Cyclic OT metabolites (**9a** – **9b**) acted as partial $G\alpha_q$ agonists at the OTR, with potency 100-150 fold lower than OT, and maximal efficacies 30 – 35% of the OT-induced response. At the $V_{1A}R$, **9a** and **9b** were neither active as agonists or antagonists of AVP-induced $G\alpha_q$ signalling. In line with the lack of observable binding at the OTR or $V_{1A}R$, no linear OT metabolites (**9c** – **9i**) were able to induce or antagonise $G\alpha_q$ signalling at either the OTR or $V_{1A}R$.

4.3.2 Cyclic and Linear Metabolites: Receptor Affinity

The OTR and $V_{1A}R$ residues that interact with OT and other peptide ligands have been investigated by means of biochemical, pharmacological, molecular modelling and site-directed mutagenesis approaches, allowing inferences to be made about receptor interactions with the OT metabolites evaluated in compound library **9**. The binding modality for OT and structurally related peptide agonists at the OTR

spans across residues in the N-terminus, extracellular loop ECL1 and transmembrane domains TM2-7 of the receptor, which are spatially arranged to form a central binding cavity on the extracellular surface [154, 247–250].

Site-directed mutagenesis studies have identified the residues Arg^{34}, Phe^{103}, Tyr^{209} and Phe^{284} as particularly important determinants of receptor affinity and ligand selectivity in the OTR [158, 232, 251, 252]. Arg^{34}, located in the N-terminus of the receptor, is conserved between the OTR/AVPR family and thought to play a role in non-selective ligand recognition via interactions with residues 7 - 9 in native peptide ligands [251]. Phe^{103} (Tyr^{115} in $V_{1A}R$) is found in ECL1, and is a determinant of ligand selectivity that interacts with the variable residue at position 8 of the peptide ligand (Ile^8 in OT, Arg^8 in AVP) [158, 252]. Tyr^{209} and Phe^{284} are evolutionarily conserved residues located in transmembrane domains TM5 and TM6 of the central binding cavity, which interact with aromatic or hydrophobic residues retained at position 2 and 3 in the cyclic core of OT and AVP [232]. Based on this information, it can be hypothesised that the cyclic core formed by residues 1 – 6 of OT and AVP may extend into the TM2-7 binding cavity, facilitating interactions between the ligand and Tyr^{209}/Phe^{284} residues in the receptor. Meanwhile, the linear tripeptide tail formed by residues 7 – 9 of OT and AVP extends to distal sites, interacting with Arg^{34}, Phe^{103} and other residues in extracellular domains of the receptor.

Truncation of the tripeptide tail of OT in **9a** and **9b** led to a dramatic reduction in OTR and $V_{1A}R$ affinity, but did not entirely abolish binding at either receptor, suggesting that interactions between residue 7 – 9 and the receptors are not a critical determinant of ligand affinity. Truncation of residues 7 – 9 also reduced the OTR binding selectivity of **9a** and **9b**, supporting earlier evidence from site-directed mutagenesis studies suggesting that the tripeptide tail of OTR and $V_{1A}R$ ligands are involved in ligand recognition [247]. In contrast to **9a** and **9b**, **9c** – **9j** were linearised through removal of the Cys^1-Cys^6 disulfide bridge. This modification led to a total loss of OTR and $V_{1A}R$ affinity, indicating that a sterically constrained cyclic moiety is a crucial determinant of affinity for peptide ligands at both receptors. The wide extracellular cavity which forms the orthosteric site of the OTR and $V_{1A}R$, identified through X-ray crystallography and molecular modelling, may have evolved to accommodate this bulky cyclic component, which is also present in the endogenous ligands. A six-membered ring is conserved in evolutionary antecedents of OT and AVP (isotocin, mesotocin, vasotocin) and all clinically used peptide OTR agonists (carbetocin, atosiban, demoxytocin), which would seem to confirm the central importance of this motif.

The finding that linear C-terminal fragments of OT do not bind to the OTR or $V_{1A}R$

sheds an interesting light on a recent animal behavioural study by Moy et al. [216], where it was found that the linear metabolite $OT_{4\text{-}9}$ (corresponding to **9e**) exerted a dose-dependent positive effect on social exploration in a mouse model of ASD. The OT analogue, carbetocin, and non-peptide OTR agonist TC-OT 39 were also evaluated, but failed to elicit prosocial effects in this behavioural assessment. Although the receptor pharmacology of $OT_{4\text{-}9}$ at the OTR and $V_{1A}R$ was not reported in this study, the authors noted the possibility that $OT_{4\text{-}9}$ may be acting through a target external to the OTR. An earlier investigation of OT metabolism by Burbach et al. also identified $OT_{4\text{-}9}$ as a bioactive metabolite with potent effects in attenuating passive avoidance behaviour in male rats, but did not disclose information on receptor affinity [213]. The lack of detectable OTR or $V_{1A}R$ affinity for $OT_{4\text{-}9}$ (**9e**) in the present study suggests that the OTR/AVPR family is not the target of $OT_{4\text{-}9}$, raising the possibility that this metabolite is exerting prosocial behavioural effects through an undetermined drug target in the CNS. Another linear product of OT metabolism – $OT_{7\text{-}9}$, (MIF-1) - is known to bind multiple targets in the brain, inhibiting μ-opioid receptor activation and acting as a positive allosteric modulator of dopamine receptors, which provides further evidence that linear OT metabolites retain biological activity and are capable of interacting with other class-A GPCRs [217, 218]. These findings strongly support the possibility of a novel and uncharacterised mechanism through which linear, C-terminal OT metabolites such as $OT_{4\text{-}9}$ are exerting behavioural effects.

4.3.3 Cyclic Metabolites: Functional Activity

Cyclic, N-terminal OT fragments **9a** and **9b** exhibited maximal efficacy values 30 – 35% of OT-induced $G\alpha_q$ response at the OTR. This suggests that truncation of $Gly^9\text{-}NH_2$ of OT in **9a** impairs interactions between the C-terminal of the peptide and residues of the OTR that mediate conformational changes necessary for signal transduction, thus negatively impacting ligand efficacy. The finding that removal of Leu^8 in **9b** has no additional negative effect on OTR efficacy suggests that the relative hydrophobicity of the residue at the C-terminal of the peptide is an important determinant of ligand-OTR interactions. Both OT and **9b** contain relatively hydrophilic C-terminal residues ($Gly^9\text{-}NH_2$, Pro^7) in comparison to **9a**, which contains a strongly hydrophobic C-terminal Leu^8 residue. OT displayed substantially higher potency for $G\alpha_q$ pathway activation than **9a**, and a similar, though not statistically significant trend was observed for **9b**.

The relative hydrophilicity of the residue in position 8 of OT and analogues has

also been reported to influence preferential activation of specific intracellular signalling pathways associated with the OTR. Naturally occurring and synthetic OT analogues which contain a hydrophilic Pro^8 residue in place of the hydrophobic Leu^8 in OT display ligand bias, with a reduced propensity for β-arrestin recruitment compared with $G\alpha_q$ signalling induction in cell-based expression systems [36, 48]. This indicates that the tripeptide tail of OTR agonists participates in receptor interactions which facilitate β-arrestin mediated endocytosis and subsequent desensitisation. Removal of the tripeptide C-terminal in **9a** and **9b** may therefore be a strategy to reduce β-arrestin recruitment to the OTR and prolong therapeutic efficacy, a possibility which warrants further investigation.

At the $V_{1A}R$, the maximal efficacy of OT was found to be 38% of AVP-induced $G\alpha_q$ response, confirming that OT acts as a partial $V_{1A}R$ agonist. This reduction in efficacy is in concordance with the established pharmacology of OT at the $V_{1A}R$, and can be attributed to the substitution of aromatic Phe^3 and polar Arg^8 residues in AVP with hydrophobic Ile^3 and Leu^8 residues in OT [253]. In comparison, cyclic metabolites **9a** and **9b** displayed no intrinsic efficacy for $G\alpha_q$ activation at the $V_{1A}R$. This suggests that C-terminal truncation of OT further impacts ligand-$V_{1A}R$ interactions, producing agonists with efficacy so low that they are essentially inactive at the $V_{1A}R$ with respect to the $G\alpha_q$ signalling pathway. The further finding that **9a** and **9b** do not antagonise AVP signalling through the $V_{1A}R$ indicates that cyclic N-terminal fragments of OT are functionally-selective, OTR partial agonists.

4.3.4 Metabolite Bioactivity in the Physiological Context

Biological activity in OT metabolites may have evolved to facilitate prolonged activation of OT-associated signalling networks in the CNS following proteolytic degradation of the parent molecule. Cyclic N-terminal fragments and linear C-terminal products of OT metabolism are able to elicit robust behavioural changes *in vivo*, suggesting that the behavioural effects attributed to OT may actually result from the combined signalling of OT and coexisting downstream metabolic products, which vary in concentration over time [242]. As N- and C-terminal degradation of OT is catalysed by different classes of peptidases, the tissue-specific distribution and expression level of these proteins could determine whether cyclic or linear OT metabolites are predominant in different regions of the CNS and periphery, potentially driving divergent signalling outcomes. For example, OT metabolism in liver, kidney and endometrial tissue is catalysed primarily by placental leucine aminopeptidase (P-LAP), which increases in expression during pregnancy, and produces linear C-

terminal OT fragments [254–256]. In contrast, previous studies have found cyclic N-terminal fragments $OT_{1\text{-}8}$ and $OT_{1\text{-}7}$ (**9a** and **9b**) to be the most prevalent metabolic products in CNS-derived synaptic membranes following incubation with OT [242].

Although the peptidase responsible for C-terminal degradation of OT in the CNS has not been characterised, an early investigation by Burbach et al. identified a C-terminal cleaving peptidase with high expression in rat brain limbic structures, which is a putative catalyst for this metabolic pathway *in vivo* [212]. C-terminal OT fragments can be detected after 1 h of incubation at 37 °C, and increase in concentration after 3 h, indicating that the biological half-life of these metabolites in the CNS may exceed that of OT [212]. If cyclic N-terminal metabolites are prevalent in the CNS and are not rapidly degraded by peptidases, as the literature suggests, then the altered pharmacology of **9a** and **9b** relative to OT may translate to different OTR signalling outcomes *in vivo*. Although the vast majority of research efforts have been focused on characterisation of linear C-terminal OT fragments, one investigation of cyclic fragment $OT_{1\text{-}8}$ (**9a**) found that in relation to OT, this metabolite exerted equal effects on passive avoidance and addictive behaviour, greater effects on grooming and no effect on penile erection or uterine contraction, highlighting the subtleties surrounding the relationship between OTR signalling and behaviour [257].

One possibility is that the greater OTR selectivity of cyclic OT fragments **9a** and **9b** may have evolved to facilitate selective activation of OTR-associated pathways in cortico-limbic circuits where the $V_{1A}R$ is also co-expressed. It is well established that OT and AVP signalling systems exert opposing influences on some aspects of behaviour [258–260]. For example, OT attenuates fear expression in the central nucleus of the amygdala, whereas AVP facilitates fear expression via distinct but overlapping neuronal populations that express the OTR or $V_{1A}R$ [256, 261]. Divergent effects between OT and AVP can also be seen in relation to memory consolidation and retrieval, avoidance behaviour and aggression [259, 260, 262]. In this light, the OTR selectivity of cyclic OT metabolites **9a** and **9b** may mitigate the undesirable effects mediated by non-selective activation of the $V_{1A}R$ by OT *in vivo*.

Although the findings of the present study confirm that linear metabolites (**9c** – **9j**) do not act via the OTR or $V_{1A}R$, there is extensive evidence that C-terminal fragments of OT are produced in the CNS and exert discernible effects on behaviour. Incubation of OT with synaptic membranes leads to the production of linear OT fragments, with $OT_{4\text{-}9}$ and $OT_{5\text{-}9}$ the most prevalent linear metabolites after 3 h incubation at 37 °C [213]. Enzymes of the leucyl-aminopeptidase family, which produce linear OT metabolites, are present throughout the CNS, with high expression

density in the medial hypothalamus, the site of OT synthesis, pointing towards a role in metabolic regulation of OT [212, 263]. Linear metabolites produced via this pathway have been implicated in the regulation of multiple behavioural domains associated with OT. The antidepressant effects of OT in mice are dependent on the presence of insulin-regulated aminopeptidase (IRAP), a neuronally expressed homologue of P-LAP [263]. In one investigation, OT was unable to ameliorate learned helplessness in *IRAP*$^{-/-}$ mice during the forced swim-test, while in another study, a similar effect was found in this behavioural model following co-infusion of OT and angiotensin-IV, an IRAP inhibitor [215, 264].

These findings strongly suggest that the antidepressant-like effects attributed to OT may actually be mediated by a linear C-terminal fragment produced via IRAP degradation of OT in the CNS. C-terminal fragments [*p*Glu^4,Cyt^6]-OT$_{4\text{-}9}$ and [*p*Glu^4,Cyt^6]-OT$_{4\text{-}8}$ have also been reported to exert potent effects on passive avoidance and social preference in animal behavioural models, providing further evidence that linear OT metabolites regulate important physiological functions in the CNS [216, 265]. The lack of OTR or $V_{1A}R$ affinity determined for OT$_{4\text{-}9}$ and OT$_{5\text{-}9}$ (**9e**, **9f**) in the present study indicates that these behavioural are mediated by an uncharacterised drug target.

4.3.5 Conclusions and Future Directions

In summary, a library of peptide fragments derived from OT (**9a** – **9j**) were evaluated for biological activity at the OTR and $V_{1A}R$ in cell-based expression systems. Cyclic N-terminal fragments **9a** and **9b** were found to be partial agonists for the $G\alpha_q$ pathway at the OTR, and neither activated or inhibited $G\alpha_q$ signalling through the $V_{1A}R$, indicating that they are functionally-selective OTR ligands. Structure activity relationship analyses of **9a** and **9b** suggest that the linear tripeptide tail in OT (residues 7 – 9) is not a crucial determinant of affinity, but strongly influences $G\alpha_q$ efficacy at both receptors, and that hydrophobic residues are preferenced in this region of the molecule. Linear C-terminal fragments **9c** – **9j** did not bind to the OTR or $V_{1A}R$, and neither activated or inhibited endogenous ligand signalling through either receptor, suggesting an unidentified drug target is mediating the behavioural effects identified for linear OT metabolites in previous studies.

Based on these promising preliminary findings, **9a** and **9b** were selected for OTR lead development in the following chapter. While these metabolites achieve greater OTR functional selectivity than OT, mitigating issues of $V_{1A}R$ crosstalk, both molecules are predicted to display limited metabolic stability *in vivo*. As such, a key objec-

tive in subsequent lead development was to incorporate structural elements in the molecule which could reduce the accessibility of peptidases, thus reducing susceptibility to degradation.

Identification of novel drug targets for linear metabolites **9c** – **9j** was beyond the scope of the present investigation, but still represents an intriguing avenue for further research. The behavioural effects elicited by $OT_{4\text{-}9}$ have been repeatedly demonstrated in animal models, strongly supporting the possibility of uncharacterised signalling pathways which could be targeted to modulate social behaviour. Identification of drug targets for linear OT metabolites could be achieved using a combination of high-throughput affinity screening, cellular thermal shift assays, proteomics and gene expression analysis [266–268]. After the selection of putative targets based on the primary screening results, cell-based expression systems could be constructed for each drug target candidate, and the pharmacology of linear OT metabolites evaluated using *in vitro* affinity and functional assays.

Chapter 5

Structural Modification of Bioactive Oxytocin Metabolites

5.1 Introduction and Rationale

Pharmacological characterisation of an OT metabolite library in Chapter 4 revealed that the macrocycle motif formed by residues 1 – 6 of the OT peptide sequence is a crucial determinant of ligand affinity at both the OTR and $V_{1A}R$. Truncation of the C-terminal linear sequence formed by Pro^7-Leu^8-Gly^9-NH_2 residues in OT produces ligands that bind to both the OTR and $V_{1A}R$, but which are functionally selective agonists for OTR-mediated $G\alpha_q$ signalling, neither activating the $V_{1A}R$-$G\alpha_q$ pathway at a detectable level in HTRF IP_1 assays or inhibiting AVP-induced $G\alpha_q$ signalling (**9a** and **9b**).

Most peptide and small-molecule OTR agonists reported in the literature display low selectivity between the OTR and $V_{1A}R$ [89]. The $V_{1A}R$ is highly expressed in limbic regions of the CNS, with spatial distribution patterns that overlap closely with OTR expression [269]. As such, off-target activation or inhibition of the $V_{1A}R$ by OT is a confounding factor in studies exploring the relationship between OTR signalling and behaviour, and may be a source of adverse health outcomes in clinical contexts. $G\alpha_q$ signalling is the predominant pathway associated with the $V_{1A}R$ in cell-based expression systems and *in vivo* [270, 271]. As OTR-selective agonists, **9a** and **9b** represent an opportunity to mitigate non-selective activation of $V_{1A}R$-mediated $G\alpha_q$ signalling, a key issue limiting the utility of OT as a therapeutic agent and investigative tool.

Truncation of the linear C-terminal sequence and retention of the cyclic motif of OT in **9a** and **9b** confers further advantages that may improve the metabolic stability, absorption and distribution of these molecules, including reduced molecular weight, polar surface area and greater conformational rigidity relative to the parent molecule [272, 273]. Cyclisation of peptides forms a bulky secondary structure, which reduces the accessibility of peptidases in comparison to linear peptide sequences [274]. Cyclic peptides also have a propensity to form reversible intramolecular hydrogen bonds (IMHBs) in non-polar environments, such as lipid membranes. IMHBs form between polar side chains and functional groups within the peptide backbone of the ring structure, improving passive permeability in non-polar environments by reducing the exposed polar surface area (EPSA) of the peptide [275]. One such example is the endogenous peptide cyclosporin-A, which can adopt different conformational states depending on the composition of the solvent environment [276]. cyclosporin-A retains sufficient polarity to bind specifically to its biological target, but can mask polarity via IMHB formation to traverse lipid membranes. As such, cyclosporin-A is highly permeable as measured by the EPSA method (EPSA = 70) [277], with

high oral bioavailability relative to other peptide drugs [278]. Removal of the linear C-terminal sequence and retention of the cyclic motif in **9a** and **9b** may therefore represent an opportunity to structurally optimise the OT molecule whilst maintaining the capacity to form IMHBs that could influence the passive permeability or pharmacological properties of the ligand.

Based on these predicted properties, compounds **9a** and **9b** were selected as lead molecules for further development. A key consideration in subsequent optimisation efforts was to introduce motifs that may enhance the metabolic stability of the structurally important cyclic motif formed by residues 1 – 6 of the peptide ligand sequence. The amide-bonded peptide backbone is the natural substrate of many classes of proteolytic enzymes. As such, metabolic instability is an inherent property of peptide ligands. In the human body this property is favourable, as it facilitates degradation and recycling of endogenous proteins, prevents the accumulation of toxic protein aggregates, and provides temporal regulation of signalling peptides. From a therapeutic perspective, however, metabolic instability substantially reduces the bioavailability and efficacy of exogenously-administered peptides. As discussed previously, OT metabolism in the CNS is catalysed by peptidases which sequentially cleave amino acids from the N- and C-termini of the molecule [213, 242]. Linearisation of the peptide, which could be catalysed *in vivo* either by aminopeptidase-mediated cleavage of the Cys^1-Tyr^2 peptide bond, or reduction of the Cys^1-Cys^6 disulfide bridge, results in metabolites which do not bind or activate the OTR (as demonstrated in Chapter 4). Preventing linearisation of the molecule was thus critical in designing effective OTR ligands based on the scaffold of **9a** and **9b**.

The literature contains numerous examples of structural modifications that successfully stabilise the disulfide bond in OT analogues without compromising biological activity [199, 200, 279], therefore we instead chose to focus our efforts on modification of the peptide backbone at the N and C-termini, an approach which has previously demonstrated success in reducing the proteolytic susceptibility of many classes of peptide drugs, [280]. These modifications were integrated in the design of compound series **10** – **12** (Table 5.1). Compounds **10a**, **11a** and **12a** contain methylation of the Tyr^2 residue α-carbon, a modification which has been shown to reduce aminopeptidase accessibility and improve the membrane permeability of peptide drugs [281]. Compounds **10b**, **11b** and **12b** are modified to incorporate the β-isomer of Tyr^2, which introduces a methylene group into the peptide backbone, reducing proteolytic cleavage of the N-terminal amide bond [282]. Compounds **11c** and **12c** are amidated at the C-terminal residue (Leu^8 in **11c**, Pro^7 in **12c**), a modification that protects the molecule from carboxypeptidase-mediated degradation,

and which has been shown

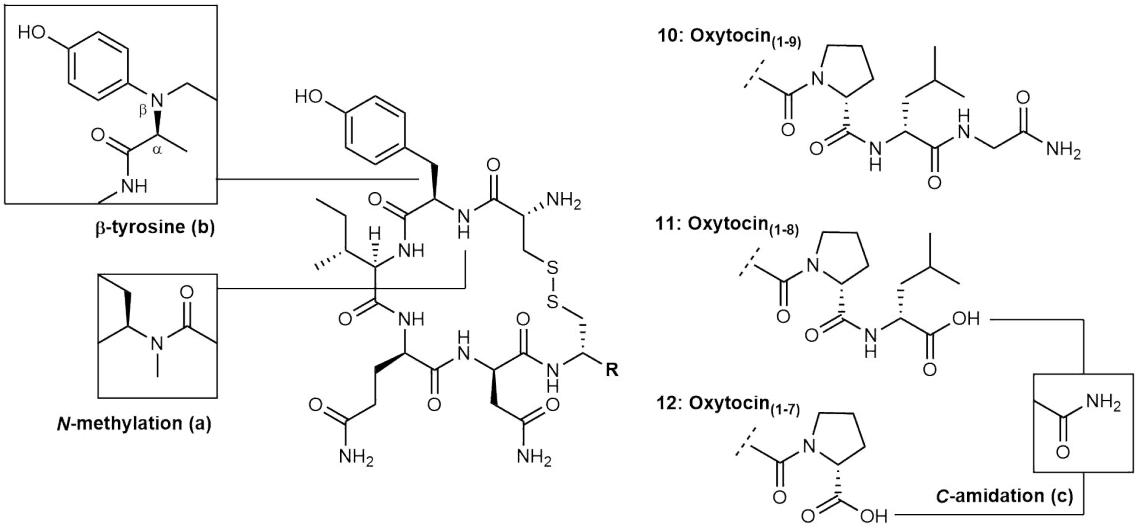

Compound	Fragment length	Sequence	Modification
OT	1 - 9	CYIQNCPLG-NH_2	none
9a	1 - 8	CYIQNCPL	none
9b	1 - 7	CYIQNCP	none
10a	1 - 9	C(*MeY*)IQNCPLG	*N*-methylation
10b	1 - 9	C(βY)IQNCPLG	β-tyrosine[2]
11a	1 - 8	C(*MeY*)IQNCPL	*N*-methylation
11b	1 - 8	C(βY)IQNCPL	β-tyrosine[2]
11c	1 - 8	CYIQNCPL-NH_2	*C*-amidation
12a	1 - 7	C(*MeY*)IQNCP	*N*-methylation
12b	1 - 7	C(βY)IQNCP	β-tyrosine[2]
12c	1 - 7	CYIQNCP-NH_2	*C*-amidation

Table 5.1: Putative stability-enhancing structural modifications incorporated into full-length oxytocin and cyclic, N-terminal fragments of the peptide sequence. Compounds designated (a) are methylated at the α-amine carbon of the cysteine[1]-tyrosine[2] peptide bond. Compounds designated (b) are substituted with the β-isomer of tyrosine[2]. Compounds designated (c) are amidated at the carboxyl terminus of the peptide sequence. *MeY*: *N*-methyl-tyrosine, *βY*: β-tyrosine.

to enhance the receptor affinity and biological activity of peptide ligands [283]. C-amidation is present as a post-translational modification in more than half of all known endogenous peptides [284], including both OT and AVP, suggesting that this

conserved motif may serve an important function in their biological activity. All modifications were incorporated separately into full-length $OT_{1\text{-}9}$, $OT_{1\text{-}8}$ (**9a**) and $OT_{1\text{-}7}$ (**9b**) to ascertain the sensitivity of each scaffold to modification.

The impact of these modifications on ligand affinity and biological activity were characterised in Section 5.2. The affinity of compound library **10 - 12** at the human OTR was first explored using a competition radioligand binding assay in Section 5.2.1. Ligand biological activity at the human OTR was then assessed using cell-based $G\alpha_q$ signalling and intracellular Ca^{2+} flux assays in Section 5.2.2 and 5.2.3.

5.2 Pharmacological Evaluation of Modified Oxytocin Metabolites

5.2.1 Ligand Affinity at the Oxytocin Receptor

The binding affinity of modified metabolite library **10** - **12** at the human OTR was indexed using a competition radioligand binding assay outlined previously (Methods 2.4.2). Data is shown in Figure 5.1 and summarised in Table 5.2. N-methylation of full-length $OT_{1\text{-}9}$ (**10a**) had a negative effect on OTR affinity, leading to a 55-fold reduction compared with the native peptide. This modification was better tolerated in the N-methylated $OT_{1\text{-}8}$ (**11a**) and $OT_{1\text{-}7}$ (**12a**) fragments, which saw only a 1.5-fold and 3.5-fold reduction in OTR affinity relative to their unmodified counterparts, respectively.

Incorporation of β-Tyr^2 exerted a more detrimental effect on receptor affinity, producing a total loss of detectable OTR binding in both the full-length and truncated peptides (**10b**, **11b**, **12b**). In contrast to these modifications, C-amidation displayed a net positive effect on OTR affinity. In the $OT_{1\text{-}8}$ fragment (**11c**), this modification led to a 8-fold increase in OTR affinity (K_i: 132 ± 66 nM) relative to the unmodified counterpart **9a**, whilst in the $OT_{1\text{-}7}$ fragment (**12c**), C-amidation increased OTR affinity by 4-fold compared with **9b**, producing the strongest binding characteristics of any peptide ligand investigated in the present study (K_i: 61 ± 22 nM).

5.2.2 Ligand Functional Activity: $G\alpha_q$ Signalling

Characterisation of OTR agonist properties for compound library **10** - **12** was performed using a $G\alpha_q$ signalling assay outlined previously (Methods 2.5.1). Data is shown in Figure 5.2 and summarised in Table 5.2. The effect of each modification on ligand-induced $G\alpha_q$ signalling mirrored the overall trend observed for OTR affinity in Section 5.2.1. N-methylation led to reduced potency in all modified peptides compared with the unmodified counterpart, although this decrease was most pronounced in the full-length peptide (**10a**), which saw a 230-fold reduction in potency relative to unmodified OT, compared with more modest 2-fold and 3.6-fold decreases for the $OT_{1\text{-}8}$ (**11a**) and $OT_{1\text{-}7}$ (**12a**) fragments, relative to their unmodified counterparts. Maximal efficacy for the full-length N-methylated peptide was also substantially lower than unmodified OT (**10a**: 39 ± 9% of OT response) and decreased with truncation of the molecule to $OT_{1\text{-}8}$ (**11a**: 16 ± 3% of OT response),

however no further reduction was observed with truncation to $OT_{1\text{-}7}$ (**12a**: 17 ± 8% of OT response).

In line with the dramatic loss of OTR affinity observed for β-Tyr^2 modified peptides in Section 5.2.1, peptides that incorporated this element (**10b**, **11b**, **12b**) also displayed low potency for activation of $G\alpha_q$ signalling. In full-length $OT_{1\text{-}9}$ (**10b**) this modification led to an 810-fold decrease in potency, with a corresponding maximal efficacy of 14 ± 3% of OT response. This low efficacy for the $G\alpha_q$ signalling pathway was further amplified in truncated peptides **11b** and **12b**, resulting in a flattened dose-response curve and precluding the extrapolation of EC_{50} values for these molecules.

C-amidation of the $OT_{1\text{-}8}$ fragment (**11c**) had little effect on $G\alpha_q$ potency, producing an EC_{50} of 626 ± 136 nM, comparable to the EC_{50} of the unmodified counterpart, **9a** (EC_{50}: 598 ± 118 nM). Although this modification had no net effect on potency for the $G\alpha_q$ signalling pathway, the maximal efficacy for **11c** was increased to 52 ± 7% of OT response, compared with 34 ± 5% for **9a**. C-amidation of the $OT_{1\text{-}7}$ fragment (**12c**) produced an EC_{50}: 244 ± 44 nM, corresponding to a 2-fold increase in potency relative to the unmodified counterpart. An increase in maximal efficacy was also observed between C-amidated and unmodified $OT_{1\text{-}7}$ fragments, increasing to 50 ± 12% of OT response in **11c**, compared with 30 ± 11% in the unmodified counterpart, **9b**.

5.2.3 Ligand Functional Activity: Intracellular Calcium Flux

Activation of the OTR leads to increases in cytosolic Ca^{2+} concentration, a downstream event which represents the convergence of multiple intracellular signal transduction pathways, and is a key mechanism translating OTR activation in the CNS to modulation of neuronal circuits associated with behaviour. To demonstrate that the $G\alpha_q$ potency and efficacy data collected in HTRF IP_1 assays is reflected in this important signalling outcome, a Ca^{2+} mobilisation assay (Methods 2.5.3) was used to index the functional activity of compound library **10 - 12**.

Data is shown in Figure 5.3 and summarised in Table 5.2. Overall, ligand potency and efficacy values estimated using Ca^{2+} mobilisation assays were considerably higher than those found in $G\alpha_q$ HTRF IP_1 assays. OT displayed an EC_{50} of 2 ± 1 nM. Truncation of the molecule led to potency and efficacy losses irrespective of modification, although a conserved pattern was observed between modifications

at each fragment length.

In line with the findings of previous assays, β-Tyr^2 incorporation was the most deleterious modification, producing a 925-fold potency decrease in the full-length peptide (**10b**), with a corresponding maximal efficacy that was 61 ± 1% of the OT response. Truncation of the peptide sequence compounded this effect, with the $OT_{1\text{-}8}$ fragment (**11b**) displaying a maximal efficacy 27 ± 3% of OT response, falling to 1 ± 1% of OT response in the $OT_{1\text{-}7}$ fragment (**12b**). N-methylation was less detrimental for functional activity, producing a 97-fold decrease in potency in the full-length peptide (**10a**) relative to OT, and a maximal efficacy 74 ± 1% of OT response. N-methylation of $OT_{1\text{-}8}$**(11a)** and $OT_{1\text{-}7}$ **(12a)** fragments did not substantially impact ligand potency in this assay, with similar EC_{50} values determined for unmodified and modified peptides (Table 5.2). C-amidated peptides retained a high degree of potency and efficacy in Ca^{2+} flux assays. The $OT_{1\text{-}7}$ fragment (**12c**) was the most potent ligand identified from compound library **10** – **12** in this assay, with an EC_{50} of 85 ± 12 nM. C-amidation was also the modification least affected by truncation of the peptide sequence – maximal efficacy was found to be 92 ± 13% of OT response for the $OT_{1\text{-}8}$ fragment (**11c**) and 75 ± 8% for the $OT_{1\text{-}7}$ fragment (**12c**), respectively.

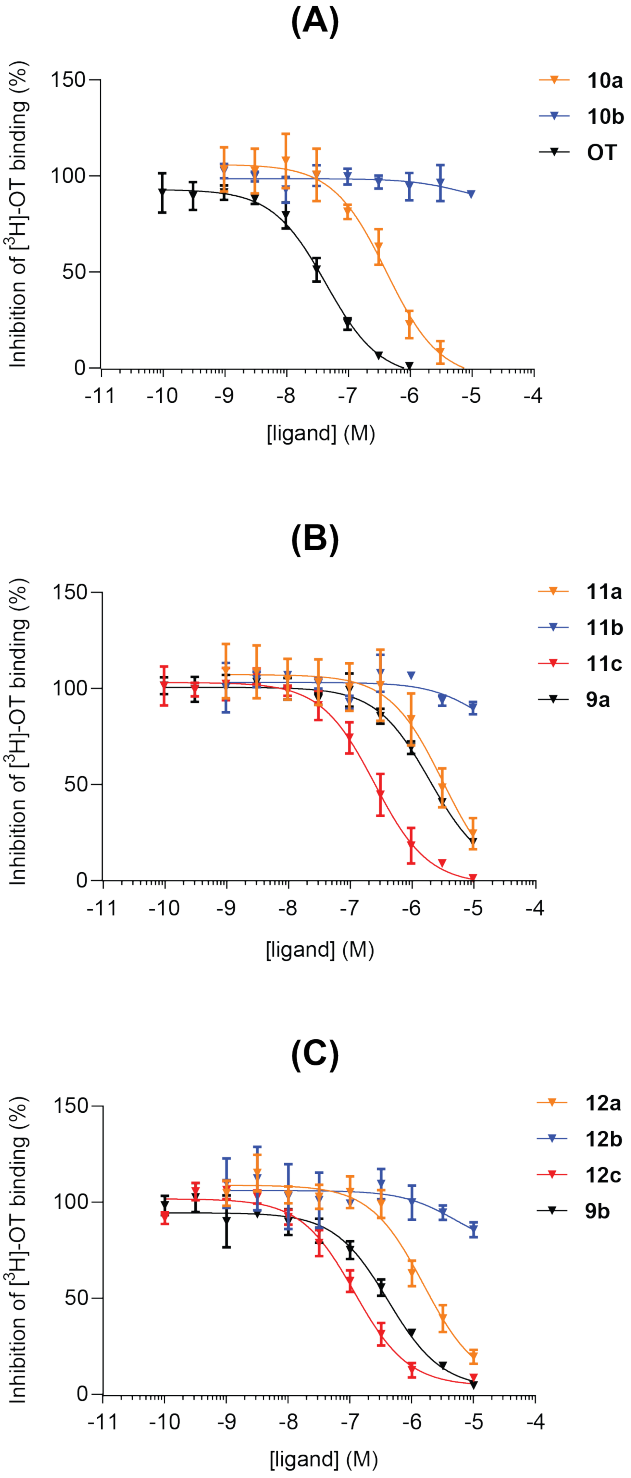

Figure 5.1: Binding affinity curves for modified, cyclic derivatives of oxytocin at the human oxytocin receptor (OTR) measured by competitive displacement of radiolabelled [^{3}H]-OT in HEK293 membrane homogenate under equilibrium conditions. **(a)** N-methylation, **(b)** β-Tyr^2 and **(c)** C-amidation modifications were incorporated separately into **(A)** the full-length $OT_{1\text{-}9}$ sequence, **(B)** $OT_{1\text{-}8}$ and **(C)** $OT_{1\text{-}7}$ fragments. Affinity data for the unmodified peptide fragments $OT_{1\text{-}8}$ **(9a)** and $OT_{1\text{-}7}$ **(9b)** are included for comparison. Data represent the mean ± the standard deviation of three independent experiments.

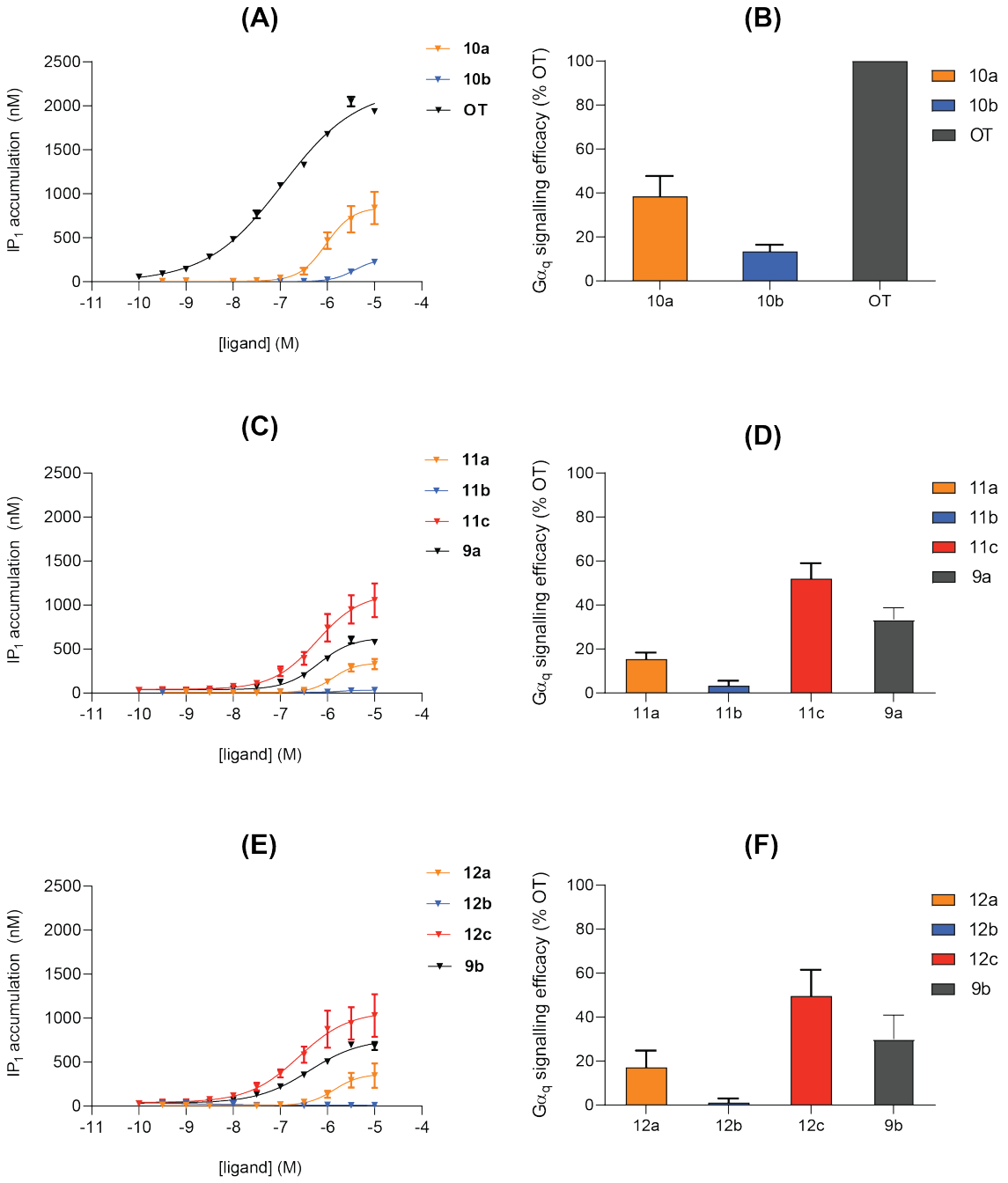

Figure 5.2: Functional activity of modified, cyclic derivatives of oxytocin at the $G\alpha_q$ signalling pathway associated with the human oxytocin receptor (OTR). Ligand potency and maximal efficacy for the $G\alpha_q$ signalling pathway was evaluated using a cell-based, homogenous-time resolved fluorescence (HTRF) assay. **(a)** N-methylation, **(b)** β-Tyr^2 and **(c)** C-amidation modifications were incorporated separately into **(A - B)** the full-length $OT_{1\text{-}9}$ sequence, **(C - D)** $OT_{1\text{-}8}$ and **(E - F)** $OT_{1\text{-}7}$ fragments. Functional data for the unmodified peptide fragments $OT_{1\text{-}8}$ **(9a)** and $OT_{1\text{-}7}$ **(9b)** are included for comparison. Data represent the mean ± the standard deviation of at least three independent experiments.

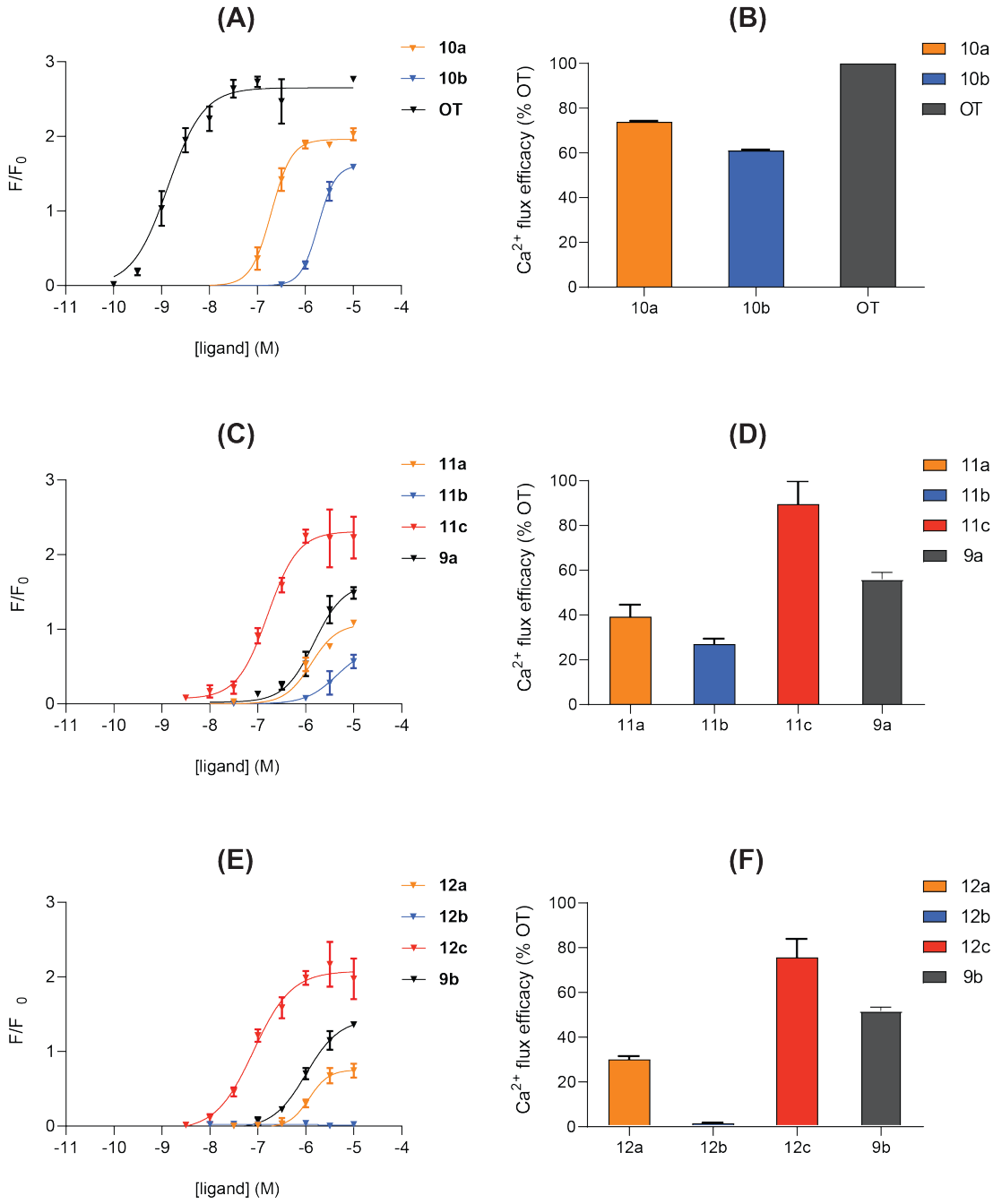

Figure 5.3: Functional effects of modified, cyclic derivatives of oxytocin on intracellular Ca^{2+} flux at the human oxytocin receptor (OTR). Ligand potency and maximal efficacy for intracellular Ca^{2+} flux was evaluated using a cell-based, real-time fluorescence assay. The t=peak fluorescence following ligand exposure was used to determine potency and efficacy data. **(a)** N-methylation, **(b)** β-Tyr^2 and **(c)** C-amidation modifications were incorporated separately into **(A - B)** the full-length $OT_{1\text{-}9}$ sequence, **(C - D)** $OT_{1\text{-}8}$ and **(E - F)** $OT_{1\text{-}7}$ fragments. Functional data for the unmodified peptide fragments $OT_{1\text{-}8}$ **(9a)** and $OT_{1\text{-}7}$ **(9b)** are included for comparison. Data represent the mean ± the standard deviation of at least three independent experiments.

Table 5.2: Affinity and functional activity of modified, cyclic derivatives of oxytocin (**10 - 12**) at the human oxytocin receptor (OTR). Receptor affinity (K_i) was measured by competitive displacement of radiolabelled oxytocin ([^{3}H]-OT) in HEK293 membrane homogenate under equilibrium binding conditions. Functional effects were determined using cellular assays in HEK293 cells expressing the OTR at 37°C. A homogenous time-resolved fluorescence (HTRF) assay was used to index activation or inhibition of the $G\alpha_q$ signalling pathway. A real-time fluorescence assay was used to index ligand-induced Ca^{2+} flux, a major signalling outcome associated with activation of the OTR. Data represent the mean ± the standard deviation of at least three independent experiments. *nd*: not determined, *OT*: oxytocin.

Compound	Affinity, K_i(nM)	$G\alpha_q$ potency, EC_{50}(nM)	$G\alpha_q$ efficacy (% OT)	Ca^{2+} flux potency, EC_{50}(nM)	Ca^{2+} flux efficacy (% OT)
OT	4 ± 2	4 ± 1	100	2 ± 1	100
carbetocin	4 ± 2	419 ± 153	36 ± 4	nd	nd
9a	1041 ± 159	598 ± 118	34 ± 5	1363 ± 169	56 ± 3
9b	232 ± 35	404 ± 91	30 ± 11	960 ± 79	51 ± 2
10a	220 ± 3	930 ± 191	39 ± 9	194 ± 6	74 ± 1
10b	>10 000	3241 ± 366	14 ± 3	1847 ± 328	61 ± 1
11a	1691 ± 379	1295 ± 199	16 ± 3	1286 ± 550	39 ± 5
11b	>10 000	>10 000	3 ± 2	4415 ± 634	27 ± 3
11c	132 ± 66	626 ± 136	52 ± 7	160 ± 30	92 ± 13
12a	809 ± 347	1476 ± 559	17 ± 8	1166 ± 149	29 ± 2
12b	>10 000	>10 000	2 ± 1	>10 000	1 ± 1
12c	61 ± 22	260 ± 44	50 ± 12	85 ± 12	75 ± 8

5.3 Lead Development of C-Amidated Cyclic Peptides

After screening a library of modified, cyclic derivatives of OT (compound library **10** – **12**) in binding and functional assays in Section 5.2, amidation of the C-terminal amino acid residue (**11c**, **12c**) emerged as a viable structural modification that could putatively increase metabolite resistance to proteolytic degradation without compromising ligand affinity, potency or efficacy at the OTR. In contrast, N-methylation of the Tyr^2 residue (**10a**, **11a**, **12a**) and replacement with β-Tyr^2 (**10b**, **11b**, **12b**) negatively impacted peptide ligand pharmacology, limiting the utility of these modifications. *In silico* structural analysis of C-amidated peptides indicates reduced polar surface area and fewer rotatable bonds in **11c** and **12c** relative to OT, factors which could improve the bioavailability and CNS penetration of these molecules (Table 5.3). From these findings, C-amidated metabolites **11c** and **12c** were identified as the most promising lead candidates within compound library **10** - **12**, and were thus selected for further preclinical development.

A key consideration in subsequent optimisation efforts was to identify whether lead molecules displayed a reduced efficacy toward OTR β-arrestin recruitment and receptor internalisation, relative to OT. While β-arrestins were initially thought to be only associated with receptor desensitisation, it is now known that β-arrestin recruitment can promote activation of alternate signalling mechanisms, by interfering with canonical G-protein/receptor interactions and acting as a scaffold for enzymes associated with other intracellular signalling pathways [285]. Once such example is the β-arrestin dependent activation of the MAPK signalling cascade following OTR activation in the PVN, which has been identified as a central factor in the anxiolytic effect of OT in males and females [226, 286, 287].

Novel insights have similarly expanded the role of receptor internalisation. While once thought to be the factor which terminates GPCR activity, evidence has emerged

Table 5.3: Physiochemical properties of oxytocin and C-amidated derivatives calculated *in silico*.

Compound	Molecular weight (g mol^{-1})	Topological polar surface area ($Å^2$)	Rotatable bonds
OT	1007.21	399.53	17
11c	951.14	364.63	15
12c	837.98	335.54	11

that sustained signalling from internalised receptors in early endosomes can occur for many GPCRS, facilitating a range of signalling outcomes that are spatiotemporally distinct from the canonical pathways associated with receptor activation at the plasma membrane [288–290]. While this paradigm has not been investigated for the OTR, it has been demonstrated for several pituitary and hypothalamic hormone receptors, including the structurally related V2R [291, 292].

The influence of these non-canonical signalling pathways on the full repertoire of OT-associated behaviours is not clearly understood, and thus, the 'ideal' signalling profile for an OTR-targeting therapeutic is not known. Identification of OTR ligands that are biased toward G-protein dependent signalling and which reduce β-arrestin recruitment or receptor internalisation may therefore serve as valuable investigative tools for *in vivo* studies seeking to delineate the impact of these pathways on OT-associated behaviour.

In Section 5.3.1, the propensity for lead molecules to induce β-arrestin recruitment was evaluated using a cell-based bioluminescence resonance energy transfer (BRET) assay. Although the human OTR interacts with both β-arrestin1 and β-arrestin2 isoforms [36], functional studies have revealed a more robust interaction between the OTR and β-arrestin2 following exposure to peptide agonists [48], a relationship which has also been widely demonstrated in other class-A GPCRs [293]. For these reasons, genetic constructs expressing the human β-arrestin2 isomer were used in subsequent assays.

The structurally related and clinically used OT analogue, carbetocin, was included in these experiments alongside OT to provide a secondary point of reference for ligand effects at the OTR, and to establish whether the pharmacological properties of **11c** and **12c** fall within a range that may be sufficient to elicit behavioural effects *in vivo*. Carbetocin has been previously reported as an OTR selective $G\alpha_q$ agonist that does not recruit β-arrestin [203], providing an interesting contrast to the effects induced by the native ligand, OT.

Using data from β-arrestin recruitment assays and ligand-induced activation of the $G\alpha_q$ pathway determined previously in Section 5.2.2, ligand signalling bias toward OTR-mediated $G\alpha_q$ signalling or β-arrestin recruitment was determined in Section 5.3.2 using an analytical approach based on the operational model of agonism developed by Black and Leff and expanded by Christopolous et al. [227, 228]. An endosomal trafficking assay was then employed in Section 5.3.3 to experimentally confirm the results derived from ligand bias analysis and provide another cellular measurement of OTR internalisation alongside β-arrestin recruitment assays.

In addition to determining potential ligand signalling bias for **11c** and **12c**, we also sought to expand the scope of the functional activity dataset generated for these molecules thus far. Although $G\alpha_q$ proteins are the primary intracellular signal transduction partners associated with the OTR [154], interactions between the OTR and $G\alpha_s$ proteins, which regulate the cyclic AMP/protein-kinase A (cAMP-PKA) signalling cascade, have been detected in neuronal and myometrial tissue [160, 161, 222]. OTR expression in the myometrium is regulated by cAMP-responsive repressor elements, and increases during parturition in a process mediated partly by $G\alpha_s$ signalling [160, 161]. In neurons, $G\alpha_s$ signalling via the cAMP-PKA cascade controls a number of biological properties such as axonal growth, synaptic transmission, regulation of excitability or long term changes in the nucleus [294], whilst OTR-mediated $G\alpha_s$ signalling specifically has been demonstrated to produce sustained, inward Na^+ currents in vagal neurons [222].

Although the relationship between OTR-mediated $G\alpha_s$ signalling in the CNS and the regulation of social behaviour is not clearly established, the known association between the OTR and $G\alpha_s$ proteins in different tissues necessitates *in vitro* screening of OTR ligand properties at this pathway. To this end, a cellular HTRF cAMP production assay was performed to index ligand-induced activation of the $G\alpha_s$-cAMP signalling cascade via the OTR in Section 5.3.4. Forskolin, a known activator of cAMP signalling [224, 295], was used as a positive control to verify functionality of the assay system. The OTR antagonist atosiban, which does not activate $G\alpha_s$ signalling [172], was used as a reference compound to compare the $G\alpha_s$ pathway activity of OT and modified metabolites **11c** and **12c**.

Finally, it is increasingly recognised that ligand receptor affinity values determined *in vitro*, under equilibrium binding conditions are not sufficient to accurately predict drug affinity or activity *in vivo*. Multiple factors present in biological systems such as incomplete tissue distribution, membrane partitioning, rapid metabolic degradation and excretion of drugs substantially reduce the likelihood that ligand binding will occur under equilibrium conditions at the site of the target receptor [296]. It is therefore important in preclinical development stages to understand the kinetics of ligand-receptor binding interactions which may determine ligand activity under non-equilibrium states *in vivo*. To this end, receptor binding kinetics data for OT, **11c**, **12c** and carbetocin was acquired at the human OTR using a series of kinetic radioligand binding assays in Section 5.3.5, providing a comprehensive preclinical dataset for future drug discovery efforts using these molecules.

Table 5.4: Effects of modified, cyclic derivatives of oxytocin on ligand-induced β-arrestin recruitment to the human oxytocin receptor (OTR). Ligand potency and efficacy toward β-arrestin recruitment was measured using a bioluminescence resonance energy transfer (BRET) assay in HEK293 cells expressing the human OTR at 37°C. The t=$\text{BRET}_{\text{peak}}$ following agonist stimulation was used to determine potency and efficacy values. Data represent the mean ± the standard deviation of three independent experiments. *OT*: oxytocin.

Compound	Potency (EC_{50}, nM)	Efficacy (% OT)
OT	1.1 ± 0.2	100
carbetocin	0.1 ± 0.04	64 ± 14
11c	25 ± 2	73 ± 11
12c	26 ± 5	60 ± 13

5.3.1 Ligand Effects on β-arrestin Recruitment to the Oxytocin Receptor

Sustained agonist activation of the OTR facilitates β-arrestin recruitment to the cytosolic domain of the receptor, a process which decouples G-protein dependent signalling, and which may subsequently activate alternate β-arrestin dependent signalling pathways or receptor internalisation mechanisms. A cell-based BRET assay (Methods 2.5.4) was used to index β-arrestin recruitment to the OTR following agonist stimulation by OT, carbetocin, **11c** or **12c**.

Sustained agonist activation of the OTR facilitates β-arrestin recruitment to the cytosolic domain of the receptor, a process which decouples G-protein dependent signalling, and which may subsequently activate alternate β-arrestin dependent signalling pathways or receptor internalisation mechanisms.

Data is shown in Figure 5.4: (A – B) and summarised in Table 5.4. OT robustly induced β-arrestin recruitment to the OTR, with an EC_{50} of 1.1 ± 0.2 nM. Interestingly, carbetocin displayed a 10-fold higher potency than OT for β-arrestin engagement (EC_{50}: 0.12 ± 0.04 nM), yet the maximal efficacy of carbetocin at this pathway was only 64 ± 14% of the OT induced response. In contrast, **11c** and **12c** were approximately 25-fold less potent than OT and 200-fold less potent than carbetocin towards β-arrestin recruitment, respectively. Despite this disparity in potency, the maximal efficacy of C-amidated peptides for β-arrestin engagement was similar to that of carbetocin - for **11c**, 73 ± 11% of OT response, and for **12c**, 59 ± 13% of OT-induced response, with no statistically significant differences between mean values (one-way ANOVA: F=1.001, p=0.4214)

5.3.2 Quantitative Analysis of Ligand Signalling Bias

Ligand efficacy towards a signalling pathway can be determined using a single functional assay with a reference agonist (OT) and non-linear regression analysis. However, to obtain meaningful comparisons of ligand efficacy between different functional assays, observational and systemic biases arising from differences in experimental conditions must be mitigated. With data from cellular functional assays, we utilised a quantitative analytical method (see Methods 2.6.3) to derive ligand signalling bias towards $G\alpha_q$ pathway activation or β-arrestin recruitment.

Relative to OT, carbetocin displayed a higher propensity towards β-arrestin recruitment than $G\alpha_q$ signalling at the OTR (*t*-test, unpaired, $p<0.05$). Carbetocin signalling bias toward the β-arrestin recruitment pathway was approximately 1.5 fold greater than **11c** and 3-fold greater than **12c**, respectively (Figure 5.4: D). In comparison, **11c** and **12c** displayed a trend towards increased $G\alpha_q$ pathway activation and away from β-arrestin recruitment with decreasing peptide length. Relative to OT, **12c** displayed a statistically significant preference toward $G\alpha_q$ signalling (*t*-test, unpaired, $p<0.001$), although significance was not achieved for **11c**.

5.3.3 Ligand Effects on Endosomal Trafficking of β-arrestin

Recruitment of β-arrestin to the OTR terminates G-protein dependent signalling and initiates internalisation and trafficking of the receptor to early endosomes [180]. To experimentally confirm the $G\alpha_q$ pathway ligand signalling bias identified for C-amidated metabolites in Section 5.3.2, OT and **12c** were screened using a PathHunter eXpress assay (Methods 2.5.5). This assay provides a quantitative measurement of internalised GPCR protein localised to the early endosome by detecting the chemiluminescent signal generated by complementation of β-galactosidase enzyme fragments expressed by a recombinant β-arrestin protein and early endosomal marker proteins following agonist stimulation.

As shown in Figure 5.4: E, exposure to OT facilitated endosomal trafficking of β-arrestin in OTR-expressing cells in a robust and dose-dependent manner (EC_{50}: 0.4 ± 0.1 nM). The maximal effect of OT (100 nM) was observed following 3 h of agonist stimulation, leading to a statistically significant, 13-fold increase in endosomal trafficking relative to the basal state (one-way ANOVA with Dunnett's test, F: 221.5, $p<0.0001$) (Figure 5.4: F). In comparison, 3 h exposure to **12c** (10 µM) did not lead to a statistically significant increase in endosomal trafficking of the OTR relative to

the basal state.

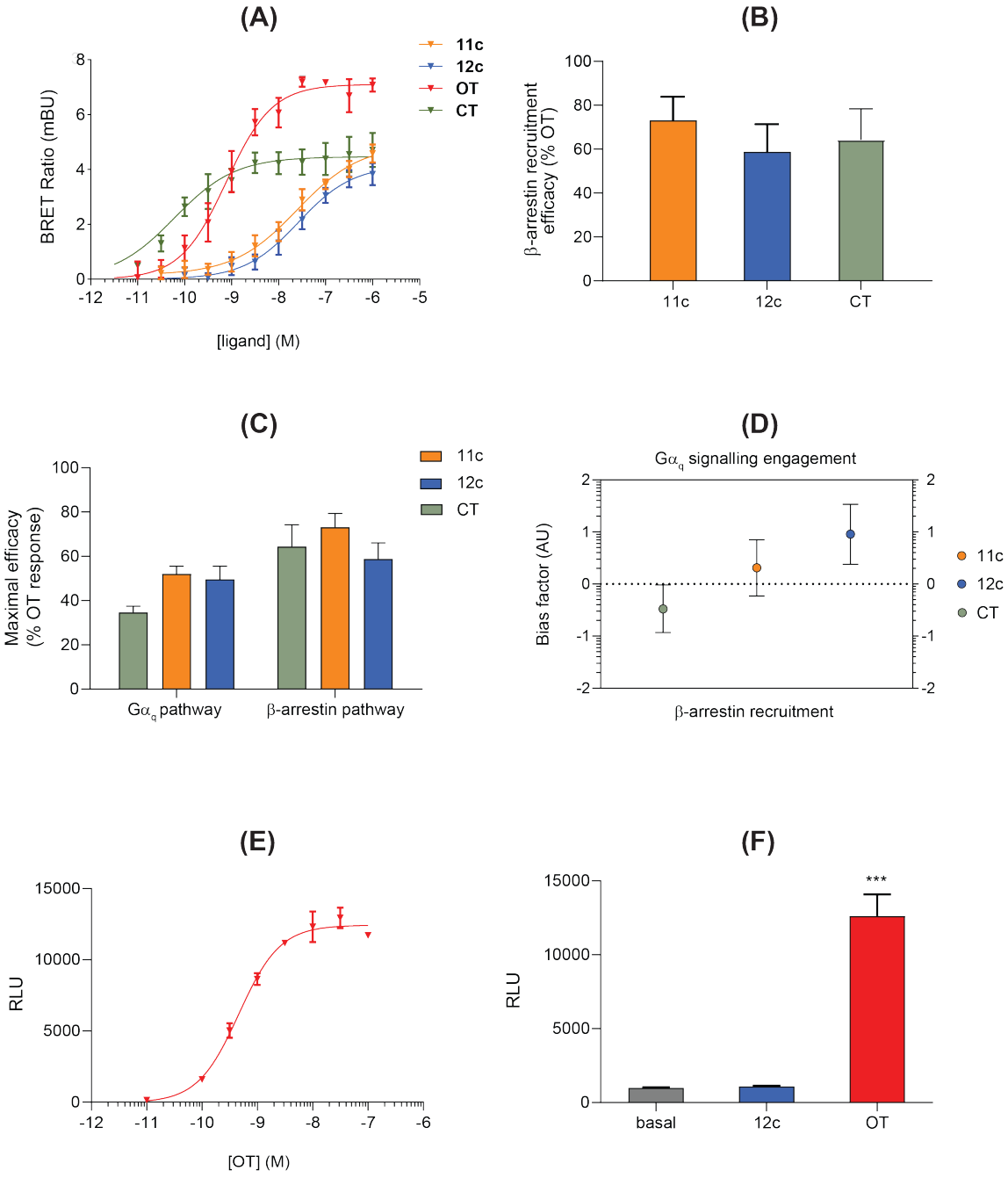

Figure 5.4: Functional effects of oxytocin, carbetocin and C-amidated, cyclic derivatives of oxytocin (**11c**, **12c**) on β-arrestin recruitment and intracellular trafficking of the human oxytocin receptor (OTR). **(A)** Ligand potency for β-arrestin recruitment at the OTR. **(B)** Maximal efficacy of ligand-induced β-arrestin recruitment at the OTR (No significant difference between means, one-way ANOVA: F=1.001, p=0.4214). **(C)** Comparison of maximal ligand efficacy values obtained from $G\alpha_q$ signalling and β-arrestin recruitment assays. **(D)** Quantitative ligand signaling bias analysis using functional data derived from $G\alpha_q$ signalling and β-arrestin recruitment assays. Relative to OT, **12c** and carbetocin (CT) displayed statistically significant differences in signalling preference (t-test, unpaired, **12c**: $p< 0.001$, carbetocin: $p<0.05$) **(E)** Oxytocin-induced OTR internalisation determined using an endosomal trafficking assay. **(F)** Comparison of ligand-induced trafficking of β-arrestin to early endosomes following agonist stimulation. 3 h of exposure to oxytocin led to a statistically significant increase in β-arrestin trafficking relative to the basal state (one-way ANOVA with Dunnett's test, F: 221.5, $^{****}p<0.0001$).

5.3.4 Ligand Effects on $G\alpha_s$ Signalling

To determine if C-amidated metabolites exhibit agonist properties at the $G\alpha_s$ signalling pathway, OT, **11c** and **12c** were screened against the cAMP activator, forskolin, and OTR antagonist, atosiban, using a HTRF cAMP production assay (Methods 2.5.2).

Forskolin robustly induced cAMP production in OTR-expressing cells, with an EC_{50} of 2820 ± 428 nM, in line with previously published potency data (Figure 5.5: A) [295]. OT acted as a low-efficacy $G\alpha_s$ agonist, producing a small but statistically significant increase in cAMP production, with an EC_{50} of 53 ± 22 nM (Figure 5.5: B). The maximal efficacy of compounds was assessed at 10 µM concentrations following 5 min of agonist exposure. Forskolin treatment produced a statistically significant 16-fold increase in cAMP production relative to basal activity, whilst OT treatment produced a 2-fold increase (one-way ANOVA with Dunnett's test, F: 114.3, forskolin: $p<0.001$, OT: $p<0.05$) (Figure 5.5: C). In contrast, the $G\alpha_s$ response induced by **11c**, **12c** and atosiban did not differ significantly from the basal state, indicating that they do not function as agonists of the $G\alpha_s$ signalling pathway via the OTR.

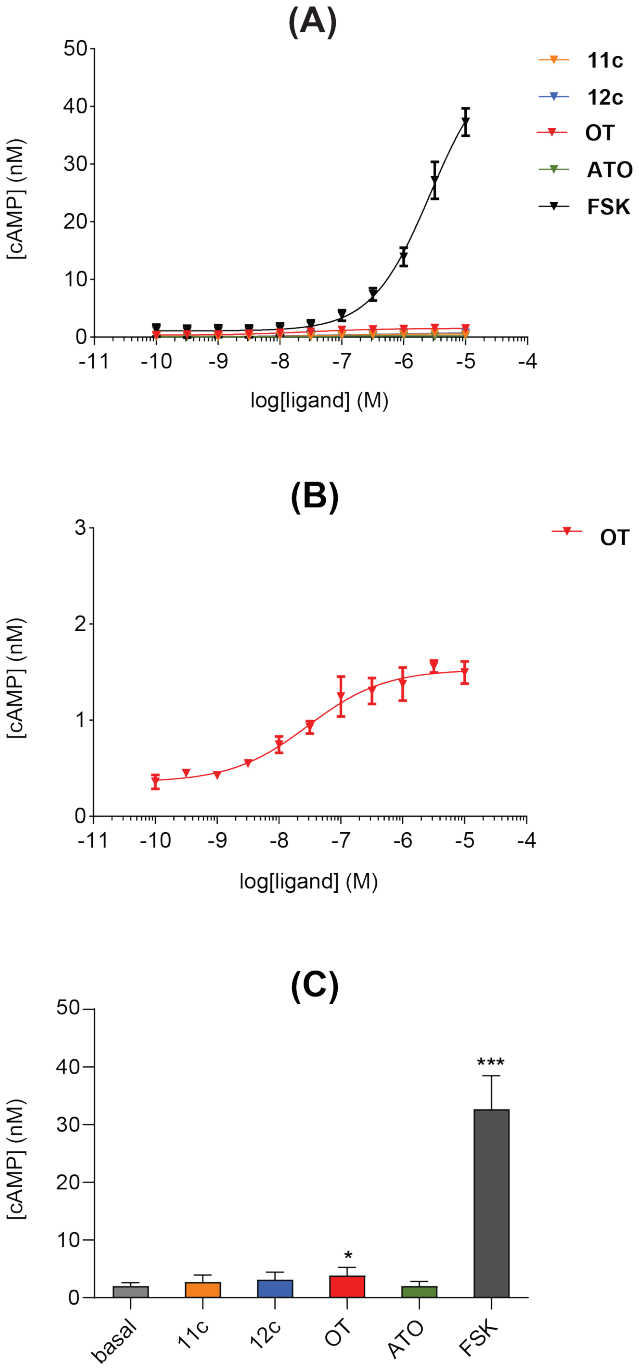

Figure 5.5: Functional effects of oxytocin, atosiban and C-amidated derivatives of oxytocin **11c** and **12c** at the $G\alpha_s$ signalling pathway. Ligand potency and maximal efficacy values for $G\alpha_s$ pathway activation were evaluated using a cell-based homogenous time-resolved fluorescence (HTRF) cAMP production assay. **(A)** Ligand dose-response data for $G\alpha_s$-mediated cAMP production. **(B)** Oxytocin dose-response curve for cAMP production. **(C)** Ligand maximal efficacy at the $G\alpha_s$ pathway. Forskolin (10 µM) and oxytocin (10 µM) treatment produced statistically significant increases in cAMP production relative to basal activity (one-way ANOVA with Dunnett's test, F: 114.3, $^{***}p<0.001$ [FSK], $^{*}p<0.05$ [OT]). Data represent the mean ± the standard deviation of three independent experiments. *ATO*: atosiban, *FSK*: forskolin, *OT*: oxytocin

5.3.5 Kinetics of Ligand Binding at the Oxytocin Receptor

To explore the receptor binding kinetics of properties of OT, carbetocin, **11c** and **12c**, we next sought to characterise ligand-receptor interactions under non-equilibrium conditions using a series of radioligand binding assays described in Methods 2.4.3.

[^{3}H]-OT was used as a radioligand probe to determine the association (k_{on}) and dissociation (k_{off}) rate constants of competing, unlabelled ligands at the OTR. The k_{off} for [^{3}H]-OT was first determined using a dissociation time-course assay. [^{3}H]-OT dissociation from the OTR was monophasic, with a radioligand-OTR complex $t_{1/2}$ of 139 min, 95% CI [117, 149] (Figure 5.6). When fitted to a one-phase exponential decay function (Methods 2.6.1), dissociation data yielded a k_{off} of 0.0050 ± 0.0005 min^{-1} for [^{3}H]-OT and a receptor residence time ($1/k_{off}$) of 200.6 min (Table 5.5). The k_{on} for [^{3}H]-OT was determined using an association time-course assay and fitted to a one-phase exponential association function (Methods 2.6.1), yielding a value of 8.8 ± 1.0 × 10^6 M^{-1} min^{-1} (Figure 5.6).

Following determination of binding rate constants for [^{3}H]-OT, k_{on} and k_{off} rates for unlabelled compounds were determined by performing a competition kinetic binding assay described in Methods 2.4.3. Data is summarised in Table 5.5. Carbetocin was the most rapidly binding OTR ligand evaluated, displaying a k_{on} faster than [^{3}H]-OT by one order of magnitude. The C-amidated metabolites **11c** and **12c** displayed comparable association kinetics and were the slowest binding ligands, with k_{on} values an order of magnitude less than [^{3}H]-OT, and two orders of magnitude less than carbetocin. Carbetocin also displayed the most rapid dissociation from the OTR, with a k_{off} 2-fold higher than **11c** and **12c**, whereas [^{3}H]-OT was the most slowly dissociating ligand, displaying a k_{off} 2-fold lower than **11c** or **12c** and 4-fold lower than carbetocin. These dissociation rates were reflected in the receptor residence time for each ligand, with [^{3}H]-OT displaying the longest receptor occupancy (201 min), followed by **12c** (109 min), **11c** (65 min) and carbetocin (35 min).

Table 5.5: Binding kinetics of [^{3}H]-oxytocin, carbetocin and C-amidated, cyclic derivatives of oxytocin at the human oxytocin receptor (OTR). Association (k_{on}) and dissociation (k_{off}) rate constants were experimentally determined using a series of timecourse radioligand binding assays performed at 20°C in OTR-expressing, HEK293 membrane homogenates. Data represent the mean ± the standard deviation of at least three independent experiments. RT: receptor residence time, OT: oxytocin.

Compound	k_{on} (M^{-1} min^{-1})	k_{off} (min^{-1})	K_d (k_{off}/k_{on}) (nM)	RT ($1/k_{off}$) (min)
[^{3}H]-OT	$8.8 \pm 1.0 \times 10^6$	0.005 ± 0.001	0.6	201
carbetocin	$3.9 \pm 1.7 \times 10^7$	0.0284 ± 0.0039	0.7	35
11c	$3.4 \pm 1.4 \times 10^5$	0.0155 ± 0.0039	46.0	65
12c	$3.0 \pm 1.5 \times 10^5$	0.0092 ± 0.0042	31.2	109

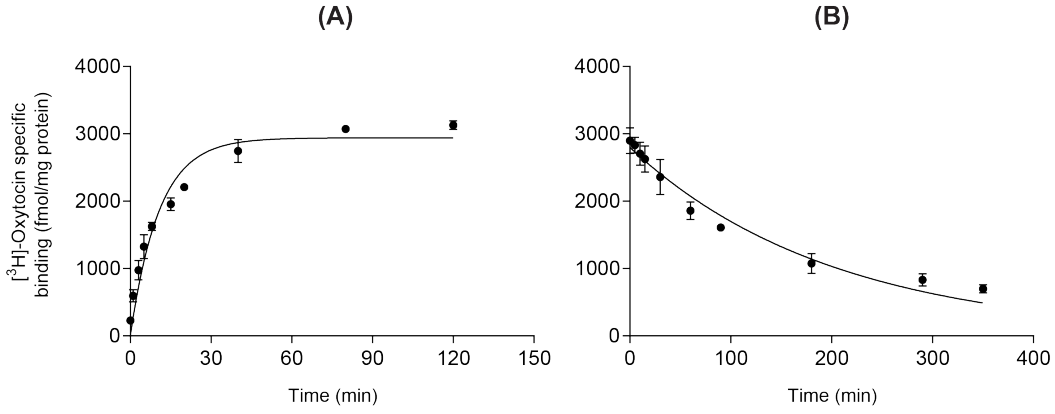

Figure 5.6: Binding kinetics of radiolabelled oxytocin ([^{3}H]-OT) at the human oxytocin receptor (OTR). Kinetic parameters were determined using timecourse radioligand binding assays performed at 20°C in OTR-expressing HEK293 membrane homogenate. **(A)** Association of [^{3}H]-OT to the the OTR over time. Data were fitted to a one-phase exponential association function to produce the association rate constant (k_{on}). **(B)** Dissociation of [^{3}H]-OT from the OTR over time. Data were fitted to a one-phase exponential decay function to produce the half-life ($t_{1/2}$) of the ligand-receptor complex and the dissociation rate constant (k_{off}) of [^{3}H]-OT. All data represent the mean ± the standard deviation of at least three independent experiments.

5.4 Discussion

5.4.1 Summary of Findings

Engineering of putatively stabilising modifications into OT and compound library **10 - 12** revealed that the cyclic portion of the molecule is highly sensitive to modification, with full-length $OT_{1\text{-}9}$ displaying the greatest degree of susceptibility. N-methylation of Tyr^2 or replacement with β-Tyr^2 in the cyclic motif reduced ligand affinity for the OTR, and negatively impacted potency and efficacy in $G\alpha_q$ signalling and intracellular Ca^{2+} flux functional assays. Of the three structural modifications evaluated, only amidation of the C-terminal residue (Leu^8 in **11c**, Pro^7 in **12c**) produced ligands with improved OTR affinity, potency and efficacy relative to their unmodified counterparts. These truncated, modified fragments of the OT peptide sequence were therefore selected as candidates for further lead development. A β-arrestin recruitment assay was first employed to evaluate the effects of **11c** and **12c** on agonist-induced OTR endocytosis, alongside an OT analogue, carbetocin. Carbetocin displayed the highest potency toward β-arrestin recruitment, greater than OT itself, whilst **11c** and **12c** displayed potencies that were several orders of magnitude weaker than OT. Interestingly this trend in potency did not correlate with ligand efficacy – carbetocin, **11c** and **12c** were found to be partial agonists for β-arrestin recruitment with similar maximal efficacies, ranging from 50 – 70% of the response induced by OT.

A quantitative analysis of ligand signalling bias was then performed to determine if **11c**, **12c** or carbetocin displayed signalling bias toward OTR-mediated $G\alpha_q$ signalling or β-arrestin recruitment, respectively. This analysis revealed a trend toward preferential $G\alpha_q$ signalling activation with decreasing peptide length in **11c** and **12c**, and a trend toward β-arrestin recruitment in carbetocin. An endosomal trafficking assay that measures β-arrestin proximity to early endosome protein biomarkers demonstrated that the low efficacy of **12c** toward β-arrestin recruitment reduces the propensity for this ligand to induce OTR internalisation. OT robustly induced β-arrestin2 localisation to early endosomes, whereas the effect induced by **12c** was not significantly different from the basal state after 3 h of agonist stimulation.

An endosomal trafficking assay that measures β-arrestin proximity to early endosome protein biomarkers demonstrated that the low efficacy of **12c** toward β-arrestin recruitment reduces the propensity for this ligand to induce OTR internalisation.

To explore the functional effects of OT and C-amidated derivatives at other intracel-

lular signalling pathways associated with the OTR, a cAMP production assay was used to determine agonist effects of **11c** and **12c** toward the $G\alpha_s$-dependent cAMP-PKA signalling cascade, alongside the OTR antagonist atosiban. In our hands, OT was a low efficacy agonist for the $G\alpha_s$ pathway, whilst **11c**, **12c** and atosiban exposure (10 µM) did not lead to a statistically significant increase in cAMP production above basal activity, indicating that they do not function as $G\alpha_s$ agonists.

Finally, a series of kinetics radioligand binding assays were used to estimate the association and dissociation rate constants of OT, **11c**, **12c** and carbetocin at the OTR, with the aim of providing a comprehensive preclinical dataset for **11c** and **12c** and identifying relationships between ligand binding kinetics, potency and efficacy. Carbetocin displayed the most rapid association and dissociation kinetics, corresponding to the shortest receptor residence time of the compounds evaluated. OT displayed a rapid association rate constant and slow dissociation rate constant, producing the longest receptor residence time of the compounds evaluated. **11c** and **12c** exhibited comparable binding kinetics, and were found to have the slowest association rate constants of the compounds evaluated, and dissociation rate constants faster than OT, but slower than carbetocin.

5.4.2 Assessing the Impact of Structural Modifications on Metabolite Biological Activity

Structural studies indicate that OT forms at least two IMHBs within the cyclic portion of the molecule (see Figure 5.7) [297–300]. Nonetheless, OT also contains multiple polar side chains and solvent-exposed amide groups, which contribute to a high exposed polarity (EPSA = 153), and corresponding low passive permeability [277, 301]. Moreover, the low biological half-life of OT (28 min in cerebrospinal fluid, 1 – 2 minutes in blood [211]) suggests that the cyclic nature of the molecule does not confer substantial protection from endogenous peptidases. We therefore sought to introduce peptide backbone modifications that could enhance both the metabolic stability and passive permeability of OT.

These modifications focused on protection of the N- and C-termini of the molecule, which are the primary substrates for the peptidases which degrade OT *in vivo* [242]. Within the macrocycle of OT, N-methylation of the Tyr^2 amine group and substitution with β-Tyr^2 serve to alter the configuration of the Cys^1-Tyr^2 peptide bond, reducing the affinity for aminopeptidases which sequentially cleave polypeptides from the N-terminal of the molecule [281, 282]. When incorporated into full-length

OT and cyclic N-terminal fragments $OT_{1\text{-}8}$ and $OT_{1\text{-}7}$, these modifications were both deleterious for ligand affinity and functional activity at the OTR.

A possible explanation for this finding may be that these modifications disrupt IMHB networks which stabilise OT when bound to the OTR orthosteric site. Site-directed mutagenesis and x-ray crystallography studies indicate that the cyclic portion of OT interacts with a hydrophobic binding cavity in the OTR formed by TM2-7 [154, 247–250], a non-polar environment conducive to the formation of IMHBs. Within the macrocycle of OT, IMHBs can form between the Tyr^2 amine and Cys^6 carbonyl group (IMHB-1), as well as the Asn^5 amine and Tyr^2 carbonyl group (IMHB-2) [297–300] (Figure 5.7). As such, N-methylation of the Tyr^2amine is likely to prevent the formation of IMHB-1, whereas incorporation of β-Tyr^2 introduces a centrally-projecting methylene group that could disrupt both IMHB-1 and IMHB-2 interactions.

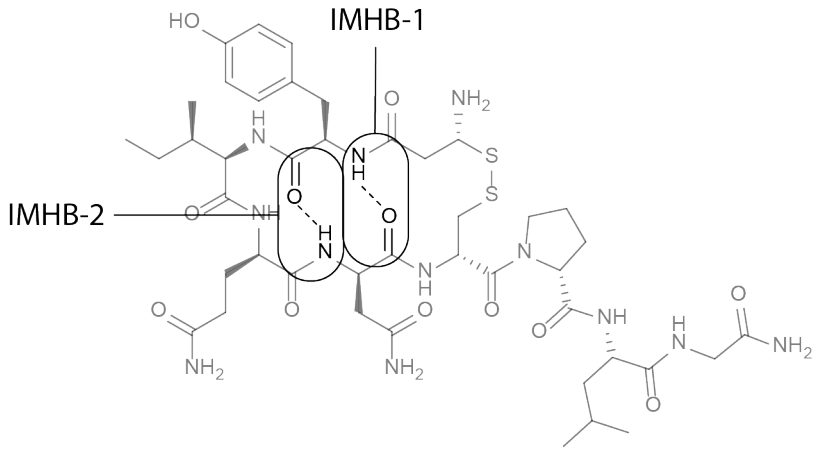

Figure 5.7: Intramolecular hydrogen bonds (IMHBs) which stabilise the secondary structure of oxytocin. IMHB-1 occurs between the Tyr^2 amine and the Cys^6 carbonyl group. IMHB-1 occurs between the Tyr^2 carbonyl group and the Asn^5 amine.

This hypothesis correlates with the affinity and functional data of the modified metabolites explored in this chapter – N-methylation led to a substantial decrease in ligand activity at the OTR, whilst β-Tyr^2 incorporation almost abolished OTR activity entirely. These findings are further supported by a recent study conducted by Sciabola et. al [302], who performed a systematic N-methylation of each residue in the OT sequence and characterised their impact on pharmacological properties and IMHB networks. N-methylation at Tyr^2, Gln^4 and Asn^5 residues in the cyclic portion of OT led to potency reductions of up to 1000-fold, and did not increase the EPSA of OT, suggesting that the amide groups of these residues form IMHBs in the

endogenous context. Conversely, N-methylation of Cys^1, Ile^3, Cys^6 in the macrocycle, as well as Leu^8 and Gly^9 in the linear C-terminal sequence of OT produced analogues that retained full agonist activity at the OTR and displayed reduced EPSA. This indicates a decrease in exposed polarity, which suggests that the amine groups of these residues do not participate in IMHBs in endogenous OT. This evidence suggests that N-methylation of the Tyr^2 residue or substitution with β-Tyr^2 are unsuitable modifications to protect the N-terminal of OT from aminopeptidase activity, as they may disrupt IMHBs which are critical for stabilising the secondary structure of OT.

In contrast to the Tyr^2 modifications which focused on the peptide N-terminus, amidation of the C-terminal Leu^8 in **11c** and Pro^7 in **12c** proved to be a more effective modification for retaining biological activity at the OTR. Relative to their non-amidated precursors **9a** and **9b**, which feature a carboxyl terminus, **11c** and **12c** displayed enhanced OTR affinity, as well as greater potency and efficacy for the OTR-associated $G\alpha_q$ signalling pathway. To contextualise how such a minor modification could impact the pharmacological properties of a peptide ligand, it is necessary to consider the endogenous role of C-amidation. Within neural and endocrine tissues, signalling peptides are typically synthesised through excision from a larger precursor protein, followed by a series of enzymatic reactions which modify the excised peptide and protect it from further metabolism [303]. C-amidation, catalysed by the enzyme peptidyl-glycine alpha-amidating monooxygenase, is a modification present in more than half of all known endogenous peptides [284]. For many of these peptides, C-amidation is necessary to achieve full biological activity [304].

Amidation confers a range of advantages on signalling peptides which correspond to their evolved mode of action in eukaryotic organisms. Signalling peptides are secreted into circulation, and generally act on discrete biological targets that are distal from their site of synthesis. The amide group enhances resistance to proteolytic degradation, facilitating this mechanism by prolonging the half-life of amidated peptides in the bloodstream [305]. In contrast to carboxyl groups, amides are also less susceptible to deprotonation, reducing peptide sensitivity to changes in physiological pH. In addition to these attributes, amidation is also known to stabilise the secondary structure of many peptides [306–308] and facilitate high affinity, specific binding to their cognate GPCR targets [248, 303, 309] factors which further contribute to their biological efficacy.

Both OT and AVP are C-amidated peptides, indicating that this conserved modification may serve a function in the endogenous OTR/AVPR signalling system. Supporting this assertion, removal of the C-terminal Gly^9 amide in OT leads to a

loss of potency in Ca^{2+} flux, $G\alpha_q$ and cAMP signalling assays, different biological indices associated with activation of the OTR in cellular expression systems [200]. Site-directed mutagenesis studies indicate that the linear C-terminal tripeptide of OT interacts with residues in the N-terminus of the OTR [248, 309]. This binding site is known to interact specifically with agonists, and as such is thought to be a driver of signal transduction via the OTR. Thus, the composition of the C-terminal in OT analogues may be an important structural determinant of agonist efficacy. When viewed in this context, the improved agonist properties of C-amidated OT fragments **11**c and **12c** relative to their deaminated counterparts in functional assays may reflect a restoration of binding interactions between the terminal amide of the peptide ligand and high affinity epitopes located in the extracellular N-terminal region of the OTR. Further modelling studies docking these ligands into the newly reported OTR crystal structure [155] may be a method to test this hypothesis.

5.4.3 C-Amidated Cyclic Peptides: Signalling Bias

Using a set of cell-based functional assays and a quantitative analysis of ligand signalling bias, **11c** and **12c** were found to display a trend towards preferential activation of OTR-mediated $G\alpha_q$ signalling and away from β-arrestin recruitment. These data suggest that the linear C-terminal portion in OT and peptide analogues participates in receptor interactions that influence GRK-mediated receptor phosphorylation or β-arrestin affinity for the OTR. As such, variations in the C-terminal peptide sequence of the ligand may produce a range of different OTR signalling outcomes, affecting the temporal profile of $G\alpha_q$ signalling, facilitating or reducing β-arrestin dependent signalling cascades and altering the dynamics of β-arrestin mediated receptor internalisation.

This hypothesis is supported by evolutionary characteristics associated with the OT/AVP peptide family, as well as similar findings from *in vitro* pharmacological screening of synthetic OT analogues. The sequence of OT is strongly conserved among eutherian mammals [154]. Recently, however, novel variants of OT have been identified in multiple species of New World monkeys, which display intense care-giving behaviour and a high incidence of social monogamy [310]. These OT analogues also display reduced β-arrestin recruitment at the OTR in cell-based assays [48], and largely feature substitutions at position 8 residue of the peptide sequence (Leu^8 in ancestral OT, substituted with Pro^8, Ala^8, Thr^8 and in New World monkey variants of OT) [47]. A key aspect of these substitutions is an increase in relative hydrophilicity relative to Leu^8-OT.

Busnelli et al. [36] have also described synthetic OT analogues that contain hydrophilic amino acid subsitutions at position 8, and which display similarly low efficacy for β-arrestin recruitment in cell-based assays. **12c** did not retain the position 8 residue but displayed reduced β-arrestin recruitment and OTR internalisation, perhaps reflecting that the complexity of receptor-ligand interactions cannot be reduced to a single position in the ligand sequence. **12c** does contain a C-terminal Pro^{7}, however, which may still be able to participate in compensatory interactions with Leu^{8}/Pro^{8}-associated residues in the flexible, extracellular portions of the OTR that are thought to interact with the linear tripeptide sequence of the ligand [309].

Site-directed mutagenesis studies of the human OTR indicate that Phe^{103} in ECL1 of the receptor interacts with the C-terminal sequence of the peptide ligand [153]. Interestingly, there is also evidence of co-evolution in the receptors of New World monkeys at this residue – the receptors of *Callithrix jacchus* contain a hydrophobic phenylalanine whereas the receptor of *Saimiri sciureus* has a hydrophilic tyrosine in this position [153]. Based on this evidence, it is possible that the relative hydrophilicity of the C-terminal tail in OTR ligands determines the strength of the interaction with Phe^{103} and other residues in ECL1 of the receptor. This interaction may lead to conformational changes in the receptor which expose a variable number of phosphorylation sites located on the intracellular domains of the OTR. β-arrestin is recruited to the OTR following GRK-2 mediated receptor phosphorylation [177], and there is evidence that the level of β-arrestin recruitment may be controlled purely by the number of intracellular receptor phosphorylation sites exposed by the agonist-induced conformational shift [311]. If this paradigm is reflected in the OT system, the hydropathicity and composition of the C-terminal ligand sequence may influence the strength of ligand-ECL1 interactions in the OTR, which could in turn lead to greater or lesser β-arrestin recruitment based on the extent of induced conformational change.

The composition of the ligand C-terminal sequence is not the only determinant of β-arrestin recruitment efficacy, as evidenced by the characterisation of carbetocin in the present study. Carbetocin retains the Pro^{7}-Leu^{8}-Gly^{9}9-NH_2 sequence of ancestral OT, but differs in the cyclic portion of the molecule, with a butyl chain replacing the Cys^{1}-Cys^{6} disulfide bridge.

In our hands, carbetocin displayed β-arrestin recruitment potency that was an order of magnitude greater than OT, corresponding to clear trend towards β-arrestin recruitment in subsequent signalling bias analysis. This suggests that interactions between the cyclic portion of the ligand and the OTR are also responsible for triggering receptor internalisation. These findings contradict a cell-based characterisation

performed by Passoni et. al [203], who found that carbetocin induces receptor internalisation via a β-arrestin independent mechanism. Interestingly, they found that in contrast to OT, carbetocin did not promote receptor recycling to the plasma membrane, suggesting instead trafficking to lysosomes and proteolytic degradation of the OTR. The disparity in findings may result from stochastic variations in the heterologous cellular expression systems used to characterise β-arrestin recruitment - the expression levels of intracellular signalling partners in these systems can be impacted by buffer composition, expression cell type and age, as well as the genetic construct used to introduce protein encoding cDNAs to the cell. As such, experimental data derived from these systems is only an approximation of signalling events that may occur *in vivo*. Nonetheless, both findings point towards altered OTR internalisation dynamics following exposure to carbetocin, which is further supported by animal behavioural data showing that carbetocin does not elicit the full range of behavioural outcomes associated with OT [216], potentially a consequence of rapid OTR depletion following carbetocin exposure.

In our hands, carbetocin displayed lower efficacy than OT toward β-arrestin recruitment, but higher potency, corresponding to clear trend towards β-arrestin recruitment in subsequent signalling bias analysis. These findings contradict a characterisation performed by Passoni et. al [203], who reported that carbetocin does not induce β-arrestin recruitment to the OTR in a cell-based BRET assay. Despite this observation, it was found that carbetocin promotes OTR internalisation following agonist exposure, suggesting activation of a β-arrestin independent endocytosis pathway.

This disparity in findings may arise from the use of different bioluminescent proteins in each investigation, resulting in differences in assay sensitivity. The study conducted by Passoni et. al utilised a *Renilla* luciferase (Rluc) construct, whereas the present study used a more recently developed bioluminescence platform – Nanoluc (Nluc) – a bioengineered luciferase derived from the deep sea shrimp *Oplophorus gracilirostris*. Nluc is smaller, more stable and produces ¿150-fold higher luminescence than Rluc [312]. The consequent advantages of Nluc include reduced steric hindrance of native protein-protein interactions by the luciferase construct, reduced assay background noise and enhanced signal sensitivity - factors which may have improved the likelihood of detecting low efficacy carbetocin-induced β-arrestin recruitment relative to earlier studies.

Assessing the β-arrestin recruitment efficacy of novel OTR ligands was a priority in the present investigation. The OTR rapidly desensitises following exposure to OT in cell-based functional assays [313], whilst in animal behavioural studies, chronic

OT exposure produces selective reductions in OT-associated social behaviours and a concomittent reduction in OTR expression across integrative centres of the limbic system, including the amygdala and bed nucleus of the stria terminalis [183, 314, 315]. In humans, prolonged OT infusion during parturition is associated with uterine atony, a condition linked to OTR desensitisation, in which the myometrial tissues of the uterus become unresponsive to endogenous OT resulting in the loss of uterine contractility and producing life-threatening complications such as postpartum haemorrhage [226]. As such, mitigating OTR desensitisation is an appealing strategy to extend the efficacy of OTR-targeting therapeutics and reduce adverse events associated with their clinical use.

Further preclinical development of **12c** may ultimately produce a lead candidate with these properties, however, there are several caveats to the current findings which can be addressed with further research. Although ligand effects at the $G\alpha_q$ and $G\alpha_s$ and β-arrestin2 signalling pathways were assessed in this investigation, OTR interactions with $G\alpha_{i/o}$ proteins and β-arrestin1 have also been detected in cell-based expression systems, neural and uterine tissue [36, 173, 226]. Ligand biological activity at these pathways was not assessed in the present investigation, and will be necessary to obtain a comprehensive picture of **11c** and **12c** signalling bias at the OTR.

In addition, some cellular events associated with the OTR, such as activation of the MAPK signalling cascade, are dependent on β-arrestin recruitment [226]. MAPK signalling in the PVN has been identified as a central factor in the anxiolytic effect of OT in males and females [286, 287]. As such, a $G\alpha_q$ signalling biased ligand such as **12c** may be less efficacious than OT in some social behavioural domains that are dependent on β-arrestin signalling. Finally, sustained signalling from internalised receptors is an emerging concept in GPCR pharmacology, in which it is recognised that in some contexts, GPCRs retain signalling activity in endosomes following β-arrestin-mediated endocytosis. The robust receptor internalisation induced by OT may have evolved to facilitate endosomal signalling, a concept which has been demonstrated for the structurally related V_2R [316], but which has not yet been explored for the OTR. A reduced propoensity toward OTR internalisation in **12c** may reduce the capacity for signalling from internalised receptors to occur.

In addition, the influence of β-arrestin recruitment and OTR internalisation on the therapeutic efficacy of OT is not yet well understood. As such, **12c**, a $G\alpha_q$ signalling biased ligand that does not induce β-arrestin recruitment, may be less efficacious than OT in social behavioural domains that are dependent on β-arrestin recruitment, including the MAPK signalling cascade. Conversely, these biased signalling

properties highlight the utility of **12c** as an investigative tool to explore the impact of non-canonical OTR signalling on behaviour *in vivo*.

5.4.4 C-Amidated Cyclic Peptides: Receptor Binding Kinetics

The process of drug development is hindered by difficulties in predicting *in vivo* efficacy based on *in vitro* affinity and potency measurements. In the open system of the body, drugs are subject to absorption, distribution, metabolism and excretion (ADME) kinetics, which cause fluctuations in the concentration of free drug over time. As a consequence, steady-state ligand binding conditions which are readily achieved *in vitro* rarely translate to the biological context. Drug development approaches which focus solely on screening with equilibrium-based parameters (K_i, EC_{50}) therefore cannot provide a comprehensive picture of how a drug will behave when administered to a living organism. For this reason, the kinetics of ligand binding to the OTR for **11c**, **12c**, OT and carbetocin was determined using a competition radioligand binding assay series and an analysis framework developed by Motulsky and Mahan [220]. Rate constants (k_{on}/k_{off}) were first determined for the radioligand probe – [^{3}H]-OT – then calculated for each compound, followed by mathematical derivation of the K_d (k_{off}/k_{on}) and receptor residence time ($1/k_{off}$) for each ligand at the OTR.

From this screening, marked differences were observed between ligand K_i values determined experimentally with equilibrium competition radioligand binding assays (Section 5.2.1), and ligand K_d values mathematically derived from association and dissociation rate constants, with the latter indicating OTR affinities for evaluated ligands 2-4 fold greater than experimental data. K_d is a temperature-dependent variable, and therefore this disparity may be attributable to the temperature difference between kinetic and equilibrium radioligand binding assays. Equilibrium radioligand binding assays were performed at 4°C to minimise the effects of non-specific ligand binding in tissue homogenate. In contrast, kinetic radioligand binding assays were performed at 21°C, as the dissociation timecourse of [^{3}H]-OT from the OTR at 4°C exceeded 12 h in optimisation experiments, limiting the utility of the assay as a medium-throughput screening platform if performed at this temperature. Neither equilibrium K_i or kinetic K_d values determined *in vitro* represent the binding affinity of a ligand in a cellular or tissue environment, and thus the ligand affinity values obtained from each assay should not be regarded as absolute. Instead, this data can be used to compare the affinity relationships between ligands. The rank order

and degree of ligand affinity between OT, **11c**, **12c** and carbetocin was concordant between equilibrium and kinetic radioligand binding assay data, thus, each dataset supports the veracity of the other.

Substantial differences were also observed between the association and dissociation rate constants of the OTR ligands evaluated. OT and carbetocin both rapidly associated with the OTR, while **11c** and **12c** associated at a slower rate. OT dissociated from the OTR slowly, producing the longest receptor residence time, followed by **12c**, **11c** and finally carbetocin, which displayed the shortest receptor residence time. The contrast between the rapid association kinetics of OT and carbetocin and the slower association kinetics of **11c** and **12c** suggest that residues in the C-terminal linear sequence of the peptide ligand facilitate receptor conformational shifts from an 'inactive' state to an agonist-bound signalling state. For most receptor-ligand interactions studied, this conformational transition follows one of two mechanisms. In the first instance (Equation 5.1), a complex (RL) is formed between the ligand (L) and receptor (R) via a one-step association (k_1) and dissociation process (k_2). In the second instance, known as the 'induced-fit' model (Equation 5.2), ligand binding to a receptor induces conformational isomerisation, leading to the formation of a complex with much higher ligand affinity (RL*). The rate constants k_3 and k_4 describe the transition between high affinity and low affinity receptor states.

$$\mathrm{R} \underset{k_2}{\overset{k_1[\mathrm{L}]}{\rightleftharpoons}} \mathrm{RL} \tag{5.1}$$

$$\mathrm{R} \underset{k_2}{\overset{k_1[\mathrm{L}]}{\rightleftharpoons}} \mathrm{RL} \underset{k_4}{\overset{k_3}{\rightleftharpoons}} \mathrm{RL}^* \tag{5.2}$$

The interaction between OT and the OTR follows the induced-fit model of ligand binding [309]. The main contribution to the increase in affinity is due to specific interactions of the flexible N-terminus and first extracellular loop of the OTR with the linear C-terminal tripeptide amide of OT. Thus, truncation of the peptide C-terminal sequence may be expected to reduce the strength of this interaction, resulting in slower receptor isomerisation and association kinetics, as demonstrated for **11c** and **12c** in the present work.

Although optimisation of slow association kinetics is achievable, there are several factors which limit the utility of this approach in a drug development program. Firstly, association rates are dependent not only on the k_{on} value of a ligand, but also the concentration [296]. Thus, a low k_{on} value for a drug could be compensated through an increase in dosage *in vivo*. Secondly, ligand-receptor association rates

are ultimately restricted by the rate at which binding partners diffuse through a solution - the diffusion limit creates an upper threshold for k_{on} values of approximately 10^8 – 10^9 M^{-1} min^{-1} which cannot be overcome through structural optimisation of a ligand. Furthermore, the ADME factors which influence drug efficacy *in vivo* can affect the local concentration of a ligand within a target tissue to such an extent that the k_{on} is no longer the primary determinant of ligand-receptor complex formation. Finally, association kinetics describe the interaction which occurs before the formation of an 'active' ligand-receptor complex and subsequent recruitment of intracellular signalling partners, whereas ligand dissociation kinetics dictate the duration of the agonist-bound receptor active state, and may be thus expected to exert a greater influence on pharmacological efficacy.

Indeed, there is extensive evidence that dissociation kinetics are a key predictor of drug efficacy and duration of effects [317, 318]. In cellular binding kinetics assays, long dissociative half lives have been associated with increased potency in several classes of drugs, including anti-tumoural epidermal growth factor receptor, tyrosine kinase inhibitors and HIV-1 antiretroviral agents [319, 320]. Dissociation kinetics also impact drug efficacy *in vivo*. The α-reductase inhibitor, finasteride, blocks the production of the male hormone dihydrotestosterone from its precursor testosterone, and is used to treat benign prostate hyperplasia, male pattern baldness and acne. Finasteride binds the α-reductase enzyme with a K_i of 0.3 pM, resulting in a complex with a dissociative half-life greater than 30 days [321]. Finasteride achieves peak plasma concentrations in humans at 1.8 – 2.8 h, with an elimination $t_{1/2}$ in systemic circulation of 4.7 – 7.1 h [322]. Despite this, a single oral dose of finasteride has been shown to suppress dihydrotestosterone formation for up to 7 days, strongly suggesting that slow dissociation kinetics are the primary driver of its anti-androgenic efficacy [296]. Similar relationships between long dissociative half life and *in vivo* efficacy have been shown for angiotensin II type 1 receptor inhibitors used to treat hypertension, purine nucleoside phosphorylase inhibitors used in the treatment of autoimmune disorders, and antipsychotics of the D_2R dopamine receptor antagonist class [323–325]. Interestingly, long dissociative half-lives in D_2R antagonists are strongly correlated with on-target adverse effects which may be associated with sustained receptor occupancy [325].

While dissociation kinetics have mainly been studied in relation to antagonists, this concept is being increasingly investigated as a strategy to optimise agonist-induced signalling at GPCRs [326, 327]. The transiency of GPCR signalling creates a more complex scenario, as receptor internalisation and desensitisation may mitigate the influence of a slowly-dissociating agonist on signalling efficacy. The dissociation kinetics of OT, carbetocin, **11c** and **12c** determined in the present work appear to

support a relationship between long dissociative half-life and $G\alpha_q$ signalling efficacy. The rank order of $G\alpha_q$ efficacy was determined to be OT > **12c** > **11c** > carbetocin, an order which was reflected in receptor residence times, but not equilibrium affinity (K_i) values. The longer OTR residence time of **12c** compared to **11c** may form the empirical basis for the higher OTR affinity and functional activity of **12c**, despite the loss of the important Leu^8 residue in the tripeptide tail of the ligand.

5.4.5 Conclusions and Future Directions

The present work extends upon the OTR peptide ligand development program which identified biologically active OT metabolites in Chapter 4. With the aim of enhancing metabolic stability, a series of modifications were incorporated into full-length $OT_{1\text{-}9}$ alongside cyclic N-terminal fragments **9a** and **9b** ($OT_{1\text{-}8}$ and $OT_{1\text{-}7}$). Amidation of the C-terminal residue in these peptides produced **11c** and **12c** - derivative molecules with improved OTR affinity and $G\alpha_q$ agonist properties relative to their unmodified counterparts, as measured in cellular assays. Moreover, textbf11c and **12c** display signalling bias toward the OTR-associated $G\alpha_q$ signalling pathway and away from β-arrestin recruitment, a factor which may reduce ligand-induced OTR desensitisation *in vivo*. In contrast to OT, neither **11c** or **12c** activated the $G\alpha_s$ pathway in cellular assays, a property which may reduce their liability to induce uncharacterised on-target effects associated with OTR-$G\alpha_s$ coupling in different tissues. The pharmacological effects of **11c** and **12c** at the OTR were comparable in a range of different functional assays, suggesting that there is no clear advantage in retaining the Leu^8 residue of **11c** in subsequent lead development. As such, **12c** is positioned as the most viable candidate for further optimisation.

While the effects of C-amidation on ligand pharmacology have been demonstrated in this work, experimental confirmation of greater metabolic stability in **12c** is a priority for further investigation. Recent years have seen the development of several specialised liquid chromatography mass-spectrometry (LC-MS) protocols for the detection of OT in biological samples [328–331]. However, most protocols require ultra-sensitive technology to achieve accurate measurements in the desired concentration range (typically ng/mL) [330]. A methodology reported by Brandtzaeg et al. [331] circumvents this issue by measuring the total OT (protein-bound and unbound) in biological samples through alkylation and reduction pretreatment steps, followed by purification of peptide analytes with solid-phase extraction. Substantial efforts were made to adapt this LC-MS protocol to assess the metabolic stability of peptide OTR agonists identified in Chapters 4 and 5, following incubation in

C57BL/6 mouse brain homogenate. In this assay format, brain tissue is incubated with a fixed concentration of peptide analyte at 37°C over a 6 h timecourse. Individual aliquots are removed over time and frozen for subsequent LC-MS analysis. Optimisation of the method could not be completed during the course of the project due to issues associated with the highly variable fragmentation patterns of cyclic peptides in LC-MS systems. However, efforts to establish this assay in our laboratory are ongoing, and a simplified LC-MS protocol based on the method of Braentzag et al. has recently been reported, which may prove more amenable to analysis of **12c** metabolic stability in future development efforts [329].

Numerous groups have sought to overcome the metabolic instability of OT by incorporating structural elements that confer resistance to proteolytic degradation. Several of these modifications have also been shown to improve OTR selectivity, receptor affinity and functional activity of OT analogues. After assessing metabolic stability with LC-MS, a logical progression in the optimisation of **12c** would be to synthesise a peptide library which incorporates these modifications, then evaluate their impact on ligand pharmacology at the OTR, metabolic stability and CNS permeability. A key finding of the present study was that the Tyr^2 amine group in **12c** is not amenable to modifications that introduce conformational changes to the peptide backbone. To reduce the aminopeptidase susceptibility of the N-terminal in **12c**, the peptide bond of Cys^1-Tyr^2 could be substituted with a trifluoroethylamine group (Figure 5.8: A), a low-basicity bioisostere which preserves the geometry of the peptide bond, as well as the capacity to engage in hydrogen-bond donating and accepting interactions [332]. An alternative strategy could be to remove the N-terminal free amine group of Cys^1 in **12c** (Figure 5.8: B), a modification which improves OTR affinity in the full-length peptide, increases hydrophobicity and impairs aminopeptidase substrate recognition [333].

Although N-methylation of Tyr^2 had a negative impact on pharmacology in **11c** and **12c**, this modification may prove more viable when applied to amine groups that do not participate in IMHBs that stabilise the secondary structure of OT, such as those of Ile^3 and Cys^6 residues (Figure 5.8: C). N-methylation of these amino acids could reduce the exposed polarity of **12c**, enhancing passive permeability through lipophilic membranes without disrupting the IMHB networks formed by the Tyr^2 and Asn^5 amine groups. Finally, the Cys^1-Cys^6 disulfide bond of **12c** could be substituted with a range of more stable surrogates, such as sulfide, diselenide, or *meta*-xylene bridges (Figure 5.8: D), all of which have been incorporated successfully into the full-length peptide sequence of OT without compromising ligand pharmacology at the OTR [199, 200, 334].

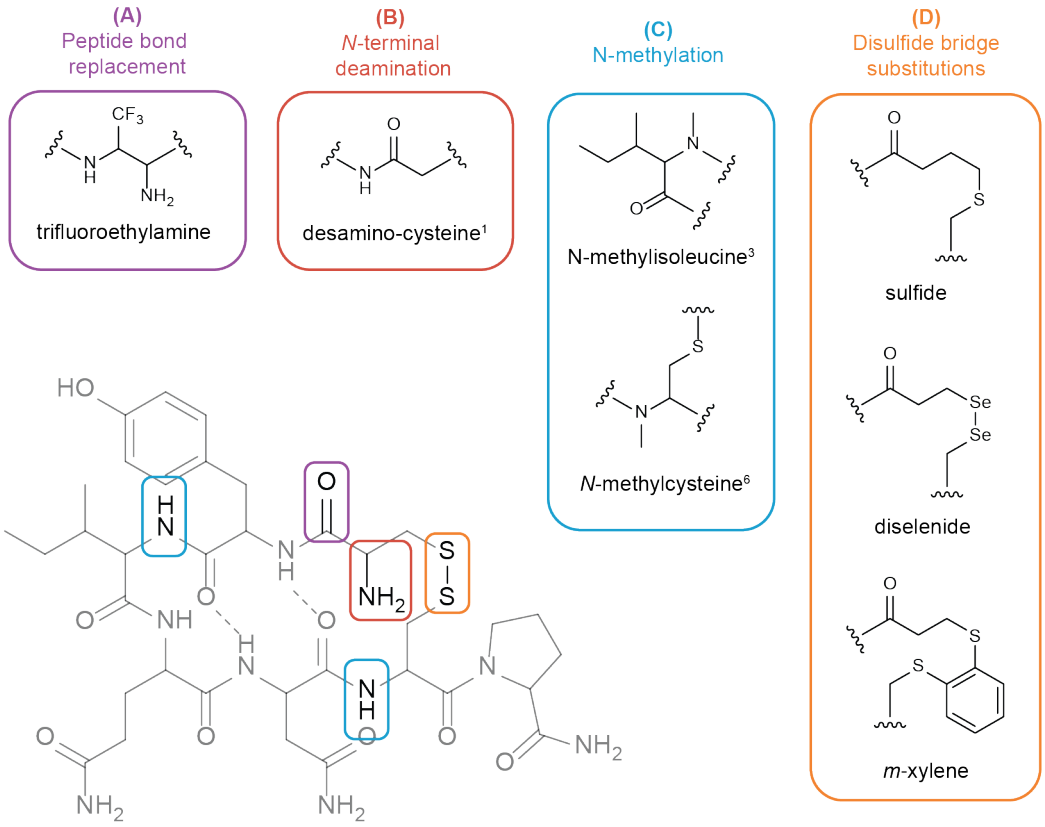

Figure 5.8: Structural modifications of **12c** to improve metabolic stability, passive permeability and oxytocin receptor affinity. **(A)** Substitution of the Cys^1-Tyr^2 peptide bond with a trifluorethylamine bioisostere improves proteolytic resistance. **(B)** Deamination of the N-terminus increases oxytocin receptor affinity and hydrophobicity. **(C)** N-methylation of residues that do not participate in intramolecular hydrogen bonding networks (IMHBs) could reduce exposed polar surface area (EPSA). **(D)** Substitution of the disulfide bond increases proteolytic resistance without impairing ligand pharmacology. Based on [199, 200, 332–334].

Chapter 6

Summary and Conclusions

This research aimed to identify and characterise novel agonists of the human OTR, a therapeutic target in neuropsychiatric disorders. While there is growing evidence that enhancing OTR signalling may be an effective strategy to treat anxiety and social dysfunction in ASD, SAD, schizophrenia and major depression, OT itself is unlikely to be therapeutically developed for these indications due to its rapid *in vivo* metabolism, low receptor selectivity, poor CNS penetration and desensitisation of the OTR with chronic administration. The present work sought to identify OTR agonists from different sources which overcame limitations inherent to the native peptide, thus providing advantageous lead candidates for the preclinical development pipeline and identifying new opportunities for lead optimisation in future studies. Drug candidates were identified from a library of pyrazolobenzodiazepine small molecules based on the structure of WAY-267,464, and a library of peptide ligands derived from the structure of known endogenous OT metabolites.

6.0.1 Small Molecule Ligands

The small molecule drug discovery program focused on two derivative compound libraries based on the structure of WAY-267,464. Previous work from our laboratory indicated that replacing the rigid benzylurea motif in WAY-267,464 with flexible alkyl tethers abolished ligand OTR activity and largely diminished OTR binding affinity [198]. This led us to hypothesise that restoring rigidity to the central moiety of WAY-267,464 via a phenylpiperazine linker may restore ligand OTR affinity and activity whilst reducing the overall structural complexity of the molecule. Screening a library of WAY-267,464 analogues containing a phenylpiperazine linker did not produce effective OTR ligands, indicating that the benzylurea motif is a pharmacophoric structural component shared by WAY-267,464 and other first-generation pyrazolobenzodiazepine OTR agonists, TC-OT 39 and LIT-001 [192, 194, 196]. As such, the findings of this work contribute to the structure-activity dataset of the pyrazolobenzodiazepine scaffold, and support retaining this structural component in the future development of WAY-267,464 analogues.

We next focused on dissecting the pharmacophoric contributions of the diazepine moiety which is conserved between WAY-267,464, LIT-001 and TC OT-39. This was achieved by synthesising and characterising a series of WAY-267,464 derivatives which retained only the diazepine heterocycle conjugated to a set of functional groups via the adjacent amide in WAY-267,464. While OTR affinity and activity was abolished by these modifications, $V_{1A}R$ affinity was retained at level comparable to the phenylpiperazine WAY-267,464 analogues, implying an alternative binding modality between phenylpiperazine and truncated diazepine derivatives within the $V_{1A}R$ orthosteric site. The truncated diazepine library produced the most potent small molecule $V_{1A}R$ ligand identified in this thesis, **5f** (K_i: 230 nM). This unexpected finding indicated that radical reductions in molecular weight, polarity and structural complexity of WAY-267,464 via removal of the benzylurea and resorcinol moeities can still produce ligands that bind to receptors in the OTR/AVPR family - a key consideration in designing effective, CNS-penetrant drugs. The loss of OTR affinity and preservation of $V_{1A}R$ affinity in both the phenylpiperazine and truncated diazepine compound libraries further suggests that the $V_{1A}R$ orthosteric site is more accessible to small ligands than that of the OTR, a factor which could inform the design of selective $V_{1A}R$ ligands derived from WAY-267,464 in future investigations.

Although $V_{1A}R$ affinity was retained by phenylpiperazine and truncated diazepine WAY-267,464 derivatives, no biological activity was detected at the $V_{1A}R$ in a cellular functional assay which indexes $G\alpha_q$ pathway activation, a canonical signalling pathway associated with the $V_{1A}R$. Although the HTRF IP1 assay used to characterise ligand activity at this pathway provides a rapid, robust indication of ligand potency and efficacy, the dynamic range is limited for low affinity compounds and can result in false negatives, which may explain the lack of observable ligand activity associated with $V_{1A}R$ ligands in this work. To accurately characterise the pharmacology of viable $V_{1A}R$ ligands **4a** (phenylpiperazine derivative) and **5f** (diazepine derivative), one strategy could be to employ cellular assays which utilise BRET and FRET-based biosensors, similar to the nanoBRET assay used to index β-arrestin recruitment to the OTR in Chapter 5. These biosensor assays provide a direct, sensitive and real-time measurement of receptor proximity to intracellular signalling partners, and have been widely developed to investigate different aspects GPCR pharmacology and protein-protein interactions, including G-protein recruitment, intracellular Ca^{2+} flux and kinase activation [36, 335–337], providing multiple indices of ligand biological activity. Nonetheless, further structural optimisation of **4a** and **5f** will be necessary to improve $V_{1A}R$ receptor affinity and potency. This course of action, if pursued, could identify novel, selective $V_{1A}R$ receptor agonists

and antagonists with applications in social behavioural research. If $V_{1A}R$ antagonism emerges as a property of optimised WAY-267,464 derivatives, then these molecules could be repurposed as AVP-signalling inhibitors, with indications for hyponatremia, congestive heart failure and liver cirrhosis [236–238].

Although no OTR agonists were directly identified from the small molecule discovery program, the structure-activity relationships of the WAY-267,464 derivatives explored in this work subsequently informed the design of potent OTR agonists by our laboratory, based on the truncated diazepine scaffold (**5f**). These novel diazepine OTR agonists represent the lowest molecular weight OTR agonists identified to date, positioning them as promising lead candidates for developing second-generation OTR agonists with improved CNS penetration over WAY-267,464, TC OT-39 and LIT-001. Intraperitoneal administration of the identified lead from this second-generation library (**5f** analogues and OTR agonists) elicits prosocial behaviour in a BALB/c social preference test at doses of 5 mg/kg. This behaviour is blocked by a CNS-permeable OTR antagonist but not by a CNS-impermeable OTR antagonist, providing evidence that these molecules can cross the blood brain barrier and exert central effects following peripheral administration [239].

6.0.2 Peptide Ligands

The peptide discovery program was inspired by reports that endogenous metabolites of OT retain biological activity in cellular assays and exert prosocial effects in animal behavioural models [213, 216]. The first stage of the program aimed to determine the receptor pharmacology of linear and cyclic peptide fragments derived from the metabolism of OT. This investigation revealed that no linear fragments of OT bound to the OTR or $V_{1A}R$ indicating that the disulfide-bridged cyclic portion of the molecule is crucial for receptor affinity in the OTR/AVPR family. Interestingly, linear fragments $OT_{4\text{-}9}$ and $OT_{5\text{-}9}$ have demonstrated robust effects on social behaviour and anxiety memory *in vivo* [213, 216], suggesting that they are exerting these effects via an unidentified drug target. The hypothalamus produces a wide range of peptide hormones, and their cognate receptors are highly expressed at the site of synthesis. These hormone signalling systems play several important regulatory roles and have been shown to influence the expression of social behaviours [338]. Thus, linear OT metabolites may be exerting behavioural effects by acting as partial agonists or allosteric modulators of these hypothalamic peptide receptors. The Pro^7-Leu^8-Gly^9-NH_2 fragment of OT (MIF-1) is a positive allosteric modulator of dopamine receptors, inhibits opioid neurotransmission and α-MSH release from the

hypothalamus, and potentiates melatonin activity, providing supporting evidence that other linear OT metabolites may have the capacity to engage with multiple targets in the CNS [217, 218]. Identification of putative drug targets for $OT_{4\text{-}9}$ and $OT_{5\text{-}9}$ fell outside the scope of this thesis, but could be achieved using a combination of high-throughput affinity screening, cellular thermal shift assays, proteomics and gene expression analysis [266–268]. A comprehensive analysis of the OT metabolome via this method may elucidate previously unidentified mechanisms through which the OT system influences behaviour, opening new avenues of research into the biology of social behaviour and revealing novel therapeutic targets to ameliorate social behavioural deficits in neuropsychiatric disorders.

In contrast to linear OT metabolites, cyclic N-terminal fragments of OT (**9a**, **9b**) bound to the OTR and $V_{1A}R$. **9a** and **9b** displayed functional selectivity - retaining a partial $G\alpha_q$ agonist profile at the OTR with no discernible functional effects at the $V_{1A}R$ in cellular assays. This stands in contrast to the parent molecule OT, which is a potent agonist of $G\alpha_q$ signalling through both receptors. Early investigations of OT metabolism indicated that N-terminal cyclic fragments are generated by endogenous peptidases in neuronal tissue [212, 213]. Based on these converging lines of evidence, it could be speculated that OT metabolism in the CNS produces cyclic products which facilitate prolonged activation of the OTR after the local concentration of OT is depleted, without inducing activation of the $V_{1A}R$. This may be a mechanism through which OT release is able to elicit long-lasting behavioural effects despite a relatively short biological half-life in the CNS. The influence of cyclic metabolites **9a** and **9b** on OT-associated behaviours could be evaluated using exogenous administration of these peptides in animal models of social behaviour, anxiety and depression. In particular, the use of $OXT^{-/-}$ knockout mice strains such as B6;129S-Oxt^{tm1Wsy} could facilitate studies exploring rescue of social deficits in OT deficient mice following administration of **9a** or **9b**. The lack of functional activity exhibited by **9a** and **9b** displayed at the $V_{1A}R$ could be confirmed *in vivo* by using a similar experimental design, with a conditional $OXTR^{-/-}$ strain such as B6.129(SJL)-$Oxtr^{tm1.1Wsy}$, allowing for spatial and temporal knockdown of the OTR. Before these further investigations of **9a** and **9b** can be undertaken, potential differences in ligand pharmacology at the mouse OTR and $V_{1A}R$ should first be determined using a secondary *in vitro* pharmacology screening of **9a** and **9b** in cell lines expressing the murine receptors.

The second stage of the peptide discovery program focused on incorporating structural modifications into **9a** and **9b** which have been demonstrated to enhance metabolic stability in other classes of peptide drugs. Modifications which enhance OTR affinity and functional activity, and those that negatively impact pharmacol-

ogy were characterised, with C-amidation (**11c**, **12c**) emerging as the most viable strategy for improving metabolic stability whilst retaining OTR activity. Although there are numerous examples within the literature that C-amidation enhances peptide stability, direct experimental evidence of this relationship for **11c** and **12c** was not concluded in the present work due to time constraints and assay optimisation issues. To derive this information in future investigations, one approach may be to implement an *ex vivo* drug metabolism assay coupled with an LC-MS analysis platform (see Chapter 5, Section 5.4.5 for further details). Such an assay would provide a robust preclinical measure of how structural modifications to cyclic OT metabolites influence metabolic stability within the CNS.

Another objective of the peptide discovery program was to identify OT analogues that may be more amenable to CNS penetration than the endogenous peptide. Truncation of the OT peptide sequence in **11c** and **12c** reduces the size, polarity and conformational flexibility of the molecule – factors which are likely to improve passive permeability through the lipid environment of the blood-brain barrier. Permeability may be further improved through structural modifications that reduce exposed polarity, such as N-methylation of the peptide backbone, or substitution of hydrophilic residues with hydrophobic amino acids, however, the present work revealed that intramolecular hydrogen-bonding networks which stabilise the secondary structure of OT must be carefully considered when introducing these modifications. The passive permeability of modified OT analogues could be determined *in vitro* using a CaCo-2 permeability assay, then evaluated *in vivo* using positron emission tomography (PET) imaging. This would, however, necessitate the synthesis of radiolabelled peptide tracers which mirror the structure of **11c**, **12c** or subsequently developed analogues.

If passive permeability is not improved through structural modification to an extent that orally-administered drug formulations become feasible, other strategies may be used to deliver physiologically relevant quantities of **11c**, **12c** or derivative OTR agonists to the CNS. Intranasal administration is the primary mode of OT drug delivery in clinical contexts, and this approach could also be applied to cyclic derivatives of OT. OT concentration increases in the CSF following intranasal administration in rodents [339], macaques [340] and humans [341]. However, questions remain surrounding the validity of this strategy for delivering consistent dosage to CNS – intranasal OT administration appears to produce concomitant increases in peripheral OT levels in most cases [342], which may lead to alterations in behaviour via afferent feedback to the CNS from peripheral tissues which richly express the OTR, such as the gastrointestinal tract [343] or cardiovascular system [344]. In other studies, a lack of correlation between the administered dose, CSF and plasma

OT concentrations have cast doubt on the reliability of this administration route [75]. To overcome these limitations, the efficacy of intranasal administration could be improved by designing novel drug formulations of **11c** or **12c** which are tailored to the architecture, structure and physiochemical characteristics of nasal mucosa [345]. The viability of this approach has been demonstrated by the preliminary success of TTA-121, a novel intranasal formulation of OT with adjusted osmolality and viscosity to facilitate passage through mucosal membranes. TTA-121 exhibits improved bioavailability relative to OT, has been evaluated for safety and toxicity in mice [346], primates [347] and humans [348], and is currently undergoing a phase II trial for efficacy on ameliorating ASD social deficits in Japanese cohorts [349].

If structural modifications to enhance passive permeability and novel drug formulations to facilitate intranasal delivery do not improve the CNS penetration of **11c**, **12c** or derivative OTR agonists, then more exotic strategies may be required to achieve the desired biodistribution of these molecules. Recently, the receptor for advanced glycation end-products (RAGE) has been identified as an active transporter of OT across brain capillary endothelial cells [350, 351]. Thus, future structural optimisation of **11c** and **12c** could be directed towards enhancing RAGE affinity as a possible strategy to increase active transport of OT into the brain. Alternatively, nanoparticle-encapsulated formulations of OT may be another strategy to harness active transport of peptides across the blood-brain barrier. Several nanoparticle formulations of OT have been developed using poly(lactic-co-glycolic acid) (PLGA) or bovine serum albumin (BSA) as the base material, conjugated to either transferrin or rabies virus glycoprotein to facilitate targeting to the CNS [352]. When administered intranasally to mice, these nanoparticle-encapsulated formulations exhibit faster initial burst release and sustained elevation of OT concentration in the CSF, relative to intranasal OT alone [353]. Moreover, nanoparticle-encapsulated OT displays greater prosocial effects relative to intranasal OT in mouse social behavioural models, in both acute and sub-chronic dosing regimes, supporting the validity of this approach for therapeutic development of other peptide OTR agonists, such as **11c** and **12c** [353]. It should be considered, however, that nanoparticle-mediated drug delivery is a nascent field, with many questions of safety, toxicity and efficacy remaining to be addressed before such a strategy could be used to formulate therapeutics for human cohorts [354].

Another objective in the peptide discovery program was to identify OT analogues with enhanced $G\alpha_q$ signalling efficacy and reduced propensity to recruit β-arrestin to the OTR. Such biased ligands could serve as investigative tools to separately evaluate the influence of transient G-protein signalling mediated by OTRs expressed on the plasma membrane, and persistent signalling mediated by arrestin-bound and

internalised OTRs, elucidating the signalling pathways which should be targeted to produce a desired therapeutic outcome in neuropsychiatric disorders.

Although β-arrestin mediated receptor desensitisation is not a prerequisite for receptor downregulation, there is evidence of a relationship between these processes in the OTR system. In cellular and *ex vivo* studies, OT rapidly induces β-arrestin recruitment, desensitisation and internalisation of the OTR, associated with a downregulation of *OXTR* mRNA [129, 180, 313, 355, 356]. Chronic OT administration in mice negatively influences aspects of social behaviour, accompanied by a concomitant downregulation in OTR expression within the CNS over time [183], suggesting that downregulation is a mechanism for OT tolerance induction. Mitigating receptor desensitisation may therefore be necessary to develop OTR-targeted therapies that retain long-term efficacy in chronic dosing regimens.

The present work identified ligand signalling bias in **11c** and **12c** toward $G\alpha_q$ pathway activation and away from β-arrestin recruitment to the OTR. Furthermore, **12c** failed to elicit OTR internalisation in an endosomal trafficking assay. This positions **11c** and **12c** as valuable molecules for future investigative studies, and highlights the feasibility of mitigating OTR desensitisation in therapeutic development through ligand structural modification.

These findings are preliminary in nature, and further investigations should aim to address several caveats. Ligand signalling bias for OT, carbetocin, **11c** and **12c** was only investigated between the $G\alpha_q$ pathway and β-arrestin recruitment pathway. Although **11c** and **12c** did not activate the $G\alpha_s$ pathway, the OTR couples with multiple intracellular partners, including $G\alpha_{i/o}$ proteins, β-arrestin1, kinases and membrane-bound signalling molecules. To obtain a more comprehensive and accurate picture of ligand signalling biases, BRET-based biosensors could be constructed for each interacting protein partner and the effects of **11c** and **12c** on recruitment to the OTR assessed in a cellular assay format. Fluorescence imaging of OTR-expressing cell lines or neuronal tissue following incubation with OT or **12c** could also provide insights into OTR expression at the plasma membrane following agonist exposure and confirm the lack of **12c**-induced β-arrestin2-mediated OTR internalisation observed in endosomal trafficking assays. Ultimately, animal behavioural studies that utilise chronic dosing regimens will be needed to confirm whether the ligand signalling bias observed for **11c** and **12c** in cellular expression systems translates to prolonged therapeutic efficacy *in vivo*.

A final objective in the peptide discovery program was to characterise the ligand binding kinetics of novel OTR agonists. Analysis of the receptor-binding kinetics of

11c, **12c**, OT and carbetocin identified the ligand dissociation rate constant (k_{off}) as a potential driver of $G\alpha_q$ signalling efficacy at the OTR, suggesting that binding kinetics assays could facilitate future efforts to optimise OTR agonist potency. The generalisability of this finding is limited by the small number of compounds evaluated in this investigation, however, there is extensive evidence to suggest that k_{off} rates are a key determinant of ligand activity *in vitro* and therapeutic efficacy *in vivo* [296, 318, 357, 358]. Incorporation of a binding kinetics screening platform for future derivative libraries of **11c** and **12c** may facilitate identification of novel OTR agonists with enhanced receptor residence time and improved $G\alpha_q$ signalling efficacy. Ligands with longer OTR residence time may also display sustained therapeutic efficacy *in vivo*, as a consequence of reduced susceptibility to drug clearance mechanisms which deplete the concentration of ligand in circulation [318].

In addition to extending exploration of k_{off} rates, there are other intriguing avenues of inquiry related to ligand binding kinetics at the OTR. Ligand rebinding has been identified as a potential explanation for why certain ligands may have longer *in vivo* efficacy than their *in vitro* receptor residence times would suggest [359]. Rebinding events are thought to occur through hindered diffusion of ligand away from a target receptor by macrostructural elements such as the cellular plasma membrane [357]. Designing peptide OTR ligands with membrane-anchoring structural motifs could facilitate rebinding events by partitioning into the plasma membrane. The known localisation of the OTR to cholesterol-enriched 'lipid raft' microdomains may constitute a further opportunity to design anchoring motifs which target OTR agonists in close proximity to the receptor [360]. Such membrane-tethered ligands could be structurally optimised toward rapid association and dissociation kinetics, producing repeated ligand-receptor interactions and inducing sustained activation of the OTR in a manner distinct from slowly dissociating ligands.

6.0.3 Concluding Remarks

Although the small molecule discovery program (Chapter 2) did not identify novel OTR agonists, two ligands (**4a**, **5f**) with non-detectable OTR affinity, high $V_{1A}R$ receptor selectivity and moderate $V_{1A}R$ affinity were characterised, which may have alternate therapeutic applications. In contrast, the peptide discovery program (Chapter 3) identified biologically active, cyclic N-terminal fragments of OT (**9a**, **9b**) which bound to the OTR with high affinity and displayed functional selectivity - acting as agonists at the OTR and neither activating or inhibiting $V_{1A}R$ signalling at a detectable level in cellular assays. Structural modification of these cyclic metabo-

lites in Chapter 4 led to the identification of peptide OTR agonists (**11c**, **12c**) with enhanced receptor affinity and signalling efficacy compared to their unmodified metabolite precursors. In contrast to OT, these modified peptides displayed more rapid dissociation kinetics than OT, ligand signalling bias toward $G\alpha_q$ pathway activation and away from β-arrestin recruitment at the OTR, and did not induce detectable β-arrestin recruitment to the early endosome following agonist exposure – factors which may indicate a capacity for reduced OTR desensitisation and prolonged therapeutic efficacy *in vivo*. The lower molecular weight, reduced polarity and greater structural rigidity of **11c** and **12c** relative to OT may facilitate greater CNS penetration than that attainable by the parent molecule, positioning them as superior candidates for further development as peptide-based OTR agonists, with therapeutic applications in the treatment of neuropsychiatric disorders.

Bibliography

[1] S Rotzinger. "Peptides and Behaviour". In: *Handbook of Biologically Active Peptides*. 2nd ed. Academic Press, 2013. Chap. 254, pp. 1858–1863.

[2] G. J. Norman, L. C. Hawkley, S. W. Cole, G. G. Berntson, and J. T. Cacioppo. "Social neuroscience: the social brain, oxytocin, and health". In: *Soc Neurosci* 7.1 (2012), pp. 18–29.

[3] J. Rault. "Be kind to others: Prosocial behavioura and their implications for animal welfare". In: *Applied Animal Behaviour Science* 210 (2019), pp. 113–123.

[4] S. A. Golden, M. Jin, and Y. Shaham. "Animal Models of (or for) Aggression Reward, Addiction, and Relapse: Behavior and Circuits". In: *J Neurosci* 39.21 (2019), pp. 3996–4008.

[5] H. Ohtsuki, C. Hauert, E. Lieberman, and M. A. Nowak. "A simple rule for the evolution of cooperation on graphs and social networks". In: *Nature* 441.7092 (2006), pp. 502–5.

[6] A. K. Beery and D. Kaufer. "Stress, social behavior, and resilience: Insights from rodents". In: *Neurobiology of Stress* 1 (2015), pp. 116–127.

[7] D. E. Jones, M. Greenberg, and M. Crowley. "Early Social-Emotional Functioning and Public Health: The Relationship Between Kindergarten Social Competence and Future Wellness". In: *Am J Public Health* 105.11 (2015), pp. 2283–90.

[8] D. P. Kennedy and R. Adolphs. "The social brain in psychiatric and neurological disorders". In: *Trends Cogn Sci* 16.11 (2012), pp. 559–72.

[9] F. Ozbay, D. C. Johnson, E. Dimoulas, C. A. Morgan, D. Charney, and S. Southwick. "Social support and resilience to stress: from neurobiology to clinical practice". In: *Psychiatry (Edgmont)* 4.5 (2007), pp. 35–40.

[10] L. A. O'Connell and H. A. Hofmann. "Evolution of a vertebrate social decision-making network". In: *Science* 336.6085 (2012), pp. 1154–7.

[11] A. H. Veenema and I. D. Neumann. "Central vasopressin and oxytocin release: regulation of complex social behaviours". In: *Prog Brain Res* 170 (2008), pp. 261–76.

[12] C. Dulac, L. A. O'Connell, and Z. Wu. "Neural control of maternal and paternal behaviors". In: *Science* 345.6198 (2014), pp. 765–70.

[13] C. Yoshihara, M. Numan, and K. O. Kuroda. “Oxytocin and Parental Behaviors”. In: *Curr Top Behav Neurosci* 35 (2018), pp. 119–153.

[14] T. A. Baskerville and A. J. Douglas. “Interactions between dopamine and oxytocin in the control of sexual behaviour”. In: *Prog Brain Res* 170 (2008), pp. 277–90.

[15] M. Kosfeld, M. Heinrichs, P. J. Zak, U. Fischbacher, and E. Fehr. “Oxytocin increases trust in humans”. In: *Nature* 435.7042 (2005), pp. 673–6.

[16] R. Hurlemann, A. Patin, O. A. Onur, M. X. Cohen, T. Baumgartner, S. Metzler, I. Dziobek, J. Gallinat, M. Wagner, W. Maier, and K. M. Kendrick. “Oxytocin enhances amygdala-dependent, socially reinforced learning and emotional empathy in humans”. In: *J Neurosci* 30.14 (2010), pp. 4999–5007.

[17] S. Shahrestani, A. H. Kemp, and A. J. Guastella. “The impact of a single administration of intranasal oxytocin on the recognition of basic emotions in humans: a meta-analysis”. In: *Neuropsychopharmacology* 38.10 (2013), pp. 1929–36.

[18] E. L. MacLean, L. R. Gesquiere, M. E. Gruen, B. L. Sherman, W. L. Martin, and C. S. Carter. “Endogenous Oxytocin, Vasopressin, and Aggression in Domestic Dogs”. In: *Front Psychol* 8 (2017), p. 1613.

[19] N. Duque-Wilckens, M. Q. Steinman, S. A. Laredo, R. Hao, A. M. Perkeybile, K. L. Bales, and B. C. Trainor. “Inhibition of vasopressin V1a receptors in the medioventral bed nucleus of the stria terminalis has sex- and context-specific anxiogenic effects”. In: *Neuropharmacology* 110.Pt A (2016), pp. 59–68.

[20] R. R. Thompson, K. George, J. C. Walton, S. P. Orr, and J. Benson. “Sex-specific influences of vasopressin on human social communication”. In: *Proc Natl Acad Sci U S A* 103.20 (2006), pp. 7889–94.

[21] A. Knafo, S. Israel, A. Darvasi, R. Bachner-Melman, F. Uzefovsky, L. Cohen, E. Feldman, E. Lerer, E. Laiba, Y. Raz, L. Nemanov, I. Gritsenko, C. Dina, G. Agam, B. Dean, G. Bornstein, and R. P. Ebstein. “Individual differences in allocation of funds in the dictator game associated with length of the arginine vasopressin 1a receptor RS3 promoter region and correlation between RS3 length and hippocampal mRNA”. In: *Genes Brain Behav* 7.3 (2008), pp. 266–75.

[22] F. Uzefovsky, I. Shalev, S. Israel, A. Knafo, and R. P. Ebstein. “Vasopressin selectively impairs emotion recognition in men”. In: *Psychoneuroendocrinology* 37.4 (2012), pp. 576–80.

[23] E. F. Coccaro, R. J. Kavoussi, R. L. Hauger, T. B. Cooper, and C. F. Ferris. "Cerebrospinal fluid vasopressin levels: correlates with aggression and serotonin function in personality-disordered subjects". In: *Arch Gen Psychiatry* 55.8 (1998), pp. 708–14.

[24] M. Heinrichs and G. Domes. "Neuropeptides and social behaviour: effects of oxytocin and vasopressin in humans". In: *Prog Brain Res* 170 (2008), pp. 337–50.

[25] Q. Lu, J. Lai, Y. Du, T. Huang, P. Prukpitikul, Y. Xu, and S. Hu. "Sexual dimorphism of oxytocin and vasopressin in social cognition and behavior". In: *Psychol Res Behav Manag* 12 (2019), pp. 337–349.

[26] D. H. Skuse and L. Gallagher. "Dopaminergic-neuropeptide interactions in the social brain". In: *Trends Cogn Sci* 13.1 (2009), pp. 27–35.

[27] R. Mottolese, J. Redoute, N. Costes, D. Le Bars, and A. Sirigu. "Switching brain serotonin with oxytocin". In: *Proc Natl Acad Sci U S A* 111.23 (2014), pp. 8637–42.

[28] R. Feldman, M. Monakhov, M. Pratt, and R. P. Ebstein. "Oxytocin Pathway Genes: Evolutionary Ancient System Impacting on Human Affiliation, Sociality, and Psychopathology". In: *Biol Psychiatry* 79.3 (2016), pp. 174–84.

[29] M. G. Di Giglio, M. Muttenthaler, K. Harpsoe, Z. Liutkeviciute, P. Keov, T. Eder, T. Rattei, S. Arrowsmith, S. Wray, A. Marek, T. Elbert, P. F. Alewood, D. E. Gloriam, and C. W. Gruber. "Development of a human vasopressin V1a-receptor antagonist from an evolutionary-related insect neuropeptide". In: *Sci Rep* 7 (2017), p. 41002.

[30] K. Yamashita and T. Kitano. "Molecular evolution of the oxytocin-oxytocin receptor system in eutherians". In: *Mol Phylogenet Evol* 67.2 (2013), pp. 520–8.

[31] C. A. Pedersen and Jr. Prange A. J. "Induction of maternal behavior in virgin rats after intracerebroventricular administration of oxytocin". In: *Proc Natl Acad Sci U S A* 76.12 (1979), pp. 6661–5.

[32] R. M. Buijs. "Intra- and extrahypothalamic vasopressin and oxytocin pathways in the rat. Pathways to the limbic system, medulla oblongata and spinal cord". In: *Cell Tissue Res* 192.3 (1978), pp. 423–35.

[33] J. Elands, C. Barberis, S. Jard, B. Lammek, M. Manning, W. H. Sawyer, and E. R. de Kloet. "125I-d(CH2)5[Tyr(Me)2, Tyr(NH2)9]AVP: iodination and binding characteristics of a vasopressin receptor ligand". In: *FEBS Lett* 229.2 (1988), pp. 251–5.

[34] J. Elands, C. Barberis, S. Jard, E. Tribollet, J. J. Dreifuss, K. Bankowski, M. Manning, and W. H. Sawyer. "125I-labelled d(CH2)5[Tyr(Me)2,Thr4,Tyr-NH2(9)]OVT: a selective oxytocin receptor ligand". In: *Eur J Pharmacol* 147.2 (1988), pp. 197–207.

[35] T. Kimura, O. Tanizawa, K. Mori, M. J. Brownstein, and H. Okayama. "Structure and expression of a human oxytocin receptor". In: *Nature* 356.6369 (1992), pp. 526–9.

[36] M. Busnelli, E. Bulgheroni, M. Manning, G. Kleinau, and B. Chini. "Selective and potent agonists and antagonists for investigating the role of mouse oxytocin receptors". In: *J Pharmacol Exp Ther* 346.2 (2013), pp. 318–27.

[37] C. S. Carter, A. C. DeVries, and L. L. Getz. "Physiological substrates of mammalian monogamy: the prairie vole model". In: *Neurosci Biobehav Rev* 19.2 (1995), pp. 303–14.

[38] G. S. Prounis, K. Thomas, and A. G. Ophir. "Developmental trajectories and influences of environmental complexity on oxytocin receptor and vasopressin 1A receptor expression in male and female prairie voles". In: *J Comp Neurol* 526.11 (2018), pp. 1820–1842.

[39] T. R. Insel and T. J. Hulihan. "A gender-specific mechanism for pair bonding: oxytocin and partner preference formation in monogamous voles". In: *Behav Neurosci* 109.4 (1995), pp. 782–9.

[40] J. T. Winslow and T. R. Insel. "The social deficits of the oxytocin knockout mouse". In: *Neuropeptides* 36.2-3 (2002), pp. 221–9.

[41] N. Egashira, A. Tanoue, G. Tsujimoto, K. Mishima, Y. Takano, K. Iwasaki, and M. Fujiwara. "[Vasopressin receptor knockout mice as an animal model of psychiatric disorders]". In: *Nihon Shinkei Seishin Yakurigaku Zasshi* 26.2 (2006), pp. 101–5.

[42] S. R. Wersinger, E. I. Ginns, A. M. O'Carroll, S. J. Lolait, and 3rd Young W. S. "Vasopressin V1b receptor knockout reduces aggressive behavior in male mice". In: *Mol Psychiatry* 7.9 (2002), pp. 975–84.

[43] A. S. Smith, A. Agmo, A. K. Birnie, and J. A. French. "Manipulation of the oxytocin system alters social behavior and attraction in pair-bonding primates, Callithrix penicillata". In: *Horm Behav* 57.2 (2010), pp. 255–62.

[44] R. M. Wittig, C. Crockford, T. Deschner, K. E. Langergraber, T. E. Ziegler, and K. Zuberbuhler. "Food sharing is linked to urinary oxytocin levels and bonding in related and unrelated wild chimpanzees". In: *Proc Biol Sci* 281.1778 (2014), p. 20133096.

[45] V. Michopoulos, M. Checchi, D. Sharpe, and M. E. Wilson. "Estradiol effects on behavior and serum oxytocin are modified by social status and polymorphisms in the serotonin transporter gene in female rhesus monkeys". In: *Horm Behav* 59.4 (2011), pp. 528–35.

[46] J. Cavanaugh, S. B. Carp, C. M. Rock, and J. A. French. "Oxytocin modulates behavioral and physiological responses to a stressor in marmoset monkeys". In: *Psychoneuroendocrinology* 66 (2016), pp. 22–30.

[47] D. Ren, G. Lu, H. Moriyama, A. C. Mustoe, E. B. Harrison, and J. A. French. "Genetic diversity in oxytocin ligands and receptors in New World monkeys". In: *PLoS One* 10.5 (2015), e0125775.

[48] E. Silva L. T. Parreiras, P. Vargas-Pinilla, D. A. Duarte, D. Longo, G. V. Espinoza Pardo, A. Dulor Finkler, V. R. Paixao-Cortes, P. Pare, D. L. Rovaris, E. B. Oliveira, R. A. Caceres, G. L. Goncalves, M. Bouvier, F. M. Salzano, A. B. Lucion, C. M. Costa-Neto, and M. C. Bortolini. "Functional New World monkey oxytocin forms elicit an altered signaling profile and promotes parental care in rats". In: *Proc Natl Acad Sci U S A* 114.34 (2017), pp. 9044–9049.

[49] G. Leng and M. Ludwig. "Intranasal Oxytocin: Myths and Delusions". In: *Biol Psychiatry* 79.3 (2016), pp. 243–50.

[50] S. A. Grace, S. L. Rossell, M. Heinrichs, C. Kordsachia, and I. Labuschagne. "Oxytocin and brain activity in humans: A systematic review and coordinate-based meta-analysis of functional MRI studies". In: *Psychoneuroendocrinology* 96 (2018), pp. 6–24.

[51] C. F. Zink and A. Meyer-Lindenberg. "Human neuroimaging of oxytocin and vasopressin in social cognition". In: *Horm Behav* 61.3 (2012), pp. 400–9.

[52] R. Thompson, S. Gupta, K. Miller, S. Mills, and S. Orr. "The effects of vasopressin on human facial responses related to social communication". In: *Psychoneuroendocrinology* 29.1 (2004), pp. 35–48.

[53] B. Jurek and I. D. Neumann. "The Oxytocin Receptor: From Intracellular Signaling to Behavior". In: *Physiol Rev* 98.3 (2018), pp. 1805–1908.

[54] R. Feldman, I. Gordon, and O. Zagoory-Sharon. "Maternal and paternal plasma, salivary, and urinary oxytocin and parent-infant synchrony: considering stress and affiliation components of human bonding". In: *Dev Sci* 14.4 (2011), pp. 752–61.

[55] K. J. Parker, J. P. Garner, R. A. Libove, S. A. Hyde, K. B. Hornbeak, D. S. Carson, C. P. Liao, J. M. Phillips, J. F. Hallmayer, and A. Y. Hardan. "Plasma oxytocin concentrations and OXTR polymorphisms predict social impairments in children with and without autism spectrum disorder". In: *Proc Natl Acad Sci U S A* 111.33 (2014), pp. 12258–63.

[56] D. LoParo and I. D. Waldman. "The oxytocin receptor gene (OXTR) is associated with autism spectrum disorder: a meta-analysis". In: *Mol Psychiatry* 20.5 (2015), pp. 640–6.

[57] D. B. Campbell, D. Datta, S. T. Jones, E. Batey Lee, J. S. Sutcliffe, E. A. Hammock, and P. Levitt. "Association of oxytocin receptor (OXTR) gene variants with multiple phenotype domains of autism spectrum disorder". In: *J Neurodev Disord* 3.2 (2011), pp. 101–12.

[58] S. Jacob, C. W. Brune, C. S. Carter, B. L. Leventhal, C. Lord, and Jr. Cook E. H. "Association of the oxytocin receptor gene (OXTR) in Caucasian children and adolescents with autism". In: *Neurosci Lett* 417.1 (2007), pp. 6–9.

[59] S. Wu, M. Jia, Y. Ruan, J. Liu, Y. Guo, M. Shuang, X. Gong, Y. Zhang, X. Yang, and D. Zhang. "Positive association of the oxytocin receptor gene (OXTR) with autism in the Chinese Han population". In: *Biol Psychiatry* 58.1 (2005), pp. 74–7.

[60] R. Feil and M. F. Fraga. "Epigenetics and the environment: emerging patterns and implications". In: *Nat Rev Genet* 13.2 (2012), pp. 97–109.

[61] S. Mamrut, H. Harony, R. Sood, H. Shahar-Gold, H. Gainer, Y. J. Shi, L. Barki-Harrington, and S. Wagner. "DNA methylation of specific CpG sites in the promoter region regulates the transcription of the mouse oxytocin receptor". In: *PLoS One* 8.2 (2013), e56869.

[62] H. Harony-Nicolas, S. Mamrut, L. Brodsky, H. Shahar-Gold, L. Barki-Harrington, and S. Wagner. "Brain region-specific methylation in the promoter of the murine oxytocin receptor gene is involved in its expression regulation". In: *Psychoneuroendocrinology* 39 (2014), pp. 121–31.

[63] B. W. Haas, M. M. Filkowski, R. N. Cochran, L. Denison, A. Ishak, S. Nishitani, and A. K. Smith. "Epigenetic modification of OXT and human sociability". In: *Proc Natl Acad Sci U S A* 113.27 (2016), E3816–23.

[64] M. Aghajani, E. T. Klapwijk, O. F. Colins, C. Ziegler, K. Domschke, Rrjm Vermeiren, and N. J. A. van der Wee. "Interactions Between Oxytocin Receptor Gene Methylation and Callous-Unemotional Traits Impact Socioaffective Brain Systems in Conduct-Disordered Offenders". In: *Biol Psychiatry Cogn Neurosci Neuroimaging* 3.4 (2018), pp. 379–391.

[65] C. Maud, J. Ryan, J. E. McIntosh, and C. A. Olsson. "The role of oxytocin receptor gene (OXTR) DNA methylation (DNAm) in human social and emotional functioning: a systematic narrative review". In: *BMC Psychiatry* 18.1 (2018), p. 154.

[66] M. Kimmel, M. Clive, F. Gispen, J. Guintivano, T. Brown, O. Cox, M. W. Beckmann, J. Kornhuber, P. A. Fasching, L. M. Osborne, E. Binder, J. L. Payne, and Z. Kaminsky. "Oxytocin receptor DNA methylation in postpartum depression". In: *Psychoneuroendocrinology* 69 (2016), pp. 150–60.

[67] M. Bang, J. I. Kang, S. J. Kim, J. Y. Park, K. R. Kim, S. Y. Lee, K. Park, E. Lee, S. K. Lee, and S. K. An. "Reduced DNA Methylation of the Oxytocin Receptor Gene Is Associated With Anhedonia-Asociality in Women With Recent-Onset Schizophrenia and Ultra-high Risk for Psychosis". In: *Schizophr Bull* 45.6 (2019), pp. 1279–1290.

[68] J. P. Gouin, Q. Q. Zhou, L. Booij, M. Boivin, S. M. Cote, M. Hebert, I. Ouellet-Morin, M. Szyf, R. E. Tremblay, G. Turecki, and F. Vitaro. "Associations among oxytocin receptor gene (OXTR) DNA methylation in adulthood, exposure to early life adversity, and childhood trajectories of anxiousness". In: *Sci Rep* 7.1 (2017), p. 7446.

[69] M. H. Puglia, T. S. Lillard, J. P. Morris, and J. J. Connelly. "Epigenetic modification of the oxytocin receptor gene influences the perception of anger and fear in the human brain". In: *Proc Natl Acad Sci U S A* 112.11 (2015), pp. 3308–13.

[70] G. Dolen, A. Darvishzadeh, K. W. Huang, and R. C. Malenka. "Social reward requires coordinated activity of nucleus accumbens oxytocin and serotonin". In: *Nature* 501.7466 (2013), pp. 179–84.

[71] H. S. Knobloch, A. Charlet, L. C. Hoffmann, M. Eliava, S. Khrulev, A. H. Cetin, P. Osten, M. K. Schwarz, P. H. Seeburg, R. Stoop, and V. Grinevich. "Evoked axonal oxytocin release in the central amygdala attenuates fear response". In: *Neuron* 73.3 (2012), pp. 553–66.

[72] H. E. Ross, C. D. Cole, Y. Smith, I. D. Neumann, R. Landgraf, A. Z. Murphy, and L. J. Young. "Characterization of the oxytocin system regulating affiliative behavior in female prairie voles". In: *Neuroscience* 162.4 (2009), pp. 892–903.

[73] C. N. Rogers, A. P. Ross, S. P. Sahu, E. R. Siegel, J. M. Dooyema, M. A. Cree, E. G. Stopa, L. J. Young, J. K. Rilling, H. E. Albers, and T. M. Preuss. "Oxytocin- and arginine vasopressin-containing fibers in the cortex

of humans, chimpanzees, and rhesus macaques". In: *Am J Primatol* 80.10 (2018), e22875.

[74] W. Bargmann and E. Scharrer. "The site of origin of the hormones of the posterior pituitary". In: *Am Sci* 39.2 (1951), pp. 255–9.

[75] S. M. Freeman and L. J. Young. "Comparative Perspectives on Oxytocin and Vasopressin Receptor Research in Rodents and Primates: Translational Implications". In: *J Neuroendocrinol* 28.4 (2016).

[76] J. Peris, K. MacFadyen, J. A. Smith, A. D. de Kloet, L. Wang, and E. G. Krause. "Oxytocin receptors are expressed on dopamine and glutamate neurons in the mouse ventral tegmental area that project to nucleus accumbens and other mesolimbic targets". In: *J Comp Neurol* 525.5 (2017), pp. 1094–1108.

[77] S. M. Freeman, K. Inoue, A. L. Smith, M. M. Goodman, and L. J. Young. "The neuroanatomical distribution of oxytocin receptor binding and mRNA in the male rhesus macaque (Macaca mulatta)". In: *Psychoneuroendocrinology* 45 (2014), pp. 128–41.

[78] S. M. Freeman, A. L. Smith, M. M. Goodman, and K. L. Bales. "Selective localization of oxytocin receptors and vasopressin 1a receptors in the human brainstem". In: *Soc Neurosci* 12.2 (2017), pp. 113–123.

[79] M. L. Boccia, P. Petrusz, K. Suzuki, L. Marson, and C. A. Pedersen. "Immunohistochemical localization of oxytocin receptors in human brain". In: *Neuroscience* 253 (2013), pp. 155–64.

[80] D. S. Quintana, J. Rokicki, D. van der Meer, D. Alnaes, T. Kaufmann, A. Cordova-Palomera, I. Dieset, O. A. Andreassen, and L. T. Westlye. "Oxytocin pathway gene networks in the human brain". In: *Nat Commun* 10.1 (2019), p. 668.

[81] T. A. Baskerville and A. J. Douglas. "Dopamine and oxytocin interactions underlying behaviors: potential contributions to behavioral disorders". In: *CNS Neurosci Ther* 16.3 (2010), e92–123.

[82] M. Yoshida, Y. Takayanagi, K. Inoue, T. Kimura, L. J. Young, T. Onaka, and K. Nishimori. "Evidence that oxytocin exerts anxiolytic effects via oxytocin receptor expressed in serotonergic neurons in mice". In: *J Neurosci* 29.7 (2009), pp. 2259–71.

[83] O. Dal Monte, M. Piva, K. M. Anderson, M. Tringides, A. J. Holmes, and S. W. C. Chang. "Oxytocin under opioid antagonism leads to supralinear enhancement of social attention". In: *Proc Natl Acad Sci U S A* 114.20 (2017), pp. 5247–5252.

[84] P. A. Brennan. “The nose knows who’s who: chemosensory individuality and mate recognition in mice”. In: *Horm Behav* 46.3 (2004), pp. 231–40.

[85] E. Tribollet, C. Barberis, S. Jard, M. Dubois-Dauphin, and J. J. Dreifuss. “Localization and pharmacological characterization of high affinity binding sites for vasopressin and oxytocin in the rat brain by light microscopic autoradiography”. In: *Brain Res* 442.1 (1988), pp. 105–18.

[86] R. A. Adan, F. W. Van Leeuwen, M. A. Sonnemans, M. Brouns, G. Hoffman, J. G. Verbalis, and J. P. Burbach. “Rat oxytocin receptor in brain, pituitary, mammary gland, and uterus: partial sequence and immunocytochemical localization”. In: *Endocrinology* 136.9 (1995), pp. 4022–8.

[87] A. C. Keebaugh and L. J. Young. “Increasing oxytocin receptor expression in the nucleus accumbens of pre-pubertal female prairie voles enhances alloparental responsiveness and partner preference formation as adults”. In: *Horm Behav* 60.5 (2011), pp. 498–504.

[88] A. C. Keebaugh, C. E. Barrett, J. L. Laprairie, J. J. Jenkins, and L. J. Young. “RNAi knockdown of oxytocin receptor in the nucleus accumbens inhibits social attachment and parental care in monogamous female prairie voles”. In: *Soc Neurosci* 10.5 (2015), pp. 561–70.

[89] M. Manning, A. Misicka, A. Olma, K. Bankowski, S. Stoev, B. Chini, T. Durroux, B. Mouillac, M. Corbani, and G. Guillon. “Oxytocin and vasopressin agonists and antagonists as research tools and potential therapeutics”. In: *J Neuroendocrinol* 24.4 (2012), pp. 609–28.

[90] E. H. Shen, C. C. Overly, and A. R. Jones. “The Allen Human Brain Atlas: comprehensive gene expression mapping of the human brain”. In: *Trends Neurosci* 35.12 (2012), pp. 711–4.

[91] D. Paval. “A Dopamine Hypothesis of Autism Spectrum Disorder”. In: *Dev Neurosci* 39.5 (2017), pp. 355–360.

[92] A. J. Rosenfeld, J. A. Lieberman, and L. F. Jarskog. “Oxytocin, dopamine, and the amygdala: a neurofunctional model of social cognitive deficits in schizophrenia”. In: *Schizophr Bull* 37.5 (2011), pp. 1077–87.

[93] M. R. Lee, M. C. Rohn, G. Tanda, and L. Leggio. “Targeting the Oxytocin System to Treat Addictive Disorders: Rationale and Progress to Date”. In: *CNS Drugs* 30.2 (2016), pp. 109–23.

[94] E. Scarr, S. Sundram, D. Keriakous, and B. Dean. “Altered hippocampal muscarinic M4, but not M1, receptor expression from subjects with schizophrenia”. In: *Biol Psychiatry* 61.10 (2007), pp. 1161–70.

[95] G. Karvat and T. Kimchi. “Acetylcholine elevation relieves cognitive rigidity and social deficiency in a mouse model of autism”. In: *Neuropsychopharmacology* 39.4 (2014), pp. 831–40.

[96] R. Cools, A. C. Roberts, and T. W. Robbins. “Serotoninergic regulation of emotional and behavioural control processes”. In: *Trends Cogn Sci* 12.1 (2008), pp. 31–40.

[97] P. Shattock and P. Whiteley. “Biochemical aspects in autism spectrum disorders: updating the opioid-excess theory and presenting new opportunities for biomedical intervention”. In: *Expert Opin Ther Targets* 6.2 (2002), pp. 175–83.

[98] L. Xiao, M. F. Priest, J. Nasenbeny, T. Lu, and Y. Kozorovitskiy. “Biased Oxytocinergic Modulation of Midbrain Dopamine Systems”. In: *Neuron* 95.2 (2017), 368–384 e5.

[99] Y. Liu and Z. X. Wang. “Nucleus accumbens oxytocin and dopamine interact to regulate pair bond formation in female prairie voles”. In: *Neuroscience* 121.3 (2003), pp. 537–44.

[100] W. Romero-Fernandez, D. O. Borroto-Escuela, L. F. Agnati, and K. Fuxe. “Evidence for the existence of dopamine D2-oxytocin receptor heteromers in the ventral and dorsal striatum with facilitatory receptor-receptor interactions”. In: *Mol Psychiatry* 18.8 (2013), pp. 849–50.

[101] O. Lindvall, A. Bjorklund, and G. Skagerberg. “Selective histochemical demonstration of dopamine terminal systems in rat di- and telencephalon: new evidence for dopaminergic innervation of hypothalamic neurosecretory nuclei”. In: *Brain Res* 306.1-2 (1984), pp. 19–30.

[102] F. Moos and P. Richard. “Excitatory effect of dopamine on oxytocin and vasopressin reflex releases in the rat”. In: *Brain Res* 241.2 (1982), pp. 249–60.

[103] S. M. Freeman, M. C. Palumbo, R. H. Lawrence, A. L. Smith, M. M. Goodman, and K. L. Bales. “Effect of age and autism spectrum disorder on oxytocin receptor density in the human basal forebrain and midbrain”. In: *Transl Psychiatry* 8.1 (2018), p. 257.

[104] E. P. Noble. “D2 dopamine receptor gene in psychiatric and neurologic disorders and its phenotypes”. In: *Am J Med Genet B Neuropsychiatr Genet* 116B.1 (2003), pp. 103–25.

[105] D. Wei, D. Lee, C. D. Cox, C. A. Karsten, O. Penagarikano, D. H. Geschwind, C. M. Gall, and D. Piomelli. "Endocannabinoid signaling mediates oxytocin-driven social reward". In: *Proc Natl Acad Sci U S A* 112.45 (2015), pp. 14084–9.

[106] J. Day and H. C. Fibiger. "Dopaminergic regulation of cortical acetylcholine release". In: *Synapse* 12.4 (1992), pp. 281–6.

[107] M. Sarter, C. Lustig, and S. F. Taylor. "Cholinergic contributions to the cognitive symptoms of schizophrenia and the viability of cholinergic treatments". In: *Neuropharmacology* 62.3 (2012), pp. 1544–53.

[108] T. A. Baskerville, J. Allard, C. Wayman, and A. J. Douglas. "Dopamine-oxytocin interactions in penile erection". In: *Eur J Neurosci* 30.11 (2009), pp. 2151–64.

[109] I. D. Neumann and D. A. Slattery. "Oxytocin in General Anxiety and Social Fear: A Translational Approach". In: *Biol Psychiatry* 79.3 (2016), pp. 213–21.

[110] A. B. Emiliano, T. Cruz, V. Pannoni, and J. L. Fudge. "The interface of oxytocin-labeled cells and serotonin transporter-containing fibers in the primate hypothalamus: a substrate for SSRIs therapeutic effects?" In: *Neuropsychopharmacology* 32.5 (2007), pp. 977–88.

[111] H. Jorgensen, M. Riis, U. Knigge, A. Kjaer, and J. Warberg. "Serotonin receptors involved in vasopressin and oxytocin secretion". In: *J Neuroendocrinol* 15.3 (2003), pp. 242–9.

[112] J. L. Eaton, L. Roache, K. N. Nguyen, B. S. Cushing, E. Troyer, E. Papademetriou, and M. A. Raghanti. "Organizational effects of oxytocin on serotonin innervation". In: *Dev Psychobiol* 54.1 (2012), pp. 92–7.

[113] K. Varnas, C. Halldin, and H. Hall. "Autoradiographic distribution of serotonin transporters and receptor subtypes in human brain". In: *Hum Brain Mapp* 22.3 (2004), pp. 246–60.

[114] K. Varnas, H. Hall, P. Bonaventure, and G. Sedvall. "Autoradiographic mapping of 5-HT(1B) and 5-HT(1D) receptors in the post mortem human brain using [(3)H]GR 125743". In: *Brain Res* 915.1 (2001), pp. 47–57.

[115] K. Varnas, Y. L. Hurd, and H. Hall. "Regional expression of 5-HT1B receptor mRNA in the human brain". In: *Synapse* 56.1 (2005), pp. 21–8.

[116] A. L. Garcia-Garcia, A. Newman-Tancredi, and E. D. Leonardo. "5-HT(1A) [corrected] receptors in mood and anxiety: recent insights into autoreceptor versus heteroreceptor function". In: *Psychopharmacology (Berl)* 231.4 (2014), pp. 623–36.

[117] E. Gur, E. Dremencov, F. Garcia, L. D. Van de Kar, B. Lerer, and M. E. Newman. "Functional effects of chronic electroconvulsive shock on serotonergic 5-HT(1A) and 5-HT(1B) receptor activity in rat hippocampus and hypothalamus". In: *Brain Res* 952.1 (2002), pp. 52–60.

[118] I. G. Makarenko, M. M. Meguid, and M. V. Ugrumov. "Distribution of serotonin 5-hydroxytriptamine 1B (5-HT(1B)) receptors in the normal rat hypothalamus". In: *Neurosci Lett* 328.2 (2002), pp. 155–9.

[119] J. Savitz, I. Lucki, and W. C. Drevets. "5-HT(1A) receptor function in major depressive disorder". In: *Prog Neurobiol* 88.1 (2009), pp. 17–31.

[120] M. Tiger, K. Varnas, Y. Okubo, and J. Lundberg. "The 5-HT1B receptor - a potential target for antidepressant treatment". In: *Psychopharmacology (Berl)* 235.5 (2018), pp. 1317–1334.

[121] P. M. Fisher, C. C. Meltzer, S. K. Ziolko, J. C. Price, E. L. Moses-Kolko, S. L. Berga, and A. R. Hariri. "Capacity for 5-HT1A-mediated autoregulation predicts amygdala reactivity". In: *Nat Neurosci* 9.11 (2006), pp. 1362–3.

[122] M. Bocchio, S. B. McHugh, D. M. Bannerman, T. Sharp, and M. Capogna. "Serotonin, Amygdala and Fear: Assembling the Puzzle". In: *Front Neural Circuits* 10 (2016), p. 24.

[123] V. M. Husarova, S. Lakatosova, A. Pivovarciova, K. Babinska, J. Bakos, J. Durdiakova, A. Kubranska, I. Ondrejka, and D. Ostatnikova. "Plasma Oxytocin in Children with Autism and Its Correlations with Behavioral Parameters in Children and Parents". In: *Psychiatry Investig* 13.2 (2016), pp. 174–83.

[124] G. Scantamburlo, M. Hansenne, S. Fuchs, W. Pitchot, P. Marechal, C. Pequeux, M. Ansseau, and J. J. Legros. "Plasma oxytocin levels and anxiety in patients with major depression". In: *Psychoneuroendocrinology* 32.4 (2007), pp. 407–10.

[125] S. K. Lawson, A. C. Gray, and N. S. Woehrle. "Effects of oxytocin on serotonin 1B agonist-induced autism-like behavior in mice". In: *Behav Brain Res* 314 (2016), pp. 52–64.

[126] D. Jin, H. X. Liu, H. Hirai, T. Torashima, T. Nagai, O. Lopatina, N. A. Shnayder, K. Yamada, M. Noda, T. Seike, K. Fujita, S. Takasawa, S. Yokoyama, K. Koizumi, Y. Shiraishi, S. Tanaka, M. Hashii, T. Yoshihara, K. Higashida, M. S. Islam, N. Yamada, K. Hayashi, N. Noguchi, I. Kato, H. Okamoto, A. Matsushima, A. Salmina, T. Munesue, N. Shimizu, S. Mochida, M. Asano, and H. Higashida. "CD38 is critical for social behaviour by regulating oxytocin secretion". In: *Nature* 446.7131 (2007), pp. 41–5.

[127] E. H. van den Burg, J. Stindl, T. Grund, I. D. Neumann, and O. Strauss. "Oxytocin Stimulates Extracellular Ca2+ Influx Through TRPV2 Channels in Hypothalamic Neurons to Exert Its Anxiolytic Effects". In: *Neuropsychopharmacology* 40.13 (2015), pp. 2938–47.

[128] T. Ohbuchi, J. Haam, and J. G. Tasker. "Regulation of Neuronal Activity in Hypothalamic Vasopressin Neurons". In: *Interdiscip Inf Sci* 21.3 (2015), pp. 225–234.

[129] S. M. Smith and W. W. Vale. "The role of the hypothalamic-pituitary-adrenal axis in neuroendocrine responses to stress". In: *Dialogues Clin Neurosci* 8.4 (2006), pp. 383–95.

[130] F. A. Antoni. "Vasopressinergic control of pituitary adrenocorticotropin secretion comes of age". In: *Front Neuroendocrinol* 14.2 (1993), pp. 76–122.

[131] E. Q. Cox, A. Stuebe, B. Pearson, K. Grewen, D. Rubinow, and S. Meltzer-Brody. "Oxytocin and HPA stress axis reactivity in postpartum women". In: *Psychoneuroendocrinology* 55 (2015), pp. 164–72.

[132] K. J. Parker, C. L. Buckmaster, A. F. Schatzberg, and D. M. Lyons. "Intranasal oxytocin administration attenuates the ACTH stress response in monkeys". In: *Psychoneuroendocrinology* 30.9 (2005), pp. 924–9.

[133] A. E. Kudwa, R. F. McGivern, and R. J. Handa. "Estrogen receptor beta and oxytocin interact to modulate anxiety-like behavior and neuroendocrine stress reactivity in adult male and female rats". In: *Physiol Behav* 129 (2014), pp. 287–96.

[134] I. D. Neumann, L. Torner, N. Toschi, and A. H. Veenema. "Oxytocin actions within the supraoptic and paraventricular nuclei: differential effects on peripheral and intranuclear vasopressin release". In: *Am J Physiol Regul Integr Comp Physiol* 291.1 (2006), R29–36.

[135] B. B. Jamieson, B. B. Nair, and K. J. Iremonger. "Regulation of hypothalamic corticotropin-releasing hormone neurone excitability by oxytocin". In: *J Neuroendocrinol* 29.11 (2017).

[136] J. Maniam, C. Antoniadis, and M. J. Morris. "Early-Life Stress, HPA Axis Adaptation, and Mechanisms Contributing to Later Health Outcomes". In: *Front Endocrinol (Lausanne)* 5 (2014), p. 73.

[137] A. Agorastos, P. Pervanidou, G. P. Chrousos, and D. G. Baker. "Developmental Trajectories of Early Life Stress and Trauma: A Narrative Review on Neurobiological Aspects Beyond Stress System Dysregulation". In: *Front Psychiatry* 10 (2019), p. 118.

[138] J. Vargas, M. Junco, C. Gomez, and N. Lajud. "Early Life Stress Increases Metabolic Risk, HPA Axis Reactivity, and Depressive-Like Behavior When Combined with Postweaning Social Isolation in Rats". In: *PLoS One* 11.9 (2016), e0162665.

[139] E. G. Spratt, J. S. Nicholas, K. T. Brady, L. A. Carpenter, C. R. Hatcher, K. A. Meekins, R. W. Furlanetto, and J. M. Charles. "Enhanced cortisol response to stress in children in autism". In: *J Autism Dev Disord* 42.1 (2012), pp. 75–81.

[140] E. Iob, C. Kirschbaum, and A. Steptoe. "Persistent depressive symptoms, HPA-axis hyperactivity, and inflammation: the role of cognitive-affective and somatic symptoms". In: *Mol Psychiatry* (2019).

[141] K. Roelofs, J. van Peer, E. Berretty, Pd Jong, P. Spinhoven, and B. M. Elzinga. "Hypothalamus-pituitary-adrenal axis hyperresponsiveness is associated with increased social avoidance behavior in social phobia". In: *Biol Psychiatry* 65.4 (2009), pp. 336–43.

[142] T. E. Bridges, E. W. Hillhouse, and M. T. Jones. "The effect of dopamine on neurohypophysial hormone release in vivo and from the rat neural lobe and hypothalamus in vitro". In: *J Physiol* 260.3 (1976), pp. 647–66.

[143] S. L. Resendez, M. Dome, G. Gormley, D. Franco, N. Nevarez, A. A. Hamid, and B. J. Aragona. "mu-Opioid receptors within subregions of the striatum mediate pair bond formation through parallel yet distinct reward mechanisms". In: *J Neurosci* 33.21 (2013), pp. 9140–9.

[144] B. J. Ragen, S. M. Freeman, S. A. Laredo, S. P. Mendoza, and K. L. Bales. "mu and kappa opioid receptor distribution in the monogamous titi monkey (Callicebus cupreus): implications for social behavior and endocrine functioning". In: *Neuroscience* 290 (2015), pp. 421–34.

[145] R. J. Bicknell, G. Leng, J. A. Russell, R. G. Dyer, S. Mansfield, and B. G. Zhao. "Hypothalamic opioid mechanisms controlling oxytocin neurones during parturition". In: *Brain Res Bull* 20.6 (1988), pp. 743–9.

[146] R. J. Bicknell and G. Leng. "Endogenous opiates regulate oxytocin but not vasopressin secretion from the neurohypophysis". In: *Nature* 298.5870 (1982), pp. 161–2.

[147] Z. D. You, J. H. Li, C. Y. Song, C. H. Wang, and C. L. Lu. "Chronic morphine treatment inhibits oxytocin synthesis in rats". In: *Neuroreport* 11.14 (2000), pp. 3113–6.

[148] I. Neumann, J. A. Russell, B. Wolff, and R. Landgraf. "Naloxone increases the release of oxytocin, but not vasopressin, within limbic brain areas of conscious parturient rats: a push-pull perfusion study". In: *Neuroendocrinology* 54.6 (1991), pp. 545–51.

[149] R. J. Bicknell, G. Leng, D. W. Lincoln, and J. A. Russell. "Naloxone excites oxytocin neurones in the supraoptic nucleus of lactating rats after chronic morphine treatment". In: *J Physiol* 396 (1988), pp. 297–317.

[150] A. Roy, M. Roy, S. Deb, G. Unwin, and A. Roy. "Are opioid antagonists effective in attenuating the core symptoms of autism spectrum conditions in children: a systematic review". In: *J Intellect Disabil Res* 59.4 (2015), pp. 293–306.

[151] E. Rubenstein, J. C. Young, L. A. Croen, C. DiGuiseppi, N. F. Dowling, L. C. Lee, L. Schieve, L. D. Wiggins, and J. Daniels. "Brief Report: Maternal Opioid Prescription from Preconception Through Pregnancy and the Odds of Autism Spectrum Disorder and Autism Features in Children". In: *J Autism Dev Disord* 49.1 (2019), pp. 376–382.

[152] P. Pare, V. R. Paixao-Cortes, L. Tovo-Rodrigues, P. Vargas-Pinilla, L. H. Viscardi, F. M. Salzano, L. E. Henkes, and M. C. Bortolini. "Oxytocin and arginine vasopressin receptor evolution: implications for adaptive novelties in placental mammals". In: *Genet Mol Biol* 39.4 (2016), pp. 646–657.

[153] J. Koehbach, T. Stockner, C. Bergmayr, M. Muttenthaler, and C. W. Gruber. "Insights into the molecular evolution of oxytocin receptor ligand binding". In: *Biochem Soc Trans* 41.1 (2013), pp. 197–204.

[154] G. Gimpl and F. Fahrenholz. "The oxytocin receptor system: structure, function, and regulation". In: *Physiol Rev* 81.2 (2001), pp. 629–83.

[155] Y Waltenspuhl, J Schoppe, J Ehrenmann, L Kummer, and A Pluckthun. "Crystal structure of the human oxytocin receptor". In: *bioRxiv* preprint (2020).

[156] C. Barberis, B. Mouillac, and T. Durroux. "Structural bases of vasopressin/oxytocin receptor function". In: *J Endocrinol* 156.2 (1998), pp. 223–9.

[157] B. Mouillac, B. Chini, M. N. Balestre, J. Elands, S. Trumpp-Kallmeyer, J. Hoflack, M. Hibert, S. Jard, and C. Barberis. "The binding site of neuropeptide vasopressin V1a receptor. Evidence for a major localization within transmembrane regions". In: *J Biol Chem* 270.43 (1995), pp. 25771–7.

[158] B. Chini, B. Mouillac, Y. Ala, M. N. Balestre, S. Trumpp-Kallmeyer, J. Hoflack, J. Elands, M. Hibert, M. Manning, S. Jard, and et al. "Tyr115 is the key residue for determining agonist selectivity in the V1a vasopressin receptor". In: *EMBO J* 14.10 (1995), pp. 2176–82.

[159] M. Birnbaumer. "Vasopressin receptors". In: *Trends Endocrinol Metab* 11.10 (2000), pp. 406–10.

[160] Z. Strakova and M. S. Soloff. "Coupling of oxytocin receptor to G proteins in rat myometrium during labor: Gi receptor interaction". In: *Am J Physiol* 272.5 Pt 1 (1997), E870–6.

[161] A. Yulia, N. Singh, K. Lei, S. R. Sooranna, and M. R. Johnson. "Cyclic AMP Effectors Regulate Myometrial Oxytocin Receptor Expression". In: *Endocrinology* 157.11 (2016), pp. 4411–4422.

[162] M. Busnelli, A. Sauliere, M. Manning, M. Bouvier, C. Gales, and B. Chini. "Functional selective oxytocin-derived agonists discriminate between individual G protein family subtypes". In: *J Biol Chem* 287.6 (2012), pp. 3617–29.

[163] V. Grinevich, H. S. Knobloch-Bollmann, M. Eliava, M. Busnelli, and B. Chini. "Assembling the Puzzle: Pathways of Oxytocin Signaling in the Brain". In: *Biol Psychiatry* 79.3 (2016), pp. 155–64.

[164] S. Chung, I. H. Kim, D. Lee, K. Park, J. Y. Kim, Y. K. Lee, E. J. Kim, H. W. Lee, J. S. Choi, G. H. Son, W. Sun, K. S. Shin, and H. Kim. "The role of inositol 1,4,5-trisphosphate 3-kinase A in regulating emotional behavior and amygdala function". In: *Sci Rep* 6 (2016), p. 23757.

[165] N. Wettschureck, A. Moers, T. Hamalainen, T. Lemberger, G. Schutz, and S. Offermanns. "Heterotrimeric G proteins of the Gq/11 family are crucial for the induction of maternal behavior in mice". In: *Mol Cell Biol* 24.18 (2004), pp. 8048–54.

[166] A. Ayar, M. Ozcan, E. Alcin, I. Serhatlioglu, S. Ozcan, S. Kutlu, and H. Kelestimur. "Oxytocin activates calcium signaling in rat sensory neurons through a protein kinase C-dependent mechanism". In: *J Physiol Biochem* 70.1 (2014), pp. 43–8.

[167] D. Di Scala-Guenot, D. Mouginot, and M. T. Strosser. "Increase of intracellular calcium induced by oxytocin in hypothalamic cultured astrocytes". In: *Glia* 11.3 (1994), pp. 269–76.

[168] T. C. Sudhof. “Calcium control of neurotransmitter release”. In: *Cold Spring Harb Perspect Biol* 4.1 (2012), a011353.

[169] H. Higashida. “Somato-axodendritic release of oxytocin into the brain due to calcium amplification is essential for social memory”. In: *J Physiol Sci* 66.4 (2016), pp. 275–82.

[170] J. L. Garibay, T. Kozasa, H. Itoh, T. Tsukamoto, M. Matsuoka, and Y. Kaziro. “Analysis by mRNA levels of the expression of six G protein alpha-subunit genes in mammalian cells and tissues”. In: *Biochim Biophys Acta* 1094.2 (1991), pp. 193–9.

[171] S. H. Kim, D. A. MacIntyre, A. C. Hanyaloglu, A. M. Blanks, S. Thornton, P. R. Bennett, and V. Terzidou. “The oxytocin receptor antagonist, Atosiban, activates pro-inflammatory pathways in human amnion via G(alphai) signalling”. In: *Mol Cell Endocrinol* 420 (2016), pp. 11–23.

[172] A. Reversi, V. Rimoldi, T. Marrocco, P. Cassoni, G. Bussolati, M. Parenti, and B. Chini. “The oxytocin receptor antagonist atosiban inhibits cell growth via a ”biased agonist” mechanism”. In: *J Biol Chem* 280.16 (2005), pp. 16311–8.

[173] M. Gravati, M. Busnelli, E. Bulgheroni, A. Reversi, P. Spaiardi, M. Parenti, M. Toselli, and B. Chini. “Dual modulation of inward rectifier potassium currents in olfactory neuronal cells by promiscuous G protein coupling of the oxytocin receptor”. In: *J Neurochem* 114.5 (2010), pp. 1424–35.

[174] J. M. Israel, D. A. Poulain, and S. H. Oliet. “Oxytocin-induced postinhibitory rebound firing facilitates bursting activity in oxytocin neurons”. In: *J Neurosci* 28.2 (2008), pp. 385–94.

[175] M. Nishizato, T. X. Fujisawa, H. Kosaka, and A. Tomoda. “Developmental changes in social attention and oxytocin levels in infants and children”. In: *Sci Rep* 7.1 (2017), p. 2540.

[176] C. P. de Kock, K. D. Wierda, L. W. Bosman, R. Min, J. J. Koksma, H. D. Mansvelder, M. Verhage, and A. B. Brussaard. “Somatodendritic secretion in oxytocin neurons is upregulated during the female reproductive cycle”. In: *J Neurosci* 23.7 (2003), pp. 2726–34.

[177] A. Hasbi, D. Devost, S. A. Laporte, and H. H. Zingg. “Real-time detection of interactions between the human oxytocin receptor and G protein-coupled receptor kinase-2”. In: *Mol Endocrinol* 18.5 (2004), pp. 1277–86.

[178] M. P. Smith, V. J. Ayad, S. J. Mundell, C. A. McArdle, E. Kelly, and A. Lopez Bernal. “Internalization and desensitization of the oxytocin receptor is inhibited by Dynamin and clathrin mutants in human embryonic kidney 293 cells”. In: *Mol Endocrinol* 20.2 (2006), pp. 379–88.

[179] Jr. Goodman O. B., J. G. Krupnick, F. Santini, V. V. Gurevich, R. B. Penn, A. W. Gagnon, J. H. Keen, and J. L. Benovic. “Beta-arrestin acts as a clathrin adaptor in endocytosis of the beta2-adrenergic receptor”. In: *Nature* 383.6599 (1996), pp. 447–50.

[180] F. Conti, S. Sertic, A. Reversi, and B. Chini. “Intracellular trafficking of the human oxytocin receptor: evidence of receptor recycling via a Rab4/Rab5 ”short cycle””. In: *Am J Physiol Endocrinol Metab* 296.3 (2009), E532–42.

[181] C. Robinson, R. Schumann, P. Zhang, and R. C. Young. “Oxytocin-induced desensitization of the oxytocin receptor”. In: *Am J Obstet Gynecol* 188.2 (2003), pp. 497–502.

[182] S. Phaneuf, G. Asboth, M. P. Carrasco, B. R. Linares, T. Kimura, A. Harris, and A. L. Bernal. “Desensitization of oxytocin receptors in human myometrium”. In: *Hum Reprod Update* 4.5 (1998), pp. 625–33.

[183] H. Huang, C. Michetti, M. Busnelli, F. Manago, S. Sannino, D. Scheggia, L. Giancardo, D. Sona, V. Murino, B. Chini, M. L. Scattoni, and F. Papaleo. “Chronic and acute intranasal oxytocin produce divergent social effects in mice”. In: *Neuropsychopharmacology* 39.5 (2014), pp. 1102–14.

[184] K. Oya, Y. Matsuda, S. Matsunaga, T. Kishi, and N. Iwata. “Efficacy and safety of oxytocin augmentation therapy for schizophrenia: an updated systematic review and meta-analysis of randomized, placebo-controlled trials”. In: *Eur Arch Psychiatry Clin Neurosci* 266.5 (2016), pp. 439–50.

[185] F. De Cagna, L. Fusar-Poli, S. Damiani, M. Rocchetti, G. Giovanna, A. Mori, P. Politi, and N. Brondino. “The Role of Intranasal Oxytocin in Anxiety and Depressive Disorders: A Systematic Review of Randomized Controlled Trials”. In: *Clin Psychopharmacol Neurosci* 17.1 (2019), pp. 1–11.

[186] A. Preti, M. Melis, S. Siddi, M. Vellante, G. Doneddu, and R. Fadda. “Oxytocin and autism: a systematic review of randomized controlled trials”. In: *J Child Adolesc Psychopharmacol* 24.2 (2014), pp. 54–68.

[187] L. R. Hanson and 2nd Frey W. H. “Intranasal delivery bypasses the blood-brain barrier to target therapeutic agents to the central nervous system and treat neurodegenerative disease”. In: *BMC Neurosci* 9 Suppl 3 (2008), S5.

[188] M. E. Modi, F. Connor-Stroud, R. Landgraf, L. J. Young, and L. A. Parr. "Aerosolized oxytocin increases cerebrospinal fluid oxytocin in rhesus macaques". In: *Psychoneuroendocrinology* 45 (2014), pp. 49–57.

[189] A. Gossen, A. Hahn, L. Westphal, S. Prinz, R. T. Schultz, G. Grunder, and K. N. Spreckelmeyer. "Oxytocin plasma concentrations after single intranasal oxytocin administration - a study in healthy men". In: *Neuropeptides* 46.5 (2012), pp. 211–5.

[190] H. Walum, I. D. Waldman, and L. J. Young. "Statistical and Methodological Considerations for the Interpretation of Intranasal Oxytocin Studies". In: *Biol Psychiatry* 79.3 (2016), pp. 251–7.

[191] T. M. Kazdoba, P. T. Leach, M. Yang, J. L. Silverman, M. Solomon, and J. N. Crawley. "Translational Mouse Models of Autism: Advancing Toward Pharmacological Therapeutics". In: *Curr Top Behav Neurosci* 28 (2016), pp. 1–52.

[192] G. R. Pitt, A. R. Batt, R. M. Haigh, A. M. Penson, P. A. Robson, D. P. Rooker, A. L. Tartar, J. E. Trim, C. M. Yea, and M. B. Roe. "Non-peptide oxytocin agonists". In: *Bioorg Med Chem Lett* 14.17 (2004), pp. 4585–9.

[193] Y. Yang, H. Li, R. Ward, L. Gao, J. F. Wei, and T. R. Xu. "Novel oxytocin receptor agonists and antagonists: a patent review (2002 - 2013)". In: *Expert Opin Ther Pat* 24.1 (2014), pp. 29–46.

[194] R. H. Ring, L. E. Schechter, S. K. Leonard, J. M. Dwyer, B. J. Platt, R. Graf, S. Grauer, C. Pulicicchio, L. Resnick, Z. Rahman, S. J. Sukoff Rizzo, B. Luo, C. E. Beyer, S. F. Logue, K. L. Marquis, Z. A. Hughes, and S. Rosenzweig-Lipson. "Receptor and behavioral pharmacology of WAY-267464, a non-peptide oxytocin receptor agonist". In: *Neuropharmacology* 58.1 (2010), pp. 69–77.

[195] C. Hicks, W. Jorgensen, C. Brown, J. Fardell, J. Koehbach, C. W. Gruber, M. Kassiou, G. E. Hunt, and I. S. McGregor. "The nonpeptide oxytocin receptor agonist WAY 267,464: receptor-binding profile, prosocial effects and distribution of c-Fos expression in adolescent rats". In: *J Neuroendocrinol* 24.7 (2012), pp. 1012–29.

[196] M. C. Frantz, L. P. Pellissier, E. Pflimlin, S. Loison, J. Gandia, C. Marsol, T. Durroux, B. Mouillac, J. A. J. Becker, J. Le Merrer, C. Valencia, P. Villa, D. Bonnet, and M. Hibert. "LIT-001, the First Nonpeptide Oxytocin Receptor Agonist that Improves Social Interaction in a Mouse Model of Autism". In: *J Med Chem* 61.19 (2018), pp. 8670–8692.

[197] C. Hicks, L. Ramos, T. A. Reekie, R. Narlawar, M. Kassiou, and I. S. McGregor. "WAY 267,464, a non-peptide oxytocin receptor agonist, impairs social recognition memory in rats through a vasopressin 1A receptor antagonist action". In: *Psychopharmacology (Berl)* 232.15 (2015), pp. 2659–67.

[198] W. T. Jorgensen, D. W. Gulliver, T. A. Katte, E. L. Werry, T. A. Reekie, M. Connor, and M. Kassiou. "Conformationally rigid derivatives of WAY-267,464: Synthesis and pharmacology at the human oxytocin and vasopressin-1a receptors". In: *Eur J Med Chem* 143 (2018), pp. 1644–1656.

[199] R. Beard, A. Stucki, M. Schmitt, G. Py, C. Grundschober, A. D. Gee, and E. W. Tate. "Building bridges for highly selective, potent and stable oxytocin and vasopressin analogs". In: *Bioorg Med Chem* 26.11 (2018), pp. 3039–3045.

[200] M. Muttenthaler, A. Andersson, I. Vetter, R. Menon, M. Busnelli, L. Ragnarsson, C. Bergmayr, S. Arrowsmith, J. R. Deuis, H. S. Chiu, N. J. Palpant, M. O'Brien, T. J. Smith, S. Wray, I. D. Neumann, C. W. Gruber, R. J. Lewis, and P. F. Alewood. "Subtle modifications to oxytocin produce ligands that retain potency and improved selectivity across species". In: *Sci Signal* 10.508 (2017).

[201] K. Wisniewski, S. Alagarsamy, R. Galyean, H. Tariga, D. Thompson, B. Ly, H. Wisniewska, S. Qi, G. Croston, R. Laporte, P. J. Riviere, and C. D. Schteingart. "New, potent, and selective peptidic oxytocin receptor agonists". In: *J Med Chem* 57.12 (2014), pp. 5306–17.

[202] N. Kablaoui, M. Vanase-Frawley, and S. Sciabola. "Hybrid peptide-small molecule oxytocin analogs are potent and selective agonists of the oxytocin receptor". In: *Bioorg Med Chem Lett* 28.3 (2018), pp. 415–419.

[203] I. Passoni, M. Leonzino, V. Gigliucci, B. Chini, and M. Busnelli. "Carbetocin is a Functional Selective Gq Agonist That Does Not Promote Oxytocin Receptor Recycling After Inducing beta-Arrestin-Independent Internalisation". In: *J Neuroendocrinol* 28.4 (2016).

[204] M. Eliava, M. Melchior, H. S. Knobloch-Bollmann, J. Wahis, M. da Silva Gouveia, Y. Tang, A. C. Ciobanu, R. Triana Del Rio, L. C. Roth, F. Althammer, V. Chavant, Y. Goumon, T. Gruber, N. Petit-Demouliere, M. Busnelli, B. Chini, L. L. Tan, M. Mitre, R. C. Froemke, M. V. Chao, G. Giese, R. Sprengel, R. Kuner, P. Poisbeau, P. H. Seeburg, R. Stoop, A. Charlet, and V. Grinevich. "A New Population of Parvocellular Oxytocin Neurons Controlling Magnocellular Neuron Activity and Inflammatory Pain Processing". In: *Neuron* 89.6 (2016), pp. 1291–1304.

[205] A. D. de Araujo, M. Mobli, J. Castro, A. M. Harrington, I. Vetter, Z. Dekan, M. Muttenthaler, J. Wan, R. J. Lewis, G. F. King, S. M. Brierley, and P. F. Alewood. "Selenoether oxytocin analogues have analgesic properties in a mouse model of chronic abdominal pain". In: *Nat Commun* 5 (2014), p. 3165.

[206] E. J. Campbell-Smith, N. M. Holmes, N. W. Lingawi, M. C. Panayi, and R. F. Westbrook. "Oxytocin signaling in basolateral and central amygdala nuclei differentially regulates the acquisition, expression, and extinction of context-conditioned fear in rats". In: *Learn Mem* 22.5 (2015), pp. 247–57.

[207] V. Klenerova, I. Krejci, P. Sida, Z. Hlinak, and S. Hynie. "Modulary effects of oxytocin and carbetocin on stress-induced changes in rat behavior in the open-field". In: *J Physiol Pharmacol* 60.2 (2009), pp. 57–62.

[208] S. Chaviaras, P. Mak, D. Ralph, L. Krishnan, and J. H. Broadbear. "Assessing the antidepressant-like effects of carbetocin, an oxytocin agonist, using a modification of the forced swimming test". In: *Psychopharmacology (Berl)* 210.1 (2010), pp. 35–43.

[209] P. Mak, C. Broussard, K. Vacy, and J. H. Broadbear. "Modulation of anxiety behavior in the elevated plus maze using peptidic oxytocin and vasopressin receptor ligands in the rat". In: *J Psychopharmacol* 26.4 (2012), pp. 532–42.

[210] M. Fabian, M. L. Forsling, J. J. Jones, and J. S. Pryor. "The clearance and antidiuretic potency of neurohypophysial hormones in man, and their plasma binding and stability". In: *J Physiol* 204.3 (1969), pp. 653–68.

[211] J. G. Veening, T. de Jong, and H. P. Barendregt. "Oxytocin-messages via the cerebrospinal fluid: behavioral effects; a review". In: *Physiol Behav* 101.2 (2010), pp. 193–210.

[212] J. P. Burbach, E. R. De Kloet, and D. De Wied. "Oxytocin biotransformation in the rat limbic brain: characterization of peptidase activities and significance in the formation of oxytocin fragments". In: *Brain Res* 202.2 (1980), pp. 401–14.

[213] J Burbach, B Bohus, G Kovacs, J Van Nispen, H Greven, and D de Wied. "Oxytocin is a precursor of potent behaviourally active neuropeptides". In: *European Journal of Pharmacology* 94.1-2 (1983), pp. 125–131.

[214] P. Popik, J. Vetulani, and J. M. Van Ree. "Facilitation and attenuation of social recognition in rats by different oxytocin-related peptides". In: *Eur J Pharmacol* 308.2 (1996), pp. 113–6.

[215] E. Loyens, D. De Bundel, H. Demaegdt, S. Y. Chai, P. Vanderheyden, Y. Michotte, P. Gard, and I. Smolders. "Antidepressant-like effects of oxytocin in mice are dependent on the presence of insulin-regulated aminopeptidase". In: *Int J Neuropsychopharmacol* 16.5 (2013), pp. 1153–63.

[216] S. S. Moy, B. L. Teng, V. D. Nikolova, N. V. Riddick, C. D. Simpson, A. Van Deusen, W. P. Janzen, M. F. Sassano, C. A. Pedersen, and M. B. Jarstfer. "Prosocial effects of an oxytocin metabolite, but not synthetic oxytocin receptor agonists, in a mouse model of autism". In: *Neuropharmacology* 144 (2019), pp. 301–311.

[217] V. Verma, A. Mann, W. Costain, G. Pontoriero, J. M. Castellano, K. Skoblenick, S. K. Gupta, Z. Pristupa, H. B. Niznik, R. L. Johnson, V. D. Nair, and R. K. Mishra. "Modulation of agonist binding to human dopamine receptor subtypes by L-prolyl-L-leucyl-glycinamide and a peptidomimetic analog". In: *J Pharmacol Exp Ther* 315.3 (2005), pp. 1228–36.

[218] A. Bocheva and E. Dzambazova-Maximova. "Antiopioid properties of the TYR-MIF-1 family". In: *Methods Find Exp Clin Pharmacol* 26.9 (2004), pp. 673–7.

[219] W. T. Jorgensen, D. W. Gulliver, E. L. Werry, T. Reekie, M. Connor, and M. Kassiou. "Flexible analogues of WAY-267,464: Synthesis and pharmacology at the human oxytocin and vasopressin 1a receptors". In: *Eur J Med Chem* 108 (2016), pp. 730–740.

[220] H. J. Motulsky and L. C. Mahan. "The kinetics of competitive radioligand binding predicted by the law of mass action". In: *Mol Pharmacol* 25.1 (1984), pp. 1–9.

[221] B. Costa, E. Da Pozzo, C. Giacomelli, E. Barresi, S. Taliani, F. Da Settimo, and C. Martini. "TSPO ligand residence time: a new parameter to predict compound neurosteroidogenic efficacy". In: *Sci Rep* 6 (2016), p. 18164.

[222] S. Alberi, J. J. Dreifuss, and M. Raggenbass. "The oxytocin-induced inward current in vagal neurons of the rat is mediated by G protein activation but not by an increase in the intracellular calcium concentration". In: *Eur J Neurosci* 9.12 (1997), pp. 2605–12.

[223] J. A. Schroeder, J. D. Ruta, J. S. Gordon, A. S. Rodrigues, and C. C. Foote. "The phosphodiesterase inhibitor isobutylmethylxanthine attenuates behavioral sensitization to cocaine". In: *Behav Pharmacol* 23.3 (2012), pp. 310–4.

[224] R. H. Alasbahi and M. F. Melzig. "Forskolin and derivatives as tools for studying the role of cAMP". In: *Pharmazie* 67.1 (2012), pp. 5–13.

[225] B. M. Sanborn, K. Dodge, M. Monga, A. Qian, W. Wang, and C. Yue. "Molecular mechanisms regulating the effects of oxytocin on myometrial intracellular calcium". In: *Adv Exp Med Biol* 449 (1998), pp. 277–86.

[226] C. A. Grotegut, L. Feng, L. Mao, R. P. Heine, A. P. Murtha, and H. A. Rockman. "beta-Arrestin mediates oxytocin receptor signaling, which regulates uterine contractility and cellular migration". In: *Am J Physiol Endocrinol Metab* 300.3 (2011), E468–77.

[227] T. Kenakin, C. Watson, V. Muniz-Medina, A. Christopoulos, and S. Novick. "A simple method for quantifying functional selectivity and agonist bias". In: *ACS Chem Neurosci* 3.3 (2012), pp. 193–203.

[228] J. W. Black and P. Leff. "Operational models of pharmacological agonism". In: *Proc R Soc Lond B Biol Sci* 220.1219 (1983), pp. 141–62.

[229] E. T. van der Westhuizen, B. Breton, A. Christopoulos, and M. Bouvier. "Quantification of ligand bias for clinically relevant beta2-adrenergic receptor ligands: implications for drug taxonomy". In: *Mol Pharmacol* 85.3 (2014), pp. 492–509.

[230] J. L. Lau and M. K. Dunn. "Therapeutic peptides: Historical perspectives, current development trends, and future directions". In: *Bioorg Med Chem* 26.10 (2018), pp. 2700–2707.

[231] A. D. Wong, M. Ye, A. F. Levy, J. D. Rothstein, D. E. Bergles, and P. C. Searson. "The blood-brain barrier: an engineering perspective". In: *Front Neuroeng* 6 (2013), p. 7.

[232] B. Chini, B. Mouillac, M. N. Balestre, S. Trumpp-Kallmeyer, J. Hoflack, M. Hibert, M. Andriolo, S. Pupier, S. Jard, and C. Barberis. "Two aromatic residues regulate the response of the human oxytocin receptor to the partial agonist arginine vasopressin". In: *FEBS Lett* 397.2-3 (1996), pp. 201–6.

[233] G. Antobreh, I. Enyedy, and A. W. Ravna. "Molecular modeling and docking studies of the oxytocin receptor". In: *Future Med Chem* 10.2 (2018), pp. 135–155.

[234] Y. Cheng and W. H. Prusoff. "Relationship between the inhibition constant (K1) and the concentration of inhibitor which causes 50 per cent inhibition (I50) of an enzymatic reaction". In: *Biochem Pharmacol* 22.23 (1973), pp. 3099–108.

[235] J. Gupte, G. Cutler, J. L. Chen, and H. Tian. "Elucidation of signaling properties of vasopressin receptor-related receptor 1 by using the chimeric receptor approach". In: *Proc Natl Acad Sci U S A* 101.6 (2004), pp. 1508–13.

[236] C. Palm, F. Pistrosch, K. Herbrig, and P. Gross. "Vasopressin antagonists as aquaretic agents for the treatment of hyponatremia". In: *Am J Med* 119.7 Suppl 1 (2006), S87–92.

[237] A. Greenberg and J. G. Verbalis. "Vasopressin receptor antagonists". In: *Kidney Int* 69.12 (2006), pp. 2124–30.

[238] J. W. Ferguson, G. Therapondos, D. E. Newby, and P. C. Hayes. "Therapeutic role of vasopressin receptor antagonism in patients with liver cirrhosis". In: *Clin Sci (Lond)* 105.1 (2003), pp. 1–8.

[239] M. Kassiou, W. Jorgensen, E. Werry, T. Reekie, M. Bowen, and I. S. McGregor. *Non-Peptide Oxytocin Receptor Agonists*. Patent. 2018.

[240] C. W. Gruber, J. Koehbach, and M. Muttenthaler. "Exploring bioactive peptides from natural sources for oxytocin and vasopressin drug discovery". In: *Future Med Chem* 4.14 (2012), pp. 1791–8.

[241] M. Petersson and K. Uvnas-Moberg. "Prolyl-leucyl-glycinamide shares some effects with oxytocin but decreases oxytocin levels". In: *Physiol Behav* 83.3 (2004), pp. 475–81.

[242] R. Stancampiano, M. R. Melis, and A. Argiolas. "Proteolytic conversion of oxytocin by brain synaptic membranes: role of aminopeptidases and endopeptidases". In: *Peptides* 12.5 (1991), pp. 1119–25.

[243] R. He, B. Finan, J. P. Mayer, and R. D. DiMarchi. "Peptide Conjugates with Small Molecules Designed to Enhance Efficacy and Safety". In: *Molecules* 24.10 (2019).

[244] K. Wisniewski. "Design of Oxytocin Analogs". In: *Methods Mol Biol* 2001 (2019), pp. 235–271.

[245] D. S. Hersh, A. S. Wadajkar, N. Roberts, J. G. Perez, N. P. Connolly, V. Frenkel, J. A. Winkles, G. F. Woodworth, and A. J. Kim. "Evolving Drug Delivery Strategies to Overcome the Blood Brain Barrier". In: *Curr Pharm Des* 22.9 (2016), pp. 1177–1193.

[246] S. Schilling, C. Wasternack, and H. U. Demuth. "Glutaminyl cyclases from animals and plants: a case of functionally convergent protein evolution". In: *Biol Chem* 389.8 (2008), pp. 983–91.

[247] S. R. Hawtin, H. C. Howard, and M. Wheatley. "Identification of an extracellular segment of the oxytocin receptor providing agonist-specific binding epitopes". In: *Biochem J* 354.Pt 2 (2001), pp. 465–72.

[248] V. J. Wesley, S. R. Hawtin, H. C. Howard, and M. Wheatley. "Agonist-specific, high-affinity binding epitopes are contributed by an arginine in the N-terminus of the human oxytocin receptor". In: *Biochemistry* 41.16 (2002), pp. 5086–92.

[249] G. Gimpl, R. Postina, F. Fahrenholz, and T. Reinheimer. "Binding domains of the oxytocin receptor for the selective oxytocin receptor antagonist barusiban in comparison to the agonists oxytocin and carbetocin". In: *Eur J Pharmacol* 510.1-2 (2005), pp. 9–16.

[250] F. Fanelli, P. Barbier, D. Zanchetta, P. G. de Benedetti, and B. Chini. "Activation mechanism of human oxytocin receptor: a combined study of experimental and computer-simulated mutagenesis". In: *Mol Pharmacol* 56.1 (1999), pp. 214–25.

[251] M. Wheatley, S. R. Hawtin, V. J. Wesley, H. C. Howard, J. Simms, A. Miles, K. McEwan, and R. A. Parslow. "Agonist binding to peptide hormone receptors". In: *Biochem Soc Trans* 31.Pt 1 (2003), pp. 35–9.

[252] B. Chini, B. Mouillac, Y. Ala, M. N. Balestre, S. Trumpp-Kallmeyer, J. Hoflack, J. Elands, M. Hibert, M. Manning, S. Jard, and C. Barberis. "Identification of a single residue responsible for agonist selectivity in the oxytocin-vasopressin receptors". In: *Ann N Y Acad Sci* 812 (1997), pp. 218–21.

[253] A. Jovanovic, S. Jovanovic, I. Tulic, and L. Grbovic. "Effect of oxytocin as a partial agonist at vasoconstrictor vasopressin receptors on the human isolated uterine artery". In: *Br J Pharmacol* 121.7 (1997), pp. 1468–74.

[254] T. Nagasaka, S. Nomura, M. Okamura, M. Tsujimoto, H. Nakazato, Y. Oiso, N. Nakashima, and S. Mizutani. "Immunohistochemical localization of placental leucine aminopeptidase/oxytocinase in normal human placental, fetal and adult tissues". In: *Reprod Fertil Dev* 9.8 (1997), pp. 747–53.

[255] T. Rogi, M. Tsujimoto, H. Nakazato, S. Mizutani, and Y. Tomoda. "Human placental leucine aminopeptidase/oxytocinase. A new member of type II membrane-spanning zinc metallopeptidase family". In: *J Biol Chem* 271.1 (1996), pp. 56–61.

[256] S. Toda, H. Ando, T. Nagasaka, S. Tsukahara, M. Nomura, Y. Kotani, S. Nomura, F. Kikkawa, M. Tsujimoto, and S. Mizutani. "Existence of placental leucine aminopeptidase/oxytocinase/insulin-regulated membrane aminopeptidase in human endometrial epithelial cells". In: *J Clin Endocrinol Metab* 87.3 (2002), pp. 1384–9.

[257] A. Argiolas and G. L. Gessa. "Central functions of oxytocin". In: *Neurosci Biobehav Rev* 15.2 (1991), pp. 217–31.

[258] D. Huber, P. Veinante, and R. Stoop. "Vasopressin and oxytocin excite distinct neuronal populations in the central amygdala". In: *Science* 308.5719 (2005), pp. 245–8.

[259] B. Bohus, G. L. Kovacs, and D. de Wied. "Oxytocin, vasopressin and memory: opposite effects on consolidation and retrieval processes". In: *Brain Res* 157.2 (1978), pp. 414–7.

[260] B. Bohus, I. Urban, T. B. van Wimersma Greidanus, and D. de Wied. "Opposite effects of oxytocin and vasopressin on avoidance behaviour and hippocampal theta rhythm in the rat". In: *Neuropharmacology* 17.4-5 (1978), pp. 239–47.

[261] D. Viviani and R. Stoop. "Opposite effects of oxytocin and vasopressin on the emotional expression of the fear response". In: *Prog Brain Res* 170 (2008), pp. 207–18.

[262] C. F. Ferris. "Vasopressin/oxytocin and aggression". In: *Novartis Found Symp* 268 (2005), 190–8; discussion 198–200, 242–53.

[263] R. N. Fernando, J. Larm, A. L. Albiston, and S. Y. Chai. "Distribution and cellular localization of insulin-regulated aminopeptidase in the rat central nervous system". In: *J Comp Neurol* 487.4 (2005), pp. 372–90.

[264] P. R. Gard, P. Daw, Z. S. Mashhour, and P. Tran. "Interactions of angiotensin IV and oxytocin on behaviour in mice". In: *J Renin Angiotensin Aldosterone Syst* 8.3 (2007), pp. 133–8.

[265] D. de Wied, O. Gaffori, J. P. Burbach, G. L. Kovacs, and J. M. van Ree. "Structure activity relationship studies with C-terminal fragments of vasopressin and oxytocin on avoidance behaviors of rats". In: *J Pharmacol Exp Ther* 241.1 (1987), pp. 268–74.

[266] Z. Zhu and J. Cuozzo. "Review article: high-throughput affinity-based technologies for small-molecule drug discovery". In: *J Biomol Screen* 14.10 (2009), pp. 1157–64.

[267] R. Jafari, H. Almqvist, H. Axelsson, M. Ignatushchenko, T. Lundback, P. Nordlund, and D. Martinez Molina. "The cellular thermal shift assay for evaluating drug target interactions in cells". In: *Nat Protoc* 9.9 (2014), pp. 2100–22.

[268] M. Jayapal and A. J. Melendez. "DNA microarray technology for target identification and validation". In: *Clin Exp Pharmacol Physiol* 33.5-6 (2006), pp. 496–503.

[269] K. M. Dumais and A. H. Veenema. "Vasopressin and oxytocin receptor systems in the brain: Sex differences and sex-specific regulation of social behavior". In: *Front Neuroendocrinol* 40 (2016), pp. 1–23.

[270] M. Thibonnier, C. Auzan, Z. Madhun, P. Wilkins, L. Berti-Mattera, and E. Clauser. "Molecular cloning, sequencing, and functional expression of a cDNA encoding the human V1a vasopressin receptor". In: *J Biol Chem* 269.5 (1994), pp. 3304–10.

[271] M. A. Wasilewski, V. D. Myers, F. A. Recchia, A. M. Feldman, and D. G. Tilley. "Arginine vasopressin receptor signaling and functional outcomes in heart failure". In: *Cell Signal* 28.3 (2016), pp. 224–233.

[272] H. Pajouhesh and G. R. Lenz. "Medicinal chemical properties of successful central nervous system drugs". In: *NeuroRx* 2.4 (2005), pp. 541–53.

[273] D. F. Veber, S. R. Johnson, H. Y. Cheng, B. R. Smith, K. W. Ward, and K. D. Kopple. "Molecular properties that influence the oral bioavailability of drug candidates". In: *J Med Chem* 45.12 (2002), pp. 2615–23.

[274] D. F. Veber and R Freidinger. "The design of metabolically stable peptide analogs". In: *Trends in Neurosciences* 8 (1985), pp. 392–396.

[275] A. T. Bockus, K. W. Lexa, C. R. Pye, A. S. Kalgutkar, J. W. Gardner, K. C. Hund, W. M. Hewitt, J. A. Schwochert, E. Glassey, D. A. Price, A. M. Mathiowetz, S. Liras, M. P. Jacobson, and R. S. Lokey. "Probing the Physicochemical Boundaries of Cell Permeability and Oral Bioavailability in Lipophilic Macrocycles Inspired by Natural Products". In: *J Med Chem* 58.11 (2015), pp. 4581–9.

[276] S. W. Fesik, Jr. Gampe R. T., H. L. Eaton, G. Gemmecker, E. T. Olejniczak, P. Neri, T. F. Holzman, D. A. Egan, R. Edalji, R. Simmer, and et al. "NMR studies of [U-13C]cyclosporin A bound to cyclophilin: bound conformation and portions of cyclosporin involved in binding". In: *Biochemistry* 30.26 (1991), pp. 6574–83.

[277] G. H. Goetz, L. Philippe, and M. J. Shapiro. "EPSA: A Novel Supercritical Fluid Chromatography Technique Enabling the Design of Permeable Cyclic Peptides". In: *ACS Med Chem Lett* 5.10 (2014), pp. 1167–72.

[278] M. G. Choc. "Bioavailability and pharmacokinetics of cyclosporine formulations: Neoral vs Sandimmune". In: *Int J Dermatol* 36 Suppl 1 (1997), pp. 1–6.

[279] T. Engstrom, T. Barth, P. Melin, and H. Vilhardt. "Oxytocin receptor binding and uterotonic activity of carbetocin and its metabolites following enzymatic degradation". In: *Eur J Pharmacol* 355.2-3 (1998), pp. 203–10.

[280] M. T. Weinstock, J. N. Francis, J. S. Redman, and M. S. Kay. "Protease-resistant peptide design-empowering nature's fragile warriors against HIV". In: *Biopolymers* 98.5 (2012), pp. 431–42.

[281] M. L. Di Gioia, A. Leggio, F. Malagrino, E. Romio, C. Siciliano, and A. Liguori. "N-Methylated alpha-Amino Acids And Peptides: Synthesis And Biological Activity". In: *Mini Rev Med Chem* 16.9 (2016), pp. 683–90.

[282] C. Cabrele, T. A. Martinek, O. Reiser, and L. Berlicki. "Peptides containing beta-amino acid patterns: challenges and successes in medicinal chemistry". In: *J Med Chem* 57.23 (2014), pp. 9718–39.

[283] K Vishwanatha, R Mains, and B Eipper. "Peptidylglycine Amidating Monooxygenase (PAM)". In: *Handbook of Biologically Active Peptides*. 2nd ed. Academic Press, 2013. Chap. 244, pp. 1780–1788.

[284] A. F. Russo. "Overview of Neuropeptides: Awakening the Senses?" In: *Headache* 57 Suppl 2 (2017), pp. 37–46.

[285] P. Y. Jean-Charles, S. Kaur, and S. K. Shenoy. "G Protein-Coupled Receptor Signaling Through beta-Arrestin-Dependent Mechanisms". In: *J Cardiovasc Pharmacol* 70.3 (2017), pp. 142–158.

[286] A. Blume, O. J. Bosch, S. Miklos, L. Torner, L. Wales, M. Waldherr, and I. D. Neumann. "Oxytocin reduces anxiety via ERK1/2 activation: local effect within the rat hypothalamic paraventricular nucleus". In: *Eur J Neurosci* 27.8 (2008), pp. 1947–56.

[287] B. Jurek, D. A. Slattery, R. Maloumby, K. Hillerer, S. Koszinowski, I. D. Neumann, and E. H. van den Burg. "Differential contribution of hypothalamic MAPK activity to anxiety-like behaviour in virgin and lactating rats". In: *PLoS One* 7.5 (2012), e37060.

[288] D. Calebiro, V. O. Nikolaev, M. C. Gagliani, T. de Filippis, C. Dees, C. Tacchetti, L. Persani, and M. J. Lohse. "Persistent cAMP-signals triggered by internalized G-protein-coupled receptors". In: *PLoS Biol* 7.8 (2009), e1000172.

[289] J. S. Retamal, P. D. Ramirez-Garcia, P. A. Shenoy, D. P. Poole, and N. A. Veldhuis. "Internalized GPCRs as Potential Therapeutic Targets for the Management of Pain". In: *Front Mol Neurosci* 12 (2019), p. 273.

[290] N. J. Pavlos and P. A. Friedman. "GPCR Signaling and Trafficking: The Long and Short of It". In: *Trends Endocrinol Metab* 28.3 (2017), pp. 213–226.

[291] L. A. Merriam, C. N. Baran, B. M. Girard, J. C. Hardwick, V. May, and R. L. Parsons. "Pituitary adenylate cyclase 1 receptor internalization and endosomal signaling mediate the pituitary adenylate cyclase activating polypeptide-induced increase in guinea pig cardiac neuron excitability". In: *J Neurosci* 33.10 (2013), pp. 4614–22.

[292] S. Ferrandon, T. N. Feinstein, M. Castro, B. Wang, R. Bouley, J. T. Potts, T. J. Gardella, and J. P. Vilardaga. "Sustained cyclic AMP production by parathyroid hormone receptor endocytosis". In: *Nat Chem Biol* 5.10 (2009), pp. 734–42.

[293] R. H. Oakley, S. A. Laporte, J. A. Holt, M. G. Caron, and L. S. Barak. "Differential affinities of visual arrestin, beta arrestin1, and beta arrestin2 for G protein-coupled receptors delineate two major classes of receptors". In: *J Biol Chem* 275.22 (2000), pp. 17201–10.

[294] L. Castro, C. Yapo, and P. Vincent. "[Physiopathology of cAMP/PKA signaling in neurons]". In: *Biol Aujourdhui* 210.4 (2016), pp. 191–203.

[295] K. B. Seamon, W. Padgett, and J. W. Daly. "Forskolin: unique diterpene activator of adenylate cyclase in membranes and in intact cells". In: *Proc Natl Acad Sci U S A* 78.6 (1981), pp. 3363–7.

[296] R. A. Copeland, D. L. Pompliano, and T. D. Meek. "Drug-target residence time and its implications for lead optimization". In: *Nat Rev Drug Discov* 5.9 (2006), pp. 730–9.

[297] A. Ohno, N. Kawasaki, K. Fukuhara, H. Okuda, and T. Yamaguchi. "Complete NMR analysis of oxytocin in phosphate buffer". In: *Magn Reson Chem* 48.2 (2010), pp. 168–72.

[298] R. Bhaskaran, L. C. Chuang, and C. Yu. "Conformational properties of oxytocin in dimethyl sulfoxide solution: NMR and restrained molecular dynamics studies". In: *Biopolymers* 32.12 (1992), pp. 1599–608.

[299] D. W. Urry, M. Ohnishi, and R. Walter. "Secondary structure of the cyclic moiety of the peptide hormone oxytocin and its deamino analog". In: *Proc Natl Acad Sci U S A* 66.1 (1970), pp. 111–6.

[300] S. P. Wood, I. J. Tickle, A. M. Treharne, J. E. Pitts, Y. Mascarenhas, J. Y. Li, J. Husain, S. Cooper, T. L. Blundell, V. J. Hruby, and et al. "Crystal structure analysis of deamino-oxytocin: conformational flexibility and receptor binding". In: *Science* 232.4750 (1986), pp. 633–6.

[301] G. H. Goetz, W. Farrell, M. Shalaeva, S. Sciabola, D. Anderson, J. Yan, L. Philippe, and M. J. Shapiro. "High throughput method for the indirect detection of intramolecular hydrogen bonding". In: *J Med Chem* 57.7 (2014), pp. 2920–9.

[302] S. Sciabola, G. H. Goetz, G. Bai, B. N. Rogers, D. L. Gray, A. Duplantier, K. R. Fonseca, M. A. Vanase-Frawley, and N. M. Kablaoui. "Systematic N-methylation of oxytocin: Impact on pharmacology and intramolecular hydrogen bonding network". In: *Bioorg Med Chem* 24.16 (2016), pp. 3513–20.

[303] I. Lindberg and C. C. Glembotski. "Physiological signaling in the absence of amidated peptides". In: *Proc Natl Acad Sci U S A* 116.40 (2019), pp. 19774–19776.

[304] D. J. Merkler. "C-terminal amidated peptides: production by the in vitro enzymatic amidation of glycine-extended peptides and the importance of the amide to bioactivity". In: *Enzyme Microb Technol* 16.6 (1994), pp. 450–6.

[305] D Kumar, B Eipper, and R Mains. "Amidation". In: *Reference Module in Biomedical Sciences*. Elsevier, 2014.

[306] M. Mura, J. Wang, Y. Zhou, M. Pinna, A. V. Zvelindovsky, S. R. Dennison, and D. A. Phoenix. "The effect of amidation on the behaviour of antimicrobial peptides". In: *Eur Biophys J* 45.3 (2016), pp. 195–207.

[307] S. Hosseini, H. Naderi-Manesh, D. Mountassif, M. Cerruti, H. Vali, and S. Faghihi. "C-terminal amidation of an osteocalcin-derived peptide promotes hydroxyapatite crystallization". In: *J Biol Chem* 288.11 (2013), pp. 7885–93.

[308] A. V. da Silva, B. M. De Souza, M. P. Dos Santos Cabrera, N. B. Dias, P. C. Gomes, J. R. Neto, R. G. Stabeli, and M. S. Palma. "The effects of the C-terminal amidation of mastoparans on their biological actions and interactions with membrane-mimetic systems". In: *Biochim Biophys Acta* 1838.10 (2014), pp. 2357–68.

[309] R. Postina, E. Kojro, and F. Fahrenholz. "Separate agonist and peptide antagonist binding sites of the oxytocin receptor defined by their transfer into the V2 vasopressin receptor". In: *J Biol Chem* 271.49 (1996), pp. 31593–601.

[310] A. G. Lee, D. R. Cool, Jr. Grunwald W. C., D. E. Neal, C. L. Buckmaster, M. Y. Cheng, S. A. Hyde, D. M. Lyons, and K. J. Parker. "A novel form of oxytocin in New World monkeys". In: *Biol Lett* 7.4 (2011), pp. 584–7.

[311] A. Mendez, M. E. Burns, A. Roca, J. Lem, L. W. Wu, M. I. Simon, D. A. Baylor, and J. Chen. "Rapid and reproducible deactivation of rhodopsin requires multiple phosphorylation sites". In: *Neuron* 28.1 (2000), pp. 153–64.

[312] C. G. England, E. B. Ehlerding, and W. Cai. "NanoLuc: A Small Luciferase Is Brightening Up the Field of Bioluminescence". In: *Bioconjug Chem* 27.5 (2016), pp. 1175–1187.

[313] J. M. Willets, P. J. Brighton, R. Mistry, G. E. Morris, J. C. Konje, and R. A. Challiss. "Regulation of oxytocin receptor responsiveness by G protein-coupled receptor kinase 6 in human myometrial smooth muscle". In: *Mol Endocrinol* 23.8 (2009), pp. 1272–80.

[314] B. C. Wilson, M. G. Terenzi, and C. D. Ingram. "Differential excitatory responses to oxytocin in sub-divisions of the bed nuclei of the stria terminalis". In: *Neuropeptides* 39.4 (2005), pp. 403–7.

[315] M. G. Terenzi and C. D. Ingram. "Oxytocin-induced excitation of neurones in the rat central and medial amygdaloid nuclei". In: *Neuroscience* 134.1 (2005), pp. 345–54.

[316] T. N. Feinstein, N. Yui, M. J. Webber, V. L. Wehbi, H. P. Stevenson, Jr. King J. D., K. R. Hallows, D. Brown, R. Bouley, and J. P. Vilardaga. "Non-canonical control of vasopressin receptor type 2 signaling by retromer and arrestin". In: *J Biol Chem* 288.39 (2013), pp. 27849–60.

[317] V. Seow, J. Lim, A. J. Cotterell, M. K. Yau, W. Xu, R. J. Lohman, W. M. Kok, M. J. Stoermer, M. J. Sweet, R. C. Reid, J. Y. Suen, and D. P. Fairlie. "Receptor residence time trumps drug-likeness and oral bioavailability in determining efficacy of complement C5a antagonists". In: *Sci Rep* 6 (2016), p. 24575.

[318] R. A. Copeland. "The dynamics of drug-target interactions: drug-target residence time and its impact on efficacy and safety". In: *Expert Opin Drug Discov* 5.4 (2010), pp. 305–10.

[319] E. R. Wood, A. T. Truesdale, O. B. McDonald, D. Yuan, A. Hassell, S. H. Dickerson, B. Ellis, C. Pennisi, E. Horne, K. Lackey, K. J. Alligood, D. W. Rusnak, T. M. Gilmer, and L. Shewchuk. "A unique structure for epidermal growth factor receptor bound to GW572016 (Lapatinib): relationships among protein conformation, inhibitor off-rate, and receptor activity in tumor cells". In: *Cancer Res* 64.18 (2004), pp. 6652–9.

[320] B. Maschera, G. Darby, G. Palu, L. L. Wright, M. Tisdale, R. Myers, E. D. Blair, and E. S. Furfine. "Human immunodeficiency virus. Mutations in the viral protease that confer resistance to saquinavir increase the dissociation rate constant of the protease-saquinavir complex". In: *J Biol Chem* 271.52 (1996), pp. 33231–5.

[321] J. E. Drury, L. Di Costanzo, T. M. Penning, and D. W. Christianson. "Inhibition of human steroid 5beta-reductase (AKR1D1) by finasteride and structure of the enzyme-inhibitor complex". In: *J Biol Chem* 284.30 (2009), pp. 19786–90.

[322] G. Tian. "In vivo time-dependent inhibition of human steroid 5 alpha-reductase by finasteride". In: *J Pharm Sci* 85.1 (1996), pp. 106–11.

[323] A. Lewandowicz, P. C. Tyler, G. B. Evans, R. H. Furneaux, and V. L. Schramm. "Achieving the ultimate physiological goal in transition state analogue inhibitors for purine nucleoside phosphorylase". In: *J Biol Chem* 278.34 (2003), pp. 31465–8.

[324] P. M. Vanderheyden, F. L. Fierens, and G. Vauquelin. "Angiotensin II type 1 receptor antagonists. Why do some of them produce insurmountable inhibition?" In: *Biochem Pharmacol* 60.11 (2000), pp. 1557–63.

[325] S. Kapur and P. Seeman. "Antipsychotic agents differ in how fast they come off the dopamine D2 receptors. Implications for atypical antipsychotic action". In: *J Psychiatry Neurosci* 25.2 (2000), pp. 161–6.

[326] Y. Yun, J. Chen, R. Liu, W. Chen, C. Liu, R. Wang, Z. Hou, Z. Yu, Y. Sun, I. Jzerman AP, L. H. Heitman, X. Yin, and D. Guo. "Long residence time adenosine A1 receptor agonists produce sustained wash-resistant antilipolytic effect in rat adipocytes". In: *Biochem Pharmacol* 164 (2019), pp. 45–52.

[327] J. D. Hothersall, A. J. Brown, I. Dale, and P. Rawlins. "Can residence time offer a useful strategy to target agonist drugs for sustained GPCR responses?" In: *Drug Discov Today* 21.1 (2016), pp. 90–96.

[328] L. Wang, D. W. Marti, and R. E. Anderson. "Development and Validation of a Simple LC-MS Method for the Quantification of Oxytocin in Dog Saliva". In: *Molecules* 24.17 (2019).

[329] A. A. Franke, A. Menden, and X. Li. "Determination of total oxytocin in human serum by traditional LCMS". In: *The FASEB Journal* 31 (2017), lb128–lb128.

[330] A. A. Franke, X. Li, A. Menden, M. R. Lee, and J. F. Lai. "Oxytocin analysis from human serum, urine, and saliva by orbitrap liquid chromatography-mass spectrometry". In: *Drug Test Anal* 11.1 (2019), pp. 119–128.

[331] O. K. Brandtzaeg, E. Johnsen, H. Roberg-Larsen, K. F. Seip, E. L. MacLean, L. R. Gesquiere, S. Leknes, E. Lundanes, and S. R. Wilson. "Proteomics tools reveal startlingly high amounts of oxytocin in plasma and serum". In: *Sci Rep* 6 (2016), p. 31693.

[332] M. Sani, A. Volonterio, and M. Zanda. "The trifluoroethylamine function as peptide bond replacement". In: *ChemMedChem* 2.12 (2007), pp. 1693–700.

[333] M. Manning, S. Stoev, B. Chini, T. Durroux, B. Mouillac, and G. Guillon. "Peptide and non-peptide agonists and antagonists for the vasopressin and oxytocin V1a, V1b, V2 and OT receptors: research tools and potential therapeutic agents". In: *Prog Brain Res* 170 (2008), pp. 473–512.

[334] M. Muttenthaler, A. Andersson, A. D. de Araujo, Z. Dekan, R. J. Lewis, and P. F. Alewood. "Modulating oxytocin activity and plasma stability by disulfide bond engineering". In: *J Med Chem* 53.24 (2010), pp. 8585–96.

[335] C. Xu, M. Peter, N. Bouquier, V. Ollendorff, I. Villamil, J. Liu, L. Fagni, and J. Perroy. "REV, A BRET-Based Sensor of ERK Activity". In: *Front Endocrinol (Lausanne)* 4 (2013), p. 95.

[336] L. L. Ong, J. D. Vasta, L. Monereau, G. Locke, H. Ribeiro, M. A. Pattoli, S. Skala, J. R. Burke, S. H. Watterson, J. A. Tino, P. L. Meisenheimer, B. Arey, J. Lippy, L. Zhang, M. B. Robers, A. Tebben, and C. Chaudhry. "A High-Throughput BRET Cellular Target Engagement Assay Links Biochemical to Cellular Activity for Bruton's Tyrosine Kinase". In: *SLAS Discov* 25.2 (2020), pp. 176–185.

[337] A. Salahpour, S. Espinoza, B. Masri, V. Lam, L. S. Barak, and R. R. Gainetdinov. "BRET biosensors to study GPCR biology, pharmacology, and signal transduction". In: *Front Endocrinol (Lausanne)* 3 (2012), p. 105.

[338] D. Suchecki and C. F. Elias. "Editorial: Neuropeptides and Behavior: From Motivation to Psychopathology". In: *Front Endocrinol (Lausanne)* 8 (2017), p. 210.

[339] I. D. Neumann, R. Maloumby, D. I. Beiderbeck, M. Lukas, and R. Landgraf. "Increased brain and plasma oxytocin after nasal and peripheral administration in rats and mice". In: *Psychoneuroendocrinology* 38.10 (2013), pp. 1985–93.

[340] O. Dal Monte, P. L. Noble, J. Turchi, A. Cummins, and B. B. Averbeck. "CSF and blood oxytocin concentration changes following intranasal delivery in macaque". In: *PLoS One* 9.8 (2014), e103677.

[341] N. Striepens, K. M. Kendrick, V. Hanking, R. Landgraf, U. Wullner, W. Maier, and R. Hurlemann. "Elevated cerebrospinal fluid and blood concentrations of oxytocin following its intranasal administration in humans". In: *Sci Rep* 3 (2013), p. 3440.

[342] M. Valstad, G. A. Alvares, M. Egknud, A. M. Matziorinis, O. A. Andreassen, L. T. Westlye, and D. S. Quintana. "The correlation between central and peripheral oxytocin concentrations: A systematic review and meta-analysis". In: *Neurosci Biobehav Rev* 78 (2017), pp. 117–124.

[343] H. J. Monstein, N. Grahn, M. Truedsson, and B. Ohlsson. "Oxytocin and oxytocin-receptor mRNA expression in the human gastrointestinal tract: a polymerase chain reaction study". In: *Regul Pept* 119.1-2 (2004), pp. 39–44.

[344] J. Gutkowska and M. Jankowski. "Oxytocin revisited: its role in cardiovascular regulation". In: *J Neuroendocrinol* 24.4 (2012), pp. 599–608.

[345] S. Ganger and K. Schindowski. "Tailoring Formulations for Intranasal Nose-to-Brain Delivery: A Review on Architecture, Physico-Chemical Characteristics and Mucociliary Clearance of the Nasal Olfactory Mucosa". In: *Pharmaceutics* 10.3 (2018).

[346] J Namekawa, E Matsumoto, H Kaneko, T Shimomoto, T Okamura, T Oshikata, R Renne, and D Miuora. "A 6-week repeated intranasal dose toxicity study of TTA-121, a novel oxytocin nasal spray, in rats". In: *Fundamental Toxicological Sciences* 6.7 (2019), pp. 259–268.

[347] J Namekawa, E Matsumoto, H Kaneko, T Shimomoto, T Okamura, T Oshikata, R Renne, and D Miuora. "A 6-week repeated intranasal dose toxicity study of TTA-121, a novel oxytocin nasal spray, in cynomolgus monkeys". In: *Fundamental Toxicological Sciences* 6.7 (2019), pp. 269–275.

[348] C. Sakanaka, R. Ihara, A. Kishi, K. Kirihara, G. Oguri, M. Shibuya, K. Suzuki, K. Ueda, Y. Kameyama, M. Yakabe, T. Haga, and H. Yamasue. *Safety and pharmacokinetics of single and repeated dose of a novel formulation of intra-nasal Oxytocin (TTA-121) in healthy Japanese volunteers (double blind, placebo-controlled Phase 1 trial).* Conference Paper. 2018.

[349] H. Yamasue. *A Trial of TTA-121 on Autism Spectrum Disorder.* Online Database. 2019.

[350] Y. Yamamoto, M Liang, S Munusue, K Deguchi, A Harashima, K Furuhaha, T Yuhi, J Zhonh, S Akther, H Goto, Y Eguchi, Y Kitao, O Hori, Y. Shiraishi, N Ozaki, Y Shimizu, T Kamide, A Yoshikawa, Y. Hayashi, M Nakada, O. Lopatina, M Gerasimenko, Y Komleva, N Malinoskaya, A. Salmina, M. Asano, K. Nishimori, S Sholesen, H Yamamoto, and H Haruhiro. "Vascular RAGE transports oxytocin into the brain to elicit its maternal bonding behaviour in mice". In: *Communications Biology volume* 2 (2019).

[351] Y. Yamamoto and H. Higashida. "RAGE regulates oxytocin transport into the brain". In: *Commun Biol* 3.1 (2020), p. 70.

[352] R. U. Zaman, N. S. Mulla, K. Braz Gomes, C. D'Souza, K. S. Murnane, and M. J. D'Souza. "Nanoparticle formulations that allow for sustained delivery and brain targeting of the neuropeptide oxytocin". In: *Int J Pharm* 548.1 (2018), pp. 698–706.

[353] A. Oppong-Damoah, R. U. Zaman, M. J. D'Souza, and K. S. Murnane. "Nanoparticle encapsulation increases the brain penetrance and duration of action of intranasal oxytocin". In: *Horm Behav* 108 (2019), pp. 20–29.

[354] D. M. Teleanu, I. Negut, V. Grumezescu, A. M. Grumezescu, and R. I. Teleanu. "Nanomaterials for Drug Delivery to the Central Nervous System". In: *Nanomaterials (Basel)* 9.3 (2019).

[355] C. A. Grotegut, L. Mao, S. L. Pierce, G. K. Swamy, R. P. Heine, and A. P. Murtha. "Enhanced Uterine Contractility and Stillbirth in Mice Lacking G Protein-Coupled Receptor Kinase 6 (GRK6): Implications for Oxytocin Receptor Desensitization". In: *Mol Endocrinol* 30.4 (2016), pp. 455–68.

[356] S. Phaneuf, G. Asboth, M. P. Carrasco, G. N. Europe-Finner, F. Saji, T. Kimura, A. Harris, and A. Lopez Bernal. "The desensitization of oxytocin receptors in human myometrial cells is accompanied by down-regulation of oxytocin receptor messenger RNA". In: *J Endocrinol* 154.1 (1997), pp. 7–18.

[357] G. Vauquelin. "Effects of target binding kinetics on in vivo drug efficacy: koff , kon and rebinding". In: *Br J Pharmacol* 173.15 (2016), pp. 2319–34.

[358] G. Vauquelin and S. J. Charlton. "Long-lasting target binding and rebinding as mechanisms to prolong in vivo drug action". In: *Br J Pharmacol* 161.3 (2010), pp. 488–508.

[359] G. Vauquelin. "Rebinding: or why drugs may act longer in vivo than expected from their in vitro target residence time". In: *Expert Opin Drug Discov* 5.10 (2010), pp. 927–41.

[360] G. Gimpl, K. Burger, E. Politowska, J. Ciarkowski, and F. Fahrenholz. "Oxytocin receptors and cholesterol: interaction and regulation". In: *Exp Physiol* 85 Spec No (2000), 41S–49S.

Appendices

Appendix A

Instrument Settings

Table A.1: Instrument settings for microplate readers and radioactivity detectors.

CLARIOStar	
Optic Module	Luminescence
Donor Bandwidth	450 ± 80 nm
Acceptor Bandwidth	660 ± 100 nm
Orbital Averaging	OFF
Multichromatics	Plate
Measurement Type	Precision
PMT Gain	3600
Focus	Perform adjustment
FlexStation 3	
Measurement Mode	FLEX
Excitation Wavelength	485 nm
Emission Wavelength	525 nm
Auto Emission Cut-Off	515 nm
PMT Sensitivity	6
Pipette Height	80 µL
Transfer Volume	20 µL
Compound Concentration	5X
Addition Speed	2
PHERAStar [Time-Resolved Fluorescence]	
Optic Module	HTRF
Simultaneous Dual Emission	ON
Signal Integration Start Time	50 µs
Signal Integration Time	400 µs
Settling time	0.1 s

No. of flashes per well	200
Focus	Perform adjustment

PHERAStar [Luminescence]	
Optic Module	LUM
Simultaneous Dual Emission	OFF
Orbital Averaging	OFF
No. Multichromatics	1
PMT gain	3600
Settling time	0.1 s
Measurement interval time	1.0 s
Focus	Perform adjustment

Appendix B

Assay Optimisation Data

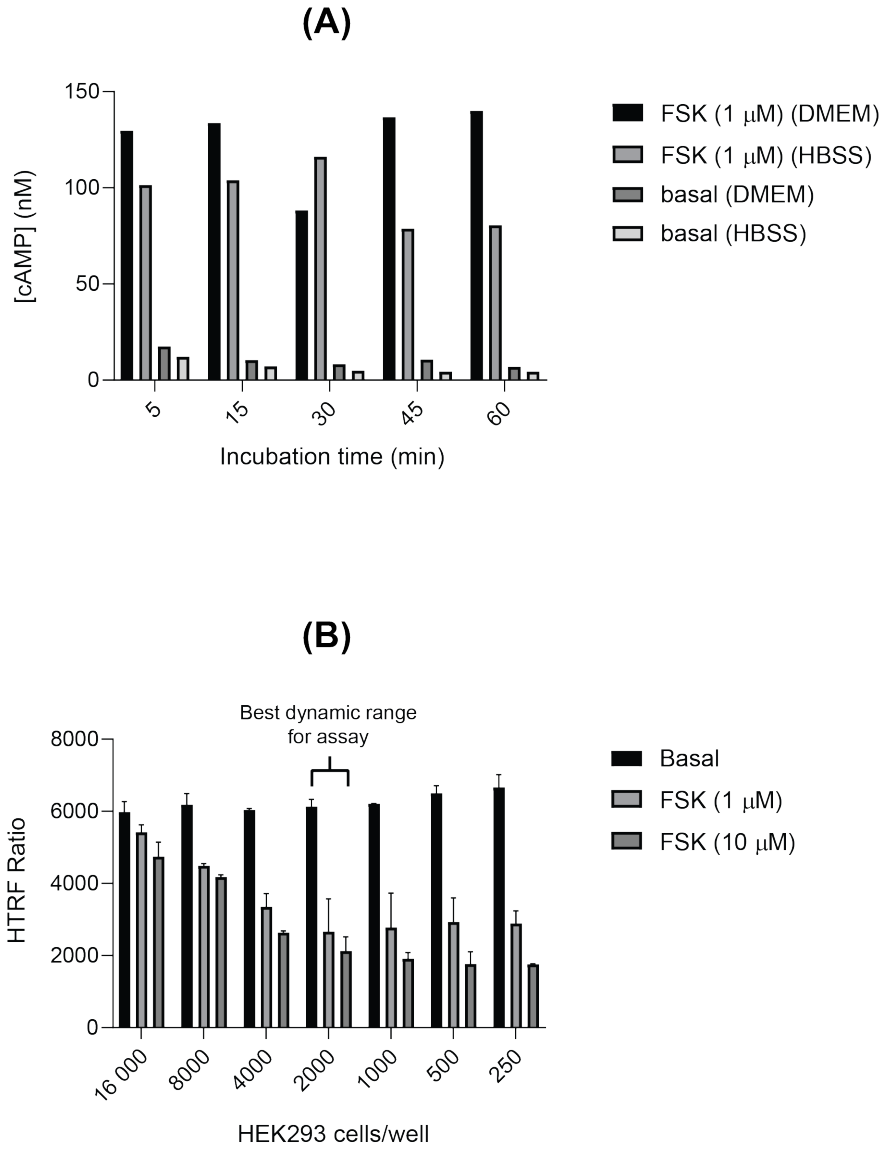

Figure B.1: Homogenous time-resolved fluorescence (HTRF) cAMP production assay optimisation (part 1). **(A)** Buffer composition and agonist incubation time. HEK293 cells expressing the human oxytocin receptor (HEK293-OTR) were incubated with forskolin (1 µM) for 5 - 60 min in HBSS or DMEM assay buffer supplemented with IBMX. **(B)** Optimal assay cell density was determined by incubating HEK293-OTR cells (0.25 - 16 $\times$ 10^3 cells/well) with forskolin (1 - 10 µM) for 5 min. The cell density which yielded the widest dynamic range between basal and forskolin-induced cAMP response was selected for subsequent assays. A higher cell density (2×10^3 cells/well) was preferenced to reduce assay variability.

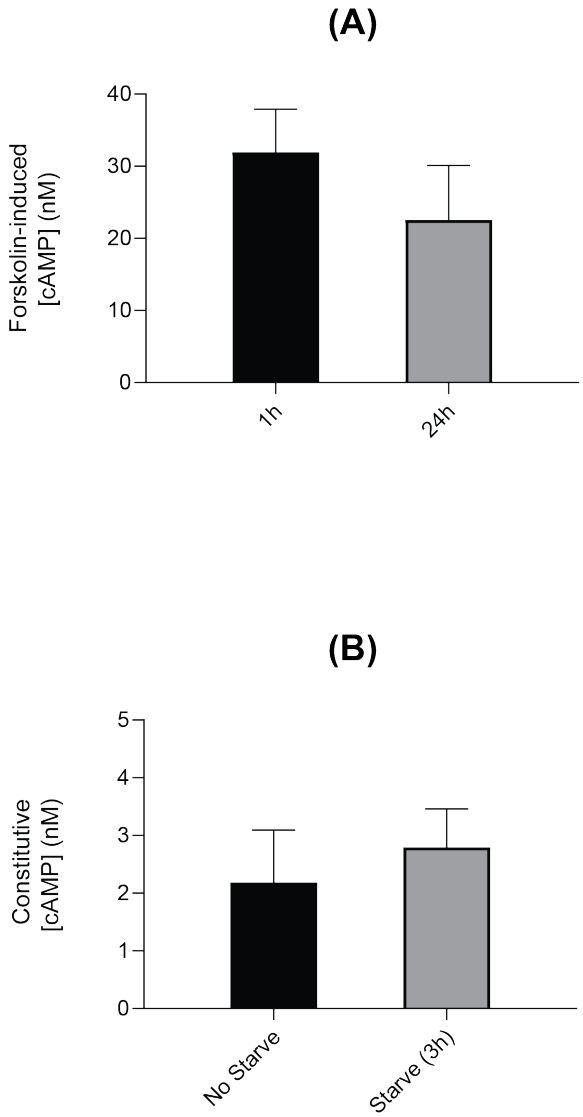

Figure B.2: Homogenous time-resolved fluorescence (HTRF) cAMP production assay optimisation (part 2). **(A)** The effect of antibody incubation time on assay sensitivity was assessed by incubating HEK293 cells expressing the human oxytocin receptor (HEK293-OTR) with forskolin (10 µM) for 5 min, followed by incubation with cAMP-d2 and Ab-cryptate fluorophores for 1 or 24 h at 20°C. No significant differences were observed between treatments (t-test, unpaired, p=0.3038). **(B)** The effect of serum starvation on constitutive cAMP production in HEK293-OTR cells. No statistically sigificant differences were observed between treatments (t-test, unpaired, p=0.3789).

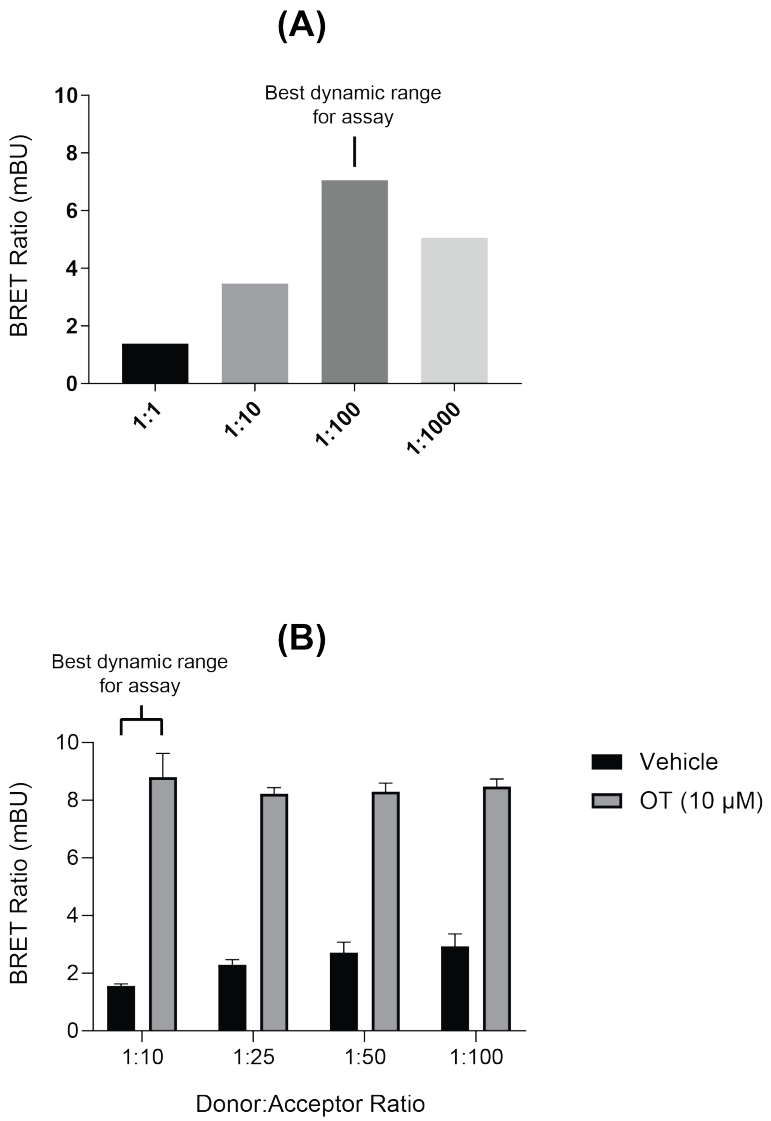

Figure B.3: Bioluminescence resonance energy transfer (BRET) β-arrestin recruitment assay - optimisation of luminescence donor and acceptor fluorophore concentration. **(A)** The optimal concentration of luminescence donor plasmid (OTR-Nluc) was determined by transfecting wild-type HEK293 cells with sequentially diluted OTR-Nluc against a fixed concentration of acceptor fluorophore plasmid (arr2-HaloTag). The donor plasmid concentration which yielded the highest BRET value following OT treatment (0.02 µg/well) was selected for subsequent assays. **(B)** The optimal concentration of acceptor fluorophore was determined by varying the concentration of (arr2-HaloTag) against a fixed concentration of OTR-Nluc previously determined in the dilution assay. The condition which yielded the highest BRET value between basal and OT (10 µM) induced recruitment of β-arrestin (1:10) was used to determine donor:acceptor ratio (1:10) and acceptor plasmid concentration (0.2 µg/well).